Ligands on Demand

Thomas Shaw

Submitted in accordance with the requirements for the degree of

Doctor of Philosophy

The University of Leeds

School of Chemical and Process Engineering

October 2024

Intellectual Property and Publications

The candidate confirms that the work submitted is his own, the contribution of the candidate and the other authors to this work has been outlined. The candidate confirms that appropriate credit has been given within the thesis where reference has been made to the work of others.

The work in Chapter 2 has appeared in: T. Shaw, A. D. Clayton, R. Labes, T. M. Dixon, S. Boyall, O. J. Kershaw, R. A. Bourne, and B. C. Hanson, React Chem Eng, 2024, 9, 426-438. TS was responsible for preparation of the manuscript and the experimental work. ADC and TMD aided TS with coding for the optimisations. RL, ADC, BCH, and SB provided feedback with the manuscript. The contribution from RAB & BCH was project supervision.

The work in Chapter 3 is set to appear in: T. Shaw, A. D. Clayton, J. M Houghton, N. Kapur, R. A. Bourne, and B. C. Hanson, Separations and Purification Technology, 2025. TS was responsible for conceptualisation, preparation of the manuscript, and the experimental work detailed. ADC and JMH aided TS with coding. NK provided the separator for the work and base code. JMH, ADC, BCH, and NK provided feedback with the manuscript. Project supervision was delivered by RAB & BCH.

The work in Chapter 4 is set to appear in: T. Shaw, A. Baker, R. A. Bourne, and B. C. Hanson, Solvent Extraction and Ion Exchange, 2025. TS was responsible for preparation of the manuscript, and the experimental work detailed. AB and BCH provided feedback with the manuscript. Project supervision was delivered by RAB & BCH.

This thesis has been submitted for the award Thesis by Publication as the work is sufficient and includes three individual papers which have a clear link between them. An initial literature review sets the scene and highlights the relevance of the work to come, the following chapters cover synthesis, purification and testing of DEHiBA respectively as individual papers. Supporting information for each chapter is indicated in the appendix.

"I alone cannot change the world, but I can cast a stone across the water to create many ripples."
Mother Theresa

"If you've got it you've got it, if you don't you don't."

Molly Thompson-Smith

I. Acknowledgements

Thank you to Professor Bruce Hanson, you were an incredible mentor, colleague, and friend. You were an inspiration who cared so much and always wanted to see others reach their potential. The nuclear industry has lost a great scientist, and the world has lost a charismatic, loving man. Thank you for your unwavering support, we had some incredible times, you are dearly missed.

I would like to thank both Professor Bruce Hanson and Professor Richard Bourne for securing the funding and turning this project into a reality, providing invaluable guidance and support throughout. Thanks to Professor Nikil Kapur and Dr. James Daglish for facilitating the continuous purification work, providing highly capable lab-scale equipment and expertise. I am extremely grateful for my colleagues past and present within the Institute of Process Research and Development and the Nuclear Engineering Group, two welcoming and passionate groups at the University of Leeds who have made my time here very enjoyable and rewarding. I am especially

grateful to Oliver Kershaw, Joseph Houghton, Sarah Boyall, Thomas Dixon, and Adam Clayton for their support and encouragement inside and outside of the lab.

I wish to thank the GREEN CDT and the EPSRC for funding my PhD giving me the opportunity to thrive and grow as passionate researcher, the industrial relevance of this research has kindled my desire to pursue a research career in radiochemistry with ambition to incorporate my learnings of digital chemistry using industry 4.0, with a desire to improve the sustainability of nuclear energy and the economics of next generation nuclear reprocessing.

I could not have made this journey without the support from my family including our beloved Spud and Chewie. I very much need to thank my parents, Steve and Fiona for my upbringing, your generosity and encouragement has provided me with passion, resilience, and integrity.

Thanks for everything Abbie, you are inspirational, I am thankful for all the sacrifices you make for us, I could not have done it without you, I love you.

II. Abstract

As the next generation of nuclear reprocessing technologies edge toward industrial readiness, concerted efforts are needed to ensure their safety, predictability, robustness, and economic viability. Organic ligands are critical to the selectivity of nuclear reprocessing, current focus is on ligands and processes that can remove long-lived radiotoxic actinides. Amides and diamides are promising ligand classes for the removal of actinides due to their selectivity for the f-block elements, with *N,N*-di-(2-ethylhexyl)isobutyramide (DEHiBA) a popular monoamide for the extraction of uranium devoid of plutonium to overcome plutonium proliferation concerns. DEHiBA is of interest to the GANEX 1st cycle process, a replacement technology to PUREX, overcoming a number of weaknesses faced by this mature industrial process. Whilst tri-*n*-butyl phosphate (TBP) is the ligand employed in the PUREX process, TBP has other uses outside of the nuclear industry, these other uses improve the economic viability of TBP, whereas specialised ligands for nuclear reprocessing like DEHiBA are more novel with limited demand at present, resulting in high costs and thus creates a barrier to research.

This work utilises industry 4.0 (the integration of artificial intelligence and automation for manufacture, otherwise referred to as smart manufacturing) to efficiently optimise the manufacture of DEHiBA, focussing on cost reduction, sustainability improvements and production throughput. Ultimately reducing a cost barrier to research and implementation of this ligand for industrial application. Specifically, the methodology utilises flow chemistry, automation, online analysis, and machine-learning algorithms to automate the optimisation of chemical space, this methodology is also applicable to other relevant ligands like the diamides or variations of DEHiBA. Four synthetic routes were optimised in this work with litres of crude DEHiBA manufacture

accessible for <£65 per litre at the time of publishing with a throughput of 15 kg L^{-1} h^{-1}, with other synthetic conditions capable of >70 kg L^{-1} h^{-1}. A purification route for the crude DEHiBA was devised and optimised to yield a product purity >99.9% in just two steps with a yield of 97% from start to end. The complete manufacture platform therefore requires at a minimum four pumps, one tubular reactor, two continuous stirred tank reactors and two coalescing separators to achieve this via two telescoped operations to yield pure DEHiBA on demand with >97% yield.

DEHiBA manufactured in this work was verified for its uranium extraction performance against literature and commercial sources, demonstrating comparable performance for the extraction of uranium(VI). The extraction of uranium(VI) was further investigated with DEHiBA, varying the ligand concentration and purity, the ratio of organic to aqueous phase and nitric acid concentration for the extraction of 0.10 M uranyl nitrate, demonstrating optimal performance with 5 M nitric acid and at least 10% extraction efficiency improvements when using 1.5 M DEHiBA instead of the typical 1.0 M DEHiBA associated with the GANEX process. A range of organic : aqueous phase ratios were also compared to see how the throughput of uranium affects the extraction efficiency of uranium(VI), identifying minimal extraction efficiency losses (5%) in exchange for a four-fold increase in throughput when using 1.5 M DEHiBA and 5 M nitric acid. These studies support the process intensification of uranium(VI) extraction with DEHiBA, comparing extraction efficiency and uranium throughput. Throughout these studies, temperature was identified to be an overlooked variable in the literature that requires future attention due to its influence on the exothermic extraction of uranium.

III. Contents

IV. List of Figures

V. List of Tables

VI. List of Schemes

VII. Abbreviations

BOAEI – Bayesian optimisation with adaptive expected improvement

CHON – Carbon, hydrogen, oxygen, and nitrogen

CMP – Carbamoyl methyl phosphonates

CMPO – Carbamoyl methyl phosphine oxides

CSTR – Continuous stirred tank reactor

DGA – Diglycolamide

DoE – Design of Experiment

EXAm - Extraction of americium

FPs – Fission products

GANEX – Grouped actinide extraction

GCIPR – Green Chemistry Institute Pharmaceutical Roundtable

GDF – Geological disposal facility

GENIORS - GEN IV Integrated Oxide fuels recycling strategies

HAR – Highly active raffinate

HLW – High level waste

iSANEX – innovative selective actinide extraction

LHC – Latin hypercube

MAs – Minor actinides

MOX – Mixed oxide

OVAT – One variable at a time

PFR – Plug flow reactor

PTs – Partitioning technologies

PUREX – Plutonium Uranium Reduction Extraction

RME – Reaction mass efficiency

SACSESS – Safety of Actinide Separation Processes

SNOBFIT - Stable Noisy Optimisation by Branch and FIT

STY – Space-time yield

TS-EMO – Thompson sampling efficient multi-objective optimisation

EDC - 1-ethyl-3-(3-dimethylaminopropyl)carbodiimide

CDI - carbonyldiimidazole

DCC - dicyclohexylcarbodiimide

T3P - *n*-propylphosphonic acid anhydride

HATU- (1-(bis(dimethylamino)methylene)-1H-1,2,3-triazolo(4,5-b)pyridinium 3-oxide hexafluorophosphate

PyBOP - benzotriazolyloxy-tris[pyrrolidino]-phosphonium hexafluorophosphate

Chapter 1: Literature Review

As the nuclear industry enters a renaissance where the world looks to it for solutions to the climate crisis, the sustainability of nuclear fission must be ensured and improved. Although nuclear energy has a low carbon footprint,[1] the fuel, uranium is a finite resource that should be managed and recycled to maximise its energy potential and minimise this threat to the long-term viability of this technology.[2] Hydrometallurgical nuclear reprocessing offers a solution to improve the sustainability and extend the supply of nuclear fuel.[3–5] Nuclear reprocessing is at present practiced on the industrial scale most notably in France, however the current technology, PUREX (Plutonium Uranium Reduction Extraction) is outdated and cost-intensive extracting both uranium and plutonium inciting proliferation concerns.[6] Replacement and complementary reprocessing technologies have been under development for decades to ensure their robustness prior to industrial implementation.[7–14] These next generation technologies primarily utilise organic ligands as extractants to selectively partition radionuclides from the irradiated nuclear fuel. These processes facilitate the selective recycling of elements primarily the actinides and lanthanides for reuse,[7] with the possibility of fabricating more nuclear fuel, and in the future the recovery of rare elements like the platinum group metals may be feasible to further extend supply.[15]

The organic ligands destined for next generation nuclear reprocessing have undergone thorough testing to ensure their effectiveness and suitability but are yet to be economically viable, an issue that surrounds nuclear reprocessing.[16] However, the literature does not focus on the synthesis and purification of these ligands at any significant scale and to our knowledge there was no literature describing and comparing synthetic routes to these ligands let alone optimising the manufacture of these high value research materials before this project began. This gap in the literature has the potential to limit the appeal and uptake of these technologies on an industrial

scale. The exploitation of flow chemistry to synthesise these ligands on demand in addition to the identification of multiple routes and conditions for their manufacture will enable cheaper and wider access to these ligands aiding to overcome cost barriers to research in this field.

1.1. Nuclear Reprocessing

The UK has declared that nuclear fission will play a pivotal role in the effort to reach carbon neutrality by 2050.[17] This emphasises the importance of research and development in the nuclear sector, with crucially improvements in the sustainability of this technology needed for long-term deployment of nuclear fission. Nuclear fission reactors are one of the lowest carbon emitting energy resources that mankind has to offer,[18] capable of producing gigawatts of electricity daily in a space efficient manner compared to renewables like wind turbines that require orders of magnitude more space to achieve similar power outputs.[19] Unfortunately however, nuclear fission is financially demanding, traditionally entailing long build times and generating long-lived radiotoxic waste.[20–24] The most infamous of which is irradiated nuclear fuel (sometimes referred to as spent/used nuclear fuel), a high-level waste (HLW) that requires careful highly specialised management. Despite its name 'spent' nuclear fuel is not entirely spent, containing a large majority of the periodic table, withholding many valuable elements that are in short supply, thus can be valued as a resource due to its rich composition. Typical compositions contain (**Figure 1**) 95-96% uranium,~1% plutonium,~0.1% minor actinides (MAs), and the remaining elements are the fission products (FPs).[25] In current commercial reactors, nuclear fuel is replaced every 18-36 months due to the conversion of uranium-235 into fission products and transuranic elements hindering the fuels efficiency. Of the 415 reactors globally in 2024, 10,000 metric tons of heavy metal (tHM) are unloaded each year, all of which must be managed safely.[26]

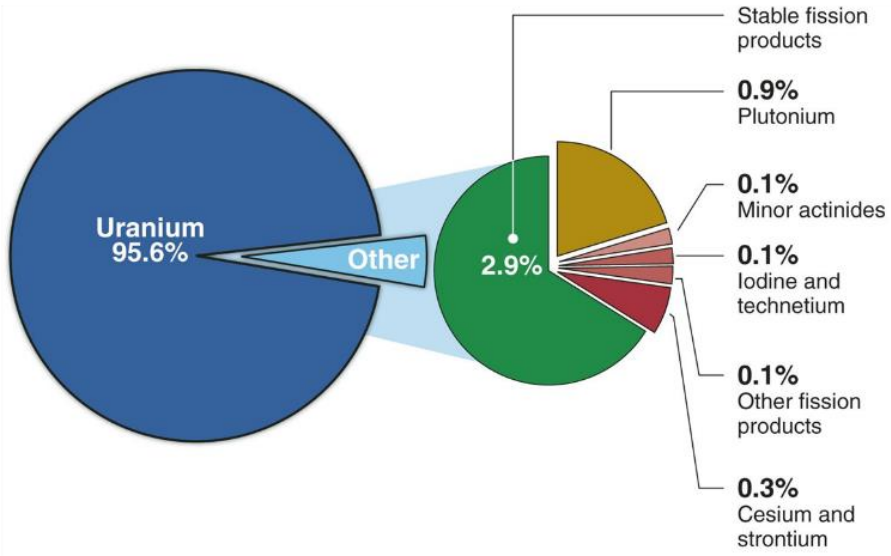

Figure 1: Typical irradiated nuclear fuel composition.[25]

The management of irradiated, high-level waste is a demanding task. The UK alone had 4.56 million cubic metres in 2019 of radioactive waste (not just irradiated nuclear fuel) in interim storage.[27,28] Any shortcuts when managing nuclear waste, particularly high-level waste could lead to disaster. The complexity of this task is due to the extreme radiotoxic nature of the irradiated fuel, the most immediate radiological concern with regard to the fuel is the radioactive decay of short-lived species resulting in deadly amounts of radiation. Cesium and strontium are particularly challenging FPs that emit beta and gamma radiation which generates significant amounts of heat. Transuranic elements such as plutonium and the minor actinides are most troublesome over a longer timeframe, accounting for most of the long-lived radiotoxicity, making safe, long-term disposal challenging as thousands of years of safe storage are needed before these elements are considered radiologically safe.[29]

At present there are two primary options for the management of irradiated nuclear fuel. Currently, the preferred method in the UK and many countries globally is direct disposal (the open fuel cycle); here, the irradiated nuclear fuel is securely packaged and relocated to a geological disposal facility (GDF) deep underground.[30] This creates a large barrier between the waste and the

biosphere in case of a breach in containment. However, a GDF must be able to guarantee safe storage of the irradiated nuclear fuel until the radiotoxicity is no longer a problem. Such a guarantee is incredibly difficult, if not impossible for roughly 200,000 years, the timespan that irradiated nuclear fuel remains more radiotoxic than natural uranium ore (**Figure 2**).[31]

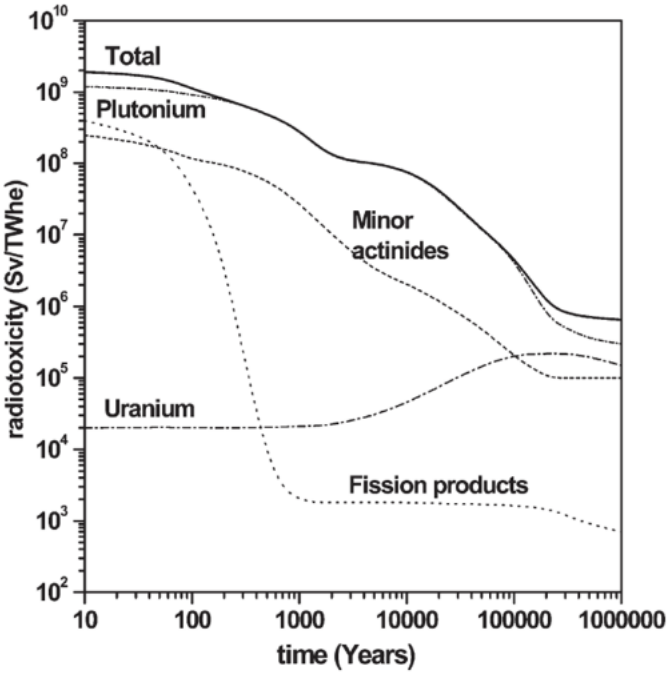

Figure 2: Comparison of irradiated nuclear fuel radiotoxicity (Total), broken down into minor actinide, uranium, plutonium and fission product radiotoxicity.[31]

Alternatively, nuclear reprocessing is a waste management option which can close the fuel cycle, improving sustainability, and can be used in conjunction with geological disposal. Reprocessing is the practice of partitioning the elements within irradiated nuclear fuel ready for recycle or disposal. Reprocessing utilises irradiated nuclear fuel as an asset that holds a wealth of materials that can be reused to generate more sustainable energy production, whilst other elements could be fed back into the economy to improve supply chains, this would improve energy and resource security, a topic of great interest at present, whilst opening avenues for nuclear medicines like targeted alpha therapy, instead of viewing irradiated nuclear fuel as a waste. To generate more sustainable energy and maximise the energy potential of uranium fissionable and fissile actinides

from irradiated fuel can be reused and fabricated back into nuclear fuel (although this does have many challenges). By recycling uranium, nuclear fission via uranium-235 will be feasible for future generations as without this uranium is a finite resource. In addition to the sustainability that reprocessing offers, the long-term radiotoxicity of irradiated nuclear fuel can be reduced for safer waste management, minimising waste volumes destined for the GDF and hence the cost of the GDF.

Figure 3: A simple illustration of the back end open and closed fuel cycles.

Despite reprocessing improving sustainability and extending the supply of resources, it is a more complex task compared to direct disposal, adding cost to nuclear programs and increasing risk.[32] In France it is estimated that reprocessing increases the cost of nuclear energy by around 5.5% compared to direct disposal (year 2000), although this is sensitive to the cost of fresh uranium ore for fuel manufacture.[33] Despite this cost burden France continues to reprocess and recycle its nuclear fuel with plans to continue this into the future. The selective extraction of elements from irradiated nuclear oxide fuel, has historically been achieved via liquid-liquid extractions. Here the irradiated nuclear fuel is dissolved in an aqueous nitric acid phase, this is then contacted with an organic phase comprised of a water immiscible solvent and an extractant such as an organic chelator to partition specific elements into the organic phase. The current industrial standard for reprocessing globally is the PUREX (Plutonium Uranium Reduction Extraction) process, a mature technology that has been used industrially since the late 1950s.[34] This process enables both plutonium and uranium to be recovered from the irradiated nuclear fuel, largely reducing the long-term toxicity of this waste (**Figure 4**).[35,36] The removal of these

radionuclides from the irradiated nuclear fuel reduces the volume of HLW destined for a GDF by ~80%, a reduction in radiotoxicity by ~90%, and a lower heat output from the waste.[37,38] A GDF is still essential for the highly active raffinate (HAR) waste stream from PUREX or other reprocessing technologies containing residual radionuclides like the MAs. Ultimately, reprocessing via PUREX results in a reduction of the storage cost for a GDF by 75%.[38,39] However, advanced reprocessing technologies like i-SANEX (innovative selective actinide extraction), AMSEL (americium selective separation) and GANEX (grouped actinide extraction) can reduced the burden on GDFs further via removal of a greater number of actinides/long-lived radionuclides, lowering the radiotoxicity and thus the required safe storage time of the waste destined for a GDF (**Figure 4**).[12,13,40–44]

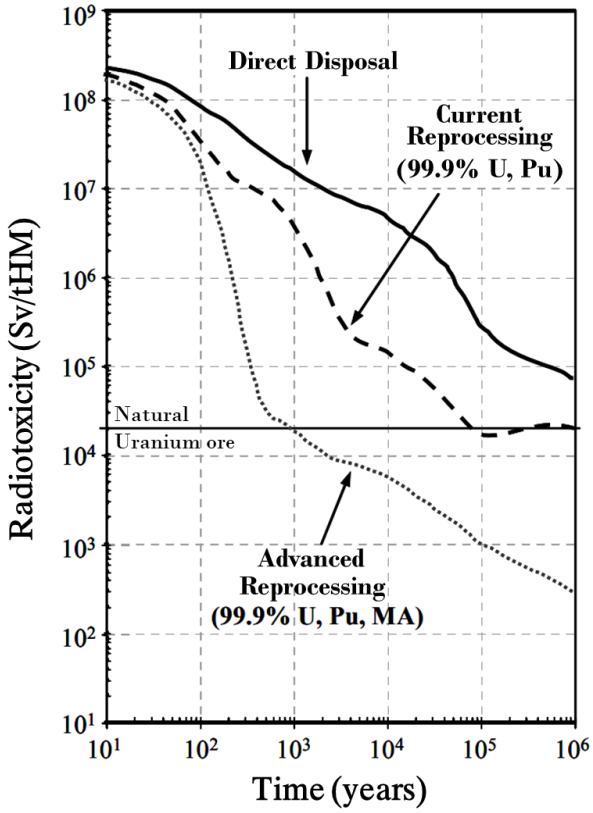

Figure 4: A comparison of the radiotoxicity of irradiated nuclear fuel/high level waste with and without different reprocessing technologies, illustrating which radionuclides are removed.[45]

In comparison to reprocessing, GDFs are immature technologies and there are no *fully* operational sites in existence today, therefore costs can only be estimated and likely an

underestimate.[30] Continued research to improve the PUREX process (**Figure 5**) and make reprocessing more appealing is ongoing and has been for decades. These new processes are referred to as advanced partitioning technologies (PTs) or next generation reprocessing flowsheets/technologies. Most of these PTs have been developed to remove more of the long-lived radionuclides from the irradiated nuclear fuel than PUREX currently offers, with focus on the MAs, namely americium. This feat would remove all the transuranic elements from irradiated nuclear fuel reducing the safe storage time of HLW to a more predictable and manageable figure in the hundreds of years. The underpinning goal of research into these technologies is to develop functional processes that are robust, well understood and economically viable. Without this, implementation on the industrial scale is insurmountable, especially due to the potential hazards involved. Efforts to minimise the complexity of these processes is continuous, with constant refinement of ligands to improve separation factors between extracted radionuclides and minimise the number of ligands used in the process.

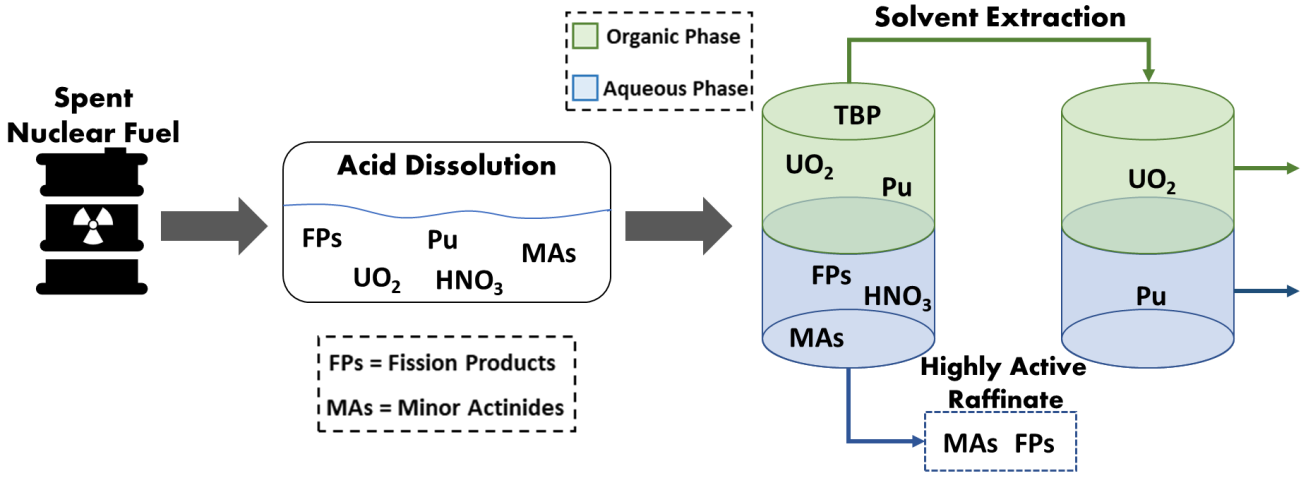

Figure 5: A simple illustration of the PUREX process.

As mentioned, organic ligands are fundamental to the success of hydrometallurgical PTs. The ligands used in nuclear reprocessing are referred to as extractants because they selectively chelate to certain species in irradiated nuclear fuel by exploiting their affinity toward different ions.[46] This process typically takes place via a liquid-liquid extraction, whereby the irradiated nuclear fuel is

dissolved in nitric acid before it is contacted with the organic (sometimes referred to as solvent) phase containing an extractant (**Figure 5**). PUREX employs the ligand tri-n-butyl phosphate (TBP) (**Figure 6**) to selectively chelate to ions in the +IV and +VI oxidation state, so uranium and plutonium are extracted, partitioning them to the organic phase for subsequent isolation.[47]

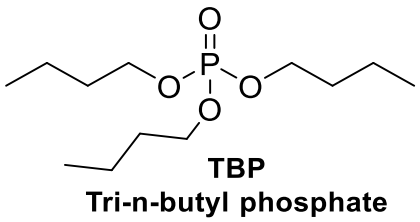

Figure 6: The chemical structure of tri-*n*-butyl phosphate (TBP).

TBP and nitrate ions typically form the following organic soluble complexes: $[Pu(NO_3)_4 \cdot 2TBP]$ and $[UO_2(NO_3)_2 \cdot 2TBP]$ (**Figure 7**), as these complexes are soluble in the organic phase, the plutonium and uranium are partitioned/extracted from the irradiated nuclear fuel in the aqueous phase.[48] By recycling uranium and plutonium, further exploitation of the energy potential from these materials is possible, thus expanding the lifetime of this energy dense resource.[49] The next generation of PTs in development use novel, specialised ligands to facilitate the extraction of trivalent f-block elements from irradiated nuclear fuel where the PUREX process targets hexa- and tetravalent f-block elements. For these ligands to be successful they must be effective at extracting specific nuclides, yet economically viable if the process is to succeed. If not, then the PT will likely be infeasible with cost barriers to research, industrial scale-up and implementation.

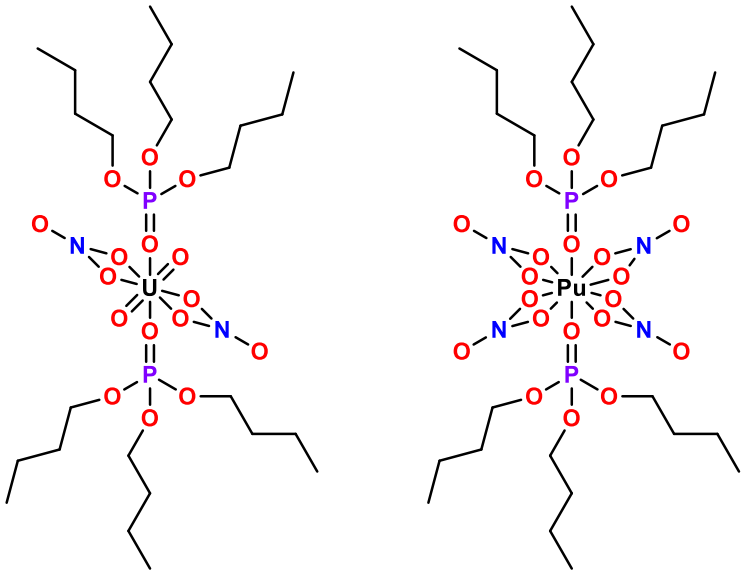

Figure 7: Two-dimensional complexation structures of TBP and NO_3 to uranium and plutonium.

One way to improve the economic viability of these ligands is through synthetic optimisation. Any metric can be optimised for a given reaction such as cost, purity, yield and throughput.[50] Often, however, the optimisation of one process metric negatively impacts another. For example if the kinetics of a reaction are slow then maximising throughput will likely hinder yield or cost metrics. Therefore, optimisation often requires a balance of process metrics to find an overall optimum.[51–53] A simple way to reduce product cost would be to find conditions that minimise cost per mole of product formed, however this could lead to lengthy reaction times and unwanted by-products, this could be avoidable by optimising multiple objectives and sacrificing some cost or assessing other synthetic routes. Prior to this work there was little to no literature investigating the synthetic optimisation of the promising ligands for nuclear reprocessing. Any literature that mentions the synthesis of these ligands typically details unrefined small scale reaction conditions to make small volumes of these ligands for testing purposes.[54–56]

As reprocessing is already an expensive area within the nuclear industry, whilst being a niche area of the chemical industry, there are few chemical vendors for these highly capable molecules. The specialised nature of these materials means that applications outside this field are limited and

thus supply is low, whereas TBP has a demand outside of nuclear reprocessing with uses in emulsions, paints and adhesives, thus is a lower cost chemical commodity due to global demand.[57] This limits the amount of research into these ligands, especially volume intensive pilot plant testing, whilst negatively impacting the economics of a next generation reprocessing facility. Further research into the synthesis of such molecules hopes to remove cost barriers to research with these important ligands whilst potentially making reprocessing of nuclear waste a more appealing route globally.

1.1.1. Disadvantages of Current PUREX Practices

Current reprocessing practices via PUREX are imperfect with ample opportunity to improve on this process by overcoming various disadvantages faced such as:[58]

- Higher proliferation risks than direct disposal due to isolation of plutonium.[59]
- Increased risk of radiation exposure to workers and the environment compared to direct disposal especially the highly active raffinate.
- Larger volumes of intermediate and low-level wastes.[60]
    - Non-CHON (purely carbon, hydrogen, oxygen, nitrogen containing) ligand so is not completely incinerable adding to waste volumes.
- Higher costs than those predicted for direct disposal.
- Degradation of TBP to hazardous and interfering materials.[61]
- Redox reliant process adding complexity.

For an advanced PT to supplant PUREX these technologies should address as many of these disadvantages as possible without compromising the advantages of PUREX that include the use of a single ligand, and maintaining or improving separation factors and distribution ratios achieved by PUREX. All these metrics are a fine balance and slight reductions in metrics like distribution ratio may be acceptable if other disadvantages are overcome.

One way to manage the proliferation risk posed by PUREX is to recycle plutonium into nuclear fuel, otherwise known as mixed-oxide (MOX) fuel as per the French closed fuel cycle.[62] Plutonium recycling reduces the volume of plutonium in storage but can add risk if the plutonium needs to be transported between secure facilities. Unfortunately, MOX fuel is not interchangeable with regular uranium dioxide fuel so manufacturing plants and reactors require modifications to accommodate MOX. A major challenge and cost when manufacturing MOX fuel is the automation required due to the higher radiation levels. These challenges are major driving forces behind the choice to store plutonium instead of recycling it. To overcome these problems, coextraction of plutonium with other elements like uranium or the MAs can be adopted. The COEX (an adaptation of the PUREX process but uranium and plutonium are coextracted and coprecipitated) process is an example of a reprocessing technology similar to PUREX but instead isolates uranium with plutonium.[63,64] Looking further forward, the GANEX (Grouped Actinide Extraction) processes are advanced PTs that enable the coextraction of plutonium with the MAs.[65]

Though PUREX vastly reduces the volume of HLW destined for a GDF, this process increases the volume of other radioactive wastes.[60] These wastes, although less radiotoxic than irradiated nuclear fuel or the HAR still require specialist disposal which incurs other complexities, risks, and costs, often requiring disposal through immobilisation within cement,[66] a material notorious for its negative environmental impact,[67] therefore, this negatively impacts the carbon footprint of nuclear energy. It is difficult to overcome the generation of other radioactive waste with advanced PTs, however most attempt to minimise secondary wastes by using completely incinerable, CHON ligands. As carbon, hydrogen, oxygen, and nitrogen (CHON) are completely incinerable elements, whereas phosphorous is not, disposal of TBP is challenging and is considered a secondary waste. The GANEX process has developed processes that utilise completely incinerable ligands, even replacing TBP with a CHON based ligand, *N,N*-di-(2-ethylhexyl)isobutyramide (DEHiBA). Where

most advanced PTs build on the PUREX process and therefore still employ TBP in the first cycle GANEX is independent of PUREX (**Figure 8**). **Figure 8** illustrates the advanced reprocessing technologies that are detailed in the SACSESS report,[7] detailing the hydrochemical and pyro reprocessing technologies that are promising for use on irradiated nuclear fuel. PUREX is the first step to many of the advanced hydrochemical PTs, which then treat the aqueous raffinate from the PUREX process containing the FPs and MAs. There are a couple of alternative hydrochemical processes that do not rely on PUREX, those being GANEX and ARTIST. These alternative technologies replace TBP with CHON based ligands, minimising secondary waste volumes due to their complete incinerability.

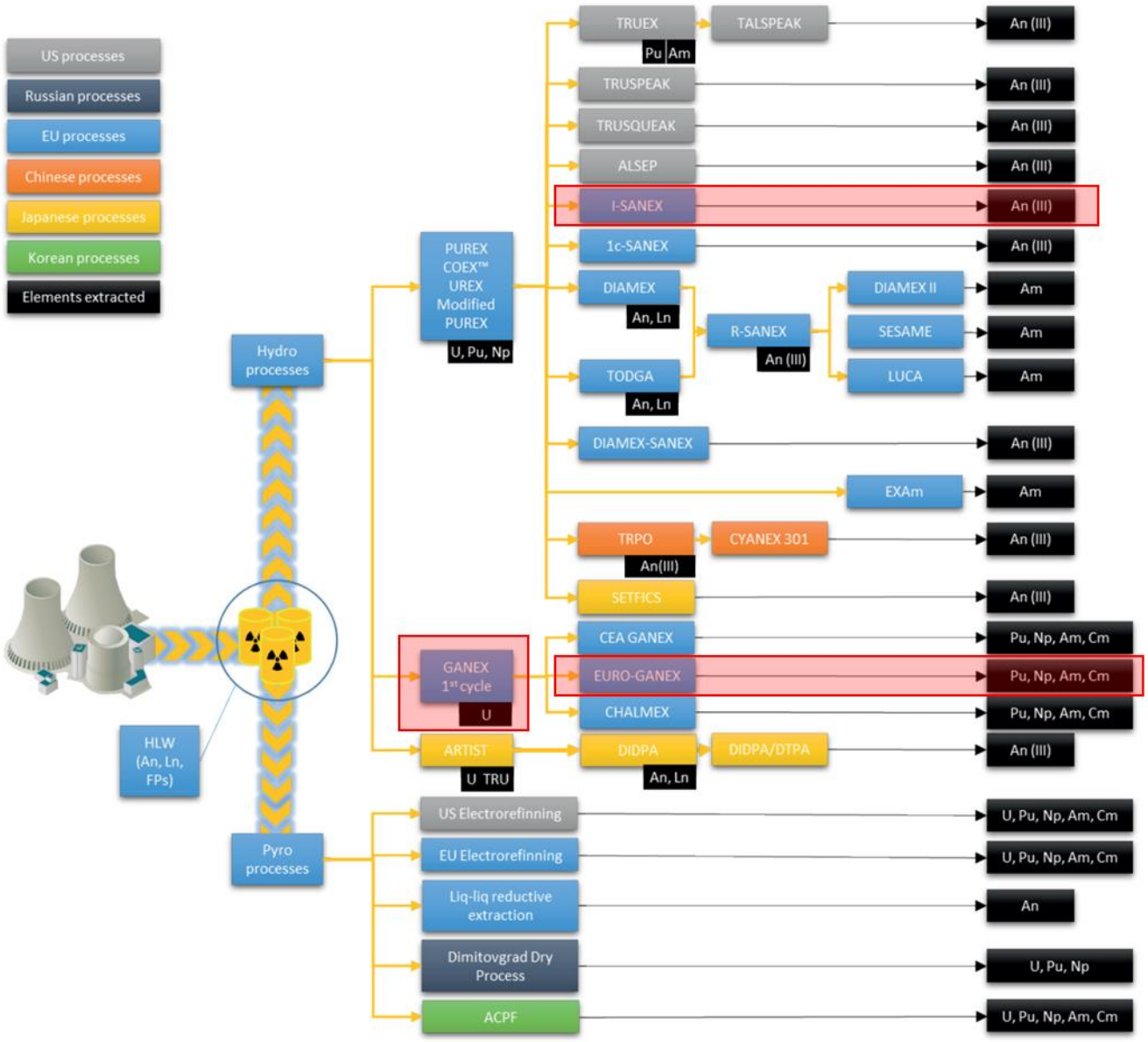

Figure 8: An overview of advanced partitioning technologies detailed in the SACSESS report.[7] The processes highlighted in red are of interest to this project.

The economic viability of reprocessing is a major drawback of this technology and often leads to open fuel cycle policies. Several studies have assessed the financial impact of reprocessing by estimating the cost of both the open and closed fuel cycles.[68–72] many factors and estimations are taken account in these studies, yet most conclude the open fuel cycle to be more cost effective despite the uncertain costs associated with a GDF and the wealth of material in used nuclear fuel that could improve the economics of nuclear reprocessing. This is due to the closed fuel cycle

requiring more steps, the continuous research that spans over decades, bespoke highly sophisticated and secure facilities, and tonnes of resources to achieve this feat of chemistry and engineering. To top this off, the need for a GDF still exists with the PUREX process and most PTs due to the HAR and secondary wastes, likely including decommissioning of the reprocessing facility. Unfortunately, for most nations, the cost and added complexity/risk outweighs the sustainability therefore, an open fuel cycle is adopted. Despite this, fissionable materials are finite resources and there will come a time when nuclear fission becomes unfeasible without recycling, therefore work is needed to improve uptake of this technology and the economic viability of the closed fuel cycle.

Unlike geological disposal, reprocessing is a mature technology that has received real-world experience, research and improvements over decades, resulting in improved understanding of the technology and proof of concept with the potential for cost reductions with iterative or next generation reprocessing facilities.[49,72] GDFs on the other hand are first of a kind technology, therefore costs are estimations with large errors. As with any first of a kind technology, complications are common and are likely to escalate the cost of these megastructures. Therefore, it is likely unfair to dismiss reprocessing as a waste management solution due to economics alone.

The radiotoxicity/composition of the HAR from PUREX is the focus of improvement for most PTs, as once this waste is vitrified it remains highly radiotoxic for over 100,000 years (**Figure 4**), an incomprehensible amount of time for civilisation.[73] The HAR comprises of mostly fission products (FPs and Mas), the FPs are less problematic, most have relatively short half-lives and account for most of the early-stage radioactivity and heat generation, whereas the MAs have longer half-lives causing most of the long-term radiotoxicity. Therefore, by partitioning and then transmutating the MAs, the safe storage time for the remainder of the waste reduces to ~1,000 years or less (**Figure 4**).[31] Removal of the MAs requires ligands with an affinity to trivalent f-block

elements due to this being the preferred oxidation states of americium and curium. To add complication the majority of the lanthanides are trivalent, thus are typically extracted alongside americium and curium.[74–77] Caesium-137 and strontium-90 are two of the long lived FPs that largely account for the remainder of the safe storage time after the MAs have been removed, therefore, the selective removal of these isotopes would further reduce the safe storage time although the current focus in this field lies in MA removal.[78] In summary the removal of all long-lived radionuclides from the HAR is possible with advanced PTs and promises to deliver a more realistic and manageable timeframe for the storage of HLW.

It is clear why the removal of long-lived radionuclides from irradiated nuclear fuel has been a primary driver behind the development of advanced PTs over the last 30+ years.[11] Many options have been developed over that time to overcome the weaknesses of the PUREX process, with work continuing to improve these processes for the next generation of nuclear reprocessing facilities to adopt. These technologies can work alongside PUREX to further improve reprocessing and make use of existing facilities, or can replace PUREX entirely working with entirely CHON ligands such as the GANEX process (**Figure 8**). To date these advanced PTs are not deemed industrially ready, with more hot tests required for some processes however further literature is needed to optimise and understand these processes to prepare the required hot tests. Of course, the risk and cost of hot tests is restrictive, however a base understanding of simplified and mock systems in preparation of such tests is paramount and beneficial to all in the field.

1.1.2. Advanced Partitioning Technologies

Partitioning is the chemical separation of elements.[31] in a nuclear context this mostly focuses on the separation of actinides from FPs. To achieve this, a majority of PTs act as additional steps

after PUREX to partition the MAs from the PUREX HAR. Whilst others like GANEX remove the need for PUREX and TBP. It is envisioned that PTs will not work alone, after the waste has been partitioned the long-lived species will be transmuted, potentially in advanced fission reactors in an effort to reach net zero carbon. For this to be successful, it is imperative that elements with large absorption cross-sections are not extracted with these fuels, such as curium and lanthanides like gadolinium as this will negatively impact transmutation in fast reactors.[79–81]

Transmutation is the conversion of one element into another,[82] thus converting long-lived radionuclides into less concerning species with shorter half-lives.[83] Transmutation of these long-lived actinides can be achieved in advanced nuclear reactors, enabling further exploitation of the untapped energy potential in uranium, thus improving nuclear sustainability. Whereas, any long-lived radioisotopes unsuitable for fission, such as curium, can be transmuted by irradiation in accelerator driven systems.[84] The introduction of partitioning and transmutation (P&T) aims to reduce environmental concerns with nuclear power, improve sustainability, and public perception of nuclear waste, paving the road to new nuclear builds to support a cleaner future.

PTs can be grouped as hydrochemical (hydrometallurgical) processes like PUREX suited for oxide fuels, or pyrochemical (electrometallurgical) processes suited for metal fuels (**Figure 8**).[7] The European Commission has funded numerous projects over the decades to assess the methodology, progress, and technological readiness of these processes through projects such as PATRICIA, GENIORS and SACSESS. This review focusses on hydrochemical processes.

Research into hydrochemical PTs has exploited and tested the selectivity of countless ligand classes such as: carbamoyl methyl phosphine oxides (CMPOs), carbamoyl methyl phosphonates (CMPs), phosphine oxides, phosphates, amides, and diamides (**Figure 9**) amongst others to advance nuclear reprocessing.[85]

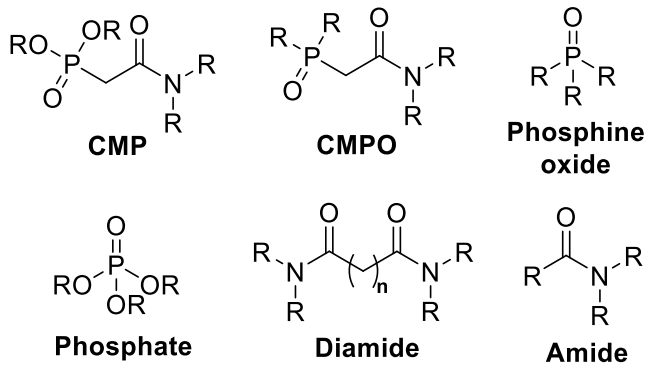

Figure 9: Commonly researched ligand structures for the partitioning of irradiated nuclear fuel

Figure 10 highlights a number of successful ligands identified for advanced PTs as described in the SACSESS report from 2015 (**Figure 10**). This report also showcases the various PT flowsheets that have been developed globally with potential operating conditions and their technology readiness levels (**Figure 8**).[7,14] Not all the ligands detailed are entirely CHON, with some still containing phosphorous, whilst others are sulfonated,[86–88] therefore there are continued efforts to identify CHON conforming replacement ligands.[89,90] As noted, many of the PTs developed build on the existing PUREX process however, GANEX has been developed an alternative technology that first extracts uranium, then the transuranics are coextracted. The replacement of TBP with DEHiBA allows the whole process to be CHON compliant, whilst improving proliferation resistance of this process and alleviating the reliance on redox chemistry. Thus GANEX, overcomes some of the disadvantages associated with PUREX, however lower distribution ratios for uranium and increased technetium uptake has been observed.[41,91–93]

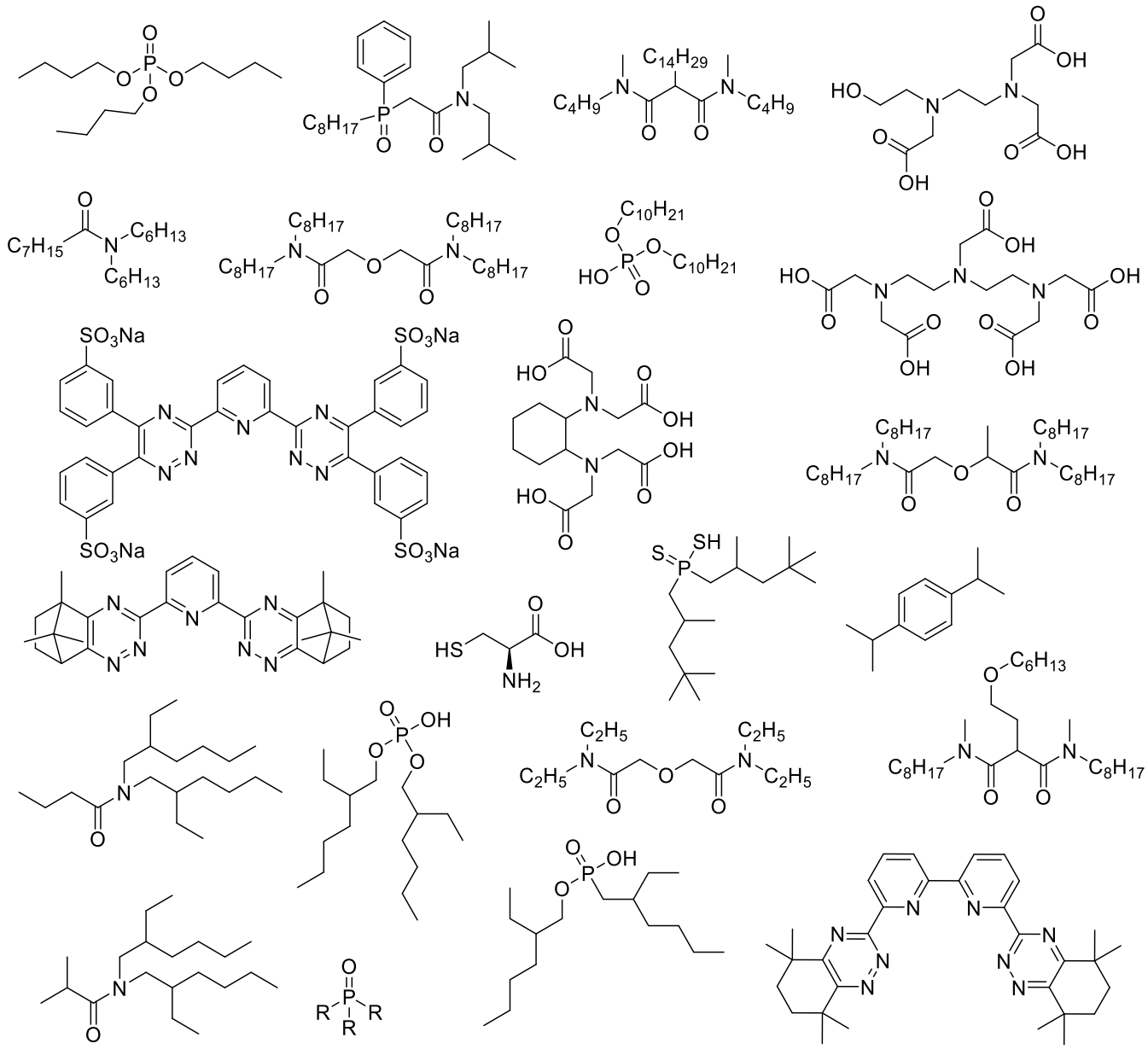

Figure 10: Examples of the diverse range of successful ligands described in the SACSESS report.[7]

Figure 10 highlights a range of molecules that are largely carbon, hydrogen, nitrogen, and oxygen, those that contain phosphorous and sulfur provided unrivalled performance at the time of publishing in 2015.[7] This collection of ligands is small in comparison to the candidates that have been tested for nuclear reprocessing,[55,94–96] with structure playing a pivotal role in controlling the selectivity of these ligands. With many of the successful ligands revolving around an amide bond, this project aims to explore, optimise and compare amide bond formation methodologies on a specific molecule of interest than can be applied to the other ligands.

Following on from the SACSESS project, GENIORS aimed to identify PTs with the least weaknesses to prioritise development, hot testing and implementation. Four priorities were identified to achieve this:[97]

- The behaviour of fission products in these systems
- Radiolytic stability of ligands and any impact of degradation products on the process
- Process related issues such as kinetics, loading, and third phase formation
- Interface between the separation processes with the dissolution and the conversion

Most hydrochemical PTs that extract the trivalent actinides such as americium and curium, rely on a three-step approach:[98]

1) Uranium (and sometimes plutonium) extraction from irradiated nuclear fuel. Here monoxide ligands such as TBP and monoamides offer good selectivity for this extraction.

2) The coextraction of trivalent lanthanides and actinides. Here di- or tridentate ligands like diamides and CMPOs offer excellent extraction for trivalent f-block elements.

3) Separation of the trivalent actinides from the lanthanides, here soft donor ligands are used to selectively extract the actinides free of the lanthanides.[99]

It must be said that PTs are not always three-step processes and although a process may be three overarching steps, each step requires a multitude of stages such as forward extraction, scrubbing, stripping and purification, therefore each of these steps is highly complex and refined. These advanced PTs are still under rigorous investigation to ensure robustness, understanding, and success if industrialised. Test results have been promising for many of these processes especially EURO-GANEX and iSANEX with >99.9% separation of the trivalent actinides from the lanthanides.[40,100–104]

In summary P&T technologies do not eliminate the need for a GDF, instead GDFs can be smaller as the volume of HLW is dramatically reduced, minimising GDF costs whilst maximising the energy potential and wealth in irradiated nuclear fuel. P&T also reduces the environmental concerns associated with the final disposal of HLW by shortening the safe storage time of this waste dramatically.[105] In the future PTs may allow near complete recyclability of irradiated nuclear fuel, supplying diminished natural resources back into the global economy, however for now, the focus lies with removing the long-lived radionuclides.

1.2. Extractant Ligands

Choice of ligand(s) is the major difference between the various hydrochemical PTs in development.[100] Whilst PUREX uses TBP, other PTs rely on alternative ligands (**Figure 9** and **Figure 10**) for their success, with research into novel extractant ligands a key driving force behind the next generation of PTs. These organic ligands preferentially extract ionic species from the irradiated nuclear fuel depending on their chemical and steric structure. Common motifs include amides/diamides, organophosphorus and hybrid ligands, although more complex structures exist with pyridine and triazole motifs.[85] A key characteristic of most is their oxygen donor sites that facilitate chelation to hard metal ions in solution.[85] Oxygen is crucial to the effectiveness of these ligands because actinides are oxophilic, therefore the extraction can selectively partition actinides. The oxophilicity of f-block elements comes from the high charge density (hard nature) of these elements.[106] This strong interaction between oxygen and f-block elements supports the hard-soft acid-base principle.[107–110] By exploiting this property, the f-block elements can be separated from the less charge dense transition metals.

The early actinides are renowned for existing in a diverse range of oxidation states, for example, neptunium can range from +III to +VII, this can be tuned via the nitric acid concentration or by redox chemistry for many of the actinides.[111] Manipulation of the acid concentration is often exploited to avoid extracting unwanted species and enables stripping of nuclides from the organic phase. When irradiated nuclear fuel is dissolved in concentrated nitric acid uranium exists as UO_2^{2+} whilst plutonium exists as Pu^{4+}.[112] For the MAs, neptunium commonly exists as NpO_2^{+} and NpO_2^{2+},[113] whilst americium and curium often exist as Am^{3+} and Cm^{3+} respectively.[114,115] Lanthanides are also preferential to the +3 oxidation state adding complexity to the selective extraction of americium and curium using oxidation state alone. The trivalent actinides are difficult to extract with monodentate ligands, therefore bi- and tridentate ligands have become the focus for trivalent actinide extraction.[116–118] Nitrogen donor ligands have become increasingly popular for the separation of trivalent lanthanides and actinides as their similarity of oxidation state makes separation difficult with a single ligand system. To overcome this, aqueous based ligands (ligands designed to only dissolve in aqueous media not the typical kerosene based organic phases) with nitrogen donor atoms have been developed such as SO_3-Ph-BTP (sulfonated bis triazinyl pyridine, **Figure 11**) to exploit the difference in charge density between the lanthanides and actinides, with softer nitrogen donor atoms favouring the softer actinides for selective stripping.[119,120]

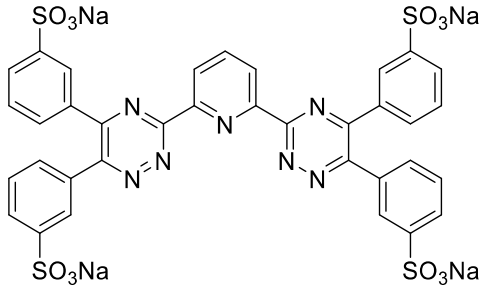

Figure 11: Chemical structure of SO_3-Ph-BTP (sulfonated bis triazinyl pyridine)

Organophosphorus ligands like phosphates (TBP) were one of the first extractants implemented for the reprocessing of irradiated nuclear fuel. They are advantageous due to their ability to preferentially extract actinides over lanthanides and FPs.[85] This is usually because these ligands are monodentate so chelate to MO_2^{2+} and M^{4+} species. The most notorious extractant in this industry is TBP, which succeeded due to the desirable properties that it exhibited for partitioning uranium and plutonium from irradiated nuclear fuel to produce nuclear weapons at the time. These properties include good radiolytic, thermal and chemical stability, low toxicity, low flammability and good extraction efficiency and separation factors for uranium and plutonium.[121]

Nevertheless, TBP has its drawbacks, such as its relatively high solubility in the aqueous phase,[122] and troublesome degradation products produced by hydrolysis or radiolysis leading to dibutyl phosphate and monobutyl phosphate. These degradation products are toxic and add complexity to the stripping stages when present,[123,124] they therefore reduce the overall extraction efficiency whilst increasing the tendency toward third phase formation. To overcome these limitations various organophosphorus ligands have been developed and tested for nuclear reprocessing.[85] Such chemistries include phosphine oxides, other phosphates and CMPOs. This review does not discuss organophosphorus ligands in detail as many organophosphorus ligands have been tested and this is not the target for this project. Many organophosphorus ligands demonstrate great promise, but all have the same limitation, their inability to completely incinerate after use, generating secondary contaminated waste. This disadvantage adds more steps and costs to reprocessing which can be overcome by use of entirely CHON containing molecules.

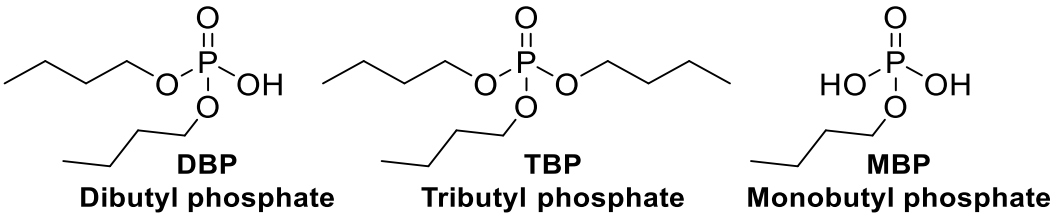

Figure 12: Chemical structures of TBP, and its troublesome degradation products dibutyl phosphate and monobutyl phosphate

In 1960, T. H. Sidall suggested *N,N*-dialkylamides as replacement extractants for TBP,[125] due to improvements over TBP as most were less soluble in the aqueous phase, less prone to hydrolysis, radiolysis, and oxidation. Despite these findings, Sidall was keen not to move away from organophosphorus ligands and published his findings on CMPs.[126] These hybrid ligands had their own degradation problems but were capable of extracting the trivalent actinides, proving the effectiveness of the amide group at chelating to the actinides and the affinity of bidentate ligands for trivalent species.[127]

Amide-based ligands such as the monoamides, diglycolamides, and malonamides have proven to be effective extractants, overcoming limitations faced by organophosphorus ligands.[128] The ligands in question are entirely CHON containing, therefore are entirely incinerable whilst also providing other favourable properties for nuclear reprocessing. Due to the prevalence of amide-based ligands among advanced PTs it is incredibly likely that the following ligands will see industrial use in the future.

1.2.1. Monoamides: Extractants for Hexavalent and Tetravalent Species

Although chemically simple, monoamides are highly effective ligands for the extraction of tetra- and hexavalent species like uranium and plutonium,[129–131] this extraction can be tailored via the structure of the alkyl groups to achieve desired separation factors. DEHiBA, *N,N*-di(2-

ethylhexyl)isobutyramide (**Figure 13**) is a specialised monoamide ligand used in step 1 of the GANEX process for the selective extraction of uranium.[132–135] The GANEX process recovers 99.9% uranium at a high purity, then coextraction of the transuranic elements ensues via more complex multidentate ligands. The initial separation of uranium simplifies any future transmutation of these materials and reduces proliferation risks.[10] Alternatively, DEHiBA has received recent attention in the US for high assay low enriched uranium (HALEU), removing reliance on Russia for valuable resources.[91,92]

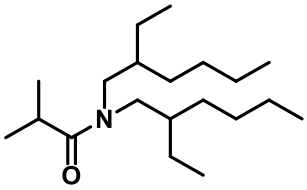

Figure 13: Chemical structure of *N,N*-di(2-ethylhexyl)isobutyramide, DEHiBA

As DEHiBA extracts uranium, GANEX has the potential to replace PUREX entirely, alternatively *N,N*-di(2-ethylhexyl)butyramide DEHBA can be used to extract uranium and plutonium due to its marginal difference in structure, if plutonium extraction is desirable. As these monoamides are compatible with nitric acid, whilst providing a good resistance to radiolysis and hydrolysis they are well suited for nuclear reprocessing.[136] DEHiBA's selectivity toward uranium is reliant on the oxygen donor atom but is heavily influenced by its alkyl groups. Modification of the branched isobutyl group to a linear butyl group, DEHBA, reduces the separation factor between uranium and plutonium facilitating the extraction of uranium and plutonium. Additionally, DEHBA demonstrates improved extraction efficiency for uranium compared to the more branched DEHiBA as it is less hindered.[137,138] As the extraction efficiency for uranium decreases when switching from DEHBA to DEHiBA so too does the extraction efficiency for plutonium, but to a greater extent, therefore, DEHiBA is more selective toward uranium alone making it the ligand of choice for GANEX.

DEHiBA addresses and overcomes many of the flaws with TBP, these include: TBPs inability to incinerate at end of life leading to large volumes of secondary low-level radioactive waste, the generation of degradation products that decrease the stripping efficiency of TBP, and third phase formation at high metal loading. These advantages make DEHiBA an attractive alternative, yet a strong driving force is necessary for the nuclear industry to adopt such a change as new facilities will be needed for this process and a multitude of hot testing is likely needed. It is imperative that work in the area of partitioning continues to support and promote this advancement in nuclear waste management. The simplicity of DEHiBA's structure is improves its chemical stability but also improves feasibility for large-scale, low-cost manufacture. This helps drive down the cost of nuclear reprocessing.

Due to the diverse structures of monoamides that have been tested and are available (**Figure 14**) it is unlikely that all reprocessing facilities in the future will adopt monoamides, or even the same monoamide.[139] However, the core synthetic step will be the amide bond formation, combining a carbonyl group typically with a bulky secondary amine, especially as many promising amide ligands have limited functional groups aside from the amide bond. The structure will likely be dictated by the process chosen and aims of the fuel cycle, for example GANEX opts to use DEHiBA due to the requirement to selectively extract only uranium in the first step. Whereas some nations/organisations may prefer DEHBA or alternative monoamides due to specific benefits. It is likely that monoamides will be employed in future industrial reprocessing, with specific interest from CEA, similar empirical formulae to DEHiBA can be expected as these medium length alkyl chains (6-8 carbons) have proven most effective in testing.[140] Alternatively, DEHBA and DHOA, (*N,N*-dihexyloctanamide) are direct replacements for TBP, offering improvements over TBP whilst still extracting both uranium and plutonium and may be preferred in some cases.[141] These

promising monoamide replacements for TBP also show potential for neptunium recovery further adding to the benefits that these extractants offer.[142]

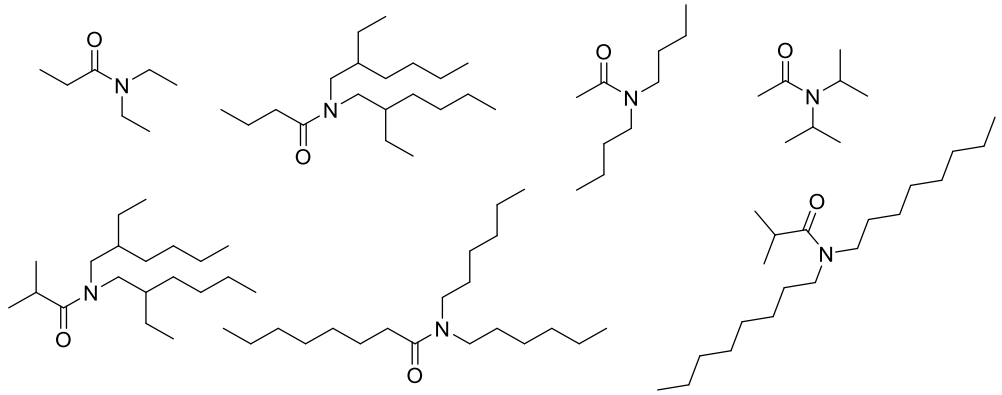

Figure 14: Chemical structures of a variety of monoamides that have been tested for nuclear reprocessing, emphasising the diversity of alkyl groups

The synthesis of DEHiBA and the other monoamide ligands is relatively simple, this is likely why there is little literature on the synthesis of this otherwise thoroughly investigated extractant. Remarkably, there is no literature optimising the synthesis of these monoamide ligands despite the limited availability and relatively high cost of these research materials. Instead, the publications that synthesise these molecules opt to enlist highly reactive (acyl chloride), costly reagents due to their effectiveness at achieving high yields and ease of purification on a small scale.[130] Despite these reagents being readily available on a small scale they are less accessible on a large scale and provide avoidable storage and handling risks in large quantities.[143] Specifically the reagents mentioned are acyl chlorides (**Scheme 1**), often derivatised from carboxylic acids. Not all publications use the acyl chloride, however the majority of the literature refers to procedures that use an acyl chloride starting material.[55,142–145] Acyl chlorides are more expensive than their respective carboxylic acid logically, generate toxic waste gases, and are prone to fast paced exothermic reactions.[146–148] If the an acyl chloride is necessary to synthesise tonnes of ligands it may be more appropriate to synthesise the acyl chloride in situ via a chlorinating agent such as thionyl chloride ($SOCl_2$), which is another highly reactive and toxic reagent (**Scheme 1**).

Although this synthetic route often leads to high product yields, the production of toxic hydrogen chloride and sulphur oxide gases plus challenging anhydrous conditions are essential increasing process complexity and cost. Of course, this route is common practice in the pharmaceutical industry, and is even used in large scale pharmaceutical manufacture,[149] however alternative routes are possible and should be compared instead of defaulting to a route, especially when manufacturing any significant volume of ligand.[150–156] With the technology available today this task can be automated via high throughput screening, although there is a significant cost/equipment barrier to this.[157,158]

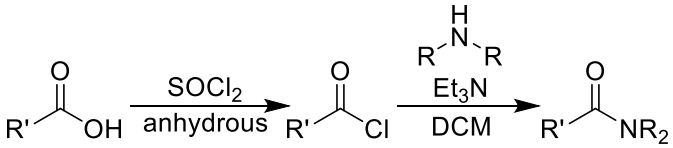

Scheme 1: A commonly published synthetic route to monoamides via an acyl chloride, with an example chlorination step included

There is a plethora of literature describing synthetic routes to amides, with new methodologies published annually. These novel methods often aim to improve environmental metrics and efficiency compared to traditional methods overcoming the need for stoichiometric activating agents that are not atom uneconomical and could be applicable to ligands like DEHiBA.[154] The main uncertainty with moving to these new techniques is that most published methods synthesise secondary amides using primary amines whereas amides of interest to PTs are typically tertiary using more hindered (branched) secondary amines so may not be applicable.[155] An example of this incompatibility is highlighted by CDI (carbonyl diimidazole), a highly effective activating agent that has been widely used for amide synthesis.[150] To its detriment CDI is typically used for secondary amide synthesis as CDI alone struggles to mediate the synthesis of bulky tertiary amides. The literature generally suggests that CDI is ineffective toward bulky secondary amines unless the amine is first combined with CDI and iodomethane.[159,160]

In conclusion, monoamides are promising ligands destined for deployment in industrial reprocessing, a good understanding of their properties has been established where DEHiBA is of most interest to a uranium only extraction such as GANEX 1st cycle or for HALEU. However, more literature is needed to better guide the synthesis of these tertiary amides, providing options and comparison of possible synthetic routes for researchers to pursue and guide estimations of cost for ligands used in economic evaluations of nuclear reprocessing. A host of synthetic routes also provides backup routes in the event that the chosen route becomes unviable due to supply chain shortcomings. Further research into the synthesis of these molecules can reduce barriers to research and the cost of these high cost research materials aiding the transition toward deployment of advanced PTs.

1.2.2. DEHiBA: The Selective Extraction of Uranium(VI)

Whilst DEHiBA has received continued interest for decades for its selective extraction of uranium which has led to the development of the GANEX flowsheet.[92,131] Many process variables have been investigated using DEHiBA to extract uranium(VI) throughout the literature, however it can be difficult to compare extractions due to the number of relevant variables: type/structure of ligand, ligand concentration, metal (uranium) concentration, nitric acid concentration, phase (SA) ratio, and temperature. The difference in uranium/metal concentration between publications often makes comparison between extraction studies challenging,[161,162] with no publications investigating all variables (to our knowledge) and few investigating more than three of these variables. The investigation of all variables would lead to hundreds if not thousands of conditions to be explored when changing one variable at a time to optimise the extraction of uranium(VI). Generally, however trends for each variable can be understood and largely predicted, particularly when using 1.0-6.0 M nitric acid concentrations, a commonly investigated variable. Therefore, models are commonly employed to predict these extractions due to good fundamental

understanding and published data.[92,135] The investigation of temperature and SA ratio has however seen little investigation despite the significant influence of temperature on the exothermic extraction and the ability to influence operational throughput respectively.[94,163] Few publications acknowledge the need to understand the influence of temperature on the extraction of species like uranium, despite the potential consequences of incomplete extraction or coextraction of nuclides. As for throughput, many publications solely investigate a 1:1 SA ratio which is likely sub-optimal in terms of loading the organic phase although the concentration of each phase can be tailored to account for this to some extent.

The majority of accessible data for the extraction of uranium with DEHiBA focuses on lab-scale batch extractions, however many variables have not been investigated in the available literature, potentially resulting in under optimised processes. It would be beneficial to see more of these variables screened and optimised in the literature, not only for DEHiBA but other ligands of interest to better inform the development of processes in the future.

G. B. Hall et al. recently published uranium extraction data using 1.5 M DEHiBA to extract varying concentrations of uranium from 0.1 M up to 1.25 M across 0.1-6.0 M nitric acid concentration. This work aimed to intensify the process of extracting uranium for the purpose of HALEU recovery in the United States. Although 1.5 M DEHiBA has been previously investigated in the literature, uranium concentrations have been very low, often using tracer concentrations and not quoting specific concentrations. These investigations used 1.5 M DEHiBA solutions to maximise uranium(VI) loading of the organic phase, demonstrating benefits in terms of the extraction efficiency over 1.0 M DEHiBA,[125,138,164] finding no issues with third phase formation. The publication mentions potential viscosity restraints for the organic phase but does not provide quantifiable data, only potential problems.[165] Despite the aim to maximise uranium loading in the organic phase, SA ratio was not investigated. Lower SA ratios (using a greater volume of aqueous

phase) would likely achieve higher uranium loading of the organic phase avoiding such high aqueous uranium concentrations that likely have high aqueous viscosity, causing handling or process issues. Additionally, this study refers to loss of performance with elevated temperature,[94] but does not reference the temperature for these extractions, it would be beneficial and interesting to measure these extractions across a range of realistic temperatures, for example 15-40 °C, in addition to monitoring the temperature of the system to see how exothermic these extractions are and whether uranium concentration affects this.

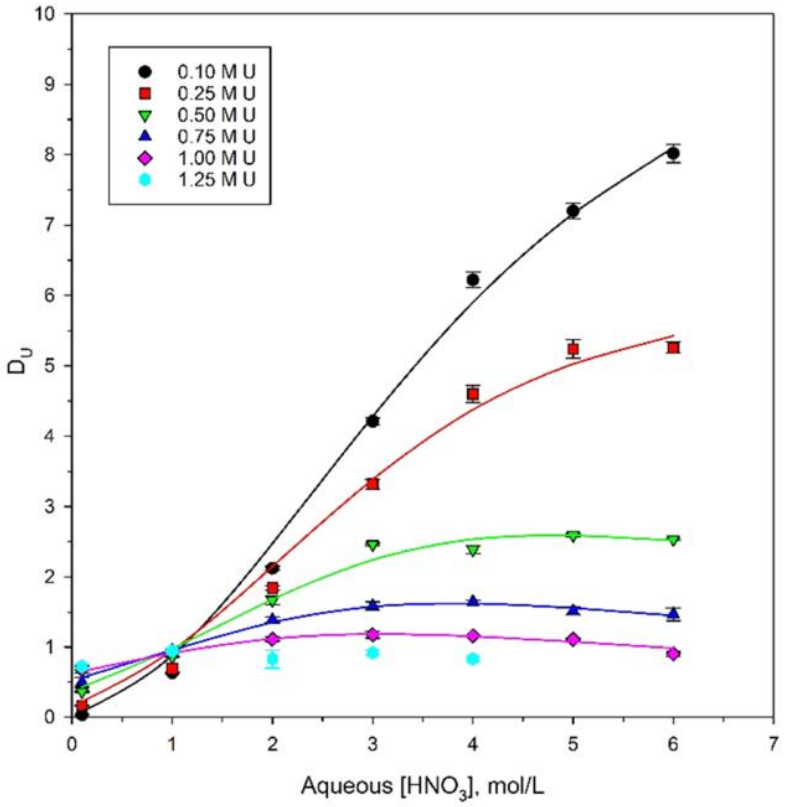

Figure 15: Distribution ratios for uranium(VI) across a range of uranium(VI) and nitric acid concentrations using 1.5 M DEHiBA at a 1:1 SA ratio, taken from G. B. Hall *et al.*[92]

1.2.3. Diamides: Targeting the Selective Extraction of Transuranic Elements

As monoamides typically favour chelation to tetra- and hexavalent metal ions, additional ligands and steps are needed to completely remove all the actinides, particularly curium and americium that typically exist in the trivalent state.[166] EURO-GANEX is one of the promising steps after GANEX 1st cycle for the extraction of plutonium, neptunium, americium, and curium via diamides with 2 or 3 oxygen donor atoms (**Figure 16**) facilitating chelation to a range of oxidation states including trivalent species. As previously mentioned, aqueous holdback/stripping agents are required to avoid the extraction of unwanted species like zirconium and the lanthanides with the actinides.[120]

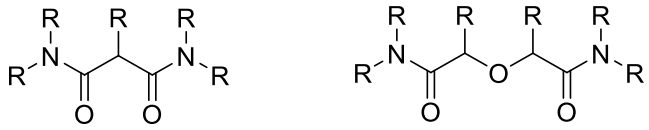

Figure 16: The chemical structure of a malonamide[167] (left) and a diglycolamide[168] (right)

Diamide ligands, most notably malonamides and diglycolamides (DGAs) have generated a lot of attention for their extraction properties in the nuclear reprocessing community (**Figure 16**).[85] Malonamides are bidentate ligands that have shown promise for the extraction of trivalent f-block elements and plutonium.[169] Their success is largely down to their ability to avoid third phase formation in most solvents and in the presence of nitric acid a common issue faced by many ligands that must be avoided in a reprocessing facility.[170]

N,N′-Dimethyl-*N,N′*-dioctylhexylethoxymalonamide (DMDOHEMA) is a ligand used in the EURO-GANEX process to reduce third phase formation whilst increasing Pu loading via its bidentate nature. The ether backbone group largely increases the complexity of DMDOHEMAs synthesis, yet it plays a pivotal role in the organic solubility and resistance to third phase formation.[171]

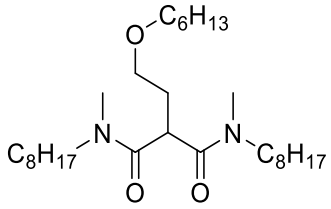

Figure 17: The chemical structure of *N,N′*-Dimethyl-*N,N′*-dioctylhexylethoxymalonamide (DMDOHEMA)

Diglycolamides emerged in the 1990s as another promising diamide extractant technology.[172] These tridentate ligands became renowned for their powerful ability to extract trivalent f-block elements, a crucial discovery for the recovery of americium. Diglycolamides offer better distribution ratios than malonamides for trivalent actinides whilst their tridentate nature reduces the number of ligands per metal ion. The use of malonamides in conjunction with diglycolamides provides an excellent framework for transuranic extraction, as seen in the EURO-GANEX process where *N,N,N′,N′*-tetra-*n*-octyl diglycolamide (TODGA, **Figure 18**) and DMDOHEMA work hand in hand. Although multi-ligand processes can achieve desired process outcomes, the complexity of the overall process escalates over time due to radiation effects on the ligands producing a multitude of degradation products that may have unfavourable interactions. This results in a concentration reduction of the desired ligands which need monitoring and adjusting to maintain performance and selective extraction. Therefore, a simpler system is desirable and constant research aims to achieve this.

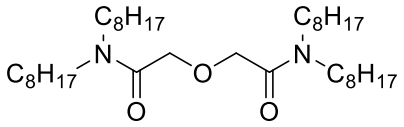

Figure 18: Chemical Structure of *N,N,N′,N′*-tetra-*n*-octyl diglycolamide (TODGA)

Diglycolamides are effective extractants for trivalent actinides and lanthanides in preference to other metal ions such as the transition metals in irradiated nuclear fuel. This is due to their tridentate nature and the hard-soft acid base concept as previously described.[108–110] Similar to the monoamides the diamides extraction properties are highly dependent on the chains bound to the

amine groups of the amide. This has been extensively tested and verified by altering these chains from straight alkyl, to branched alkyl, through to aryl groups.[173,174] To summarise, bulkier, sterically hindered ligands demonstrate reduced complexation ability, compared to shorter chains that provide more effective chelation, and so, higher distribution ratios. Despite this, diglycolamides with short alkyl chains have higher aqueous solubility and are more prone to third phase formation, therefore a balance between short and long alkyl chains is needed to be optimum. Aryl groups were not found to be as suitable, therefore, the most promising diglycolamide was identified as TODGA (**Figure 18**) as the medium length alkyl groups provide well balanced properties.

Nevertheless, TODGA is not a perfect ligand, foremost it has reduced extraction efficiency to improve its solubility, however there are other diglycolamides of interest that are utilised across different advanced PTs. Two of which have modified alkyl groups, whilst the other possess a slightly modified backbone (**Figure 19**). The first to mention is TEDGA, *N,N,N',N'*-tetraethyl diglycolamide, a water soluble diglycolamide used as a 'hold-back' reagent for similar motivations to SO_3-Ph-BTBP however in this case preferentially chelating to the lanthanides not the trivalent actinides. TEDGA is used in the EXAm (extraction of americium) process and is present in the aqueous phase to hinder the extraction of unwanted lanthanides into the organic phase for selective americium extraction, beneficially this hold back reagent is CHON compliant however the organic extractants are not.[73] Alternatively, T2EHDGA, *N,N,N',N'*-tetra-2-ethylhexyl diglycolamide is a similar ligand to TODGA empirically but with branched alkyl chains adding further steric hinderance.[173] T2EHDGA is under consideration for use in the ALSEP (actinide-lanthanide separation) process as an alternative TODGA exhibiting similar overall performance with some loss in extraction efficiency and the need for a phase modifier to avoid third phase formation.[175,176] Although TEDGA and T2EHDGA are structurally different to TODGA their synthesis will be very

similar to the synthesis of TODGA revolving around the necessary amide bond formations. Therefore, by optimising the synthesis of TODGA the optimal reaction conditions and workup will likely be similar. Recent literature has shown an interest in diglycolamides with modified backbones, a common example is 2-(2-(dioctylamino)-2-oxoethoxy)-*N*,*N*-dioctylpropanamide (TWE21), however more extensive modifications have also been investigated such as the replacement of the ether linkage with a nitrogen, and a "rigidified glycolamide".[177] TWE21 is another potential alternative to TODGA that possesses an extra methyl on its backbone and could see use in the iSANEX and EURO-GANEX processes as a replacement for TODGA.[7,14,65] The extra methyl group influences the basicity of the central oxygen atom whilst modifying the steric interaction of this molecule with ionic species, both of which are known to impact a the ligands performance. Iqbal *et al.*[177] found that the increased basicity of the central oxygen atom from the methyl group in TWE21 did not make up for the more challenging steric constraint, resulting in a poorer performance compared to TODGA.

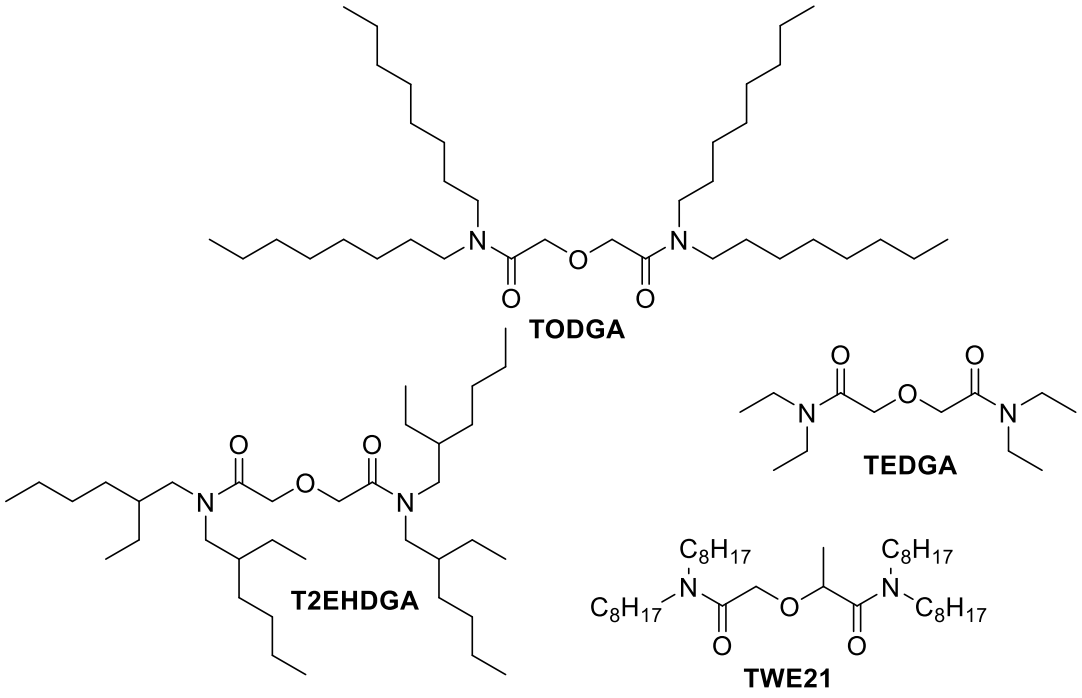

Figure 19: The chemical structures of TODGA, T2EHDA, TEDGA and TWE21

In summary, a whole host of interesting ligands for the partitioning of irradiated nuclear fuel have been identified and efforts continue to improve on the current state of the art to alleviate problems faced by current flowsheets. Many of these ligands show promise and offer highly desirable properties for reprocessing, however, most of these technologies rely on ligand combinations for actinide-lanthanide partitioning, increasing the complexity and cost of reprocessing. The future of reprocessing will likely see the simplification of PTs by reducing the number of ligands used. However, any successful ligands must meet many demands whilst being economically viable, therefore the synthesis of promising ligands requires more attention and optimisation. As amides and diamides are very popular groups of ligands it is imperative that their synthesis is investigated to ensure their viability. The next section introduces the topic of amide synthesis, a transformation that is crucial to the success of this work and of extreme importance to the chemical industry.

1.3. Amide Bond Formations

Amide bonds are abundant in everyday life, forming the DNA upon which life relies, to the pharmaceuticals, medicines, and vaccines that we rely upon. Amide bond formations are essential in both the natural and synthetic world, and yet we still have not mastered this 'simple' transformation, relying on atom inefficient processes to achieve a task so common in nature. Finding a general "green" method to amide bonds that avoids the use of additional, stoichiometric reagents that do not contribute to the final product mass is of great importance to pharmaceutical and specialty chemical manufacturers and has been for well over a decade.[150,155,178]

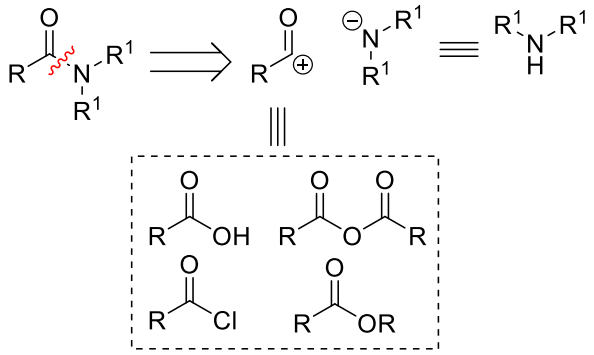

Scheme 2: The retrosynthesis of a tertiary amide

Carboxylic acids (**Scheme 2**) are often used by process chemists as a starting material for amide synthesis due to their abundance and low cost, in addition to being more benign than other functional groups like anhydrides and acyl chlorides which may be commercially available but are typically more expensive. Such functionalities are often derived from the carboxylic acid, hence the increased cost, yet the need for activating agents with the carboxylic acids can outweigh the benefits of using these materials.

In addition to a carboxylic acid, the corresponding amine is also required, unfortunately the transformation does not progress upon the combination of these raw materials alone. Instead, the combination results in a proton shift from the carboxylic acid to the amine (**Scheme 3**).[154]

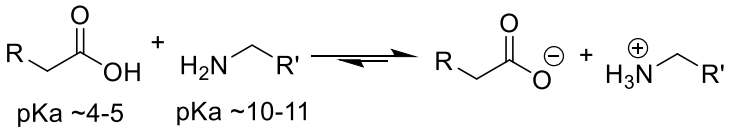

Scheme 3: Salting upon combination of a carboxylic acid and primary amine

Consequently, this salting hinders nucleophilic attack from the amine, requiring the need to overcome a high energy barrier to achieve amide bond formation. Instead of forcing this direct amidation with high temperatures and pressures that can degrade organic materials, synthetic chemists more commonly exploit stoichiometric coupling reagents. These reagents lower the energy barrier by generating a reactive intermediate prior to amide bond formation and are discussed in more detail later in this section (**Scheme 4**).

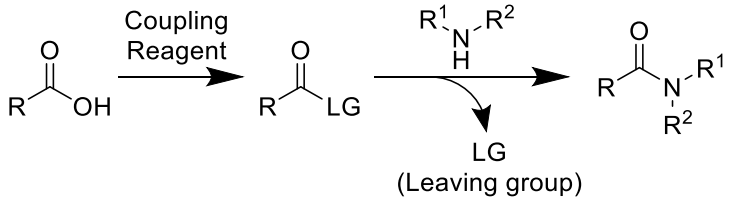

Scheme 4: Activation of a generalised carboxylic acid via a coupling reagent, followed by a nucleophilic substitution from the amine, removing the good leaving group

The reagents listed in **Table 1** are examples of common coupling reagents, employed to enhance the reactivity of carboxylic acids, generating an activated intermediate susceptible to nucleophilic attack, resulting in a subsequent reaction like amination to yield an amide bond (**Scheme 4**); Ultimately, this transformation is at the expense of a stoichiometric reagent that does not contribute to the mass of the final product resulting in increased waste volumes and further waste when purifying the product. Coupling reagents are often highly reactive towards water, for some the reagent is simply deactivated, whereas for others the reaction is vicious adding safety considerations and challenges when working with large volumes of these materials.

Table 1: A comparison of molecular weights for common coupling agents highlighting the atom efficiency when employing each. (see list of abbreviations for compound names.)

Coupling Reagent	Molecular weight (g/mol)
Phosgene	99
$SOCl_2$	119
$(COCl)_2$	127
EDC.HCl	155
CDI	162
DCC	206
Triphosgene	297
T3P®	318
HATU	380
PyBOP	520

Thionyl chloride and oxalyl chloride are excellent chlorinating reagents that have seen use for decades, however upon exposure to water the reaction is vigorous and releases toxic gases. The danger and toxicity of coupling reagents is understandable from the previous statement alone, however, their ability to cross link amino acids and interfere with DNA should not be underestimated. These properties make it difficult to work with these reagents, especially on the large scale. Not to mention the wasteful nature of these reagents due to their poor atom efficiency.

Without a good leaving group the conversion of carboxylic aids to amides requires a high energy barrier to be overcome. To overcome this energy barrier, high temperatures (for organic chemistry) and/or catalysis are alternative methodologies to coupling reagents (**Scheme 5**). Other reaction pathways to amide bonds can be found in the literature. However, these methods are often immature with niche applications, thus are yet to replace coupling reagents as a general approach to amide bond formations.[155,179–183]

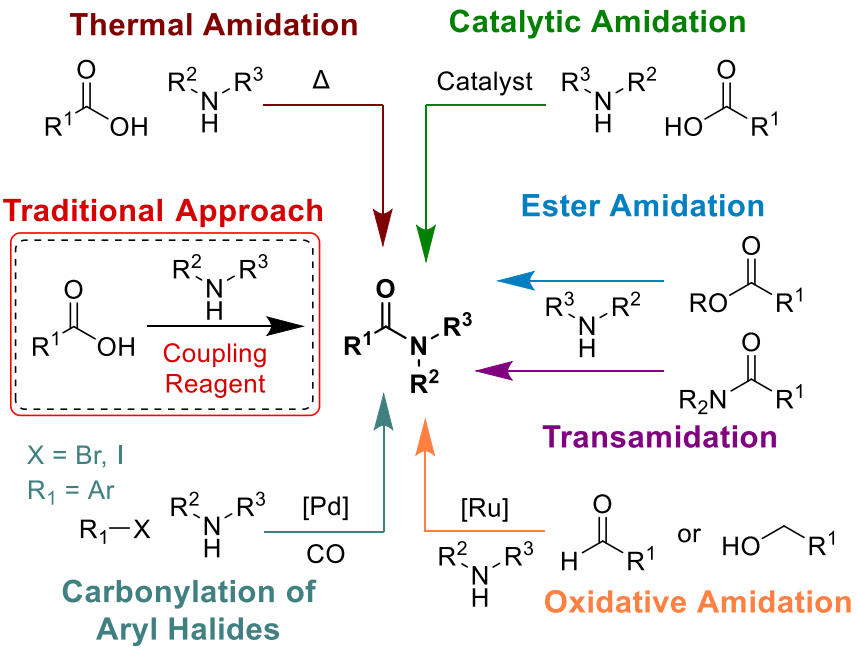

Scheme 5: Examples of amide bond formation reactions. A modified figure from T. Sheppard *et al.*[155]

In 2007 the ACS Green Chemistry Institute Pharmaceutical Roundtable (GCIPR) voted "amide bond formations avoiding poor atom economy reagents" as a high priority challenge that needs addressing.[184] Since 2007 research has continued globally to develop greener strategies for amide synthesis, most of which focus on catalytic methods. Despite its sustainable reputation, catalysis does not ensure that the reaction will be greener or cleaner. This has been highlighted by Sheppard et al.[155] who identified and discussed the advantages and disadvantages of catalytic amide bond formations. This paper included process mass intensity (PMI) data for various amidation methods in the literature to compare the green credentials of various routes, finding that current catalytic techniques do not yet meet all the requirements to replace coupling reagents and can often be more wasteful. It is often desirable for reactions to feature low PMI, whilst providing high product yields with high purity and retrievability using affordable, cost friendly reagents that do not possess risks that infringe on safety especially when large scale production is required. In 2018, 11 years on from the ACS GCIPR meeting and publication a follow up paper was published,[185] this time involving more pharmaceutical companies and again green issues in the industry were discussed and assessed. Unsurprisingly, cleaner amide synthesis was again a top requirement, this time titled "General methods for catalytic/sustainable amide synthesis". This further reinforces that since the initial publication in 2007 the scientific community has yet to find an all-purpose, atom efficient route to the amide bond, hence the reliance on stoichiometric coupling reagents remains prevalent in the chemical industry.

Dunetz *et al.*[186] further emphasised the reliance on coupling reagents by publishing a review on large scale amide bond formations in the pharmaceutical industry. This review showcases the abundance of coupling reagents that are used on the large scale whilst discussing the pros and cons from an industrial perspective.

The popularity of EDC, 1-ethyl-3-(3′-dimethylaminopropyl)-carbodiimide hydrochloride is highlighted as the coupling reagent of choice for amide synthesis (**Figure 20**). This carbodiimide, EDC and its corresponding urea by-product, EDU (1-ethyl-3-(3′-dimethylaminopropyl)-urea) are considerably more soluble than other popular carbodiimides such as DCC (N,N'-dicyclohexylcarbodiimide) and DIC (N,N'-diisopropylcarbodiimide) providing much of its success. Of all the reagents described in **Figure 20** boric acid and the boronic acids are the only catalytic reagents listed. As previously mentioned, catalytic amidations are a relatively immature technology that often lacks general applicability. However, with more time and research, catalytic methods may start to displace the dominance of stoichiometric reagents, alas for now reagents like EDC, thionyl chloride, and CDI are here to stay.

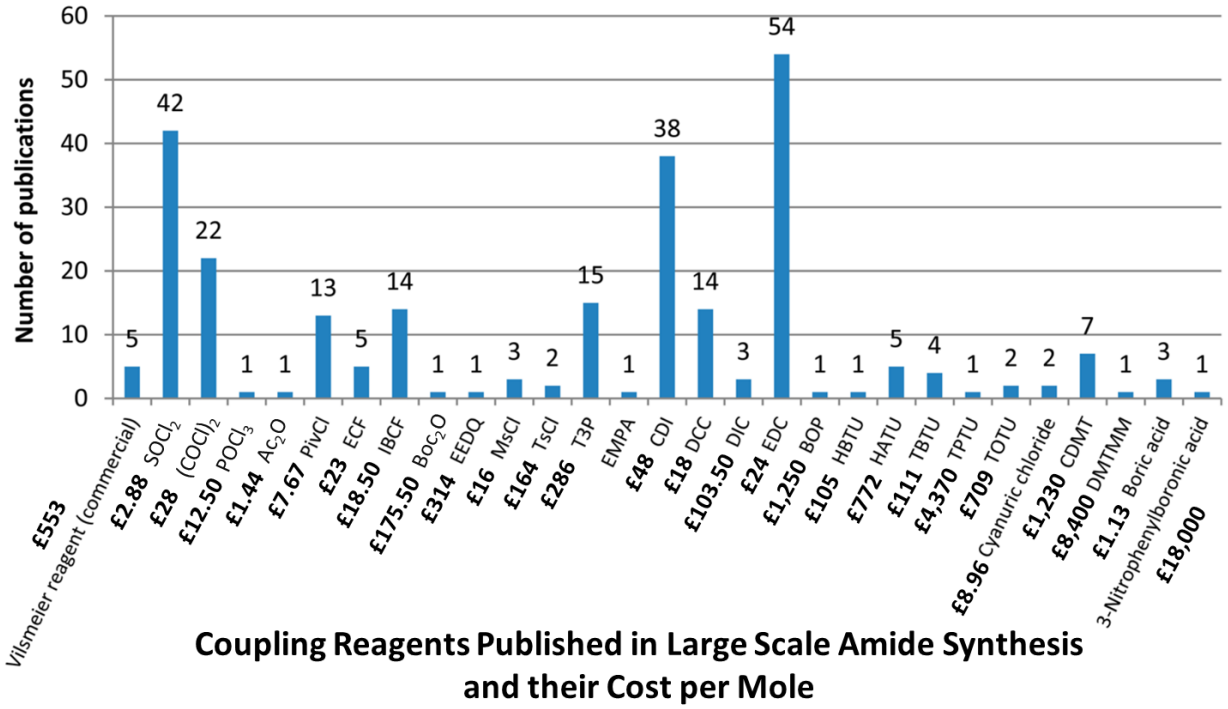

Figure 20: A modified figure displaying the popularity of coupling reagents used for amide bond formations on the industrial scale.[186] See the reference for the full names of these coupling reagents. Costs were mostly taken from Merck/Sigma Aldrich in 2022 although some could not be found the volume or weight costs were then calculated as a cost per mole.

Carbodiimides like EDC are so effective because they are prone to nucleophilic attack from a wide range of carboxylic acid containing target molecules to yield an activated ester, otherwise known as the *O*-acylisourea.[187] This reactive intermediate then has three options, it can undergo nucleophilic attack from the amine to yield the amide. This process eliminates the urea by-product EDU. Alternatively, another carboxylic acid can attack the reactive intermediate to yield the corresponding anhydride which is still susceptible to nucleophilic attack from the amine, regenerating the carboxylic acid and forming the amide but consuming an equivalent of coupling reagent. Disadvantageously, the *O*-acylisourea can rearrange via an acyl shift to yield the unreactive *N*-acylurea by-product, as indicated in **Figure 21**, consequently this consumes the carboxylic acid and coupling reagent. These three routes are illustrated in **Figure 21** for benzoic acid and a general secondary amine, illustrating general pathways by which EDC and other carbodiimides like DCC can follow.

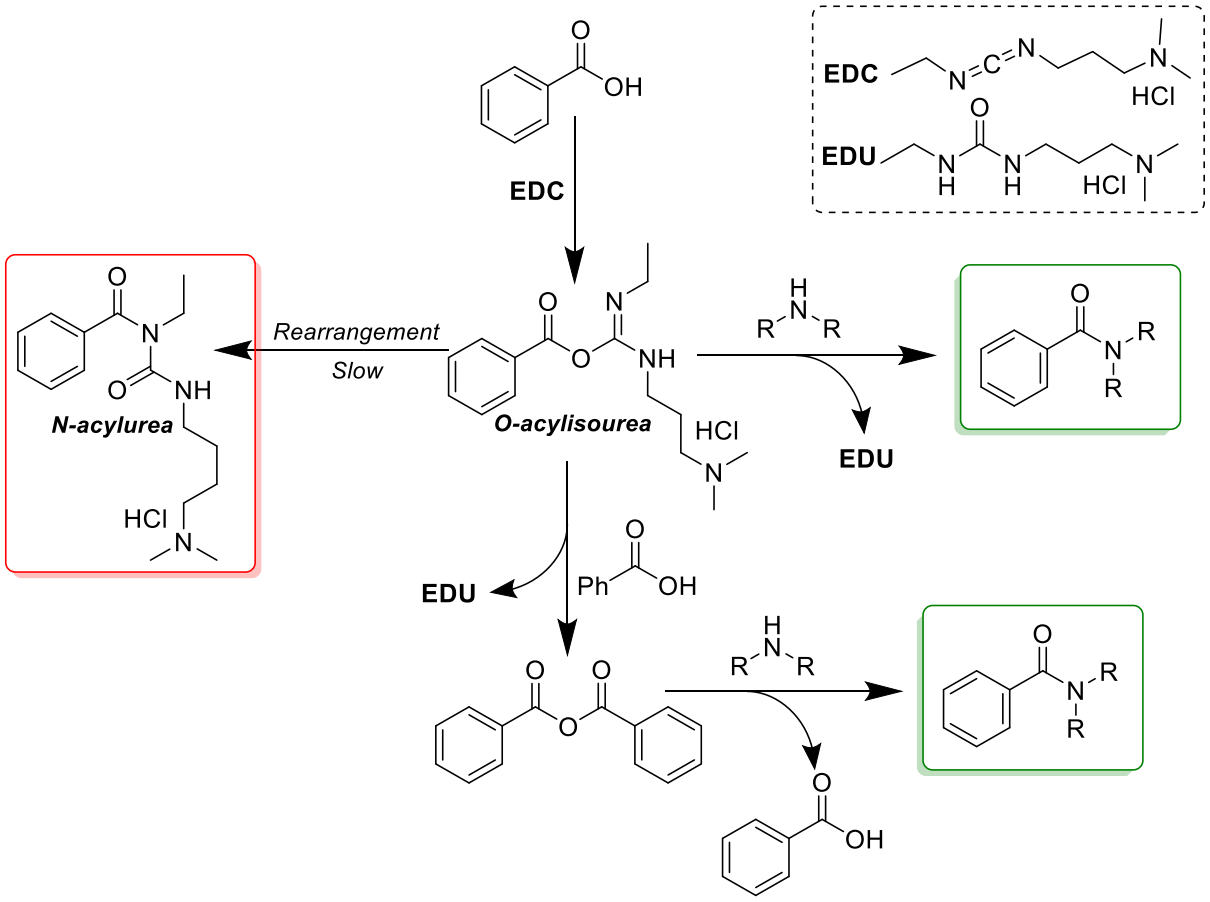

Figure 21: Three reaction pathways for amide synthesis using EDC, benzoic acid, and a general amine.

EDC is advantageous when it comes to product purification as both EDC and EDU are highly water soluble and can be removed via a simple water wash. This is often true for the *N*-acylurea by-product; hence the crude product can be mostly purified with relative ease. However, other carbodiimides like DCC, the urea by-product, DCU (*N,N*-dicyclohexylurea) is insoluble in most organic solvents, therefore reactions result in precipitation and frequently require filtration to remove this by-product, this adds further cost and process steps/complications reinforcing the preference for EDC over other carbodiimides.

Chlorinating agents are another widely used coupling reagent in academia and industry for the generation of acyl chlorides that can then react with an amine to yield the amide (

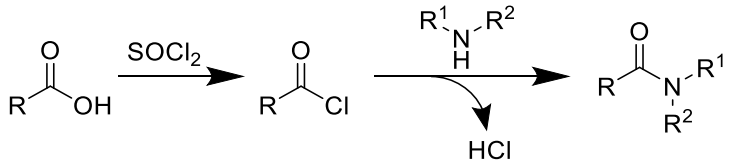

Scheme 6). Thionyl chloride and oxalyl chloride are two popular chlorination agents being somewhat safer than alternatives like phosgene and triphosgene that are more difficult to handle especially on the large scale adding an often avoidable risk. Though it should be noted that these reagents are all heavily toxic and release toxic gases when making and using them, therefore are harmful reagents to the environment. These reagents still see widespread use and popularity because of their exceptional compatibility and ability to achieve high product yields in a short time with ease of purification. As chemistry moves toward net zero, alternatives will be needed and these reagents may be phased out, therefore it is essential that significant investment in generalised, green methodologies for amide bond formation are pursued and identified.

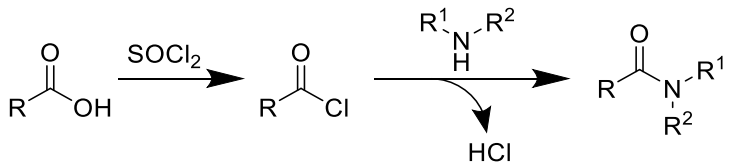

Scheme 6: Generalised chlorination of a carboxylic acid and subsequent amination to yield an amide.

The Schotten-Bauman reaction (**Scheme 7**) is commonly practiced for amide synthesis and has been used to synthesise amide containing ligands like TODGA.[188] Here, an aqueous base such as sodium hydroxide is employed to mop up the eliminated HCl. Alternatively, organic bases like triethylamine can be employed avoiding the use of an aqueous phase, proving to be a popular methodology for the synthesis of amides like DEHiBA.[54] As most of the publications that synthesise extractants for nuclear reprocessing require small quantities of these molecules for testing, acyl chloride is often the starting material of choice due to availability and robustness of these

reactions.[188] This avoids the more challenging chlorination step and achieves a good yield in a single step. Alternatively early publications that discuss the synthesis of diglycolamides start with the cyclic anhydrides whilst later publications use a chlorinating agent to generate the acyl chloride. To our knowledge ligands for nuclear reprocessing have not yet been synthesised without the use of a coupling reagent or an activated starting material. As these ligands are chemically simple (despite the use of secondary amines), in comparison to active pharmaceutical ingredients (APIs), an effort should be made for these amides to be synthesised via alternative, cleaner routes, reducing the cost of manufacture and environmental burden prior to scale-up.

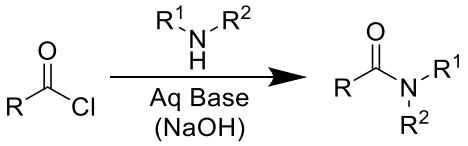

Scheme 7: Generalised tertiary amide bond formation via the Schotten-Baumann reaction.

It should be mentioned that enzymatic amidation reactions are reported in the literature,[189] and even used in for large-scale manufacture of amide bonds by giants like Pfizer.[190] However, these enzymes are typically highly specialised and limited in their substrate scope, often requiring days for reactions to complete, this makes them unlikely candidates for the synthesis of ligands like DEHiBA and TODGA without targeted research to identify a suitable enzyme. Beneficially however, when a suitable enzyme is identified the synthetic process is highly efficient and selective which is beneficial for complicated and typically highly selective pharmaceutical synthesis.

The screening of amide bond transformations is often vital to find suitable reagents compatible with the desired starting materials. This process is typically time consuming, labour intensive and wasteful, however automated solid and liquid handlers paired with well plates allows dozens of batch reactions and conditions to be screened with minimal interaction, speeding up the screening process prior to the optimisation and comparison of promising synthetic routes.[158,191–196]

Unfortunately however, there is a significant cost barrier to this equipment hindering access to this powerful resource. Self-optimising flow reactors offer the capability to screen multiple synthetic routes at once, by exploring and optimising multiple continuous and discrete variables,[197] however this is more complex than an automated batch system with more limitations. These limitations include incompatibility with non-homogenous reactions, limited solvent screening and an inability to perform reactions simultaneously. Additionally, each solution must be prepared likely by a human and as some solutions are unstable degradation over the course of the campaign can lead to bias. A simpler option is the individual screening and optimisation of synthetic routes in continuous flow using self-optimising flow reactors. The data from each synthetic route can then be compared to identify an optimum route and conditions.[156]

1.4. Flow Chemistry

Over recent years the organic chemist's toolkit has improved and diversified with influence from industry 3.0 and 4.0.[198–200] One of the most significant changes has been the development of continuous flow chemistry, especially small scale flow reactors for lab-scale research purposes.[189,190] Batch chemistry in glass vessels has long been the primary option for chemists when synthesising and purifying target materials, however, flow chemistry provides ample and new opportunities especially automation and process intensification.[201–206] Despite many considering flow chemistry as a replacement to traditional batch chemistry, the reality is more complex and flow chemistry should be considered a complementary technique to conventional batch chemistry as not all chemistry is suited for continuous flow.[207] Flow chemistry is the act of flowing reagents as a continuous stream, this can take place through various media such as reactors and separators to achieve chemical transformations or purifications respectively. The

development of lab-scale flow equipment enables more efficient process development to take this. This can minimise waste volumes , and the ease of scalability means that little R&D is required to transition a lab-scale flow reaction to a larger flow platform so long as the flow path and heat transfer does not change significantly.[208,209] The term flow reactor encompasses both continuous stirred tank reactors (CSTRs) and plug flow reactors (PFRs, **Figure 22**) such as tubular, plate, and microfluidics.[210–213]

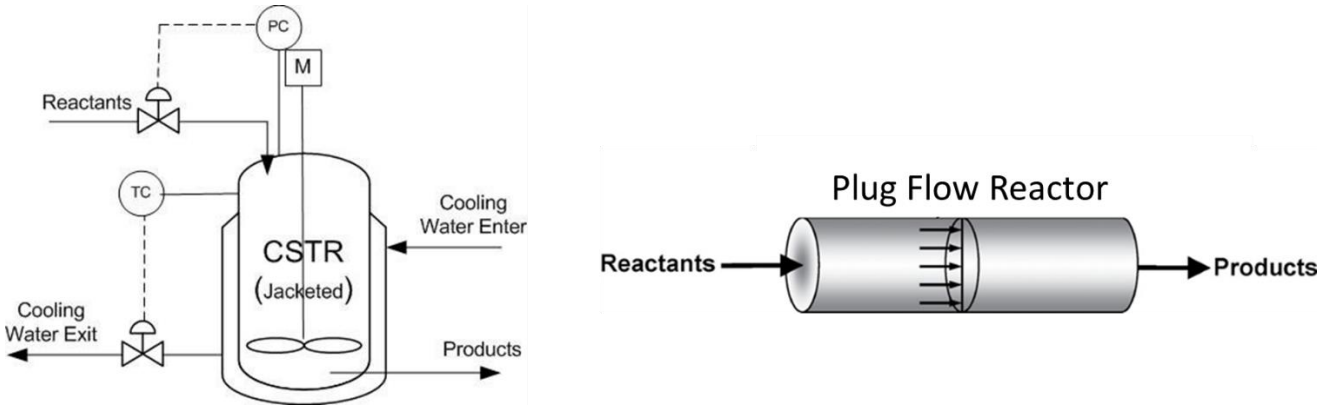

Figure 22: illustrations of typical continuous stirred tank reactor,[214] and a plug flow reactor.[215]

Plug flow reactors are beneficial for high throughput reaction optimisation due to their compatibility with automation and ability to reach steady state quickly with certainty when changing reaction conditions, minimising waste volumes which can be essential when using costly materials.[216] Comparatively, CSTRs have broader residence time distributions than PFRs (**Figure 23**) which can lead to cross contamination between reaction conditions and longer wait times for steady state which extends the overall optimisation time whilst consuming more material than an automated optimisation in a PFR.[217] Advantageously CSTRs can handle solids better than PFRs and provide better mixing, which can be needed when performing liquid-liquid extractions in continuous flow or for multiphasic reactions like the Schotten-Baumann reaction.[218] Overall PFRs are well suited to research where small scale, high throughput experimentation is of great importance, offering greater experimental throughput whilst using less material per experiment

which can save on reagent costs which could be essential when using costly reagents and intermediates. To further reduce this cost, slug flow can be adopted removing diffusion across the reactor and thus the need to wait for steady state, although this adds complexity to the setup and sampling for online or offline analysis.[216,219]

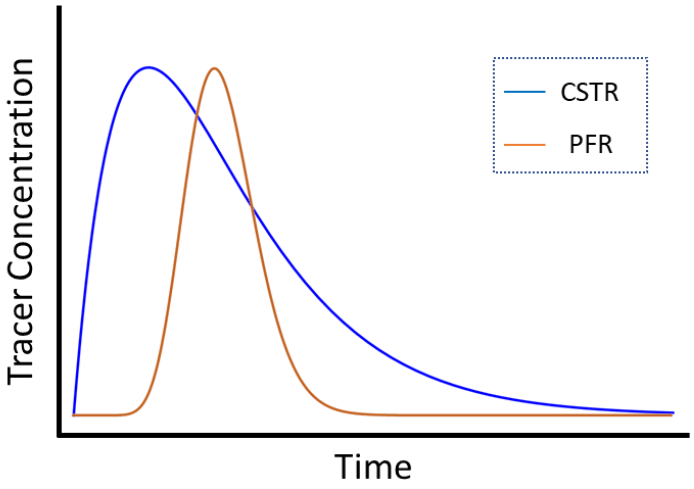

Figure 23: Typical residence time distribution of a CSTR and a PFR, reproduced from N. Kapur[220]

Despite the advantages that continuous flow chemistry offers, batch reactors and processes have been standard practice at both the small and large scale for decades. This is mostly due to their robustness and operational ease, yet batch chemistry carries limitations, most notably the level of control over the reaction and difficulties with process intensification. PFRs possess smaller dimensions for enhanced control over the reaction, such as better mixing, and enhanced heat transfer.[221,222] These offerings can enhance product quality and reaction efficiency by hindering unwanted side reactions.[223] A major benefit of PFRs is the excellent heat transfer properties, requiring reduced energy input to heat or cool solutions, further reducing operational costs.[224–227] Thus solutions can be evenly heated or cooled for enhanced process control ensuring quality control. Additionally, when heated reaction solutions are exposed to ambient conditions they equilibrate quickly to the surrounding temperature unless insulated.[224] This can be used to quench

reactions quickly, aids to control of exothermic runaway reactions and reduces safety concerns of hot effluents.

PFRs are popular due to their narrow temperature profiles across the reaction mixture in combination with enhanced mixing, facilitating the ability to avoid unwanted reaction pathways, minimising the formation of by-products or degradation products.[228] Additionally, flow chemistry supports the safer use of toxic reagents, pressurised reactions, and gases as reagents with relative ease.[224,229] The hazard of using dangerous and toxic reagents or intermediates can be heavily reduced due to small reaction volumes without limiting product volumes,[230] additionally, hazardous and sensitive intermediates can be telescoped allowing a secondary chemical transformation to take place removing the need to isolate and handle dangerous materials.[231]

Flow chemistry opens the door to new possibilities for new and old chemistry allowing access to novel process windows and cost savings that can be achieved via improved energy efficiency when heating or cooling solutions, simpler purifications due to reduced by-products, higher yields/purity or select starting material consumption. These are prime examples why flow chemistry is becoming extremely attractive in both academia and industry with giants like BASF, AstraZeneca, and Pfizer transitioning chemistry into continuous flow as early as the discovery stage.[209,232–237]

Despite the potential advantages of flow chemistry, not all chemistry is suited for continuous flow, and does not always provide advantages over batch chemistry. A review by Hartman et al.[238] discusses the merits of batch and flow chemistry, finding that reaction performance when using flow does not necessarily exceed batch, plus developing a process in flow is often more time-consuming and requires a more specialist skillset and equipment.[207,238] Flow chemistry does however offer an easier route to scale-up compared to batch chemistry due to better mixing of

reagents and even temperature profiles across the reactions. Alternatively reactions can be scaled out and product can be generated continuously.[115] Further limitations for continuous flow typically include an incompatibility with solids and precipitate formation, therefore starting materials must be soluble prior to the reaction, following this the reaction mixture should remain in the liquid phase to avoid problems.[204] Not all reactors and pumps are incompatible with solids, for example nanoparticle synthesis and catalysis are accessible in flow, however these chemistries are particularly prone to reactor fouling.[238]

To its benefit, flow chemistry is compatible with automation and high throughput experimentation for both reaction screening and optimisation.[239] This allows a large number of reaction conditions to be investigated in a short amount of time or continuously without the need for human interaction.[240] Traditional reaction screening and optimisation is a long, expensive and tedious process in batch when performed manually. The long process of repeatedly weighing out material for each reaction vessel can be mostly avoided in flow where several reservoirs can be used for hundreds of experiments. This can further enhance the reproducibility of these reactions reducing human error from repeated weighing, although degradation or precipitation of stock solutions can be problematic and should be monitored.

Flow chemistry is therefore a complementary technology to batch chemistry, allowing suitable chemistry to be investigated in novel ways, facilitating process intensification to improve process metrics. Yet continuous flow is not compatible with all chemistries and may not offer benefits over batch chemistry, particularly for reactions with slow kinetics or liquid-solid systems that can be better suited to batch chemistry. To summarise, flow chemistry can be a powerful synthetic tool when used under the correct circumstances, facilitating process intensification via access to novel process windows, but is not a replacement technology.[241,242]

1.4.1. Self-Optimising Flow Platforms

The integration of automation (industry 3.0) with flow chemistry has become popular for chemical synthesis over recent years.[243,244] To expand and improve on this, the inclusion of machine learning (industry 4.0) with automated flow chemistry has seen the rise of self-optimising flow reactors/platforms capable of optimising single and multi-step synthesis.[245] These machine-learning driven platforms can locate optimum conditions for a given reaction in minimal time and experiments compared to traditional one variable at a time synthetic optimisation.[246] Automated chemical optimisation via self-optimising flow platforms is typically more accessible than published automated batch platforms that employ robotic liquid and solid handlers used for automated library synthesis only requiring pumps and temperature controllers capable of communicating with a computer and the ability to code.[247–249] The use of machine learning algorithms to optimise objectives is an efficient advancement over statistically driven Design of Experiments (DoE) capable of solving more complex problems and identifying global optima.[250] DoE has been used in abundance to optimise many reaction steps but it does not enable complete autonomy.[251,252] To complete the automation loop self-optimising flow platforms require a form of inline/online analytics for process monitoring and the quantification of experimental outcomes, this adds complexity and cost to these setups depending on the analysis however a simple UV-Vis spectrometer can be sufficient. A whole host of process analytics have been used in combination with flow such as infrared (IR) spectroscopy, UV-Vis spectroscopy, high performance liquid chromatography (HPLC), benchtop NMR spectroscopy, gas chromatography (GC), and mass spectrometry.[243,253–256]

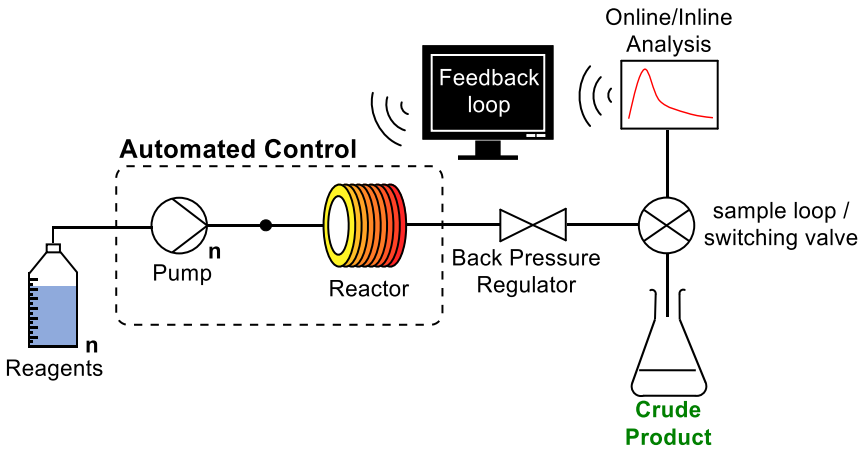

Figure 24: A simple self-optimising flow reactor setup where the pump and reactor temperature are controlled by the optimisation algorithm via a feedback loop.

As flow chemistry is so well suited to automation plus the ability to conduct chemical manufacture in an economic and sustainable manner, especially with lab-scale flow equipment, there is no wonder why reaction optimisation in continuous flow has received great interest.[233,257,258] Continuous flow enables temperature, residence time, pressure, reactant concentration, and equivalency to be accurately controlled with ease, reducing error and improving repeatability. With such a range of variables that can be optimised the task becomes very complex and time consuming for a human. Machine-learning algorithms such as SNOBFIT (Stable Noisy Optimisation by Branch and FIT),[259] BOAEI (Bayesian Optimisation with Adaptive Expected Improvement),[260] and TS-EMO (Thompson sampling efficient multi-objective optimisation) provide efficient solutions to this complex task, allowing multiple variables to be changed at once where a human could only change one to understand the impact of that variable.[261] These algorithms are not discussed in detail here (see references for further detail), but are able to find global or local optima for a given objective. Whilst SNOBFIT an BOAEI work towards the optimisation of a single objective such as yield or purity, TS-EMO can optimise multiple objectives simultaneously. Typically, multi-objective algorithms are employed for conflicting objectives such as product throughput/space-time yield (STY) and reaction mass

efficiency (RME). If a reaction has slow kinetics these objectives usually compete.[156,197] The algorithm optimises each objective individually as well as the conditions in between where a trade-off between the two objectives is met. As both objectives cannot be optimised under the same conditions, a trade-off curve is identified, otherwise known as the Pareto front (**Figure 25**).[262] The Pareto front contains a host of promising conditions from which the 'best' can be chosen for scale-up subjective to which objective is more favourable alongside any other process metrics of interest such as cost or yield.

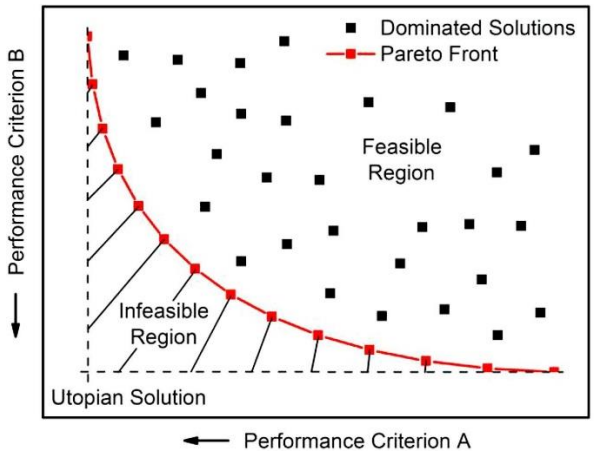

Figure 25: A depiction of the Pareto front for two given objectives.[262]

Examples of self-optimising flow chemistry are demonstrated throughout the literature, mostly focussing on the synthesis of molecules and a recent focus on telescoping chemical transformations, again mostly the synthesis steps.[156,228,243,245,255,260,263–266] Crucially the success of these platforms has been demonstrated through the optimisation of synthetic steps to the industrially relevant Osimertinib (AZD9291) using the SNOBFIT algorithm.[245] Other successes include nanoparticle synthesis,[267] Claisen condensation reactions,[266] and S_NAr transformations[53] to name a few. Overall, a high level of success has been achieved with these reactors, where optimum reaction conditions are identifiable in minimal experiments compared to traditional approaches. However, these case-studies typically focus on the front end of chemical manufacture achieving a crude product with exceptional process metrics without obtaining a pure product

which is usually required. The purification of organic material can be complex, with many options and variables to be optimised. The development of methodologies for lab-scale purification optimisations is a logical progression for self-optimising flow platforms. Lab scale purification/separation equipment is available and has been applied to purifications in continuous flow, however the optimisation of such processes has seen limited interest in the literature.[268–274]

This area of research is applicable to real world problems where it can cut down on costs and labour so that chemists can focus on more pressing problems instead of monotonous manual tasks that can be achieved through automation. As the nuclear reprocessing field focuses on testing the performance of ligands and flowsheets, the cost-effective large-scale manufacture of ligands to achieve this requires more attention. The application of self-optimising flow platforms is a promising route and methodology to achieve this task in a resource, time, and cost-effective manner.

1.5. Summary

This literature review introduces the benefits and challenges faced by the next generation of nuclear reprocessing flowsheets that can extend the supply of energy dense materials and rare earth metals. The industrial uptake of such processes is cost intensive, firstly requiring highly tailored processes and ligands to selectively extract target nuclides from a hostile environment in a safe and predictable manner. The ligands in question are constantly under development and testing, but a few of these are highly likely to be implemented in a future reprocessing facility. There are limited suppliers for these high value research materials and with little to no demand outside of the nuclear industry the cost to purchase these materials can be limiting with many publications choosing to manufacture the materials themselves, albeit on a small gram scale.

Large-scale testing of these ligands is necessary to ensure scalability of these processes, therefore access to large volumes of ligands is required but can be a barrier to research due to high costs and unoptimized synthetic routes to these ligands in the literature. The development, optimisation, and publication of different routes to these molecules of interest would alleviate this barrier to research, allowing researchers to further the technology readiness level of flowsheets like GANEX as well as optimise these processes and future processes.

DEHiBA has been identified as a molecule of great interest to the research community whilst being a simpler ligand with minimal steps for manufacture. Recent attention from the United States further demonstrates the relevance of this material and need for further research into its manufacture and performance testing. Currently it is unknown what effect impurities will have on the extraction of uranium or other radionuclides therefore the testing of DEHiBA from differing synthetic routes will aid to understand the effect of potential degradation products or impurities. There are many variables that can be optimised for the extraction of elements from irradiated nuclear fuel with major factors being type/structure of ligand, ligand concentration, metal (uranium) concentration, nitric acid concentration, phase (SA) ratio, and temperature. Although the type/structure of ligand is commonly compared throughout the literature, other variables, particularly ligand and metal concentration, SA ratio, and temperature receive lesser attention. The optimisation of these variables can maximise throughput reducing operational time ensuring irradiated fuel that can be reprocessed in a timely manner, whilst increasing extraction efficiency, minimising the number of extraction stages and thus capital and operational cost.

Although DEHiBA has been identified for this work, more complex ligands like TODGA are of great interest and require similar research and optimisation. The methodologies employed in this work are applicable to various other ligands, so long as each step is broken down individually and not telescoped, it is possible to optimise a telescoped flow platform, however more advanced

methodologies will likely be needed for such multi-step, telescoped reaction optimisations. Nevertheless it is possible through these methodologies to optimise the manufacture of other ligands, including more complex structures by investigating the efficient manufacture of DEHiBA allowing specialised ligands to be tested more thoroughly by reducing a cost barrier to research.

1.6. Project Motivations

As the nuclear industry enters a new era where the world looks to it for a solution to the climate crisis, the sustainability of nuclear fission must be ensured. Although nuclear energy has a low carbon footprint, the fuel, uranium is a finite resource. This is a threat that impacts the long-term viability of this technology. Nuclear reprocessing and recycling offer a solution to improve the sustainability and extend the supply of nuclear fuel.[1, 2] Nuclear reprocessing is practiced on the industrial scale, however the current technology is old, expensive, and deemed unfeasible by most nations. Replacement and complimentary reprocessing technologies have been under development for decades to ensure their robustness prior to industrial implementation.[3] These technologies primarily utilise organic ligand extractants to selectively partition nuclear fuel. This enables the selective recycling of elements for reuse as more nuclear fuel, in the future the recovery of other rare, less radioactive elements like Iridium may be feasible to further extend supply.

These organic ligands have undergone thorough testing to ensure their effectiveness and suitability but have not yet been deemed economically viable. The literature is sparse with specific synthetic routes to these ligands and to our knowledge there is no literature describing and comparing suitable synthetic routes to these ligands. Furthermore, the synthetic optimisation of these ligands to reduce their cost is yet to be published. This gap in the literature may well limit the appeal and uptake of these technologies.

The implementation of flow chemistry to synthesise these ligands in addition to the identification of multiple routes and conditions for their manufacture will enable cheaper and wider access to these ligands.

1.7. Project Aims & Objectives

This project aims to identify an efficient process/methodology for the manufacture of organic ligands for use in advanced nuclear reprocessing, specifically focussing on the synthesis and subsequent purification of *N,N*-(di-2-ethylhexyl)isobutyramide (DEHiBA). This involves the exploration, optimisation, and evaluation of synthetic and purification routes, using industry 4.0 optimisation techniques to identify a highly efficient and scalable process. Specifically, the project employs automated flow reactor platforms for the optimisation of chemical transformations via machine-learning algorithms to efficiently optimise key process metrics and identify promising reaction conditions for continuous on-demand manufacture.

Subsequently, DEHiBA from these optimisations will be tested for the forward extraction of uranium and verified against commercially sourced DEHiBA and the available literature data. The suitability of the optimised manufacture routes will be assessed here ensuring that starting materials, impurities and degradation products do not hinder the forward extraction of uranium, ensuring DEHiBA can be manufactured via these routes. To expand on the available literature data, variables like SA ratio, nitric acid concentration, and ligand concentration will be investigated for a more efficient extraction of uranium(VI).

1.8. Thesis Overview

The results chapters of this thesis are in the order: DEHiBA synthesis optimisation, continuous DEHiBA purification optimisation, and then performance testing of DEHiBA, benchmarking against literature data by extracting uranium(VI) from aqueous media. The work in these chapters was not completed in that order due to equipment development needed for the purification in flow optimisations. The synthesis chapter was first completed, next purification studies began in batch of differing crude products that were available from the synthetic optimisations, this generated enough purified DEHiBA for uranium extraction studies to begin, finally the purification of DEHiBA was optimised in continuous flow. During the uranium extraction work the bulb for the UV-Vis spectrometer deteriorated and halted repeats and further optimisation work that was planned. A new bulb could not be sourced as the supplier would not ship to the UK, instead a different UV-Vis spectrometer was purchased, however this arrived too late into my PhD studies and no further work was completed or analysed with this new spectrometer. The inability to analyse the extraction experiments meant that work then began on the continuous purification optimisations. Thus, these chapters are not in chronological order and the uranium extraction chapter does not use purified DEHiBA from the continuous purification optimisation chapter.

Repeatability was ensured for the continuous flow optimisation chapters prior to any optimisation, this ensured reliability of the data as sampling/analysis only occurred when steady state had been achieved. This was done using random experimental conditions and analysing via online HPLC and offline GC-FID where applicable. Experiments were repeated in randomised orders and a range of wait times/reactor volumes to determine when steady state had been achieved. Process metrics quoted were highly reproducible due to the exceptional control that continuous flow has over the reaction or purification. Following the optimisation promising conditions were repeated along with random experimental conditions to ensure reliability, all of

which were highly repeatable to the significant figures quoted, plus HPLC and GC-FID analysis were found to be in agreement with one another.

1.9. References

1 M. Usman and M. Radulescu, Examining the role of nuclear and renewable energy in reducing carbon footprint: does the role of technological innovation really create some difference?, *Science of The Total Environment*, 2022, **841**, 156662.

2 S. Gabriel, A. Baschwitz, G. Mathonnière, T. Eleouet and F. Fizaine, A critical assessment of global uranium resources, including uranium in phosphate rocks, and the possible impact of uranium shortages on nuclear power fleets, *Ann Nucl Energy*, 2013, **58**, 213–220.

3 R. Taylor, *Reprocessing and recycling of spent nuclear fuel*, Elsevier, 2015.

4 S. Widder, Benefits and concerns of a closed nuclear fuel cycle, *Journal of renewable and sustainable energy*.

5 J. R. Eiser and J. Van der Pligt, Belief and values in the nuclear debate 1, *J Appl Soc Psychol*, 1979, **9**, 524–536.

6 J. E. Birkett, M. J. Carrott, O. D. Fox, C. J. Jones, C. J. Maher, C. V Roube, R. J. Taylor and D. A. Woodhead, Recent developments in the Purex process for nuclear fuel reprocessing: Complexant based stripping for uranium/plutonium separation, *Chimia (Aarau)*, 2005, **59**, 898.

7 A. Geist, R. Taylor, C. Ekberg, P. Guilbaud, G. Modolo and S. Bourg, The SACSESS hydrometallurgy domain—an overview, *Procedia Chem*, 2016, **21**, 218–222.

8 P. Baron, S. M. Cornet, E. D. Collins, G. DeAngelis, G. Del Cul, Y. Fedorov, J. P. Glatz, V. Ignatiev, T. Inoue and A. Khaperskaya, A review of separation processes proposed for advanced fuel cycles based on technology readiness level assessments, *Progress in Nuclear Energy*, 2019, **117**, 103091.

9 K. L. Nash and G. J. Lumetta, *Advanced separation techniques for nuclear fuel reprocessing and radioactive waste treatment*, Elsevier, 2011.

10 G. Modolo, A. Geist and M. Miguirditchian, Minor actinide separations in the reprocessing of spent nuclear fuels: recent advances in Europe, *Reprocessing and recycling of spent nuclear fuel*, 2015, 245–287.

11 A. Geist, J.-M. Adnet, S. Bourg, C. Ekberg, H. Galán, P. Guilbaud, M. Miguirditchian, G. Modolo, C. Rhodes and R. Taylor, An overview of solvent extraction processes developed in Europe for advanced nuclear fuel recycling, part 1—Heterogeneous recycling, *Sep Sci Technol*, 2021, **56**, 1866–1881.

12 M. Carrott, K. Bell, J. Brown, A. Geist, C. Gregson, X. Hères, C. Maher, R. Malmbeck, C. Mason and G. Modolo, Development of a new flowsheet for co-separating the transuranic actinides: the "EURO-GANEX" process, *Solvent Extraction and Ion Exchange*, 2014, **32**, 447–467.

13 M. Miguirditchian, L. Chareyre, C. Sorel, I. Bisel, P. Baron and M. Masson, Development of the GANEX process for the reprocessing of Gen IV spent nuclear fuels.

14 S. Bourg, A. Geist, J.-M. Adnet, C. Rhodes and B. C. Hanson, Partitioning and transmutation strategy R&D for nuclear spent fuel: the SACSESS and GENIORS projects, *EPJ Nuclear Sciences & Technologies*, 2020, **6**, 35.

15 A. F. Holdsworth, H. Eccles, C. A. Sharrad and K. George, in *Waste*, MDPI, 2023, vol. 1, pp. 249–263.

16 M. Bunn, J. P. Holdren, S. Fetter and B. Van Der Zwaan, The economics of reprocessing versus direct disposal of spent nuclear fuel, *Nucl Technol*, 2005, **150**, 209–230.

17 E. UK and I. Strategy, 'Energy white paper: Powering our net zero future, *Dept. Bus., Energy Ind. Strategy, UK, Tech. Rep. CCS0220144090, CP*.

18 J. B. Greenblatt, N. R. Brown, R. Slaybaugh, T. Wilks, E. Stewart and S. T. McCoy, The future of low-carbon electricity, *Annu Rev Environ Resour*, 2017, **42**, 289–316.

19 A. Cherp, V. Vinichenko, J. Jewell, M. Suzuki and M. Antal, Comparing electricity transitions: A historical analysis of nuclear, wind and solar power in Germany and Japan, *Energy Policy*, 2017, **101**, 612–628.

20 G. Harris, P. Heptonstall, R. Gross and D. Handley, Cost estimates for nuclear power in the UK, *Energy Policy*, 2013, **62**, 431–442.

21 M. Berthélemy and L. E. Rangel, Nuclear reactors' construction costs: The role of lead-time, standardization and technological progress, *Energy Policy*, 2015, **82**, 118–130.

22 A. Cherp, V. Vinichenko, J. Jewell, M. Suzuki and M. Antal, Comparing electricity transitions: A historical analysis of nuclear, wind and solar power in Germany and Japan, *Energy Policy*, 2017, **101**, 612–628.

23 M. Berthélemy and L. E. Rangel, Nuclear reactors' construction costs: The role of lead-time, standardization and technological progress, *Energy Policy*, 2015, **82**, 118–130.

24 P. Slovic, J. H. Flynn and M. Layman, Perceived risk, trust, and the politics of nuclear waste, *Science (1979)*, 1991, **254**, 1603–1607.

25 United States Government Accountability Office, *NUCLEAR FUEL CYCLE OPTIONS DOE Needs to Enhance Planning for Technology Assessment and Collaboration with Industry and Other*, 2011.

26 IAEA.org, The Database on Nuclear Power Reactors.

27 D. for B. E. and I. S. Gov. U. Nuclear Decommissioning Authority, *2019 UK Radioactive Waste Inventory*, 2019.

28 G. MacKerron, Multiple challenges: Nuclear waste governance in the United Kingdom, *Nuclear waste governance: An international comparison*, 2015, 101–116.

29 C. Poinssot, C. Rostaing, S. Greandjean and B. Boullis, Recycling the actinides, the cornerstone of any sustainable nuclear fuel cycles, *Procedia Chem*, 2012, **7**, 349–357.

30 K. S. Shrader-Frechette, *Burying uncertainty: Risk and the case against geological disposal of nuclear waste*, Univ of California Press, 1993.

31 S. A. Ansari, P. Pathak, P. K. Mohapatra and V. K. Manchanda, Chemistry of diglycolamides: promising extractants for actinide partitioning, *Chem Rev*, 2012, **112**, 1751–1772.

32 World Nuclear Association, NUCLEAR FUEL CYCLE Processing of Used Nuclear Fuel.

33 M. Schneider and Y. Marignac, *Spent nuclear fuel reprocessing in France*, International Panel on Fissile Materials (IPFM), 2008.

34 K. L. Nash and G. R. Choppin, in *Separations of f Elements*, Springer, 1995, pp. 1–8.

35 L. B. Silverio and W. de Queiroz Lamas, An analysis of development and research on spent nuclear fuel reprocessing, *Energy Policy*, 2011, **39**, 281–289.

36 B. H. Park, F. Gao, E. Kwon and W. Il Ko, Comparative study of different nuclear fuel cycle options: quantitative analysis on material flow, *Energy Policy*, 2011, **39**, 6916–6924.

37 G. De Roo and J. E. Parsons, A methodology for calculating the levelized cost of electricity in nuclear power systems with fuel recycling, *Energy Econ*, 2011, **33**, 826–839.

38 S. Widder, Benefits and concerns of a closed nuclear fuel cycle, *Journal of renewable and sustainable energy*.

39 G. De Roo and J. E. Parsons, Nuclear fuel recycling, the value of the separated transuranics and the levelized cost of electricity, *Available at SSRN 1470926*.

40 R. Malmbeck, M. Carrott, B. Christiansen, A. Geist, X. Hérès, D. Magnusson, G. Modolo, C. Sorel, R. Taylor and A. Wilden, in *Proceedings of Sustainable Nuclear Energy Conference*, 2014.

41 M. Miguirditchian, H. Roussel, L. Chareyre, P. Baron, D. Espinoux, J. N. Calor, C. Viallesoubranne, B. Lorrain and M. Masson, HA demonstration in the Atalante facility of the Ganex 2. cycle for the grouped TRU extraction.

42 M. Miguirditchian, H. Roussel, L. Chareyre, P. Baron, D. Espinoux, J. N. Calor, C. Viallesoubranne, B. Lorrain and M. Masson, in *Proceedings Global*, 2009.

43 A. C. Edwards, P. Mocilac, A. Geist, L. M. Harwood, C. A. Sharrad, N. A. Burton, R. C. Whitehead and M. A. Denecke, Hydrophilic 2, 9-bis-triazolyl-1, 10-phenanthroline ligands enable selective Am (III) separation: a step further towards sustainable nuclear energy, *Chemical Communications*, 2017, **53**, 5001–5004.

44 C. Wagner, U. Müllich, A. Geist and P. J. Panak, Selective extraction of Am (III) from PUREX raffinate: the AmSel system, *Solvent Extraction and Ion Exchange*, 2016, **34**, 103–113.

45 K. Van Hecke and P. Goethals, Research on advanced aqueous reprocessing of spent nuclear fuel: literature study.

46 J. R. Kumar, J.-S. Kim, J.-Y. Lee and H.-S. Yoon, A brief review on solvent extraction of uranium from acidic solutions, *Separation & Purification Reviews*, 2011, **40**, 77–125.

47 T. Sekine and D. Dyrssen, Solvent extraction of metal ions with mixed ligands—V: adduct formation of some Tris-TTA complexes, *Journal of Inorganic and Nuclear Chemistry*, 1967, **29**, 1481–1487.

48 A. P. Paiva and P. Malik, Recent advances on the chemistry of solvent extraction applied to the reprocessing of spent nuclear fuels and radioactive wastes, *J Radioanal Nucl Chem*, 2004, **261**, 485–496.

49 L. B. Silverio and W. de Queiroz Lamas, An analysis of development and research on spent nuclear fuel reprocessing, *Energy Policy*, 2011, **39**, 281–289.

50 A. F. De Almeida, R. Moreira and T. Rodrigues, Synthetic organic chemistry driven by artificial intelligence, *Nat Rev Chem*, 2019, **3**, 589–604.

51 M. Bortz, J. Burger, N. Asprion, S. Blagov, R. Böttcher, U. Nowak, A. Scheithauer, R. Welke, K.-H. Küfer and H. Hasse, Multi-criteria optimisation in chemical process design and decision support by navigation on Pareto sets, *Comput Chem Eng*, 2014, **60**, 354–363.

52 Z. Wang and G. P. Rangaiah, Application and analysis of methods for selecting an optimal solution from the Pareto-optimal front obtained by multiobjective optimisation, *Ind Eng Chem Res*, 2017, **56**, 560–574.

53 A. M. Schweidtmann, A. D. Clayton, N. Holmes, E. Bradford, R. A. Bourne and A. A. Lapkin, Machine learning meets continuous flow chemistry: Automated optimisation towards the Pareto front of multiple objectives, *Chemical Engineering Journal*, 2018, **352**, 277–282.

54 G. Thiollet and C. Musikas, Synthesis and uses of the amides extractants, *Solvent Extraction and Ion Exchange*, 1989, **7**, 813–827.

55 V. K. Manchanda and P. N. Pathak, Amides and diamides as promising extractants in the back end of the nuclear fuel cycle: an overview, *Sep Purif Technol*, 2004, **35**, 85–103.

56 G. M. Casparini and G. Grossi, Application of N, N-dialkyl aliphatic amides in the separation of some actinides, *Sep Sci Technol*, 1980, **15**, 825–844.

57 R. A. P. Thomas and L. E. Macaskie, Biodegradation of tributyl phosphate by naturally occurring microbial isolates and coupling to the removal of uranium from aqueous solution, *Environ Sci Technol*, 1996, **30**, 2371–2375.

58 T. Lee, Assessment of safety culture at a nuclear reprocessing plant, *Work Stress*, 1998, **12**, 217–237.

59 M. Lehtveer and F. Hedenus, Nuclear power as a climate mitigation strategy–technology and proliferation risk, *J Risk Res*, 2015, **18**, 273–290.

60 A. Blowers, in *UK Environmental Policy in the 1990s*, Springer, 1995, pp. 210–236.

61 A. Dodi and G. Verda, Improved determination of tributyl phosphate degradation products (mono-and dibutyl phosphates) by ion chromatography, *J Chromatogr A*, 2001, **920**, 275–281.

62 D. Haas, A. Vandergheynst, J. van Vliet, R. Lorenzelli and J.-L. Nigon, Mixed-oxide fuel fabrication technology and experience at the Belgonucléaire and CFCa plants and further developments for the MELOX plant, *Nucl Technol*, 1994, **106**, 60–82.

63 C. G. Bathke, B. B. Ebbinghaus, B. A. Collins, B. W. Sleaford, K. R. Hase, M. Robel, R. K. Wallace, K. S. Bradley, J. R. Ireland and G. D. Jarvinen, The attractiveness of materials in advanced nuclear fuel cycles for various proliferation and theft scenarios, *Nucl Technol*, 2012, **179**, 5–30.

64 C. Poinssot, C. Rostaing, S. Greandjean and B. Boullis, Recycling the actinides, the cornerstone of any sustainable nuclear fuel cycles, *Procedia Chem*, 2012, **7**, 349–357.

65 M. Carrott, A. Geist, X. Hères, S. Lange, R. Malmbeck, M. Miguirditchian, G. Modolo, A. Wilden and R. Taylor, Distribution of plutonium, americium and interfering fission products between nitric acid and a mixed organic phase of TODGA and DMDOHEMA in kerosene, and implications for the design of the "EURO-GANEX" process, *Hydrometallurgy*, 2015, **152**, 139–148.

66 M. I. Ojovan, W. E. Lee and S. N. Kalmykov, *An introduction to nuclear waste immobilisation*, Elsevier, 2019.

67 C. Chen, G. Habert, Y. Bouzidi and A. Jullien, Environmental impact of cement production: detail of the different processes and cement plant variability evaluation, *J Clean Prod*, 2010, **18**, 478–485.

68 R. Peters, P. Seshadri, G. Aubert, T. Barracco and L. Billès-Garabédian, 2006.

69 F. N. Von Hippel, *Science (1979)*, 2001, 293, 2397–2398.

70 D. E. Shropshire, *Advanced fuel cycle economic analysis of symbiotic light-water reactor and fast burner reactor systems*, Idaho National Lab.(INL), Idaho Falls, ID (United States), 2009.

71 M. Bunn, H. Zhang and L. W. Kang, The Cost of Reprocessing in China.

72 M. Bunn, J. P. Holdren, S. Fetter and B. Van Der Zwaan, The economics of reprocessing versus direct disposal of spent nuclear fuel, *Nucl Technol*, 2005, **150**, 209–230.

73 M. Miguirditchian, V. Vanel, C. Marie, V. Pacary, M.-C. Charbonnel, L. Berthon, X. Hérès, M. Montuir, C. Sorel and M.-J. Bollesteros, Americium recovery from highly active PUREX raffinate by solvent extraction: The EXAm process. A review of 10 years of R&D, *Solvent Extraction and Ion Exchange*, 2020, **38**, 365–387.

74 K. L. Nash, C. Madic, J. N. Mathur and J. Lacquement, in *The chemistry of the actinide and transactinide elements*, Springer, 2006, pp. 2622–2798.

75 S. A. Ansari, P. Pathak, P. K. Mohapatra and V. K. Manchanda, Aqueous partitioning of minor actinides by different processes, *Separation & Purification Reviews*, 2011, **40**, 43–76.

76 A. V Gelis and G. J. Lumetta, Actinide Lanthanide Separation Process□ ALSEP, *Ind Eng Chem Res*, 2014, **53**, 1624–1631.

77 K. L. Nash, Separation chemistry for lanthanides and trivalent actinides, *Handbook on the physics and chemistry of rare earths*, 1994, **18**, 197–238.

78 C. Xu, J. Wang and J. Chen, Solvent extraction of strontium and cesium: a review of recent progress, *Solvent Extraction and Ion Exchange*, 2012, **30**, 623–650.

79 K. Street Jr and G. T. Seaborg, The separation of americium and curium from the rare earth elements, *J Am Chem Soc*, 1950, **72**, 2790–2792.

80 M. P. Jensen, R. Chiarizia, I. A. Shkrob, J. S. Ulicki, B. D. Spindler, D. J. Murphy, M. Hossain, A. Roca-Sabio, C. Platas-Iglesias and A. de Blas, Aqueous complexes for efficient size-based separation of americium from curium, *Inorg Chem*, 2014, **53**, 6003–6012.

81 G. Modolo, P. Kluxen and A. Geist, Demonstration of the LUCA process for the separation of americium (III) from curium (III), californium (III), and lanthanides (III) in acidic solution using a synergistic mixture of bis (chlorophenyl) dithiophosphinic acid and tris (2-ethylhexyl) phosphate, *rca-Radiochimica Acta*, 2010, **98**, 193–201.

82 N. R. Council, D. on Earth, L. Studies, C. on Geosciences, C. on S. Technology and T. Systems, Nuclear wastes: technologies for separations and transmutation.

83 J. Tommasi, M. Delpech, J.-P. Grouiller and A. Zaetta, Long-lived waste transmutation in reactors, *Nucl Technol*, 1995, **111**, 133–148.

84 J. Martinez-Val and H. A. Abderrahim, D6. 2 P&T Roadmap proposal for Advanced Fuel Cycles leading to a Sustainable Nuclear Energy, *Sixth Framework Programme–Partitioning and Transmutation European Roadmap for Sustainable nuclear Energy (PATEROS)*.

85 A. Leoncini, J. Huskens and W. Verboom, Ligands for f-element extraction used in the nuclear fuel cycle, *Chem Soc Rev*, 2017, **46**, 7229–7273.

86 F. W. Lewis, L. M. Harwood, M. J. Hudson, A. Geist, V. N. Kozhevnikov, P. Distler and J. John, Hydrophilic sulfonated bis-1, 2, 4-triazine ligands are highly effective reagents for separating actinides (III) from lanthanides (III) via selective formation of aqueous actinide complexes, *Chem Sci*, 2015, **6**, 4812–4821.

87 A. Geist, U. Müllich, D. Magnusson, P. Kaden, G. Modolo, A. Wilden and T. Zevaco, Actinide (III)/lanthanide (III) separation via selective aqueous complexation of actinides (III) using a hydrophilic 2, 6-bis (1, 2, 4-triazin-3-yl)-pyridine in nitric acid, *Solvent Extraction and ion exchange*, 2012, **30**, 433–444.

88 F. W. Lewis, L. M. Harwood, M. J. Hudson, M. G. B. Drew, V. Hubscher-Bruder, V. Videva, F. Arnaud-Neu, K. Stamberg and S. Vyas, BTBPs versus BTPhens: some reasons for their differences in properties concerning the partitioning of minor actinides and the advantages of BTPhens, *Inorg Chem*, 2013, **52**, 4993–5005.

89 P. Zsabka, A. Wilden, K. Van Hecke, G. Modolo, M. Verwerft and T. Cardinaels, Beyond U/Pu separation: Separation of americium from the highly active PUREX raffinate, *Journal of nuclear materials*, 2023, **581**, 154445.

90 T. H. Vu, J.-P. Simonin, A. L. Rollet, R. J. M. Egberink, W. Verboom, M. C. Gullo and A. Casnati, Liquid/liquid extraction kinetics of Eu (III) and Am (III) by extractants designed for the industrial reprocessing of nuclear wastes, *Ind Eng Chem Res*, 2020, **59**, 13477–13490.

91 G. B. Hall, N. P. Bessen, P. R. Zalupski, E. L. Campbell, T. S. Grimes, D. R. Peterman and G. J. Lumetta, Extraction of Neptunium, Plutonium, Americium, Zirconium, and Technetium by Di-(2-Ethylhexyl)-Iso-Butyramide (DEH i BA) at High Metal Loadings, *Solvent Extraction and Ion Exchange*, 2023, **41**, 545–563.

92 G. B. Hall, E. L. Campbell, N. P. Bessen, T. R. Graham, H. Cho, M. RisenHuber, F. D. Heller and G. J. Lumetta, Extraction of Nitric Acid and Uranium with DEHiBA under High Loading Conditions, *Inorg Chem*, 2023, **62**, 6711–6721.

93 J.-P. Glatz, P. Souček and R. Malmbeck, in *Reprocessing and recycling of spent nuclear fuel*, Elsevier, 2015, pp. 49–62.

94 P. N. Pathak, L. B. Kumbhare and V. K. Manchanda, Effect of structure of N, N dialkyl amides on the extraction of U (VI) and Th (IV): a thermodynamic study, *Radiochim Acta*, 2001, **89**, 447–452.

95 S. A. Ansari, P. Pathak, P. K. Mohapatra and V. K. Manchanda, Chemistry of diglycolamides: promising extractants for actinide partitioning, *Chem Rev*, 2012, **112**, 1751–1772.

96 P. N. Pathak, N, N-Dialkyl amides as extractants for spent fuel reprocessing: an overview, *J Radioanal Nucl Chem*, 2014, **300**, 7–15.

97 T. Lyseid Authen, J.-M. Adnet, S. Bourg, M. Carrott, C. Ekberg, H. Galán, A. Geist, P. Guilbaud, M. Miguirditchian and G. Modolo, An overview of solvent extraction processes developed in Europe for advanced nuclear fuel recycling, Part 2—homogeneous recycling, *Sep Sci Technol*, 2022, **57**, 1724–1744.

98 P. J. Panak and A. Geist, Complexation and extraction of trivalent actinides and lanthanides by triazinylpyridine N-donor ligands, *Chem Rev*, 2013, **113**, 1199–1236.

99 B. Weaver and F. A. Kappelmann, *TALSPEAK: a new method of separating americium and curium from the lanthanides by extraction from an aqueous solution of an aminopolyacetic acid complex with a monoacidic organophosphate or phosphonate*, Oak Ridge National Lab.(ORNL), Oak Ridge, TN (United States), 1964.

100 R. Taylor, M. Carrott, H. Galan, A. Geist, X. Hères, C. Maher, C. Mason, R. Malmbeck, M. Miguirditchian and G. Modolo, The EURO-GANEX process: current status of flowsheet development and process safety studies, *Procedia Chem*, 2016, **21**, 524–529.

101 M. Carrott, K. Bell, J. Brown, A. Geist, C. Gregson, X. Hères, C. Maher, R. Malmbeck, C. Mason and G. Modolo, Development of a new flowsheet for co-separating the transuranic actinides: the "EURO-GANEX" process, *Solvent Extraction and Ion Exchange*, 2014, **32**, 447–467.

102 G. Modolo, A. Wilden, P. Kaufholz, D. Bosbach and A. Geist, Development and demonstration of innovative partitioning processes (i-SANEX and 1-cycle SANEX) for actinide partitioning, *Progress in nuclear energy*, 2014, **72**, 107–114.

103 D. Whittaker, M. Sarsfield, R. Taylor, D. Woodhead, K. Taylor, M. Carrott, C. Mason, H. Colledge, R. Sanderson and B. Keywood, Process flowsheet test of the i-SANEX process with CHON-compliant ligands in aqueous and organic phases, *Progress in Nuclear Energy*, 2023, **166**, 104956.

104 M. J. Carrott, C. J. Maher, C. Mason, M. J. Sarsfield, D. Whittaker and R. J. Taylor, Experimental Test of a Process Upset in the EURO-GANEX Process and Spectroscopic Study of the Product, *Solvent Extraction and Ion Exchange*, 2023, **41**, 88–117.

105 M. Salvatores and G. Palmiotti, Radioactive waste partitioning and transmutation within advanced fuel cycles: Achievements and challenges, *Prog Part Nucl Phys*, 2011, **66**, 144–166.

106 K. P. Kepp, A quantitative scale of oxophilicity and thiophilicity, *Inorg Chem*, 2016, **55**, 9461–9470.

107 R. G. PEARSON, Of the American chemical society, *J Am Chem Soc*, 1963, **85**, 3533–3539.

108 R. G. Pearson, Hard and soft acids and bases, *J Am Chem Soc*, 1963, **85**, 3533–3539.

109 P. W. Ayers, The physical basis of the hard/soft acid/base principle, *Faraday Discuss*, 2007, **135**, 161–190.

110 T.-L. Ho, Hard soft acids bases (HSAB) principle and organic chemistry, *Chem Rev*, 1975, **75**, 1–20.

111 G. T. Seaborg, Overview of the actinide and lanthanide (the f) elements, *Radiochim Acta*, 1993, **61**, 115–122.

112 J. M. McKibben, Chemistty of the purex process, *Radiochim Acta*, 1984, **36**, 3–16.

113 A. Paulenova, *Factors Controlling Redox Speciation of Plutonium and Neptunium in Extraction Separation Processes*, Oregon State Univ., Corvallis, OR (United States), 2013.

114 W. W. Schulz, *Chemistry of americium*, Atlantic Richfield Hanford Co., Richland, WA (United States), 1976.

115 J. Narbutt, in *Liquid-phase extraction*, Elsevier, 2020, pp. 725–744.

116 P. J. Panak and A. Geist, Complexation and extraction of trivalent actinides and lanthanides by triazinylpyridine N-donor ligands, *Chem Rev*, 2013, **113**, 1199–1236.

117 K. L. Nash, Separation chemistry for lanthanides and trivalent actinides, *Handbook on the physics and chemistry of rare earths*, 1994, **18**, 197–238.

118 A. Rout, K. A. Venkatesan, M. P. Antony and P. R. V. Rao, Comparison in the extraction behavior of uranium (VI) from nitric acid medium using CHON based extractants, monoamide, malonamide, and diglycolamide, dissolved in piperidinium ionic liquid, *Sep Sci Technol*, 2016, **51**, 474–484.

119 A. Geist, U. Müllich, D. Magnusson, P. Kaden, G. Modolo, A. Wilden and T. Zevaco, Actinide (III)/lanthanide (III) separation via selective aqueous complexation of actinides (III) using a hydrophilic 2, 6-bis (1, 2, 4-triazin-3-yl)-pyridine in nitric acid, *Solvent Extraction and ion exchange*, 2012, **30**, 433–444.

120 D. Magnusson, A. Geist, R. Malmbeck, G. Modolo and A. Wilden, Flow-sheet design for an innovative SANEX process using TODGA and SO3-Ph-BTP, *Procedia Chem*, 2012, **7**, 245–250.

121 L. L. Burger, Uranium and plutonium extraction by organophosphorus compounds, *J Phys Chem*, 1958, **62**, 590–593.

122 C. V. S. Brahmmananda Rao, T. G. Srinivasan and P. R. Vasudeva Rao, Studies on the extraction of actinides by substituted butyl phosphonates, *Solvent Extraction and Ion Exchange*, 2012, **30**, 262–277.

123 G. Koch, W. Ochsenfeld, H. Schmieder and W. Weinlaender, Chemical aspects in the design of a flowsheet for a large-scale LWR reprocessing plant.

124 C. Lamouroux, H. Virelizier, C. Moulin, J. C. Tabet and C. K. Jankowski, Direct determination of dibutyl and monobutyl phosphate in a tributyl phosphate/nitric aqueous-phase system by electrospray mass spectrometry, *Anal Chem*, 2000, **72**, 1186–1191.

125 T. H. Siddall III, Effects of structure of N, N-disubstituted amides on their extraction of actinide and zirconium nitrates and of nitric acid1, *J Phys Chem*, 1960, **64**, 1863–1866.

126 T. H. Siddall III, *Bidentate Organophosphorus Compounds as Extractants. I. Extraction of Cerium, Promethium, and Americium Nitrates*, Du Pont de Nemours (EI) & Co. Savannah River Lab., Aiken, SC, 1962.

127 K. De Jesus, R. Rodriguez, D. L. Baek, R. V Fox, S. Pashikanti and K. Sharma, Extraction of lanthanides and actinides present in spent nuclear fuel and in electronic waste, *J Mol Liq*, 2021, **336**, 116006.

128 S. A. Ansari, P. Pathak, P. K. Mohapatra and V. K. Manchanda, Aqueous partitioning of minor actinides by different processes, *Separation & Purification Reviews*, 2011, **40**, 43–76.

129 N. Condamines and C. Musikas, The extraction by NN-dialkylamides. II. Extraction of actinide cations, *Solvent extraction and ion exchange*, 1992, **10**, 69–100.

130 G. Thiollet and C. Musikas, Synthesis and uses of the amides extractants, *Solvent Extraction and Ion Exchange*, 1989, **7**, 813–827.

131 N. Condamines and C. Musikas, THE EXTRACTION BY N, N-DIALKYLAMIDES. I. HNO3 AND OTHER INORGANIC ACIDS., *Solvent extraction and ion exchange*, 1988, **6**, 1007–1034.

132 G. M. Casparini and G. Grossi, Application of N, N-dialkyl aliphatic amides in the separation of some actinides, *Sep Sci Technol*, 1980, **15**, 825–844.

133 K. McCann, B. J. Mincher, N. C. Schmitt and J. C. Braley, Hexavalent actinide extraction using N, N-dialkyl amides, *Ind Eng Chem Res*, 2017, **56**, 6515–6519.

134 S. Suzuki, Y. Sasaki, T. Yaita and T. Kimura, *Study on selective separation of uranium by N, N-dialkyl-amide in ARTIST process*, Department of Materials Science, 2004.

135 P. Moeyaert, T. Dumas, D. Guillaumont, K. Kvashnina, C. Sorel, M. Miguirditchian, P. Moisy and J.-F. Dufrêche, Modeling and speciation study of uranium (VI) and technetium (VII) coextraction with DEHiBA, *Inorg Chem*, 2016, **55**, 6511–6519.

136 J. Drader, G. Saint-Louis, J. M. Muller, M. C. Charbonnel, P. Guilbaud, L. Berthon, K. M. Roscioli-Johnson, C. A. Zarzana, C. Rae and G. S. Groenewold, Radiation chemistry of the branched-chain monoamide di-2-ethylhexyl-isobutyramide, *Solvent Extraction and Ion Exchange*, 2017, **35**, 480–495.

137 D. Prabhu, G. Mahajan and G. Nair, Di (2-ethyl hexyl) butyramide and di (2-ethyl hexyl) isobutyramide as extractants for uranium (VI) and plutonium (IV), *J Radioanal Nucl Chem*, 1997, **224**, 113–117.

138 K. McCann, B. J. Mincher, N. C. Schmitt and J. C. Braley, Hexavalent actinide extraction using N, N-dialkyl amides, *Ind Eng Chem Res*, 2017, **56**, 6515–6519.

139 P. N. Pathak, L. B. Kumbhare and V. K. Manchanda, Structural effects in N, N-dialkyl amides on their extraction behavior toward uranium and thorium, *Solvent Extraction and Ion Exchange*, 2001, **19**, 105–126.

140 K. McCann, J. A. Drader and J. C. Braley, Comparing branched versus straight-chained monoamide extractants for actinide recovery, *Separation & Purification Reviews*, 2018, **47**, 49–65.

141 V. K. Manchanda, P. B. Ruikar, S. Sriram, M. S. Nagar, P. N. Pathak, K. K. Gupta, R. K. Singh, R. R. Chitnis, P. S. Dhami and A. Ramanujam, Distribution behavior of U (VI), Pu (IV), Am (III), and Zr (IV) with N, N-dihexyl octanamide under uranium-loading conditions, *Nucl Technol*, 2001, **134**, 231–240.

142 N. Kumari, P. N. Pathak, D. R. Prabhu and V. K. Manchanda, Comparison of extraction behavior of neptunium from nitric acid medium employing tri-n-butyl phosphate and N, N-dihexyl octanamide as extractants, *Sep Sci Technol*, 2012, **47**, 1492–1497.

143 G. M. Gasparini and G. Grossi, Review article long chain disubstituted aliphatic amides as extracting agents in industrial applications of solvent extraction, *Solvent Extraction and Ion Exchange*, 1986, **4**, 1233–1271.

144 J. M. Gogolski and M. P. Jensen, Using N, N-dialkylamides for neptunium purification from other actinides for space applications, *Sep Sci Technol*, 2021, **56**, 2775–2788.

145 J. M. Gogolski, P. R. Zalupski, T. S. Grimes and M. P. Jensen, Neptunium extraction by N, N-dialkylamides, *Radiochim Acta*, 2020, **108**, 707–716.

146 C. D. Hurd and R. I. Mori, On acylhydrazones and 1, 2, 3-thiadiazoles, *J Am Chem Soc*, 1955, **77**, 5359–5364.

147 P. Four and F. Guibe, Palladium-catalyzed reaction of tributyltin hydride with acyl chlorides. A mild, selective, and general route to aldehydes, *J Org Chem*, 1981, **46**, 4439–4445.

148 T. P. Smyth and B. W. Corby, Industrially viable alternative to the friedel− crafts acylation reaction: tamoxifen case study, *Org Process Res Dev*, 1997, **1**, 264–267.

149 A. Hadfield, H. Schweitzer, M. P. Trova and K. Green, Practical, large-scale synthesis of 2, 2-dimethyl-5-hydroxy-4-oxo-benzo-1, 4-dioxin, *Synth Commun*, 1994, **24**, 1025–1028.

150 V. R. Pattabiraman and J. W. Bode, Rethinking amide bond synthesis, *Nature*, 2011, **480**, 471–479.

151 C. A. G. N. Montalbetti and V. Falque, Amide bond formation and peptide coupling, *Tetrahedron*, 2005, **61**, 10827–10852.

152 C. L. Allen and J. M. J. Williams, Metal-catalysed approaches to amide bond formation, *Chem Soc Rev*, 2011, **40**, 3405–3415.

153 R. M. De Figueiredo, J.-S. Suppo and J.-M. Campagne, Nonclassical routes for amide bond formation, *Chem Rev*, 2016, **116**, 12029–12122.

154 E. Valeur and M. Bradley, Amide bond formation: beyond the myth of coupling reagents, *Chem Soc Rev*, 2009, **38**, 606–631.

155 M. T. Sabatini, L. T. Boulton, H. F. Sneddon and T. D. Sheppard, A green chemistry perspective on catalytic amide bond formation, *Nat Catal*, 2019, **2**, 10–17.

156 T. Shaw, A. D. Clayton, R. Labes, T. M. Dixon, S. Boyall, O. J. Kershaw, R. A. Bourne and B. C. Hanson, A self-optimised approach to synthesising DEHiBA for advanced nuclear reprocessing, exploiting the power of machine-learning, *React Chem Eng*, 2024, **9**, 426–438.

157 K. H. Bleicher, H.-J. Böhm, K. Müller and A. I. Alanine, Hit and lead generation: beyond high-throughput screening, *Nat Rev Drug Discov*, 2003, **2**, 369–378.

158 N. M. Morato, M. T. Le, D. T. Holden and R. Graham Cooks, Automated high-throughput system combining small-scale synthesis with bioassays and reaction screening, *SLAS TECHNOLOGY: Translating Life Sciences Innovation*, 2021, **26**, 555–571.

159 J. A. Grzyb, M. Shen, C. Yoshina-Ishii, W. Chi, R. S. Brown and R. A. Batey, Carbamoylimidazolium and thiocarbamoylimidazolium salts: novel reagents for the synthesis of ureas, thioureas, carbamates, thiocarbamates and amides, *Tetrahedron*, 2005, **61**, 7153–7175.

160 J. A. Grzyb and R. A. Batey, Carbamoylimidazolium salts as diversification reagents: an application to the synthesis of tertiary amides from carboxylic acids, *Tetrahedron Lett*, 2003, **44**, 7485–7488.

161 P. N. Pathak, R. Veeraraghavan, D. R. Prabhu, G. R. Mahajan and V. K. Manchanda, Separation studies of uranium and thorium using di-2-ethylhexyl isobutyramide (D2EHIBA), *Sep Sci Technol*, 1999, **34**, 2601–2614.

162 Y. Ban, S. Hotoku, Y. Tsubata and Y. Morita, Uranium and plutonium extraction from nitric acid by N, N-di (2-ethylhexyl)-2, 2-dimethylpropanamide (DEHDMPA) and N, N-di (2-ethylhexyl) butanamide (DEHBA) using mixer-settler extractors, *Solvent Extraction and Ion Exchange*, 2014, **32**, 348–364.

163 F. Rodrigues, G. Ferru, L. Berthon, N. Boubals, P. Guilbaud, C. Sorel, O. Diat, P. Bauduin, J. P. Simonin and J.-P. Morel, New insights into the extraction of uranium (VI) by an N, N-dialkylamide, *Mol Phys*, 2014, **112**, 1362–1374.

164 P. Moeyaert, T. Dumas, D. Guillaumont, K. Kvashnina, C. Sorel, M. Miguirditchian, P. Moisy and J.-F. Dufrêche, Modeling and speciation study of uranium (VI) and technetium (VII) coextraction with DEHiBA, *Inorg Chem*, 2016, **55**, 6511–6519.

165 M. Pleines, M. Hahn, J. Duhamet and T. Zemb, A minimal predictive model for better formulations of solvent phases with low viscosity, *EPJ N-Nuclear Sciences & Technologies*, 2020, **6**, 3.

166 C. Musikas, N. Condamines and C. Cuillerdier, Separation chemistry for the nuclear industry, *Analytical sciences*, 1991, **7**, 11–16.

167 B. Gannaz, R. Chiarizia, M. R. Antonio, C. Hill and G. Cote, Extraction of lanthanides (III) and Am (III) by mixtures of malonamide and dialkylphosphoric acid, *Solvent Extraction and Ion Exchange*, 2007, **25**, 313–337.

168 S. Kannan, M. A. Moody, C. L. Barnes and P. B. Duval, Lanthanum (III) and uranyl (VI) diglycolamide complexes: synthetic precursors and structural studies involving nitrate complexation, *Inorg Chem*, 2008, **47**, 4691–4695.

169 C. Cuillerdier, C. Musikas, P. Hoel, L. Nigond and X. Vitart, Malonamides as new extractants for nuclear waste solutions, *Sep Sci Technol*, 1991, **26**, 1229–1244.

170 G. R. Mahajan, D. R. Prabhu, V. K. Manchanda and L. P. Badheka, Substituted malonamides as extractants for partitioning of actinides from nuclear waste solutions, *Waste Management*, 1998, **18**, 125–133.

171 A. B. Patil, V. S. Shinde, P. N. Pathak, P. K. Mohapatra and V. K. Manchanda, Modified synthesis scheme for N, N-dimethyl-N, N-dioctyl-2,(2-hexyloxyethyl) malonamide (DMDOHEMA) and its comparison with proposed solvents for actinide partitioning, *Radiochim Acta*, 2013, **101**, 93–100.

172 Y. Sasaki and R. Choppin, Solvent extraction of Eu, Th, U, Np and Am with N, N'-dimethyl-N, N'-dihexyl-3-oxapentanediamide and its analogous compounds, *Analytical sciences*, 1996, **12**, 225–230.

173 Y. Sasaki, Y. Sugo, K. Morita and K. L. Nash, The effect of alkyl substituents on actinide and lanthanide extraction by diglycolamide compounds, *Solvent Extraction and Ion Exchange*, 2015, **33**, 625–641.

174 A. Sengupta, A. Bhattacharyya, W. Verboom, S. M. Ali and P. K. Mohapatra, Insight into the complexation of actinides and lanthanides with diglycolamide derivatives: experimental and density functional theoretical studies, *J Phys Chem B*, 2017, **121**, 2640–2649.

175 P. Deepika, K. N. Sabharwal, T. G. Srinivasan and P. R. Vasudeva Rao, Studies on the use of N, N, N, N-tetra (2-ethylhexyl) diglycolamide (TEHDGA) for actinide partitioning. I: Investigation on third-phase formation and extraction behavior, *Solvent Extraction and Ion Exchange*, 2010, **28**, 184–201.

176 P. Deepika, K. N. Sabharwal, T. G. Srinivasan and P. R. Vasudeva Rao, Studies on the use of N, N, N', N'-tetra (2-ethylhexyl) diglycolamide (TEHDGA) for actinide partitioning II: Investigation on radiolytic stability, *Solvent Extraction and Ion Exchange*, 2011, **29**, 230–246.

177 M. Iqbal, J. Huskens, W. Verboom, M. Sypula and G. Modolo, Synthesis and Am/Eu extraction of novel TODGA derivatives, *Supramol Chem*, 2010, **22**, 827–837.

178 E. Massolo, M. Pirola and M. Benaglia, Amide bond formation strategies: Latest advances on a dateless transformation, *European J Org Chem*, 2020, **2020**, 4641–4651.

179 N. Shimada, M. Hirata, M. Koshizuka, N. Ohse, R. Kaito and K. Makino, Diboronic acid anhydrides as effective catalysts for the hydroxy-directed dehydrative amidation of carboxylic acids, *Org Lett*, 2019, **21**, 4303–4308.

180 A. Taussat, R. M. de Figueiredo and J.-M. Campagne, Direct catalytic amidations from carboxylic acid and ester derivatives: A review, *Catalysts*, 2023, **13**, 366.

181 Z. Zhang, Y.-H. Liu, X. Zhang and X.-C. Wang, KMnO4-mediated oxidative CN bond cleavage of tertiary amines: Synthesis of amides and sulfonamides, *Tetrahedron*, 2019, **75**, 2763–2770.

182 D. C. Braddock, P. D. Lickiss, B. C. Rowley, D. Pugh, T. Purnomo, G. Santhakumar and S. J. Fussell, Tetramethyl orthosilicate (TMOS) as a reagent for direct amidation of carboxylic acids, *Org Lett*, 2018, **20**, 950–953.

183 D. D. S. Sharley and J. M. J. Williams, Acetic acid as a catalyst for the N-acylation of amines using esters as the acyl source, *Chemical Communications*, 2017, **53**, 2020–2023.

184 D. J. C. Constable, P. J. Dunn, J. D. Hayler, G. R. Humphrey, J. L. Leazer Jr, R. J. Linderman, K. Lorenz, J. Manley, B. A. Pearlman and A. Wells, Key green chemistry research areas—a perspective from pharmaceutical manufacturers, *Green Chemistry*, 2007, **9**, 411–420.

185 M. C. Bryan, P. J. Dunn, D. Entwistle, F. Gallou, S. G. Koenig, J. D. Hayler, M. R. Hickey, S. Hughes, M. E. Kopach and G. Moine, Key Green Chemistry research areas from a pharmaceutical manufacturers' perspective revisited, *Green Chemistry*, 2018, **20**, 5082–5103.

186 J. R. Dunetz, J. Magano and G. A. Weisenburger, Large-scale applications of amide coupling reagents for the synthesis of pharmaceuticals, *Org Process Res Dev*, 2016, **20**, 140–177.

187 N. Nakajima and Y. Ikada, Mechanism of amide formation by carbodiimide for bioconjugation in aqueous media, *Bioconjug Chem*, 1995, **6**, 123–130.

188 A. Leoncini, J. Huskens and W. Verboom, Preparation of Diglycolamides via Schotten–Baumann Approach and Direct Amidation of Esters, *Synlett*, 2016, **27**, 2463–2466.

189 M. R. Petchey and G. Grogan, Enzyme-catalysed synthesis of secondary and tertiary amides, *Adv Synth Catal*, 2019, **361**, 3895–3914.

190 M. S. Brown, M. A. Caporello, A. E. Goetz, A. M. Johnson, K. N. Jones, K. M. Knopf, S. A. Kulkarni, T. Lee, B. Li and C. V Lu, Streamlined Synthesis of a Bicyclic Amine Moiety Using an Enzymatic Amidation and Identification of a Novel Solid Form, *Org Process Res Dev*, 2021, **25**, 1419–1430.

191 S. Rudnicki and S. Johnston, Overview of liquid handling instrumentation for high-throughput screening applications, *Curr Protoc Chem Biol*, 2009, **1**, 43–54.

192 L. M. Mayr and D. Bojanic, Novel trends in high-throughput screening, *Curr Opin Pharmacol*, 2009, **9**, 580–588.

193 L. M. Mayr and P. Fuerst, The future of high-throughput screening, *SLAS Discovery*, 2008, **13**, 443–448.

194 J. Bajorath, Integration of virtual and high-throughput screening, *Nat Rev Drug Discov*, 2002, **1**, 882–894.

195 R. P. Hertzberg and A. J. Pope, High-throughput screening: new technology for the 21st century, *Curr Opin Chem Biol*, 2000, **4**, 445–451.

196 J. R. Broach and J. Thorner, High-throughput screening for drug discovery, *Nature*, 1996, **384**, 14–16.

197 O. J. Kershaw, A. D. Clayton, J. A. Manson, A. Barthelme, J. Pavey, P. Peach, J. Mustakis, R. M. Howard, T. W. Chamberlain and N. J. Warren, Machine learning directed multi-objective optimisation of mixed variable chemical systems, *Chemical Engineering Journal*, 2023, **451**, 138443.

198 K. H. Tantawi, A. Sokolov and O. Tantawi, in *2019 4th Technology Innovation Management and Engineering Science International Conference (TIMES-iCON)*, IEEE, 2019, pp. 1–4.

199 Z. Jiang, S. Yuan, J. Ma and Q. Wang, The evolution of production scheduling from Industry 3.0 through Industry 4.0, *Int J Prod Res*, 2022, **60**, 3534–3554.

200 S. V. Mohan and R. Katakojwala, The circular chemistry conceptual framework: A way forward to sustainability in industry 4.0, *Curr Opin Green Sustain Chem*, 2021, **28**, 100434.

201 A. R. Bogdan and A. W. Dombrowski, Emerging trends in flow chemistry and applications to the pharmaceutical industry, *J Med Chem*, 2019, **62**, 6422–6468.

202 N. Hartrampf, A. Saebi, M. Poskus, Z. P. Gates, A. J. Callahan, A. E. Cowfer, S. Hanna, S. Antilla, C. K. Schissel and A. J. Quartararo, Synthesis of proteins by automated flow chemistry, *Science (1979)*, 2020, **368**, 980–987.

203 C. P. Breen, A. M. K. Nambiar, T. F. Jamison and K. F. Jensen, Ready, set, flow! Automated continuous synthesis and optimisation, *Trends Chem*, 2021, **3**, 373–386.

204 K. F. Jensen, Flow chemistry—microreaction technology comes of age, *AIChE Journal*, 2017, **63**, 858–869.

205 K. Boodhoo and A. Harvey, *Process intensification technologies for green chemistry: engineering solutions for sustainable chemical processing*, John Wiley & Sons, 2013.

206 V. Hessel, Novel process windows–gate to maximizing process intensification via flow chemistry, *Chemical Engineering & Technology: Industrial Chemistry-Plant Equipment-Process Engineering-Biotechnology*, 2009, **32**, 1655–1681.

207 M. B. Plutschack, B. Pieber, K. Gilmore and P. H. Seeberger, The hitchhiker's guide to flow chemistry‖, *Chem Rev*, 2017, **117**, 11796–11893.

208 R. Porta, M. Benaglia and A. Puglisi, Flow chemistry: recent developments in the synthesis of pharmaceutical products, *Org Process Res Dev*, 2016, **20**, 2–25.

209 M. Baumann, T. S. Moody, M. Smyth and S. Wharry, A perspective on continuous flow chemistry in the pharmaceutical industry, *Org Process Res Dev*, 2020, **24**, 1802–1813.

210 Y. Mo and K. F. Jensen, A miniature CSTR cascade for continuous flow of reactions containing solids, *React Chem Eng*, 2016, **1**, 501–507.

211 A. Lakshmanan and L. T. Biegler, Synthesis of optimal chemical reactor networks, *Ind Eng Chem Res*, 1996, **35**, 1344–1353.

212 D. L. Penry and P. A. Jumars, Modeling animal guts as chemical reactors, *Am Nat*, 1987, **129**, 69–96.

213 D. L. Penry and P. A. Jumars, Chemical reactor analysis and optimal digestion, *Bioscience*, 1986, **36**, 310–315.

214 S. Deepa, N. Anipriya and R. Subbulakshmy, Design of controllers for continuous stirred tank reactor, *International Journal of Power Electronics and Drive Systems*, 2015, **5**, 576.

215 P. Jaibiba, S. N. Vignesh and S. Hariharan, in *Bioreactors*, Elsevier, 2020, pp. 145–173.

216 Z. Arshad, A. J. Blacker, T. W. Chamberlain, N. Kapur, A. D. Clayton and R. A. Bourne, Droplet microfluidic flow platforms for automated reaction screening and optimisation, *Curr Opin Green Sustain Chem*, 2024, 100940.

217 V. Balakotaiah and D. Luss, Multiplicity features of reacting systems: dependence of the steady-states of a CSTR on the residence time, *Chem Eng Sci*, 1983, **38**, 1709–1721.

218 R. Krishna and S. T. Sie, Strategies for multiphase reactor selection, *Chem Eng Sci*, 1994, **49**, 4029–4065.

219 H. Song, D. L. Chen and R. F. Ismagilov, Reactions in droplets in microfluidic channels, *Angewandte chemie international edition*, 2006, **45**, 7336–7356.

220 N. 'Kapur and Asynt, fReactor Unlocking the Power of Flow Chemistry.

221 H. Wu, M. A. Khan and A. S. Hussain, Process control perspective for process analytical technology: integration of chemical engineering practice into semiconductor and pharmaceutical industries, *Chem Eng Commun*, 2007, **194**, 760–779.

222 I. R. Baxendale, The integration of flow reactors into synthetic organic chemistry, *Journal of Chemical Technology & Biotechnology*, 2013, **88**, 519–552.

223 S. Kobayashi, Flow "fine" synthesis: high yielding and selective organic synthesis by flow methods, *Chemistry–An Asian Journal*, 2016, **11**, 425–436.

224 S. V Ley, On being green: can flow chemistry help?, *The Chemical Record*, 2012, **12**, 378–390.

225 J. M. Coulson, J. F. Richardson, J. R. Backhurst and J. H. Harker, *Chemical Engineering: Fluid flow, heat transfer and mass transfer*, Pergamon press, 1990, vol. 1.

226 V. Hessel, Novel process windows–gate to maximizing process intensification via flow chemistry, *Chemical Engineering & Technology: Industrial Chemistry-Plant Equipment-Process Engineering-Biotechnology*, 2009, **32**, 1655–1681.

227 J. Wegner, S. Ceylan and A. Kirschning, Flow chemistry–a key enabling technology for (multistep) organic synthesis, *Adv Synth Catal*, 2012, **354**, 17–57.

228 A. D. Clayton, E. O. Pyzer-Knapp, M. Purdie, M. F. Jones, A. Barthelme, J. Pavey, N. Kapur, T. W. Chamberlain, A. J. Blacker and R. A. Bourne, Bayesian Self-Optimisation for Telescoped Continuous Flow Synthesis, *Angewandte Chemie*, 2023, **135**, e202214511.

229 S. Fuse, N. Tanabe and T. Takahashi, Continuous in situ generation and reaction of phosgene in a microflow system, *Chemical communications*, 2011, **47**, 12661–12663.

230 C. Wiles and P. Watts, Continuous flow reactors: a perspective, *Green Chemistry*, 2012, **14**, 38–54.

231 J. A. Bennett, Z. S. Campbell and M. Abolhasani, Role of continuous flow processes in green manufacturing of pharmaceuticals and specialty chemicals, *Curr Opin Chem Eng*, 2019, **26**, 9–19.

232 R. Heusch and B. A. G. Leverkusen, Ullmann's Encyclopedia of Industrial Chemistry, *Wiley-VCH, DOI*, 2000, **10**, a09_297.

233 R. Porta, M. Benaglia and A. Puglisi, Flow chemistry: recent developments in the synthesis of pharmaceutical products, *Org Process Res Dev*, 2016, **20**, 2–25.

234 M. Colombo and I. Peretto, Chemistry strategies in early drug discovery: an overview of recent trends, *Drug Discov Today*, 2008, **13**, 677–684.

235 E. López, M. L. Linares and J. Alcázar, Flow chemistry as a tool to access novel chemical space for drug discovery, *Future Med Chem*, 2020, **12**, 1547–1563.

236 M. Ding, R. Clark, C. Bardelle, A. Backmark, T. Norris, W. Williams, M. Wigglesworth and R. Howes, Application of high-throughput flow cytometry in early drug discovery: an AstraZeneca perspective, *SLAS Discovery: Advancing Life Sciences R&D*, 2018, **23**, 719–731.

237 A. R. Bogdan and A. W. Dombrowski, Emerging trends in flow chemistry and applications to the pharmaceutical industry, *J Med Chem*, 2019, **62**, 6422–6468.

238 R. L. Hartman, J. P. McMullen and K. F. Jensen, Deciding whether to go with the flow: evaluating the merits of flow reactors for synthesis, *Angewandte Chemie International Edition*, 2011, **50**, 7502–7519.

239 M. Baumann and I. R. Baxendale, The synthesis of active pharmaceutical ingredients (APIs) using continuous flow chemistry, *Beilstein journal of organic chemistry*, 2015, **11**, 1194–1219.

240 L. Buglioni, F. Raymenants, A. Slattery, S. D. A. Zondag and T. Noël, Technological innovations in photochemistry for organic synthesis: flow chemistry, high-throughput experimentation, scale-up, and photoelectrochemistry, *Chem Rev*, 2021, **122**, 2752–2906.

241 T. Razzaq and C. O. Kappe, Continuous flow organic synthesis under high-temperature/pressure conditions, *Chemistry–An Asian Journal*, 2010, **5**, 1274–1289.

242 V. Hessel, D. Kralisch, N. Kockmann, T. Noël and Q. Wang, Novel process windows for enabling, accelerating, and uplifting flow chemistry, *ChemSusChem*, 2013, **6**, 746–789.

243 C. Mateos, M. J. Nieves-Remacha and J. A. Rincón, Automated platforms for reaction self-optimisation in flow, *React Chem Eng*, 2019, **4**, 1536–1544.

244 C. P. Breen, A. M. K. Nambiar, T. F. Jamison and K. F. Jensen, Ready, set, flow! Automated continuous synthesis and optimisation, *Trends Chem*, 2021, **3**, 373–386.

245 N. Holmes, G. R. Akien, A. J. Blacker, R. L. Woodward, R. E. Meadows and R. A. Bourne, Self-optimisation of the final stage in the synthesis of EGFR kinase inhibitor AZD9291 using an automated flow reactor, *React Chem Eng*, 2016, **1**, 366–371.

246 M. K. Sharma, J. Raval, G.-N. Ahn, D.-P. Kim and A. A. Kulkarni, Assessing the impact of deviations in optimized multistep flow synthesis on the scale-up, *React Chem Eng*, 2020, **5**, 838–848.

247 D. A. Armbruster, D. R. Overcash and J. Reyes, Clinical chemistry laboratory automation in the 21st century-amat victoria curam (Victory loves careful preparation), *Clin Biochem Rev*, 2014, **35**, 143.

248 J. Villanueva, J. Philip, D. Entenberg, C. A. Chaparro, M. K. Tanwar, E. C. Holland and P. Tempst, Serum peptide profiling by magnetic particle-assisted, automated sample processing and MALDI-TOF mass spectrometry, *Anal Chem*, 2004, **76**, 1560–1570.

249 C. De Bellefon, R. Abdallah, T. Lamouille, N. Pestre, S. Caravieilhes and P. Grenouillet, High-throughput screening of molecular catalysts using automated liquid handling, injection, and microdevices, *Chimia (Aarau)*, 2002, **56**, 621.

250 K. C. Felton, J. G. Rittig and A. A. Lapkin, Summit: benchmarking machine learning methods for reaction optimisation, *Chemistry-Methods*, 2021, **1**, 116–122.

251 R. Carlson and J. E. Carlson, *Design and optimisation in organic synthesis*, Elsevier, 2005.

252 D. E. Fitzpatrick and S. V Ley, Engineering chemistry for the future of chemical synthesis, *Tetrahedron*, 2018, **74**, 3087–3100.

253 S. M. Mugo and K. Ayton, Lipase immobilized methacrylate polymer monolith microreactor for lipid transformations and online analytics, *J Am Oil Chem Soc*, 2013, **90**, 65–72.

254 D. Hebrault, A. J. Rein and B. Wittkamp, Chemical knowledge via in situ analytics: advancing quality and sustainability, *ACS Sustain Chem Eng*, 2022, **10**, 5072–5077.

255 D. C. Fabry, E. Sugiono and M. Rueping, Online monitoring and analysis for autonomous continuous flow self-optimizing reactor systems, *React Chem Eng*, 2016, **1**, 129–133.

256 P. Sagmeister, R. Lebl, I. Castillo, J. Rehrl, J. Kruisz, M. Sipek, M. Horn, S. Sacher, D. Cantillo and J. D. Williams, Advanced real-time process analytics for multistep synthesis in continuous flow, *Angewandte Chemie International Edition*, 2021, **60**, 8139–8148.

257 F. Fanelli, G. Parisi, L. Degennaro and R. Luisi, Contribution of microreactor technology and flow chemistry to the development of green and sustainable synthesis, *Beilstein Journal of Organic Chemistry*, 2017, **13**, 520–542.

258 S. V Ley, On being green: can flow chemistry help?, *The Chemical Record*, 2012, **12**, 378–390.

259 W. Huyer and A. Neumaier, SNOBFIT--stable noisy optimisation by branch and fit, *ACM Transactions on Mathematical Software (TOMS)*, 2008, **35**, 1–25.

260 A. D. Clayton, J. A. Manson, C. J. Taylor, T. W. Chamberlain, B. A. Taylor, G. Clemens and R. A. Bourne, Algorithms for the self-optimisation of chemical reactions, *React Chem Eng*, 2019, **4**, 1545–1554.

261 E. Bradford, A. M. Schweidtmann and A. Lapkin, Efficient multiobjective optimisation employing Gaussian processes, spectral sampling and a genetic algorithm, *Journal of global optimisation*, 2018, **71**, 407–438.

262 A. M. Schweidtmann, A. D. Clayton, N. Holmes, E. Bradford, R. A. Bourne and A. A. Lapkin, Machine learning meets continuous flow chemistry: Automated optimisation towards the Pareto front of multiple objectives, *Chemical Engineering Journal*, 2018, **352**, 277–282.

263 A. D. Clayton, J. A. Manson, C. J. Taylor, T. W. Chamberlain, B. A. Taylor, G. Clemens and R. A. Bourne, Algorithms for the self-optimisation of chemical reactions, *React Chem Eng*, 2019, **4**, 1545–1554.

264 A. D. Clayton, L. A. Power, W. R. Reynolds, C. Ainsworth, D. R. J. Hose, M. F. Jones, T. W. Chamberlain, A. J. Blacker and R. A. Bourne, Self-optimising reactive extractions: towards the efficient development of multi-step continuous flow processes, *J Flow Chem*, 2020, **10**, 199–206.

265 A. D. Clayton, A. M. Schweidtmann, G. Clemens, J. A. Manson, C. J. Taylor, C. G. Niño, T. W. Chamberlain, N. Kapur, A. J. Blacker and A. A. Lapkin, Automated self-optimisation of multi-step reaction and separation processes using machine learning, *Chemical Engineering Journal*, 2020, **384**, 123340.

266 M. I. Jeraal, N. Holmes, G. R. Akien and R. A. Bourne, Enhanced process development using automated continuous reactors by self-optimisation algorithms and statistical empirical modelling, *Tetrahedron*, 2018, **74**, 3158–3164.

267 B. L. Hall, C. J. Taylor, R. Labes, A. F. Massey, R. Menzel, R. A. Bourne and T. W. Chamberlain, Autonomous optimisation of a nanoparticle catalysed reduction reaction in continuous flow, *Chemical Communications*, 2021, **57**, 4926–4929.

268 C. Khositanon, K. Adpakpang, S. Bureekaew and N. Weeranoppanant, Continuous-flow purification of silver nanoparticles and its integration with flow synthesis, *J Flow Chem*, 2020, **10**, 353–362.

269 N. Weeranoppanant, A. Adamo, G. Saparbaiuly, E. Rose, C. Fleury, B. Schenkel and K. F. Jensen, Design of multistage counter-current liquid–liquid extraction for small-scale applications, *Ind Eng Chem Res*, 2017, **56**, 4095–4103.

270 L. Yang, N. Weeranoppanant and K. F. Jensen, Characterization and modeling of the operating curves of membrane microseparators, *Ind Eng Chem Res*, 2017, **56**, 12184–12191.

271 K. K. Sirkar, Membrane separation technologies: current developments, *Chem Eng Commun*, 1997, **157**, 145–184.

272 R. Rautenbach and R. Albrecht, Membrane separation processes.

273 A. Adamo, P. L. Heider, N. Weeranoppanant and K. F. Jensen, Membrane-based, liquid–liquid separator with integrated pressure control, *Ind Eng Chem Res*, 2013, **52**, 10802–10808.

274 J. Daglish, A. J. Blacker, G. de Boer, S. J. Russell, M. Tausif, D. R. J. Hose, A. R. Parsons, A. Crampton and N. Kapur, A Coalescing Filter for Liquid–Liquid Separation and Multistage Extraction in Continuous-Flow Chemistry, *Org Process Res Dev*, 2024, **28**, 1979–1989.

275 A. Tessier, P. G. C. Campbell and M. Bisson, Sequential extraction procedure for the speciation of particulate trace metals, *Anal Chem*, 1979, **51**, 844–851.

276 N. Condamines and C. Musikas, THE EXTRACTION BY N, N-DIALKYLAMIDES. I. HNO3 AND OTHER INORGANIC ACIDS., *Solvent extraction and ion exchange*, 1988, **6**, 1007–1034.

277 N. Condamines and C. Musikas, The extraction by NN-dialkylamides. II. Extraction of actinide cations, *Solvent extraction and ion exchange*, 1992, **10**, 69–100.

278 M. L. Hill, C. Pereira and A. G. Servis, Kinetics and Mechanism of Ce (IV) Phase Transfer by the Neutral Extractants Tributyl Phosphate and N, N-Di (2-ethylhexyl) isobutyramide, *Ind Eng Chem Res*.

279 J. Drader, G. Saint-Louis, J. M. Muller, M. C. Charbonnel, P. Guilbaud, L. Berthon, K. M. Roscioli-Johnson, C. A. Zarzana, C. Rae and G. S. Groenewold, Radiation chemistry of the branched-chain monoamide di-2-ethylhexyl-isobutyramide, *Solvent Extraction and Ion Exchange*, 2017, **35**, 480–495.

280 G. M. Gasparini and G. Grossi, Review article long chain disubstituted aliphatic amides as extracting agents in industrial applications of solvent extraction, *Solvent Extraction and Ion Exchange*, 1986, **4**, 1233–1271.

281 E. R. Bertelsen, M. R. Antonio, M. P. Jensen and J. C. Shafer, Electrochemistry of PUREX: R is for reduction and ion transfer, *Solvent Extraction and Ion Exchange*, 2022, **40**, 64–85.

282 H. A. C. McKay, in *Science and technology of tribuytl phosphate*, 1990.

283 J. M. McKibben, Chemistty of the purex process, *Radiochim Acta*, 1984, **36**, 3–16.

284 R. S. Herbst, P. Baron and M. Nilsson, in *Advanced separation techniques for nuclear fuel reprocessing and radioactive waste treatment*, Elsevier, 2011, pp. 141–175.

285 W. B. Lanham and T. C. Runion, *PUREX process for plutonium and uranium recovery*, Oak Ridge National Lab.(ORNL), Oak Ridge, TN (United States), 1949.

286 J. E. Birkett, M. J. Carrott, O. D. Fox, C. J. Jones, C. J. Maher, C. V Roube, R. J. Taylor and D. A. Woodhead, Recent developments in the Purex process for nuclear fuel reprocessing: Complexant based stripping for uranium/plutonium separation, *Chimia (Aarau)*, 2005, **59**, 898.

287 G. Modolo, A. Wilden, A. Geist, D. Magnusson and R. Malmbeck, A review of the demonstration of innovative solvent extraction processes for the recovery of trivalent minor actinides from PUREX raffinate, *Radiochim Acta*, 2012, **100**, 715–725.

288 R. J. Taylor, C. R. Gregson, M. J. Carrott, C. Mason and M. J. Sarsfield, Progress towards the full recovery of neptunium in an advanced PUREX process, *Solvent Extraction and Ion Exchange*, 2013, **31**, 442–462.

289 J. Drader, G. Saint-Louis, J. M. Muller, M. C. Charbonnel, P. Guilbaud, L. Berthon, K. M. Roscioli-Johnson, C. A. Zarzana, C. Rae and G. S. Groenewold, Radiation chemistry of the branched-chain monoamide di-2-ethylhexyl-isobutyramide, *Solvent Extraction and Ion Exchange*, 2017, **35**, 480–495.

290 M. Salvatores and G. Palmiotti, Radioactive waste partitioning and transmutation within advanced fuel cycles: Achievements and challenges, *Prog Part Nucl Phys*, 2011, **66**, 144–166.

291 T. A. Kurniawan, M. H. D. Othman, D. Singh, R. Avtar, G. H. Hwang, T. Setiadi and W. Lo, Technological solutions for long-term storage of partially used nuclear waste: A critical review, *Ann Nucl Energy*, 2022, **166**, 108736.

292 R. S. Herbst, P. Baron and M. Nilsson, in *Advanced separation techniques for nuclear fuel reprocessing and radioactive waste treatment*, Elsevier, 2011, pp. 141–175.

293 S. Bourg, A. Geist and J. Narbutt, SACSESS–the EURATOM FP7 project on actinide separation from spent nuclear fuels, *Nukleonika*, 2015, **60**, 809–814.

294 C. Poinssot, C. Rostaing, P. Baron, D. Warin and B. Boullis, Main results of the French program on partitioning of minor actinides, a significant improvement towards nuclear waste reduction, *Procedia Chem*, 2012, **7**, 358–366.

295 R. Malmbeck, D. Magnusson, S. Bourg, M. Carrott, A. Geist, X. Hérès, M. Miguirditchian, G. Modolo, U. Müllich and C. Sorel, Homogenous recycling of transuranium elements from irradiated fast reactor fuel by the EURO-GANEX solvent extraction process, *Radiochim Acta*, 2019, **107**, 917–929.

296 R. Malmbeck, D. Magnusson, S. Bourg, M. Carrott, A. Geist, X. Hérès, M. Miguirditchian, G. Modolo, U. Müllich and C. Sorel, Homogenous recycling of transuranium elements from irradiated fast reactor fuel by the EURO-GANEX solvent extraction process, *Radiochim Acta*, 2019, **107**, 917–929.

297 A. Tessier, P. G. C. Campbell and M. Bisson, Sequential extraction procedure for the speciation of particulate trace metals, *Anal Chem*, 1979, **51**, 844–851.

298 J. Daglish, A. J. Blacker, G. de Boer, S. J. Russell, M. Tausif, D. R. J. Hose, A. R. Parsons, A. Crampton and N. Kapur, A Coalescing Filter for Liquid–Liquid Separation and Multistage Extraction in Continuous-Flow Chemistry, *Org Process Res Dev*, 2024, **28**, 1979–1989.

Chapter 2: A Self-Optimised Approach to Synthesising DEHiBA for Advanced Nuclear Reprocessing, Exploiting the Power of Machine-Learning

Thomas Shaw, Adam D. Clayton, Ricardo Labes, Thomas M. Dixon, Sarah Boyall, Oliver J. Kershaw, Richard A. Bourne and Bruce C. Hanson

2.1 Abstract

In an effort to advance the development of hydrometallurgical reprocessing of used nuclear fuel across the globe, this work sets out to explore and identify an optimised cost-effective pathway to synthesise the ligand DEHiBA (N,N-di-(2-ethylhexyl)isobutyramide). Currently, very few chemical suppliers stock and distribute this specialist ligand, designed for the purpose of selective uranium chelation and extraction from nuclear fuel. The high cost of DEHiBA therefore restricts access to essential large-scale testing of this promising ligand designed to advance nuclear reprocessing. This work utilises an automated flow reactor platform for the efficient optimisation of four synthetic routes to DEHiBA. These optimisations focus on optimising cost, reagent efficiency, yield and productivity target functions by exploiting the power of machine-learning algorithms for rapid process development. Ultimately, we have identified an efficient and cost-effective solvent-free route to DEHiBA from isobutyric anhydride and di-2-ethylhexylamine for <£100 (current prices) per litre of DEHiBA in reagent costs enabling affordable access to litres of this material for subsequent testing. The exothermic nature of this reaction proved that a tubular flow reactor mitigated this safety risk, whilst also continuously producing crude DEHiBA with yields up to

99+% at a purity of 76% and a process mass intensity of 1.29 g g^{-1} with conditions also capable of productivities around 75 kg L^{-1} h^{-1}, all whilst maintaining a high level of process control with outlet temperatures not exceeding 35 °C.

2.2 Introduction

The demand for nuclear energy has surged in recent years due to a global drive toward sustainability. In line with this, the UK government stated in its 2020 energy white paper that nuclear energy would play a key role in decarbonising Britain over the next 30 years,[1] which has resulted in multi-billion pound investments in large nuclear reactors at Hinkley and Sizewell. The recent rise in interest towards nuclear fission as a means to not only decarbonise power, but other, "more difficult to decarbonise industries",[2-4] brings the question of how sustainable is nuclear fission as a whole? The clean energy benefits and low carbon emissions associated with energy production from nuclear power is indisputable.[5, 6] Yet, an open fuel cycle remains popular for most, despite its unsustainable nature.[7-9] To improve the sustainability of nuclear fission the appropriate management of used nuclear fuel is vital for nuclear fission to be sustainable for future generations over a long time-frame. Currently, two overarching routes exist for the management of used nuclear fuel: direct disposal in geological facilities, and nuclear reprocessing/recycle.[10] For nuclear fission to be truly sustainable, the employment of a closed fuel cycle that avoids wasting this valuable resource, rich in elements from across the periodic table, is critical.[10-13] Yet, at present, few reprocessing facilities are in operation and these only employ the limited, but mature PUREX (Plutonium Uranium Reduction EXtraction) process for the selective extraction of uranium and plutonium.[14-17] This selective extraction is achieved through a series of liquid-liquid extractions and is governed by the ligand tri-n-butyl phosphate (TBP).[18-20]

The selectivity of hydrometallurgical reprocessing is defined by organic ligands like TBP, due to their affinity for chelation of specific metal ions.[21, 22] To enhance the capability of nuclear reprocessing, researchers have developed and tested a host of different ligands over a series of decades.[23-26] Dialkylamide and diamide ligands are two successful groups of ligands for the removal of long-lived radionuclides such as the actinides, with the dialkylamide, DEHiBA (*N*,*N*-di-(2-ethylhexyl)isobutyramide) proving to be an ideal replacement for TBP.[11, 27-29] DEHiBA offers improved selectively for uranium and does not extract plutonium,[30-32] thus enhances proliferation resistance for processes that employ DEHiBA like the GANEX (Grouped Actinide Extraction) process.[33, 34] Notably, the GANEX second cycle flowsheets employ more complex ligands like the diamides to facilitate transuranic extraction downstream.[35-37] Recent publications from Hall et al. highlight the continued interest and relevance of DEHiBA for the selective extraction of uranium, their research focussing on process intensification of uranium extraction, ensuring performance under various conditions.[38, 39]

The specialist nature of DEHiBA makes it a high-cost research material with limited suppliers. This is not only detrimental to the economics of advanced reprocessing, but also restricts access to research in this field, in particular large-scale performance testing that is necessary to further the technology readiness level. A less costly approach is to synthesise ligands like DEHiBA in-house using procedures outlined in the available literature,[40] with Thiollet and Musikas being frequently referenced.[41] This approach employs isobutyryl chloride (iBCl), triethylamine, and di-(2-ethylhexyl)amine (DiEHA) to yield DEHiBA, via an effective method in a lab environment. Unfortunately, iBCl is currently more costly than alternative materials such as isobutyric acid (iBA), whilst also being highly toxic, halogenated, and violently reacting with water, thus being unfavourable for scale-up. These issues are avoidable through alternative synthetic pathways (**Figure 26**). An ideal manufacture process for DEHiBA would minimise the use of toxic/hazardous

reagents, avoid halogenated reagents and solvents whilst minimising process mass intensity (PMI) in order to reduce safety concerns and reduce environmental impact. Desirably one condition would grant minimum reagent cost, with little trade-off between productivity and reaction mass efficiency (RME), finally a high yield with minimal by-products will reduce downstream purification costs.

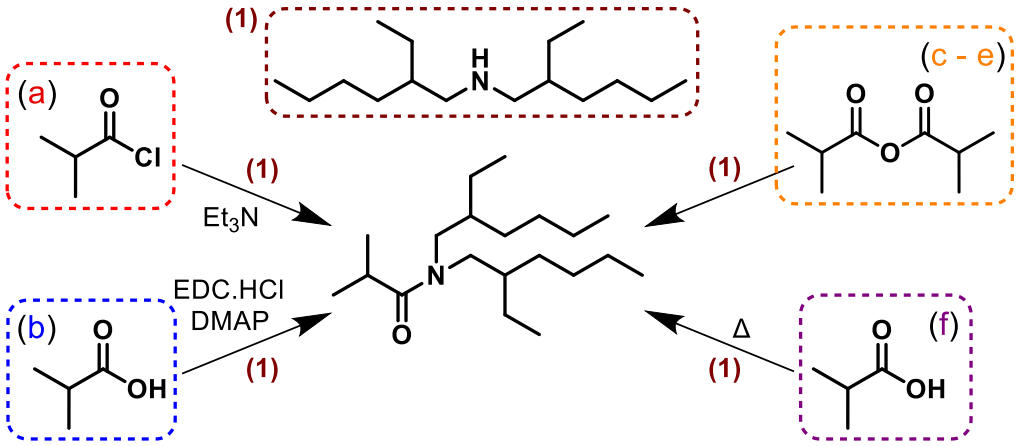

Figure 26: Four synthetic pathways to DEHiBA, (a-f) are the different routes that have been investigated in this work, where routes (c-e) represent one synthetic pathway but with different solvent systems.

To identify the optimum route and conditions to DEHiBA, each process will be optimised and compared in this work. Traditionally this can take months if not years to find an optimised solution depending on the chemistry and objectives chosen. However, recent advances at the interface between chemistry, chemical engineering and computer science has led to the development of platforms capable of rapid process development and optimisation.[42-48] The emergence and success of these technologies has been largely driven and adopted by academia with the chemical industry to save valuable time and money needed for chemical development.[49-51] Self-optimising flow reactors that utilise machine-learning algorithms in conjunction with online/inline analysis and a feedback loop are one of these technologies that has gained considerable interest of late.[47, 52] These advanced chemical reactors, automatically adjust operating conditions depending on the reaction outcome in order to optimise reaction performance.[52-58] As traditional process optimisation

campaigns are renowned for being research and labour intensive, the utilisation of these more efficient, machine learning driven technologies (**Figure 27**), enables the reduction of chemical consumption, labour, risk, and optimisation time-lines.[53, 59, 60] Furthermore, a continuous flow process facilitates continuous manufacture with enhanced process control, offering high product throughput with the beneficial ease of real-time process monitoring.[47]

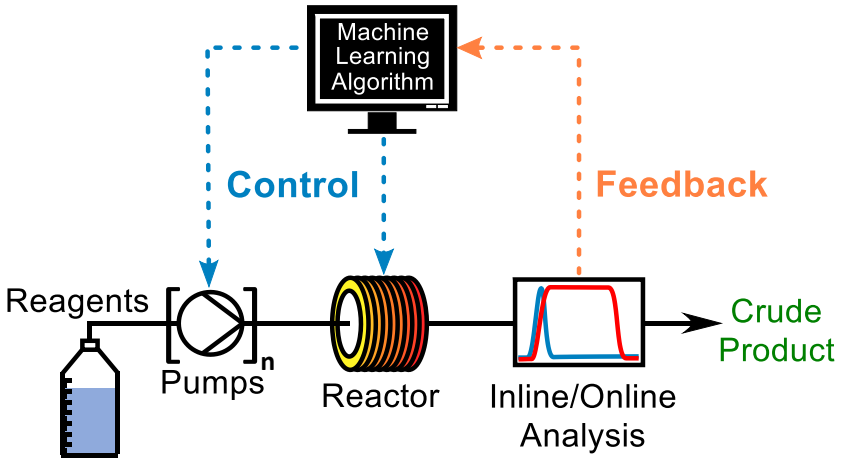

Figure 27: An illustration of a self-optimising flow reactor platform for the automated process optimisation of chemical reactions.

In this work we have employed self-optimising flow reactor platforms to optimise key process metrics of the four synthetic pathways to DEHiBA. This data has enabled identification of the best performing route for the large-scale manufacture of DEHiBA in continuous flow. Tubular flow was utilised for its ease of access to more expansive operating windows such as pressures over 200 bar and temperatures well in excess of typical boiling points when compared to batch chemistry.[61] This facilitated process intensification of each route and enhanced reaction kinetic understanding, all whilst enhancing process control and safety by minimising reaction volumes for controlling exothermic reactions. Batch chemistry was used as a screening tool to ensure reaction feasibility and suitability in continuous flow and was not optimised in this work. This work focussed on identifying the most cost effective, reagent efficient conditions that are suitable for large-scale continuous manufacture. The productivity of each process is of importance and has been optimised

in this work, here Pareto fronts have been identified to understand any trade-offs between process metrics for each route.[52] This is particularly important if there is a trade-off between cost or reagent efficiency and productivity, therefore Pareto fronts aid the identification of conditions that balance these metrics and enhance the understanding of each route, supporting the decision making process for scale up. A combination of single- and multi-objective optimisation algorithms have been exploited to optimise product yield, reaction mass efficiency (RME), space-time yield (STY), and reagent cost per moles of DEHiBA produced. A range of high performing reaction conditions across the four synthetic pathways have been identified in this work to inform key decisions for an optimised synthesis of DEHiBA prior to scale-up of DEHiBA in the future. This work further validates the power of self-optimising flow platforms by identifying a scalable, high-performance route to DEHiBA, a specialist ligand for advanced nuclear reprocessing, via the rapid optimisation of four synthetic pathways.

2.3 Experimental

2.3.1 Chemicals

All of the following commercially available compounds were purchased and used without further purification. *N,N*-di-(2-ethylhexyl)isobutyramide (DEHiBA; >99%) was purchased from Technocomm Ltd. Di-(2-ethylhexyl)amine (DiEHA, 99%), isobutyric acid (iBA; 99+%) and triethylamine (99%) were purchased from Acros Organics. 4-dimethylaminopyridine (DMAP; 99%), acetonitrile (MeCN; HPLC grade), *N,N*-dimethylformamide (DMF; Extra Pure), hexane (97%) and chloroform (99+%) were purchased from Fisher Scientific Ltd. Isobutyric anhydride (iBAnhydride, 99%), 1-ethyl-3-(3-dimethylaminopropyl)carbodiimide hydrochloride (EDC.HCl; 99%), and isobutyryl chloride (iBCl; 97%) were purchased from Fluorochem. Biphenyl (99+%) was purchased from Merck Life Science UK Ltd.

Reagent costs were acquired as of March 2022 and can be found in **Table S1**.

2.3.2 The Self-Optimising Flow Reactor Platform

The flow platform is illustrated in **Figure 28** where reagents were pumped using JASCO PU-2080 dual piston HPLC pumps and flow paths were mixed using Swagelok SS-100–3 tee-pieces. Reactors of desired volumes were made from either PFA, PTFE or 316 stainless steel (SS) tubing (1/16'' OD, 1.59 mm ID for PFA and PTFE and 1/32" ID for SS tubing), supplied by Polyflon Technology Ltd and Cole Parmer, these were fitted to a cylindrical aluminium block and heated via a Eurotherm 3200 temperature controller. Sampling was achieved using a VICI Valco EUDA-CI4W sample loop (4-port) with 0.5-0.06 μL injection volume. Reactions were maintained under fixed back pressures using Upchurch Scientific back pressure regulators (100/250 psi), whilst route (e) employed the Tescom™ 26-1762-22 control pressure regulator to achieve a pressure of 210 bar. Quantitative analysis was performed on an Agilent 1260 Infinity II series HPLC instrument fitted with an Agilent Poroshell 120 EC-C18 reverse phase column (5 cm length, 4.6 mm ID and 2.7 μm particle size). The HPLC method can be found in Chapter 6, Section 1 (HPLC and GC-FID Methods) experimental section. The automated platform was controlled using a custom written MATLAB program, the optimisation algorithms were also written and implemented in MATLAB. Calibration curves (**Figure S5**) were obtained to quantify the analysis using biphenyl as the internal standard.

MATLAB was used to control pump flow rates, reactor temperature and sampling. For each iteration the reactor was allowed to stabilize at the desired operating temperature; the pumps were set to the required flow rates and left for three reactor volumes to reach steady state; then finally, the sampling valve was triggered alongside HPLC analysis. To minimize the duration and material consumption per iteration: (i) pump flow rates were reduced to a minimum during the heating/cooling of the reactor; (ii) initial LHC experiments were sorted in order of increasing

temperature; (iii) sequential LHC experiments were started whilst analysis of the previous experiment was running. Responses for each objective were calculated from HPLC chromatograms and used to inform the optimisation algorithm of the reactions' outcome and generate the next set of reaction conditions.

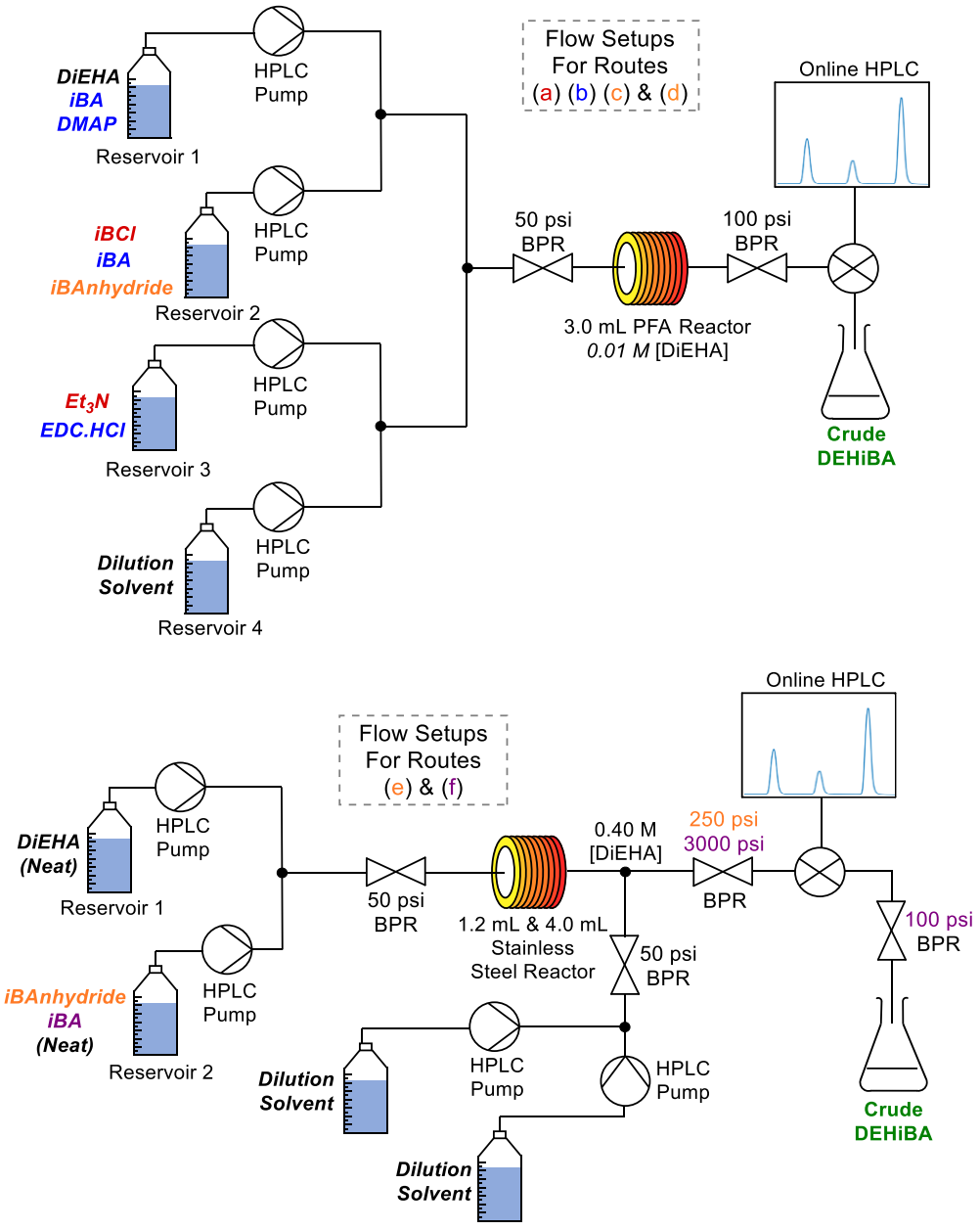

Figure 28: (Top) This illustrates the flow reactor setups for the self-optimisation of the solvated routes (a-d), where a reaction concentration of 0.01 M (DiEHA in the reactor) was maintained. All reagents in black text are used in all setups, whilst the colour coded reagents refer to the setups for each specific route as defined in **Figure 26:** Four synthetic pathways to DEHiBA, (a-f) are the different routes that have been investigated in this work, where routes (c-e) represent one

synthetic pathway but with different solvent systems. and the dashed boxes atop the setups. (Bottom) The solvent-free routes (e) and (f) were set up as illustrated, utilising solvent dilution pumps to enable quantitative online analysis.

2.4 Results and Discussion

2.4.1 Overview of Optimisations and Comparisons

This work compares routes (a-f) using the process metrics Yield, RME, STY, and reagent cost throughout. It is improbable that one route and condition will provide the lowest cost whilst maximising yield, RME, and STY, therefore conditions that minimise trade-offs between key process metrics are optimal for scale-up. This section provides an overview of how each route has been optimised, whilst the parameter bounds for each optimisation are detailed in Chapter 6.1. The solvated routes (a-d) were optimised at 0.01 mol dm^{-3} of DEHiBA to minimise chemical consumption and facilitate fair comparison between routes due to the effect of concentration on STY, a concentration limitation with route (b) defined the reaction concentration for (a-d). In **Figure 29**, the minimum residence time was limited to 0.5 minutes for ease of STY comparison between routes (a-d). Maximum/minimum theoretical limits for each route are defined in the 2D metric comparison plots.

As the ultimate driving force behind this work was to identify a cost-effective process to synthesise DEHiBA on demand, RME was utilised as the optimisation objective to achieve this. Simply minimising the amount of reagent used whilst maximising the amount of product meant that the algorithm located low reagent costs per mole of DEHiBA formed, omitting changes in reagent cost over time. The low cost of iBA added complexity to this for route (f), therefore reagent cost was instead minimised during this optimisation. Maximising STY was another key objective for this work due to its large role to play in the economics of a manufacture process.

Each optimisation utilised Latin hypercube sampling to initiate the optimisation,[62] following this Bayesian optimisation was employed to maximise yield for (a-e) to ensure setup and parameter space feasibility.[48, 53, 63] The core optimisation for each route was facilitated by the Thompson Sampling Efficient Multi-objective Optimisation (TSEMO) algorithm to maximise STY and RME or reagent cost.[55,64-68]

The discussion for each route focusses on comparing the RME, STY Pareto fronts, reagent costs, and product yield to aid identification of optimum conditions. Comparisons of key process metrics for the different routes are illustrated by **Figure 29**, whilst **Figure 30** compares the RME relative to the conditions explored for each route. STY, yield, and reagent cost, plots in the format of **Figure 30** can be found in Chapter 6.1 with additional process data such as **Table S2**.

2.4.2 Route (a): Synthesis from Isobutyryl Chloride

The most common synthetic route to DEHiBA found in the literature employs isobutyryl chloride (iBCl),[40, 41, 69-71] as a highly reactive starting material capable of yielding the product in a single step (**Figure 26**). The prevalence of this route meant that route (a) was the obvious starting point for this research. This chemistry was transitioned into continuous flow and optimised for comparison with the other routes in this work. Concerns with the environmental footprint, reactivity and toxicity of iBCl when considering scale-up are unfavourable. Additionally, the demanding safeguards required could heighten the cost of this route and burden plant design compared to alternative routes. Beneficially however, the utilisation of continuous flow here improves process safety via enhanced process control and improved heat transfer properties, enabling greater regulation of exothermic, runaway reactions.

The reaction screening of route (a) was trialled in batch prior to a transition to continuous flow to verify the suitability of the reaction. Incompatibility issues were encountered with the majority of common laboratory solvents due to the precipitation of triethylamine hydrochloride, this forced the adoption of chloroform to solubilise this salt and ensure homogeneity. Again, this further reduced the desire to implement this route for large-scale manufacture due to the environmental drawbacks of chloroform.[72, 73]

Multiple flow setups were investigated for the optimisation of route (a) (Figure S7), however the setup detailed in **Figure 28** proved most suitable, with many conditions reaching the maximum theoretical STY (374 g L^{-1} h^{-1}) which is largely limited by the residence time range specified, and is thus the upper limit for all three solvated routes, but falling slightly short of the maximum theoretical RME (69.4%). The fast reaction kinetics for this route granted almost no trade-off between RME and STY (**Figure 29**), whereby the data formed a right angle along a STY of 374 g L^{-1} h^{-1} and an RME of 65% (**Table 2**). No trade-off was observed beyond 300 g L^{-1} h^{-1}, however a gain in RME to 68% was observed around 280-300 g L^{-1} h^{-1}, this equated to a reduction in reagent cost from £37 mol^{-1} to £35 mol^{-1} but at the loss of 70-90 g L^{-1} h^{-1}. This breakthrough in RME was achieved with sub stoichiometric equivalents of iBCl and triethylamine at 150 °C. The preference for short residence times was clear, with product yield typically diminishing as residence time increased, likely due to the increased exposure of iBCl to elevated temperature. Ultimately this benefitted reaction performance due to minimal trade-off between these key process metrics.

It was observed that the minimum residence time of 0.5 minutes limited the performance of route (a), therefore shorter residence times as low as 12 seconds were explored. This again resulted in product yields up to 99+%, no loss in RME, and product throughputs up to 944 g L^{-1} h^{-1} (**Figure S9**). This further highlights the rapid reaction kinetics of route (a) even at 0.01 mol dm^{-3}.

These shorter residence times also provided minor performance improvements, with RMEs of 66% even at 900+ g L^{-1} h^{-1}, potentially due to the reduced exposure of iBCl to elevated temperature.

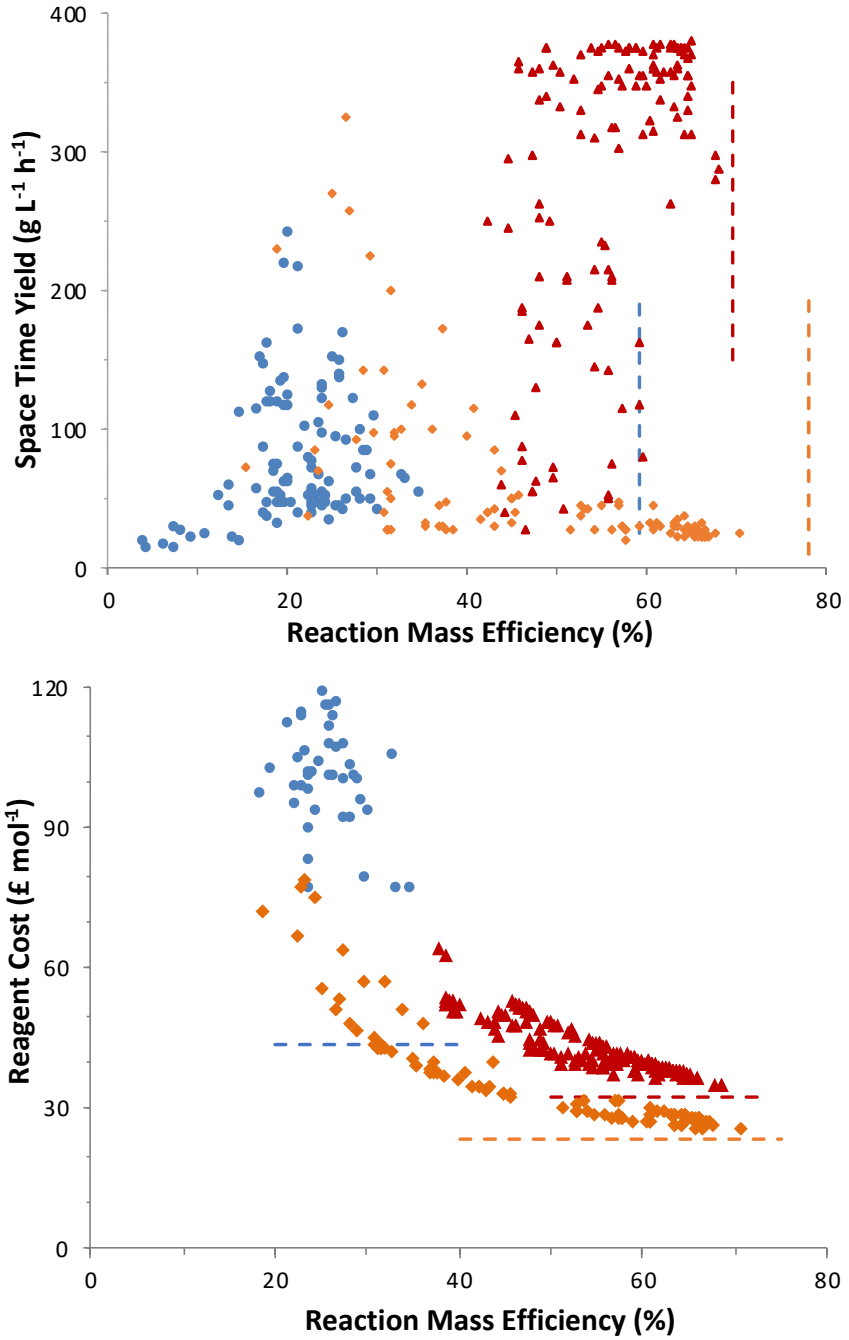

Figure 29: Space-time yield and reagent cost vs reaction mass efficiency data demonstrating Pareto fronts for the solvated routes (a) △, (b) ○, & (c) ◇, where the dashed lines indicate the maximum theoretical limits for the respective process metrics.

Six promising reaction conditions have been identified as candidates for scale up in **Table 2**.

The most cost-effective condition, £35 mol^{-1} equated to the optimum RME of 67.8%, and a STY of

285 g L^{-1} h^{-1}, whilst the best STY and RME at 374 g L^{-1} h^{-1} and 64.8% respectively required just 35 °C, and a slight excess of iBCl and triethylamine. The lowest cost per mole of DEHiBA for this route was identified to be £35 mol^{-1}. This reaction appears to be kinetically limited at 35 °C due to the need for greater equivalents to achieve similar performance to reactions beyond 100 °C. Whereas the final two conditions at 12 second residence times demonstrate some loss in performance due to the short reaction time despite temperatures well in excess of 35 °C.

Table 2: Four optimum conditions identified via the Pareto fronts in **Figure 29** of route (a), whilst the last two were found to be optimal for 0.2 minute residence time conditions. The colour coding is used for ease of comparison between the performance metrics for each route where green illustrates better performance than red.

Residence Time (min)	Equivalents. iBCl	Et_3N	Temperature (°C)	Yield of DEHiBA (%)	Reaction Mass Efficiency (%)	Space-Time Yield (g L^{-1} h^{-1})	Cost of DEHiBA (£ mol^{-1})
0.6	0.95	0.95	150.0	99.9	68.6	285	35.0
0.5	1.19	1.15	35.0	99.9	64.8	374	37.4
0.5	1.09	1.44	35.5	99.2	61.4	374	36.9
0.5	1.09	1.19	70.5	98.4	64.1	371	36.9
0.2	1.12	1.08	71.0	98.8	65.6	933	36.9
0.2	1.24	1.18	124.0	99.9	63.2	944	38.5

In summary, route (a) demonstrates fast reaction kinetics at this concentration, favouring shorter residence times with optimal temperature depending on the available equivalents of iBCl and triethylamine (**Figure 30**). High yields were achieved throughout the optimisation and the insignificant trade-off between RME and STY provided hard to beat process metrics at this concentration, thus route (a) is a convenient and effective route for the lab scale synthesis of DEHiBA. Nevertheless, the hazards and halogenated nature of iBCl and chloroform introduce avoidable complications and concerns. Therefore, the following sections explore and optimise alternative routes to identify an optimised route to DEHiBA to improve access to large-scale reprocessing testing that is currently economically restrictive if purchasing ligands from commercial suppliers.

2.4.3 Route (b). The Coupling Reagent Approach: EDC.HCl Mediated Synthesis

Coupling reagents are popular in the pharmaceutical industry for amide/peptide and ester formations, with their highly effective and robust nature seemingly outweighing their inherent atom inefficiency.[74] This popularity is prevalent even for the large-scale manufacture of pharmaceuticals as highlighted by Dunetz *et al.*[75] where popular coupling reagents like thionyl chloride, 1,1'-carbonyldiimidazole (CDI) and 1-ethyl-3-(3-dimethylaminopropyl)carbodiimide hydrochloride (EDC.HCl) are discussed and compared. The dominance of EDC.HCl for amide bond formations in the pharmaceutical industry is largely due to its ease of purification and applicability to a broad range of substrates. These characteristics are beneficial for the successful manufacture of troublesome tertiary amides and may prove effective for the sterically bulky DEHiBA target in this case. Further to these benefits, Pfizer's' publication discussing amide bond formations in continuous flow,[76] identifies EDC.HCl as one of the few coupling reagents suitable for continuous flow. Therefore, route (b) was attempted and optimised in continuous flow to assess this alternative route to DEHiBA that starts with isobutyric acid (iBA), a more benign and cost-effective raw material than iBCl.

Batch screening led to the adoption of acetonitrile (MeCN) as the reaction solvent due to comparatively good product yields and the limited solubility of EDC.HCl in most organic solvents .[77] Solubility limitations with DiEHA required the inclusion of iBA to the reservoir to ensure homogeneity of the solution due to immiscibility of DiEHA and MeCN alone. Additive screening in batch led to the addition of 4-dimethylaminopyridine (DMAP) to the flow setup, as 5 mol% saw product yields rise from 50% to 99+% at room temperature.

The optimisation of route (b) in continuous flow required the exploration of a wider equivalent range to route (a), as ≥2 equivalents of both EDC.HCl and iBA was necessary to achieve comparable

product yields. This inefficient reagent excess was extreme when compared to a batch setup, whereby equimolar amounts of DiEHA, iBA and EDC.HCl, yielded almost complete conversion to DEHiBA, although a 6 hour reaction time was required. The setup also demonstrated a requirement for temperatures >75 °C, else little or no product formation for residence times as long as 10 minutes, whilst the best conditions showed a preference for >140 °C (**Table 3**). We hypothesise that the elevated temperature required by this setup encourages the formation of *N*-acylurea, an unwanted, unreactive by-product formed by the rearrangement of *O*-acylisourea (**Scheme S3**).[78] This hypothesis was confirmed via kinetic batch studies, where an increase in temperature led to the loss of product yield (**Figure S11**).

Table 3: Six optimum conditions identified via the Pareto fronts in **Figure 29** of route (b).

Residence Time (min)	Equivalents. EDC	iBA	Temperature (°C)	Yield of DEHiBA (%)	Reaction Mass Efficiency (%)	Space-Time Yield (g L^{-1} h^{-1})	Cost of DEHiBA (£ mol^{-1})
1.4	1.66	2.53	169	75.6	29.9	98.2	79.7
3.3	1.90	1.70	153	84.8	34.7	47.6	77.3
0.7	4.90	2.64	150	91.2	20.0	240	151
1.0	3.08	3.16	144	93.8	26.2	168	101
3.1	2.20	2.50	149	95.0	33.3	57.1	77.1
3.0	2.50	2.10	151	96.2	32.9	60.0	83.3

Although a number of competitive yields (>90%) were achieved here in continuous flow the typical requirement for large reagent excesses proved to be detrimental to the RME and hence results in an increased reagent cost for this route. The best RMEs (33-35%, 59% of the theoretical maximum) were achieved when using approximately 2 equivalents of EDC.HCl and iBA, this led to uncompetitive reagent costs as low as £77 mol^{-1}. These poor RME and reagent cost metrics result in an uneconomic manufacture route with this setup.

As it was unclear why an excess of iBA and EDC.HCl is needed in continuous flow but not in batch, further kinetic studies investigated the effect of concentration on the batch reaction. It was observed that over a concentration range of 0.15 to 0.01 mol dm^{-3}, a drop in yield from 99+% to

42% was observed respectively (**Figure S11**). We hypothesise that this is due to the reduction in the rate of collision between DiEHA and the activated intermediate of iBA (*O*-acylisourea) as concentration reduces, whereas the rate of rearrangement from the *O*-acylisourea to *N*-acylurea is unaffected by this change and remains constant at the same temperature. Therefore, as concentration reduces, so too does the yield due to increased by-product formation. We expect that the RME would improve if this optimisation was conducted at a greater concentration. To improve the competitiveness of this reaction we focussed on increasing the reservoir concentration of EDC.HCl as this largely limited the reaction concentration. The addition of bases such as di-isopropyl ethylamine (DIPEA) resulted in a dramatic improvement in solubility of EDC.HCl, unfortunately this led to a 60-70% reduction in reaction yield in addition to further setup challenges. Consequently, attempts to increase the reaction concentration were abandoned and work progressed to routes (c-f) in hope these would provide competitiveness. Ultimately, the current flow setup limitations mean this reaction is better suited to batch chemistry if RME or reagent cost are important process metrics.

Six conditions that exhibit the most promise for this route are detailed in **Table 3**. The lack of competitiveness of this route led to the pursuit of other synthetic routes before further continued on the optimisation of route (b) to increase the reaction concentration. The next route utilises isobutyric anhydride directly, removing the need for EDC.HCl.

2.4.4 Routes (c) & (d). A Direct Route from Isobutyric Anhydride – Acetonitrile and Hexane Solvated Reactions

The direct combination of DiEHA and isobutyric anhydride (iBAnhydride) for the synthesis of DEHiBA is pursued here. Theoretically this synthetic pathway has the capability to outperform the

reagent cost and RME of routes (a) and (b), with the added benefits that iBAnhydride is a readily available, cost-effective reagent, with reduced hazards relative to iBCl whilst also being ideal for continuous flow due to the enhanced heat transfer that facilitates the control of exothermic reactions. Though it should be noted that for each equivalent of iBAnhydride consumed an equivalent of iBA is produced, burdening the purification process.

Preliminary batch studies were limited due to the nature of the exothermic, runaway reactions. No solubility issues were encountered unlike routes (a) and (b), opening the reaction to a range of solvents and facilitating a quick transition of this reaction to continuous flow. The diverse solvent compatibility of this reaction enabled the pursuit of two optimisation setups to evaluate the effect of solvent on this chemistry.

Acetonitrile and hexane, routes (c) and (d) respectively were chosen as the solvents for this comparison. The optimisation of route (c) showcased excellent conversion even at low equivalents (<2), with nearly half of the 116 conditions attaining yields ≥90%. The best conditions for RME and reagent cost exhibited a distinct preference for 100-130 °C, low iBAnhydride equivalents (1.0-1.8), and longer residence times (up to seven minutes). Shorter residence times were typically poorer yielding unless combined with greater equivalents, though this largely reduced the RME and added cost for the price of improving productivity. Consequently, this gave rise to a significant trade-off between RME and STY for this route, a stark contrast to route (a). In this case the cost for improving the STY dramatically reduces the RME, for example a maximum RME of 70.4% at a STY of 24 g L^{-1} h^{-1}, reduced dramatically to 45.6% for a minor increase in STY to 51 g L^{-1} h^{-1}or an RME of 26.5% to achieve a STY of 326 g L^{-1} h^{-1}. This trade-off was uncompetitive with route (a), as illustrated in **Figure 29**, if both productivity and cost are valued as important.

Route (c) is however the most cost-effective manufacture route to DEHiBA with reagent costs as low as £26 mol^{-1}. Still, a reasonable STY is necessary for continuous large-scale manufacture to be viable. Therefore, this setup requires further optimisation before it can be scaled up.

Six of the best conditions for route (c) are defined in **Table 4** covering a range of performance metrics for a more holistic understanding of this route. The trade-off between RME and STY is further emphasised by this data, whilst the high temperature and equivalent dependence for improved STY is best highlighted by this data.

Table 4: Six optimum conditions identified via the Pareto fronts in **Figure 29** of route (c).

Residence Time (min)	Equivalents. iBAnhydride	Temperature (°C)	Yield of DEHiBA (%)	Reaction Mass Efficiency (%)	Space-Time Yield (g L^{-1} h^{-1})	Cost of DEHiBA (£ mol^{-1})
0.5	5.00	150.0	83.2	26.3	326	51.2
7.0	1.00	127.5	86.1	70.4	24.1	26.0
0.8	5.00	128.5	91.4	28.9	224	46.6
0.9	4.50	143.5	91.8	31.5	200	43.7
7.0	1.50	127.5	96.0	65.5	26.9	25.9
6.5	1.80	127.0	97.5	60.6	29.4	27.1

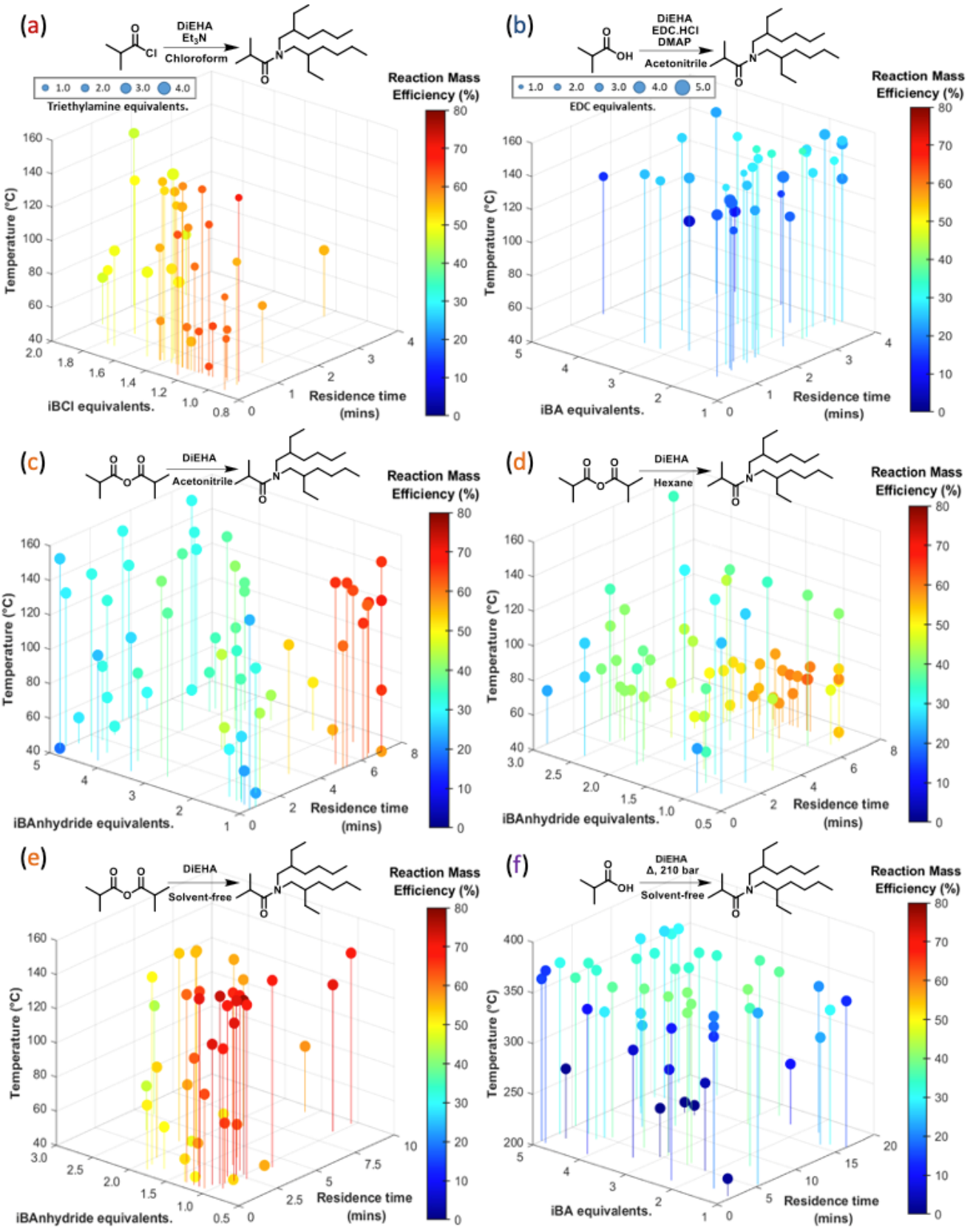

Figure 30: Six 4/5D plots demonstrating the reaction mass efficiency for routes (a-f), the synthetic route for each is defined above the plots for ease of comparison. A consistent colour bar is illustrated throughout, ranging between 0 80%, whilst the x, y, z and size ranges are subject to

the parameter space for each optimisation, finally a reduced dataset has been presented for clarity. Whilst Figures S2-4 in Chapter 6.1 illustrate reagent cost, space-time yield and DEHiBA yield respectively for these reactions.

The second optimisation of this synthetic pathway utilised hexane as the solvent (route (d)) to improve process understanding in an attempt to improve the RME, STY Pareto front. Solvent often plays a highly influential role in promoting and controlling chemical reactions,[79,80] such as influencing key process metrics like cost and purity. Therefore, the understanding of solvent effect on a given reaction is of great interest for process optimisation and cost minimisation. In this case the change in solvent results not only results in a shift in the conditions required to achieve the optimum RME but also a difference in the optimum RME. **Figure 30** illustrates this change, through the difference in optimal conditions for RME whereby the reaction in hexane (route (d)) favours a lower temperature of 70 °C to achieve the optimum RME of 62.4% for this optimisation, whereas higher temperatures are favoured when using acetonitrile and this results in a greater RME of 70.4%. The optimisation of route (d) was completed in less than 48 hours, emphasising the power of self-optimising flow reactor platforms by relocating process optima for a new solvent system.

Overall, routes (c) and (d) largely demonstrated similar trends for the process metrics of interest, with the exception of the difference in temperature preference between these routes. Route (d) did however underperform with respect to (c), potentially due to the reduced parameter space for the optimisation of route (d), although the STY, RME Pareto front trends are in agreement with one another (**Figure S15**).

Table 5 defines six of the best performing conditions for route (d) for contrast with **Table 4**. Route (c) proves to be the most promising candidate to compete with route (a), therefore further optimisation of this route is needed to improve the productivity.

Table 5: Six optimum conditions identified via the Pareto fronts in **Figure S15** of route (d).

Residence Time (min)	Equivalents. iBAnhydride	Temperature (°C)	Yield of DEHiBA (%)	Reaction Mass Efficiency (%)	Space-Time Yield (g L^{-1} h^{-1})	Cost of DEHiBA (£ mol^{-1})
0.7	2.50	105.0	54.2	26.5	145	58.0
2.4	1.35	70.5	64.9	44.4	51.6	39.0
7.0	1.21	69.7	86.8	62.4	23.2	28.4
3.7	2.15	71.5	86.8	46.5	43.8	34.1
7.0	1.45	69.0	90.5	59.9	24.2	28.6
3.9	3.00	91.5	95.8	41.7	46.5	35.6

2.4.5 Comparison of Solvated Routes (a), (b), (c) and (d)

To summarise the performance of routes (a-d), this section will briefly compare these routes. Route (a) demonstrated near perfect performance with little to no trade-off between RME and STY resulting in unmatched performance when considering all process metrics equally. Route (a) even proved highly successful for 12 second residence times, producing excellent product throughput given the concentration in addition to near perfect RME. The downfalls of route (a) arose from iBCl as it is around 3 times the price of iBAnhydride, limiting the reagent cost to £35 mol^{-1} whilst route (c) was capable of £26 mol^{-1}. Further to this the hazards of iBCl outweighed those of iBAnhydride, these factors are of great importance when moving towards large-scale manufacture as they add cost and risk. Unfortunately however, the large trade-off between RME and STY for route (c) largely hinders its performance making it unfavourable to scale-up at this stage despite the low reagent cost involved with the synthesis. In an attempt to improve this the setup of route (c) was further optimised, the results of which led to route (e), a solvent-free synthesis that utilises the same synthetic pathway as routes (c) and (d) but with massive gains in concentration and hence reaction kinetics. Route (a) was not scaled up in a similar way due to the corrosive nature of the chemistry and safety concerns with these neat materials.

Route (b) was inspired by the pharmaceutical industry, with the hope that EDC.HCl would afford an alternative, competitive manufacture route to DEHiBA. Unfortunately, the performance of this route was far from competitive due to limitations of this chemistry in continuous flow and the current setup for this optimisation. The batch synthesis of route (b) was however very reagent and temperature efficient requiring little to no reagent excess for near complete conversion at room temperature, although 6 hour reaction times were necessary.

2.4.6 Towards Scale-up: A Solvent-free Synthesis of Route (e)

In an effort to enhance the performance and scalability of route (c/d), process intensification led to a productive and efficient solvent-free synthesis with close to perfect PMI, albeit disregarding purification. The flow setup was tailored towards the optimisation via the inclusion of solvent pumps following the reactor, a continuous manufacture platform would not need these (**Figure 28**). Undoubtedly, the elimination of solvent removes an element of process control in the form of a heat sink, however the excellent heat transfer of the tubular flow platform facilitates the pursuit of this chemistry. This undertaking carried too much risk in a batch reactor so was conducted in continuous flow to enable sufficient cooling after the reactor, this ensured a high level of control over the outlet temperature of the crude product measured to be 32 °C and no runaway reactions were observed even without solvent dilution.

Initially the optimisation of this route was confined between 1-10 minute residence times, however this route now exhibited a preference for short residence times to achieve optimum performance, therefore this limit was extended to 0.5 minutes part way through the optimisation. Both these optimisations yielded excellent process metrics, demonstrating an extensive improvement over the solvated syntheses. The shift in optimisation parameters to 0.5 minute

residence times resulted in a STY improvement from 37.1 and 74.7 kg L^{-1} h^{-1}, with RMEs of 72.2% and 72.6% respectively, plus reagent costs at £25 mol^{-1} (**Table 6**), demonstrating no loss in RME at these STYs. STY was the most notable improvement of route (e) over routes (c/d), this was achieved due to the greater reaction concentration and the preference towards shorter reaction times, a consequence of the concentration increase.

Table 6: Five optimum conditions for (e) identified via the Pareto fronts in **Figures 31 & 32**.

Residence time (min)	iBAnhydride equivalents.	Temperature (°C)	Yield of DEHiBA (%)	Reaction Mass Efficiency (%)	Space-Time Yield (g L^{-1} h^{-1})	Cost of DEHiBA (£ mol^{-1})
0.7	1.00	147.9	92.1	71.9	51590	25.4
1.0	1.07	122.3	95.1	72.2	37140	25.0
0.5	1.07	149.0	95.5	72.6	74700	24.9
1.3	1.02	150.0	96.0	74.3	30090	24.5
2.7	1.00	141.9	99.3	77.5	14720	23.6

A further illustration of the enhanced performance is the optimum RME of 77.5%, this equated to the lowest reagent cost per mole of DEHiBA at £23.60, and practically complete product conversion, with both RME and reagent cost also close to their theoretical maxima. A 2.7 minute residence time was however required for this, resulting in a STY of 14.7 kg L^{-1} h^{-1}, a large improvement over route (c), but a far from the optimum STY. Advantageously, the STY, RME trade-off for route (e) presented a considerably different 2D profile to routes (c/d) (**Figure 31**), due to the shift in preference to shorter residence times for optimum overall performance. This minimised the RME loss with increasing STY, but notably the trade-off was more pronounced at lower STY as demonstrated by **Figure 30** with an RME loss of 5%. The minimisation of this trade-off is highly desirable, facilitating an efficient, low cost, and highly productive manufacture route to DEHiBA.

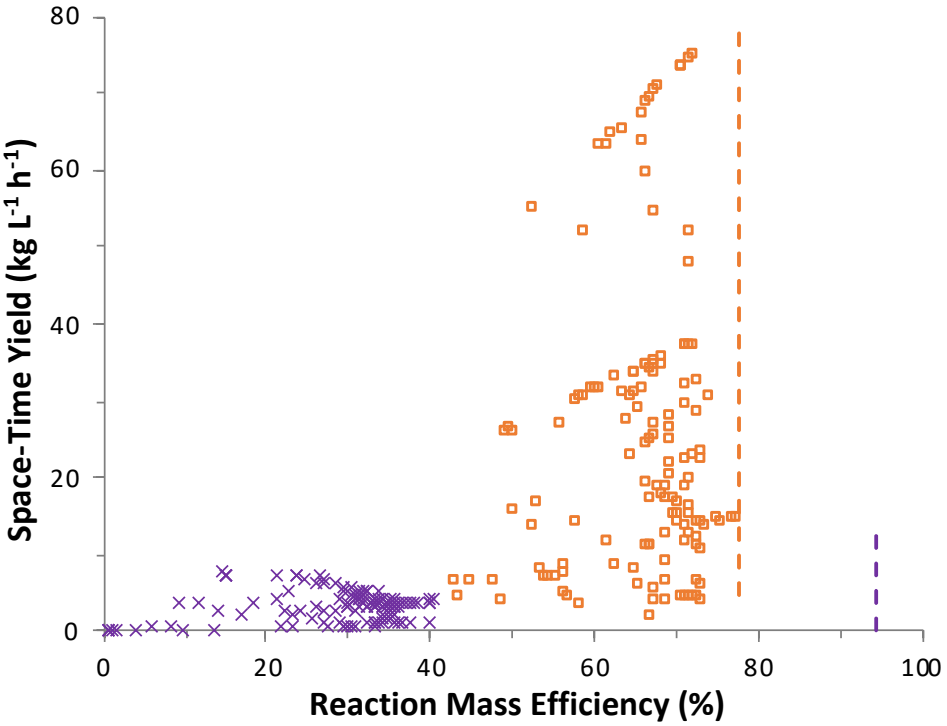

Figure 31: Space-time yield vs reaction mass efficiency data with Pareto fronts for routes (e) □, and (f) x, with their maximum theoretical RME limits as dashed lines.

The optimum conditions for this route were all identified above 100 °C, with roughly 1 equivalent of iBAnhydride, and a variety of relatively short residence times. These conditions have led to process metrics that possess exceptional performance, with STY figures in the tens of kilograms per litre per hour in comparison with the solvated routes that were only capable of hundreds of grams per litre per hour. Finally, the RME here outperforms all other routes and provides a low reagent cost, with single reaction conditions capable of desirable RME and STY.

The optimum RME and STY conditions were utilised in two continuous runs on the flow platform but without dilution solvent to manufacture 5 litres of crude DEHiBA without the presence of biphenyl. Yields were determined via an external standard to be 99.7% and 97.2% for the optimum RME of 77.5% and STY of 74.7 kg L^{-1} h^{-1} respectively throughout the 32 and 5 hour continuous runs. The slight improvement in yield led to an improvement in other process metrics, especially STY for the second run up to 75.8 kg L^{-1} h^{-1} however the PMIs are most noteworthy for

these runs at 1.29 and 1.36 g g^{-1} respectively due to the slight excess of iBAnhydride and elimination of solvent facilitating the lessened environmental impact of this process.

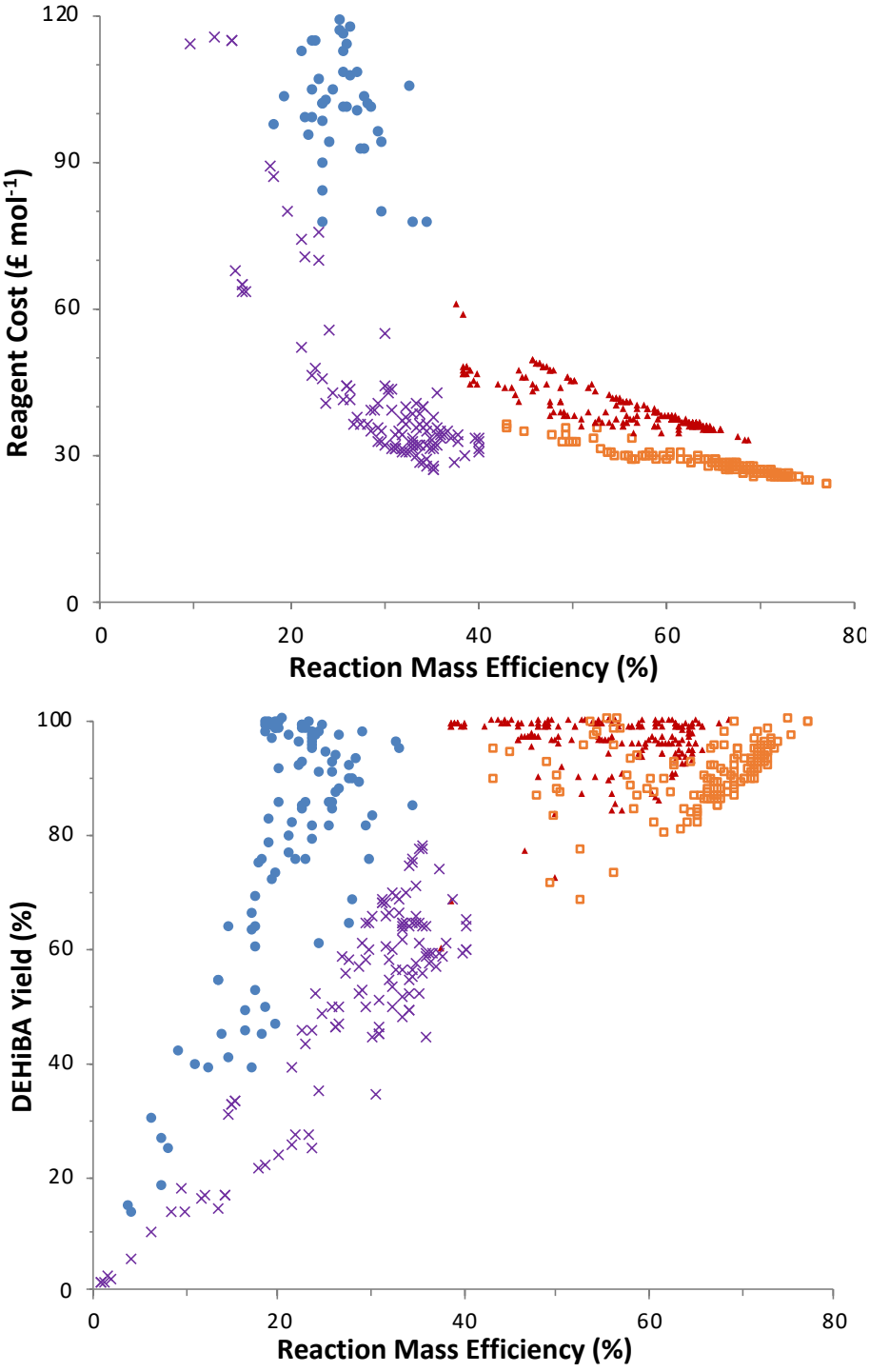

Figure 32: Reagent cost and DEHiBA yield metrics vs reaction mass efficiency comparison plots for routes (a) △, (b) ○, (e) □, and (f) x.

2.4.7 Route (f). Solvent-free Direct Thermal Amidation

Route (f) is an alternative solvent-free route with the potential to achieve a RME of 94.4% and costs as low as £18.80 mol^{-1} due to the low cost of iBA, with water as the by-product of this coupling. Therefore, this direct thermal amidation was screened and optimised in the search for another competitive route to DEHiBA, especially as the solvent-free synthesis of route (a) presented unnecessary risks and precipitation issues that required the omission or replacement of triethylamine whilst not offering cost or RME improvements.

Ideally the preparation of an amide bond would proceed through the direct coupling of carboxylic acid and amine, the only by-product being water. Unfortunately a large energy barrier must be overcome to achieve this, such as temperatures in excess of 150 °C. Often, such temperatures are too extreme and cause chemical degradation, thus limiting the applicability of this methodology, therefore this route is not common- practice for the creation of amide bonds.[74] In this work the stainless steel reactor tubing was pressurised to 210 bar to access temperatures up to 370 °C. This ensured that the reagents would not undergo a phase change to guarantee accurate residence times and reproducibility.

Preliminary temperature screening in the continuous flow reactor identified minimal product formation below 250 °C, whilst temperatures above 370 °C required greater reactor pressure. The crude product from these reactions eluted at 25 °C despite reactor temperatures of up to 370 °C, whilst the emission of gas was noted after the final BPR (back pressure regulator) and was identified as gaseous carbon dioxide and propane, products of the degradation of iBA. Additional signals were observed during the analysis and were confirmed to be the thermal degradation products of DEHiBA: *N*-(2-ethylhexyl)isobutyramide and 3-methylheptane (**Figure S19**), the formation of which increased with relation to increasing temperature and residence time. This

degradation adds complexity to the purification of DEHiBA as this amide may interfere with the extraction of uranium.

Two reactor volumes were employed for the optimisation of this route to explore a wide residence time range between 1 and 18 minutes. A wide equivalent range (1-5) proved necessary as the reaction demonstrated poor conversion at low iBA equivalents. Yields of up to 77.8% were achieved, with the highest yielding conditions proving to be the most cost effective at £27.20 mol^{-1}, despite the need for 5 equivalents of iBA. The low reagent cost of iBA results in a lesser relationship between RME and reagent cost, instead reagent cost reduced with increasing yield. This difference is also due to the poorer conversions achieved by this route.

Overall, route (f) performed poorly at the shortest residence times, with the best STY conditions requiring high equivalents of iBA and leading to poor yields, RMEs and reagent costs. Consequently, a large trade-off between STY and the other process metrics is apparent and largely affects the performance of this route. This chemistry demonstrates a preference for temperatures between 330 and 370 °C, with the best yields demanding 340-350 °C, roughly 5 equivalents of iBA, and a range of residence times between 5-13 minutes. Interestingly as the temperature neared 370 °C, lower residence times granted better yields, likely due to the reduced thermal degradation of DEHiBA.

Table 6 defines the best conditions for route (f), highlighting the best process metrics and conditions along the key Pareto-fronts. In conclusion, route (f) offers a reagent cost competitive route to DEHiBA, however the additional capital for equipment, heating and safeguards require significant consideration when comparing to other routes. Additionally, the poor STY of route (f) compared to route (e) results in an uncompetitive manufacture route despite the low reagent cost.

Table 7: Seven optimum conditions for (f) identified via the Pareto fronts in **Figures 31 & 32**.

Residence time (min)	iBA equivalents.	Temperature (°C)	Yield of DEHiBA (%)	Reaction mass efficiency (%)	Space-Time Yield (g L^{-1} h^{-1})	Cost of DEHiBA (£/mol)
1.7	5.0	366	52.3	23.8	7320	40.5
4.8	4.6	369	69.8	33.5	3731	30.0
6.3	4.5	353	71.0	34.7	2921	29.4
5.5	4.2	348	73.7	37.4	3619	28.1
13.2	5.0	338	74.3	33.8	1378	28.5
10.6	5.0	339	75.6	34.4	1734	28.0
5.4	5.0	346	77.7	35.4	3495	27.2

2.5 Conclusions

This research has utilised an advanced, fast-paced approach to successfully optimise four synthetic pathways to DEHiBA in continuous flow, whereby a favourable manufacture route to DEHiBA has been identified for large scale manufacture. Initial optimisation work, routes (a-d), employed solvent to control these reactions and their concentration for fair cross-comparison. Pareto fronts for key process metrics were analysed and provided insight into the performance of each route by highlighting optimum and scalable reaction conditions. Routes (a) and (c) were most promising in the search for a cost-effective, scalable route to DEHiBA, whereas route (b) underperformed in continuous flow, and the solvent choice for route (d) resulted in performance loss compared to (c).

Due to limitations and issues with route (a), route (c) was developed into route (e) via the mitigation of solvent, facilitated by the excellent heat transfer properties of tubular flow this enhanced all key process metrics, yielding a very desirable manufacture route. The increased reaction concentration and lower reagent cost of iBAnhydride in comparison to iBCl resulted in a route capable of manufacturing DEHiBA for just £23.60 mol^{-1} (not bulk costs), with product throughputs up to 75.8 kg L^{-1} h^{-1}. Most advantageously, the trade-off between RME and STY has been suppressed due to the improved reaction kinetics, where only a 5% loss in RME is observed along the Pareto front, to contrast, route (c) suffers from a 44% loss. Notably, further process

optimisation of route (a) could improve competitiveness through base optimisation and reaction concentration, however this was not pursued here due to the increased risk and environmental footprint driving us away from this chemistry. The solvent-free process in route (e) has largely aided develop a cleaner more economical well-rounded and scalable manufacture route.

Route (f) was designed and optimised as another solvent-free route to DEHiBA, possessing the potential to be the most cost effective and atom efficient route by directly coupling iBA and DiEHA with temperatures up to 370 °C and a pressure of 210 bar. Thermal degradation of iBA resulted in RME losses, whilst the relatively slow reaction kinetics resulted in uncompetitive STYs with route (e). Fortunately, the low cost of iBA afforded reagent costs as low as £27.20 mol^{-1}, however the requirement for relatively extreme operating conditions burdens the capital and operational cost, whilst the degradation products from the thermal amidation add further complexity to purification, thus scalability is less favourable.

The methodology used to optimise these routes aids to improve access to specialist chemicals like DEHiBA to promote large-scale testing and advance the technology readiness level of advanced nuclear reprocessing technologies like GANEX. This methodology largely reduces process optimisation timelines and overall costs, whilst providing holistic understandings of each process in the lead up to large-scale manufacture. The application of this approach to other promising ligands for nuclear reprocessing will aid improve accessibility to these specialist molecules that require large scale testing in order to advance nuclear reprocessing so that a more diverse range of radionuclides can be recovered from used nuclear fuel in the future. In this work continuous flow has facilitated the safe exploration of these routes, with the large datasets gathered in this research available in Chapter 6.2 for further use by researchers, whereby alternative conditions may be preferred for their own synthesis of DEHiBA.

2.6 Future Work

As this work focusses on improving economic and environmental metrics for the formation of DEHiBAs amide bond, future work should optimise the manufacture of DiEHA (di-(2-ethylhexyl)amine) as this is the most costly starting material. Additionally, this work does not include purification work which will add cost and complexity to the manufacture, this work is investigated in the following chapter, Chapter 3 and provides a complete manufacture route for DEHiBA.

Although this work highlights the capability of self-optimising flow platforms for chemical synthesis, DEHiBA is a simpler ligand with only one synthetic step required. Further work is needed to simplify telescoped, multi-step synthesis in continuous flow as this can be challenging to optimise in continuous flow, enabling ligands like TODGA to be more effectively optimised. It should be noted that this is not necessary for the synthesis of more complex ligands like TODGA, as each step could be optimised individually and then telescoped using optimum crude or purified material from the step before, however this could lead to less optimal conditions than if the telescoped synthesis was optimised.

2.7 References

1. UK Government, UK Energy White Paper: Powering Our Net Zero Future, UK Government, London, 2020.
2. IAEA, Nuclear Technology Review, IAEA.org, 2020.
3. A. Peakman and B. Merk, Energies, 2019, 12, 3664.
4. P. Ekins, Energy Policy, 2004, 32, 1891-1904.
5. J. B. Greenblatt, N. R. Brown, R. Slaybaugh, T. Wilks, E. Stewart and S. T. McCoy, Annual Review of Environment and Resources, 2017, 42.
6. A. Cherp, V. Vinichenko, J. Jewell, M. Suzuki and M. Antal, Energy Policy, 2017, 101, 612-628.

7. M. Gong, Y. Gao, L. Koh, C. Sutcliffe and J. Cullen, International Journal of Production Economics, 2019, 217, 88-96.
8. Z. Liu, Z. Deng, S. J. Davis, C. Giron and P. Ciais, Nature Reviews Earth & Environment, 2022, 3, 217-219.
9. C. Poinssot, S. Bourg, N. Ouvrier, N. Combernoux, C. Rostaing, M. Vargas-Gonzalez and J. Bruno, Energy, 2014, 69, 199-211.
10. P. Wattal, Progress in Nuclear Energy, 2017, 101, 133-145.
11. M. Carrott, C. Maher, C. Mason, M. Sarsfield, D. Whittaker and R. Taylor, Solvent Extraction and Ion Exchange, 2023, 41, 88-117.
12. J. M. Pearce, Sustainability, 2012, 4, 1173-1187.
13. C. W. Forsberg, Progress in Nuclear energy, 2009, 51, 192-200.
14. I. Denniss and A. Jeapes, in The nuclear fuel cycle from ore to wastes, 1996.
15. K. L. Nash and G. J. Lumetta, Advanced separation techniques for nuclear fuel reprocessing and radioactive waste treatment, Elsevier, 2011.
16. R. Herbst, P. Baron and M. Nilsson, in Advanced separation techniques for nuclear fuel reprocessing and radioactive waste treatment, Elsevier, 2011, pp. 141-175.
17. M. F. Simpson and J. D. Law, in Nuclear Energy, Springer, 2018, pp. 187-204.
18. E. Aneheim, C. Ekberg, A. Fermvik, M. R. S. J. Foreman, B. Grűner, Z. Hájková and M. Kvičalová, Solvent Extraction and Ion Exchange, 2011, 29, 157-175.
19. G. Modolo, A. Wilden, A. Geist, D. Magnusson and R. Malmbeck, Radiochimica acta, 2012, 100, 715-725.
20. R. S. Herbst, P. Baron and M. Nilsson, in Advanced Separation Techniques for Nuclear Fuel Reprocessing and Radioactive Waste Treatment, 2011, DOI: 10.1533/9780857092274.2.141, pp. 141-175.
21. J. M. MCKIBBEN, Radiochimica Acta, 1984, 36, 3-16.
22. W. B. Lanham and T. C. Runion, 1949.
23. A. Geist, J.-M. Adnet, S. Bourg, C. Ekberg, H. Galán, P. Guilbaud, M. Miguirditchian, G. Modolo, C. Rhodes and R. Taylor, Separation science and technology, 2021, 56, 1866-1881.

24. T. Lyseid Authen, J.-M. Adnet, S. Bourg, M. Carrott, C. Ekberg, H. Galán, A. Geist, P. Guilbaud, M. Miguirditchian and G. Modolo, Separation Science and Technology, 2022, 57, 1724-1744.
25. R. Garbil, S. Bourg, A. Geist, J.-M. Adnet, C. Rhodes, B. C. Hanson, C. Davies and D. Diaconu, EPJ Nuclear Sciences & Technologies, 2020, 6.
26. A. Geist, R. Taylor, C. Ekberg, P. Guilbaud, G. Modolo and S. Bourg, Procedia Chemistry, 2016, 21, 218-222.
27. J. Martinez-Val, P&T Roadmap proposal for Advanced Fuel Cycles leading to a Sustainable Nuclear Energy - Syntheses Report, Euratom, 2008.
28. R. Taylor, W. Bodel, L. Stamford and G. Butler, Energies, 2022, 15, 1433.
29. A. Rout, K. Venkatesan, M. Antony and P. V. Rao, Separation Science and Technology, 2016, 51, 474-484.
30. M. Carrott, A. Geist, X. Heres, S. Lange, R. Malmbeck, M. Miguirditchian, G. Modolo, A. Wilden and R. Taylor, Hydrometallurgy, 2015, 152, 139-148.
31. M. Miguirditchian, C. Sorel, B. Camès, I. Bisel, P. Baron, D. Espinoux, J. Calor, C. Viallesoubranne, B. Lorrain and M. Masson, 2009.
32. R. Taylor, M. Carrott, H. Galan, A. Geist, X. Hères, C. Maher, C. Mason, R. Malmbeck, M. Miguirditchian, G. Modolo, C. Rhodes, M. Sarsfield and A. Wilden, Procedia Chemistry, 2016, 21, 524-529.
33. J. Drader, G. Saint-Louis, J. M. Muller, M. C. Charbonnel, P. Guilbaud, L. Berthon, K. M. Roscioli-Johnson, C. A. Zarzana, C. Rae, G. S. Groenewold, B. J. Mincher, S. P. Mezyk, K. McCann, S. G. Boyes and J. Braley, Solvent Extraction and Ion Exchange, 2017, 35, 480-495.
34. A. Leoncini, J. Huskens and W. Verboom, Chem Soc Rev, 2017, 46, 7229-7273.
35. M. Carrott, K. Bell, J. Brown, A. Geist, C. Gregson, X. Hères, C. Maher, R. Malmbeck, C. Mason and G. Modolo, Solvent extraction and ion exchange, 2014, 32, 447-467.
36. K. Bell, C. Carpentier, M. Carrott, A. Geist, C. Gregson, X. Hérès, D. Magnusson, R. Malmbeck, F. McLachlan and G. Modolo, Procedia Chemistry, 2012, 7, 392-397.
37. R. Taylor, M. Carrott, H. Galan, A. Geist, X. Hères, C. Maher, C. Mason, R. Malmbeck, M. Miguirditchian and G. Modolo, Procedia Chemistry, 2016, 21, 524-529.

38. G. B. Hall, N. P. Bessen, P. R. Zalupski, E. L. Campbell, T. S. Grimes, D. R. Peterman and G. J. Lumetta, Solvent Extraction and Ion Exchange, 2023, 1-19.
39. G. B. Hall, E. L. Campbell, N. P. Bessen, T. R. Graham, H. Cho, M. RisenHuber, F. D. Heller and G. J. Lumetta, Inorganic Chemistry, 2023, 62, 6711-6721.
40. G. M. Gasparini and G. Grossi, Solvent Extraction and Ion Exchange, 1986, 4, 1233-1271.
41. G. Thiollet and C. Musikas, Solvent Extraction and Ion Exchange, 1989, 7, 813-827.
42. N. Cherkasov, Y. Bai, A. J. Expósito and E. V. Rebrov, Reaction Chemistry & Engineering, 2018, 3, 769-780.
43. B. Lin, J. L. Hedrick, N. H. Park and R. M. Waymouth, Journal of the American Chemical Society, 2019, 141, 8921-8927.
44. C. J. Taylor, A. Baker, M. R. Chapman, W. R. Reynolds, K. E. Jolley, G. Clemens, G. E. Smith, A. J. Blacker, T. W. Chamberlain, S. D. R. Christie, B. A. Taylor and R. A. Bourne, Journal of Flow Chemistry, 2021, DOI: 10.1007/s41981-020-00135-0.
45. L. Buglioni, F. Raymenants, A. Slattery, S. D. Zondag and T. Noël, Chemical Reviews, 2021, 122, 2752-2906.
46. S. Langner, F. Häse, J. D. Perea, T. Stubhan, J. Hauch, L. M. Roch, T. Heumueller, A. Aspuru-Guzik and C. J. Brabec, Advanced Materials, 2020, 32, 1907801.
47. M. Christensen, L. P. Yunker, F. Adedeji, F. Häse, L. M. Roch, T. Gensch, G. dos Passos Gomes, T. Zepel, M. S. Sigman and A. Aspuru-Guzik, Communications Chemistry, 2021, 4, 112.
48. B. J. Shields, J. Stevens, J. Li, M. Parasram, F. Damani, J. I. M. Alvarado, J. M. Janey, R. P. Adams and A. G. Doyle, Nature, 2021, 590, 89-96.
49. N. Holmes, G. R. Akien, A. J. Blacker, R. L. Woodward, R. E. Meadows and R. A. Bourne, Reaction Chemistry & Engineering, 2016, 1, 366-371.
50. A. D. Clayton, L. A. Power, W. R. Reynolds, C. Ainsworth, D. R. Hose, M. F. Jones, T. W. Chamberlain, A. J. Blacker and R. A. Bourne, Journal of Flow Chemistry, 2020, 10, 199-206.
51. H. L. Carter, A. W. Connor, R. Hart, J. McCabe, A. C. McIntyre, A. E. McMillan, N. R. Monks, A. K. Mullen, T. O. Ronson and A. Steven, Reaction Chemistry & Engineering, 2019, 4, 1658-1673.
52. A. M. Schweidtmann, A. D. Clayton, N. Holmes, E. Bradford, R. A. Bourne and A. A. Lapkin, Chemical Engineering Journal, 2018, 352, 277-282.

53. A. D. Clayton, J. A. Manson, C. J. Taylor, T. W. Chamberlain, B. A. Taylor, G. Clemens and R. A. Bourne, Reaction Chemistry & Engineering, 2019, 4, 1545-1554.
54. M. I. Jeraal, N. Holmes, G. R. Akien and R. A. Bourne, Tetrahedron, 2018, 74, 3158-3164.
55. P. Müller, A. D. Clayton, J. Manson, S. Riley, O. S. May, N. Govan, S. Notman, S. V. Ley, T. W. Chamberlain and R. A. Bourne, Reaction Chemistry & Engineering, 2022, 7, 987-993.
56. A. D. Clayton, E. O. Pyzer-Knapp, M. Purdie, M. F. Jones, A. Barthelme, J. Pavey, N. Kapur, T. W. Chamberlain, A. J. Blacker and R. A. Bourne, Angewandte Chemie International Edition, 2023, 62, e202214511.
57. O. J. Kershaw, A. D. Clayton, J. A. Manson, A. Barthelme, J. Pavey, P. Peach, J. Mustakis, R. M. Howard, T. W. Chamberlain and N. J. Warren, Chemical Engineering Journal, 2023, 451, 138443.
58. D. Fabry, E. Sugiono and M. Rueping, Reaction Chemistry & Engineering, 2016, 1, 129-133.
59. A.-C. Bédard, A. Adamo, K. C. Aroh, M. G. Russell, A. A. Bedermann, J. Torosian, B. Yue, K. F. Jensen and T. F. Jamison, Science, 2018, 361, 1220-1225.
60. S. V. Ley, Catalysis Science & Technology, 2016, 6, 4676-4677.
61. B. Gutmann, D. Cantillo and C. O. Kappe, Angewandte Chemie International Edition, 2015, 54, 6688-6728.
62. V. R. Joseph and Y. Hung, Statistica Sinica, 2008, 171-186.
63. P. Jorayev, D. Russo, J. D. Tibbetts, A. M. Schweidtmann, P. Deutsch, S. D. Bull and A. A. Lapkin, Chemical Engineering Science, 2022, 247, 116938.
64. E. Bradford, A. M. Schweidtmann and A. Lapkin, Journal of global optimisation, 2018, 71, 407-438.
65. S. T. Knox, S. J. Parkinson, C. Y. Wilding, R. A. Bourne and N. J. Warren, Polymer Chemistry, 2022, 13, 1576-1585.
66. A. D. Clayton, A. M. Schweidtmann, G. Clemens, J. A. Manson, C. J. Taylor, C. G. Niño, T. W. Chamberlain, N. Kapur, A. J. Blacker and A. A. Lapkin, Chemical Engineering Journal, 2020, 384, 123340.
67. P. Sagmeister, F. F. Ort, C. E. Jusner, D. Hebrault, T. Tampone, F. G. Buono, J. D. Williams and C. O. Kappe, Advanced Science, 2022, 9, 2105547.

68. F. Wagner, P. Sagmeister, C. E. Jusner, T. G. Tampone, V. Manee, F. G. Buono, J. D. Williams and C. O. Kappe, 2023.
69. C. Musikas, Inorganica Chimica Acta, 1987, 140, 197-206.
70. D. R. Prabhu, G. R. Mahajan and G. M. Nair, Journal of Radioanalytical and Nuclear Chemistry, 1997, 224, 113-117.
71. N. Condamines and C. Musikas, Solvent extraction and ion exchange, 1988, 6, 1007-1034.
72. D. R. Joshi and N. Adhikari, J. Pharm. Res. Int, 2019, 28, 1-18.
73. T. Welton, Proceedings of the Royal Society A: Mathematical, Physical and Engineering Sciences, 2015, 471, 20150502.
74. M. T. Sabatini, L. T. Boulton, H. F. Sneddon and T. D. Sheppard, Nature Catalysis, 2019, 2, 10-17.
75. J. R. Dunetz, J. Magano and G. A. Weisenburger, Organic Process Research & Development, 2016, 20, 140-177.
76. B. Li, G. A. Weisenburger and J. C. McWilliams, Organic Process Research & Development, 2020, 24, 2311-2318.
77. D. Prat, J. Hayler and A. Wells, Green Chemistry, 2014, 16, 4546-4551.
78. C. Wang, Q. Yan, H.-B. Liu, X.-H. Zhou and S.-J. Xiao, Langmuir, 2011, 27, 12058-12068.
79. M. H. Abraham, P. L. Grellier, J.-L. M. Abboud, R. M. Doherty and R. W. Taft, Canadian Journal of Chemistry, 1988, 66, 2673-2686.
80. T. Welton and C. Reichardt, Solvents and solvent effects in organic chemistry, John Wiley & Sons, 2011.

Chapter 3: Multi-Objective Bayesian Optimisation of Continuous Purifications with Automated Phase Separation for On-Demand Manufacture of DEHiBA

Thomas Shaw, Adam D. Clayton, Joseph A. Houghton, Nikil Kapur, Richard A. Bourne,* and Bruce C. Hanson

3.1 Abstract

The optimisation of purifications has received little attention in an era of machine-learning driven optimisation technologies that focus on synthesis, despite purifications being equally challenging and critical. This work utilizes lab-scale continuous purification equipment to automate the mixing and separation of phases for the purification of *N,N*-di-(2-ethylhexyl)isobutyramide (DEHiBA), a specialized ligand in demand for advanced nuclear reprocessing. Bayesian optimisation drove the purifications via feedback from HPLC and GC-FID quantitative analysis to maximize purity and product recovery via a weighted single objective. Batch purification screening found removal of *N,N*-di-(2-ethylhexyl)amine (DiEHA) to be problematic with aqueous only extractions, adding complexity to the purification. Three purification routes were optimized in continuous flow and compared for their efficacy after a single extraction stage. Optimisation of both product purity and recovery process metrics was crucial to identify optimum Pareto conditions. Product purities >95% were attainable for all routes, but the target of >99.9% was eluded after a single extraction in continuous flow. Product loss to the aqueous phase could be limited to <5%, but at the expense of product purity for all routes. Ultimately, a two-step process was devised from this work, employing a combination of water or 0.2 M nitric acid and acetonitrile to remove DiEHA and ~90% isobutyric acid, subsequent sodium bicarbonate extraction yielded >99.9% purity.

3.2 Introduction

Product purification is a key step in chemical manufacture, particularly for highly selective, specialized pharmaceuticals and extractants. Whilst high purities are prioritized, other metrics like waste reduction, sustainability, and cost are factors that can be optimized alongside purity, attaining a similar product with a reduced impact.[1] Publications that optimize processes focus on synthetic optimisation with purification optimisation escaping the spotlight.[2,3] Purification screening and optimisation can be time consuming and labour intensive but can be overcome via the adoption of automation and machine-learning (Industry 4.0) for batch or flow processes.[3,4]

Industrial batch chemistry traditionally involves discrete steps with intermittent transfer or storage of crude products and intermediates, often necessitating downtime for cleaning and preparation between batches.[5] This not only limits productivity but increases the risk of human error and contamination.[6] In contrast, flow chemistry facilitates the uninterrupted flow of reactants and products through reactors and purification equipment, resulting in constant product output.[7] The nature of continuous processes boosts productivity whilst improving product quality and consistency, with the telescoping of multiple steps into a single platform enabling robust on-demand product manufacture.[8] Despite recent advancements focusing on multi-step synthetic optimisation,[9] optimized continuous purification has garnered lesser attention.[10] Traditionally purification methods consume large volumes of solvents and aqueous phases to remove impurities, leading to poor process sustainability and economics.[11] The application of machine-learning algorithms to chemical purifications offers the possibility to improve multiple process metrics whilst yielding pure material.[12,13] Self-optimizing purification platforms explored in this work provide opportunity to simplify and automate the optimisation of operating conditions reducing the cost and time required to develop profitable, sustainable, and effective industrial processes from start to end.

Liquid-liquid extraction is well-suited for continuous flow, and the development of lab-scale purification equipment,[14] such as membrane separators and coalescing filtration,[15, 16] presents new opportunities for streamlined chemical manufacture. Access to highly capable and scalable equipment facilitates the optimisation of process conditions in the lab before pilot-plant operations, reducing the cost and complexity. Advantageously liquid-liquid extractions in flow can be automated, requiring little human intervention, reduced equipment downtime, and no solid waste disposal costs. By adapting self-optimizing flow reactor platforms to incorporate continuous separation/purification equipment, the automated optimisation of purification routes and conditions is increasingly feasible. AD Clayton et al.[17] has demonstrated the self-optimisation of an amine purification in continuous flow focusing on a single objective, purity, for this purification. To develop a balanced process, the work described herein optimizes product purity and recovery alongside sustainability, and economic process metrics.

Optimized and telescoped continuous synthesis and purification promises enhanced efficiency, improved safety, reduced environmental impact, and greater scalability;[18] Thus positioning continuous processes at the forefront in advancing the modern chemical industry, driving progress and innovation for the production of a wide range of chemical products.

The complete on demand manufacture of DEHiBA is a crucial step towards improving the economics and accessibility to ligands for advanced nuclear reprocessing.[19-22] Therefore, as previous work has optimized the synthesis of DEHiBA in continuous flow,[22] this work aims to achieve a fully optimized and integrated process by optimizing the purification of crude DEHiBA. Thus, the optimized, on-demand manufacture of other ligands and chemicals can follow. The objective for these optimisations is to produce DEHiBA with >99.9% purity, recovering maximum product with minimal waste across the whole platform. By optimizing the purification of crude DEHiBA (the output material from the synthetic optimisation of DEHiBA[22]) for product purity and

recovery whilst minimizing aqueous waste, this work overcomes the challenge of multi-step process optimisation where early changes impact later steps. Ultimately, the optimum synthetic and purification conditions can then be combined into a single platform, yielding a complete and efficient continuous manufacture route to pure DEHiBA on demand, granting improved accessibility to large volumes of industrially relevant extractants with less economic burden. Key advantages of this work is the ability to telescope the synthesis into the purification, leading to the continuous manufacture of DEHiBA on demand. No challenges are expected from the telescoping of these process due to the repeatability of both processes from the high level of control that continuous flow offers.

Additionally, insights gained from this work can be used to guide the development of purification (solvent wash) steps in nuclear reprocessing flowsheets to overcome challenges with removing fatty amines like DiEHA (*N,N*-di-(2-ethylhexyl)amine) or *N,N*-dioctylamine, typical degradation products of popular amide ligands like DEHiBA or TODGA (*N,N,N',N'*-tetraoctyldiglycolamide).[23-27]

3.3 Experimental

3.3.1 Chemicals and Crude Materials

All compounds were used as received. Acetonitrile (MeCN; HPLC grade), biphenyl (99%), naphthalene (99%), sodium bicarbonate, and hexane were purchased from Fisher Scientific Ltd. Nitric acid (68%) was purchased from VWR Chemicals. Ethyl acetate was purchased from Merck Life Science UK Ltd. Sodium naphthalenesulfonate (99%) was purchased from Fluorochem.

Two crude DEHiBA materials from chapter 2 (Figure S31) were purified in this work, batch work utilized the less pure (44%) DEHiBA obtained from high throughput synthetic conditions,

whilst the continuous flow work used purer (49%) DEHiBA from the reagent efficient synthesis. Compositions and synthetic conditions can be found in Chapter 6.2, **Figure S31**.

3.3.2 Optimisation Platform and Procedure

The flow platforms are detailed individually in Chapter 6.2 and were setup as per **Figure 33** for all optimisations, only the aqueous reservoir was changed between optimisations between nitric acid, water and sodium bicarbonate. Industrially available 2 mL fReactors (CSTRs) were used to mix the phases whilst a 2 mL coalescing separator was employed (chosen to minimise waste volumes whilst being large enough that phase separation can be maintained) to automate the phase separation via conductivity measurements and a needle valve connected to a servo motor (**Figure S24** and J. Daglish *et al.*[16]). The platform was controlled via a custom written MATLAB script, where the optimisation algorithms were also written and implemented. Automated multi-point sampling facilitated online analysis: each experiment was allowed to stabilize over a total flow equal to eight times the volume of the entire platform to reach steady state (**Figure S25**); then the sampling valve was triggered, sampling the aqueous outlet to the HPLC initializing the analysis, after 3 minutes the sampling valve for the organic outlet was triggered, again sampling to the HPLC.[18] Steady state and the performance of the separator was confirmed by testing identical conditions in batch and comparing to the results obtained in continuous flow for a variety of conditions. During this time samples of the organic phase were collected and quantified via GC-FID analysis. Process metrics were determined automatically from these chromatograms for feedback to the optimisation algorithm to generate the next batch of conditions.

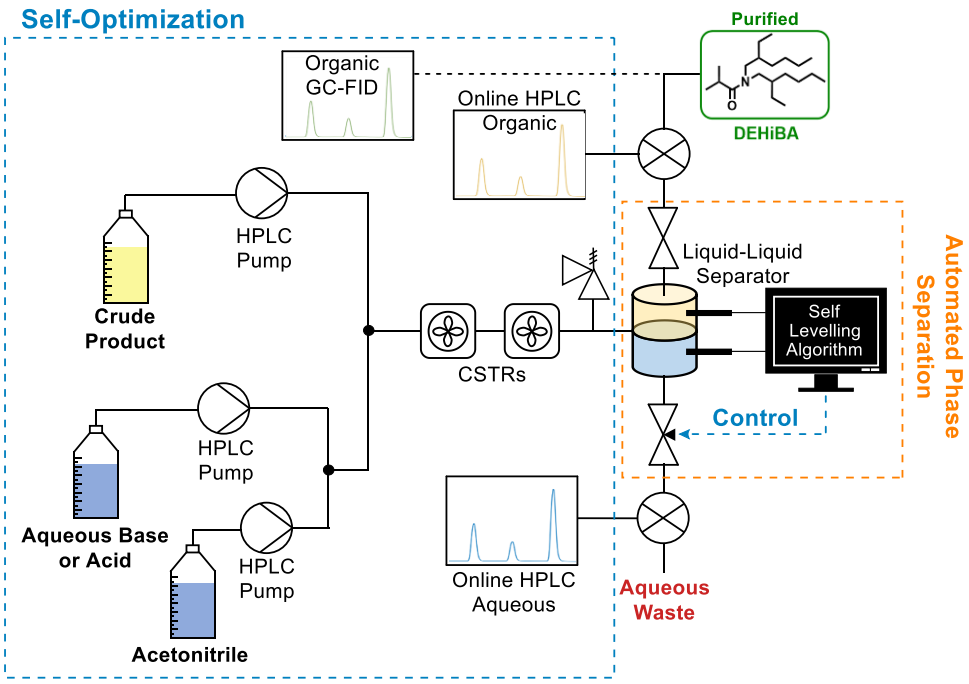

Figure 33: The self-optimizing flow purification platform employed in this work to automate the optimisation of purification conditions.

The concentration of DEHiBA in the aqueous and organic phases was quantified via online HPLC analysis using internal standards to determine volume changes and thus the loss of DEHiBA. Sodium naphthalenesulfonate (NSA) was used as the aqueous internal standard and was not found in the organic phase post extraction. As the starting materials and by-products are not UV-active their concentrations were quantified by GC-FID analysis, therefore organic samples were collected at steady state and diluted for GC-FID analysis using naphthalene as the external standard.

Bayesian Optimisation with Adaptive Expected Improvement (BOAEI)[18] was integrated for the closed-loop self-optimisation of chemical purification routes, identifying global optima in minimal experiments and thus minimal waste, time, and cost. This optimisation approach minimized periods of inactivity due to the time cost of GC-FID analysis, by suggesting new experiments in batches of four.

A weighted objective was used with BOAEI to target high purity, low product loss conditions whilst avoiding excessive material consumption needed to explore the whole Pareto front, solving

this expensive-to-evaluate optimisation with minimal experiments. The weighted objective combines and normalizes purity and product loss metrics, favouring purities >95% and minimal product loss. The algorithm employs a Bayesian optimisation methodology utilizing Gaussian processes (GPs) as the surrogate models for the objective. The acquisition function uses adaptive expected improvement to balance exploration and exploitation. The algorithm was terminated once convergence on the optimum was realized or crude material was exhausted.

3.4 Results and Discussion

3.4.1 Purification Goals

This work sets out to optimize the purification of crude products, specifically DEHiBA in continuous flow using Bayesian optimisation algorithms to optimize both product purity and recovery alongside minimizing the volume of aqueous waste. Ultimately, a product purity >99.9% is required but can be achieved whilst optimizing sustainability and economic process metrics. The automated extraction/separation equipment benefits economics further by reducing time and labor required for process optimisation. Batch purification screening was utilized to identify a suitable purification route to optimize in continuous flow.

Preliminary purification work found the removal of DiEHA from the crude product proved challenging with an aqueous only liquid-liquid extraction. Overcoming this challenge led to product losses due to addition of acetonitrile to the aqueous phase, it was therefore paramount that both product purity and recovery were maximized in this work. Although it may be possible to achieve the desired purity in a single stage with a large volume ratio of aqueous to organic phase or other wasteful methods, the goal is to minimize waste, risk and thereby cost so limits for volume ratios were set for the optimisations (**Table S17**).

Ideally the optimum purification route here maximizes purity and product recovery, whilst minimizing the number of extraction stages/steps, cost, and waste. This work prioritizes maximizing product purity and recovery using the defined weighted objective and BOAEI to optimize a single stage/step, with minimal aqueous waste a secondary objective. This work only uses one stage to identify ideal conditions and compare routes to simplify the optimisation and minimize costs, but the incorporation of multiple stages and steps is calculable and can be verified.

3.4.2 Batch Purification Screening

Batch purifications were employed to screen a range of purification routes and conditions to develop a promising system that could be transitioned into continuous flow. The crude material used was collected from a 5-hour synthesis run using high throughput conditions identified in previous work, to yield 72 kg L^{-1} h^{-1} DEHiBA from iBAnhydride and DiEHA.[22] The composition of the crude material before and after base extraction is quantified via GC-FID analysis (**Tables 8 & S14**), where purity is calculated using moles. The starting material has a 44% product purity with ~1% DiEHA and 55% iBA.

Table 8: Comparison of batch purifications varying the amount of base and hexane

Volume Ratio and Composition		Purity (%)	mol% DiEHA wrt DEHiBA	mol% iBA wrt DEHiBA
	Crude DEHiBA	44.0	2.9	125.4
1:1	DEHiBA : sat. NaHCO3	85.4	3.3	13.7
1:2		97.6	2.4	0.0
1:3		97.6	2.4	0.0
1:1:1	DEHiBA : hexane : sat. $NaHCO_3$	84.1	2.3	16.6
1:1:2		97.8	2.2	0.0
1:1	DEHiBA : NaOH	97.5	2.6	0.0
1:2		97.7	2.4	0.0
1:3		97.7	2.4	0.0
1:1:1	DEHiBA : hexane : NaOH	83.0	2.6	17.9
1:1:2		85.8	2.2	14.4

As iBA is the major impurity, purification screening began with bases such as saturated sodium bicarbonate and 1 M sodium hydroxide. The volume ratio of crude DEHiBA to aqueous phase was varied for each extraction, and hexane was added as a variable to aid separation and compare performance. Hexane improved separation in all cases, reducing the separation time, though separation was possible without. Purifications with base targeted iBA removal, with little to no removal of DiEHA as expected. Saturated sodium bicarbonate was selected as a cheap, relatively benign reagent, for comparison with 1 M NaOH, a more powerful, but also more hazardous and corrosive base with a greater pH.

1 M NaOH proved to be more volume effective, but both were only able to achieve purities <98%. Inclusion of hexane hindered iBA extraction when using NaOH, leading to a drop in product purity, but did not reduce product purity when using $NaHCO_3$. Overall, the combination of $NaHCO_3$ and hexane was most promising, offering a benign, cost-effective route, with the addition of hexane improving phase separation reducing operational complexity. Alternative bases like methylamine, pyridine, and ammonium hydroxide were also screened but afforded no benefit (**Table S15**). To

improve purity to >99.9% a different purification route was needed to remove DiEHA and iBA, ideally in a single step to minimize complexity and cost.

Next, DiEHA was targeted for its removal via acid extractions, this fatty amine oxidizes over time from colourless to yellow interfering with UV-Vis analysis a technique often employed to monitor and quantify uranium extraction.[28-30] It was therefore paramount that this material be removed to avoid complications downstream when performance testing DEHiBA. An efficient methodology for DiEHA removal would also support reprocessing development. 1 M sulfuric acid, 2 M nitric acid, and saturated ammonium chloride were compared for the purification of crude DEHiBA (**Table S16**). However as nitric acid is already utilized in nuclear reprocessing and to avoid entrainment of ions like sulfate or chloride, as these are known to interfere with UV-Vis absorption of uranium(VI),[31] nitric acid is the preferred acid for this work. Nevertheless, the performance of these acid must be assessed.

Screening of these acids alone did not achieve the desired >99.9% purity, instead achieving up to ~76% purity via the extraction of iBA but not DiEHA. Removal of DiEHA was unexpectedly poor and did not improve when increasing the amount of acid, likely due to the insolubility of the fatty chains in the polar aqueous phase. Nitric acid performed best with 70-77% purities, whilst sulfuric acid and ammonium chloride produced purities between 64-71%, both benefitting from the inclusion of hexane, nitric acid purifications were seemingly unaffected by the presence of hexane here. Notably, no significant benefit was gained by increasing the volume of each acid present.

To overcome this lack in performance and the poor extraction of DiEHA with acid alone, acetonitrile (MeCN) was incorporated into the aqueous phase, hoping to aid solubilize the greasy DiEHA and improve product purity. This study (**Table S17**) utilized the same acids, again with and without hexane, incorporating equal volumes of acetonitrile whilst increasing the amount of acid.

These extractions achieved up to 88% purity using nitric acid, MeCN and hexane, again with nitric acid outperforming the other acids that achieved a maximum of 80% purity for sulfuric acid and no significant improvement for ammonium chloride. For both nitric acid and sulfuric acid, lower acid content in the aqueous phase improved DiEHA removal.

As nitric acid outperformed the other acids it proved to be most suitable for further investigation, this time increasing the ratio of MeCN to DEHiBA (**Table 9**). This work highlights the importance of the DEHiBA to MeCN ratio for extracting DiEHA where increased MeCN improves extraction, but increased nitric acid hinders DiEHA extraction. Additionally, the absence of hexane reduced the overall purity and extraction of DiEHA. Greater than 99.9% purity was achieved in a single step for the greatest ratios explored using equal volumes of crude DEHiBA, hexane, and nitric acid, but a large excess of MeCN (4x the volume of crude DEHiBA). These extractions removed DiEHA and iBA without the need for base, streamlining the process potentially to a single step, reducing process complexity.

Table 9: Comparison of batch purifications varying the amount of acid, hexane, and the importance of acetonitrile.

Volume Ratio and Composition		Purity (%)	mol% DiEHA wrt DEHiBA	mol% iBA wrt DEHiBA
1:1:1	DEHiBA : MeCN : HNO_3	73.3	2.0	34.4
1:1:2		75.7	2.2	29.9
1:1:3		76.2	2.3	28.9
1:2:1	DEHiBA : MeCN : HNO_3	81.0	1.0	22.5
1:3:1		86.1	0.6	15.6
1:1:2:1	DEHiBA : hexane : MeCN : HNO_3	89.1	0.0	12.3
1:1:3:1		95.2	0.0	5.1
1:1:4:1		100.0	0.0	0.0
1:1:5:1		100.0	0.0	0.0

Overall, nitric acid outperformed sulfuric acid and ammonium chloride even in the presence of acetonitrile, suggesting both nitric acid and acetonitrile facilitated the removal of iBA and DiEHA. The combination of hexane, acetonitrile and nitric acid benefitted the purification most, with

hexane improving purity and separation. Ultimately, an excess of acetonitrile provided the best performance, facilitating the complete removal of DiEHA and iBA in a single step. Despite the obvious benefits acetonitrile provides, these extractions are now more complex due to increased solubility of DEHiBA in the aqueous phase leading to greater product losses. This added complexity lends itself to multi-objective optimisation where the trade-off between product purity and recovery can be minimized.

3.4.3 Continuous Flow Purifications

Following the identification of a single-step purification route in batch, focus moved to optimizing this system in continuous flow aiming to achieve similar performance and optimize process conditions. Ultimately, a purity >99.9% is required, whilst minimizing the loss of DEHiBA to the aqueous phase, ideally in a single step or with minimal steps/stages, minimizing aqueous waste and thus cost.

The same crude product was used for these purifications for fair comparison (**Figure S31**), differing from the batch purifications with greater DEHiBA content and less impurity. DEHiBA makes up 49% of this material with 50% iBA and ~1% DiEHA as a molar composition. This crude DEHiBA was used as its synthesis was best suited for scale-up, being most cost effective.

The nitric acid optimisations utilized BOAEI to maximize purity then moved to TSEMO to maximize purity and minimize DEHiBA loss, however TSEMO did not perform as intended, prioritising minimal product loss avoiding high purity conditions. Therefore, BOAEI was reintroduced, this time with the weighted objective which focused on identifying conditions of most interest with little product loss but maximum purity to more effectively solve this expensive-to-evaluate optimisation. BOAEI and the weighted objective were solely used for the water and sodium bicarbonate optimisations due to the improved efficacy.

3.4.3.1 Nitric Acid and Acetonitrile Purifications

Nitric acid concentration was reduced from 2.0 M used in batch work, to 0.2 M for the initial purification optimisation in flow, reducing the risk associated with mixing nitric acid with organic materials. Purity and DEHiBA loss data for this optimisation is plotted across the design space in **Figure 34**, highlighting the effect of each variable. Purity benefitted most from high ratios of MeCN to crude DEHiBA, whilst nitric acid had minimal effect on purity besides providing phase separation, as low nitric acid ratios resulted in miscibility for certain organic, acetonitrile ratios (dark blue markers). To contrast, minimal DEHiBA loss favoured opposite trends, favouring lower acetonitrile to crude DEHiBA ratios, crucially increased nitric acid content hindered DEHiBA extraction. Product loss can therefore be minimized at high purity conditions by increasing nitric acid content.

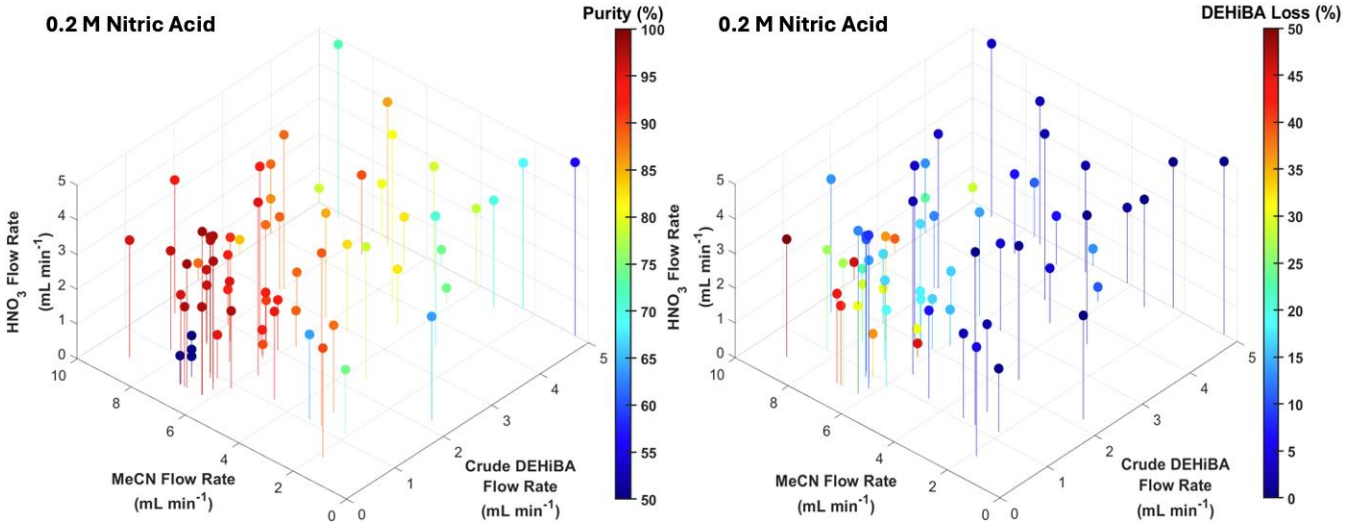

Figure 34: Purity and product loss across the parameter space for the optimisation with 0.2 M nitric acid and acetonitrile.

Purity and product loss are the primary process metrics optimized in this work, however, the amount and composition of waste is detailed in **Table 10** for comparison of relative cost and sustainability, allowing identification of balanced, yet optimum process conditions. For example,

the most optimal condition here only produces 94% pure DEHiBA after a single stage, however low product losses of 1.5% and comparatively low volumes of aqueous waste after a single stage yields optimum overall performance. The target purity of >99.9% is still feasible using this condition but would theoretically require at least three extraction stages, only losing ~5% DEHiBA overall. In comparison, conditions that yield 97.8% or even 98.6% purity lose 8-12% DEHiBA and >2 times the aqueous waste without achieving the desired purity in a single stage, justifying the importance of optimizing and comparing these metrics.

Table 10: Performance metrics for the optimal conditions when using acetonitrile and 0.2 M nitric acid to purify crude DEHiBA.

Crude DEHiBA Flow Rate (mL min^{-1})	MeCN Flow Rate (mL min^{-1})	0.2 M HNO_3 Flow Rate (mL min^{-1})	MeCN:HNO_3 Flow Ratio	Purity (%)	DEHiBA Loss (%)	Aqueous: Organic Ratio
1.575	5.387	5.000	1.08	94.0	1.5	6.6
1.370	5.746	5.000	1.15	95.4	2.3	7.8
1.481	5.803	2.569	2.26	95.9	9.9	5.7
0.888	6.659	4.071	1.64	97.4	9.6	12.1
0.727	6.239	4.270	1.46	97.8	8.8	14.5
0.705	6.226	4.431	1.41	97.8	8.5	15.1
0.518	6.291	4.703	1.34	98.6	12.7	21.2

A similar optimisation was executed using 1.0 M nitric acid to understand and optimize the influence of nitric acid concentration. Purity and DEHiBA loss comparison, **Figure 35 & S33** shows little difference between 0.2 M and 1.0 M nitric acid concentrations, with the optimum conditions highlighted using the weighted objective function as the colourbar for the 4D plot. Thus, indicating that the concentration of nitric acid has little effect on the purification in continuous flow for these conditions.

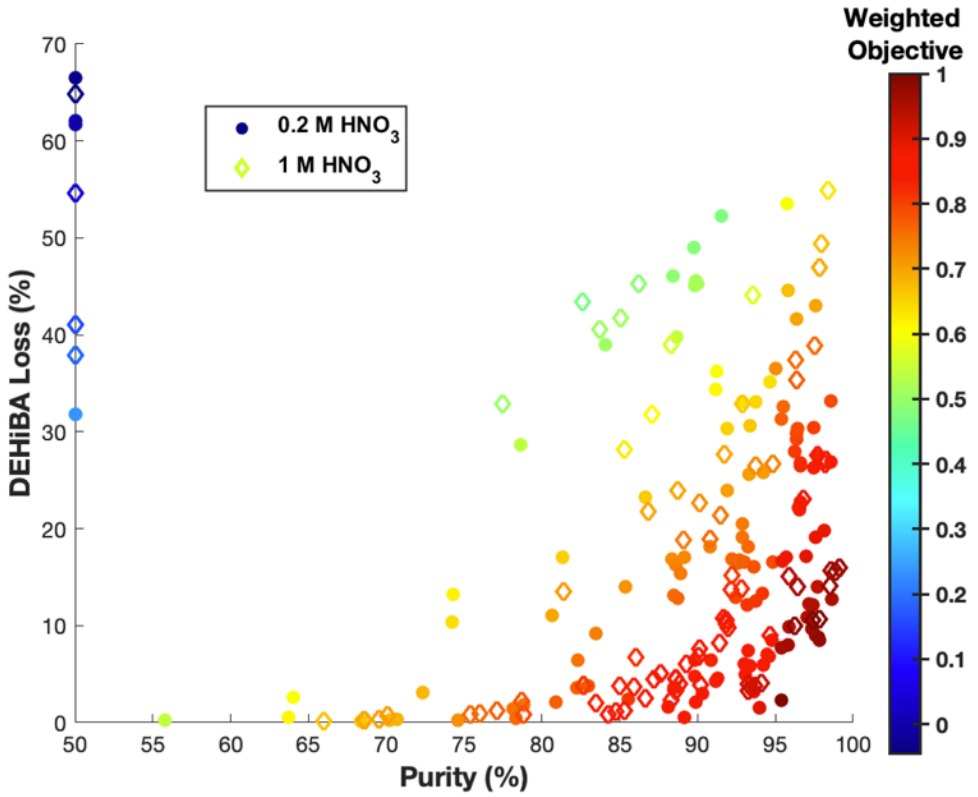

Figure 35: Comparing purity and product loss metrics for the purifications with 0.2 M and 1.0 M nitric acid using the weighted objective (defined in the methodology) as a visual aid, indicating the more optimal conditions.

Both nitric acid concentrations are capable of 98-99% product purity, although product losses >9% are met above 96% purity and increase with higher purity as illustrated in **Figure 35**. By operating at 94-95% purity, product losses can be limited to 1-2%. Whereas by operating at 97-98% purity 9-10% DEHiBA is lost per stage, which despite potentially requiring less extraction stages to achieve a product purity >99.9%, overall DEHiBA losses are greater. The performance of each condition must therefore be weighed up with the theoretical minimum number of extraction stages to achieve >99.9% purity before identifying optimum purification conditions and route.

Further work with 0.2 M nitric acid proved this routes capability for removing greater quantities of DiEHA, as well as removal of iBAnhydride. This is highly desirable, as in the event of differing crude product composition from manufacture, this purification route is more than capable, though more extraction stages may be needed to achieve the desired purity. The nature

of this continuous process allows integration of inline and online process analytics to monitor purity, regularly ensuring product quality with less manual intervention reducing human error and risk. The process can therefore be understood and adjusted in real-time with this technology to account for any process upset.

As it is unclear whether nitric acid is beneficial to the purification, the next optimisation employed water to replace the nitric acid instead of optimizing for nitric acid concentration.

3.4.3.2 Evaluating the Need for Nitric Acid: Purifications with Water and Acetonitrile

This purification exchanged nitric acid for deionized water, only using the weighted objective optimisation methodology to reach an optimum in fewer experiments saving time and waste. Visually, phase separation was less problematic with water, which advantageously is a cheaper, less hazardous material to store and use, thereby reducing operational and disposal costs. The water, acetonitrile waste stream offers simplified recovery and recycle of starting materials, by-products and solvents, lending to a greener, cleaner process, avoiding concerns with nitric acid, improving safety and sustainability whilst minimizing raw material cost.

Purity and product loss trends from this optimisation were analogous to the nitric acid optimisations (**Figure S35**), with maximum purity favouring high acetonitrile to crude DEHiBA ratios, and seemingly independent of water. Again, the opposite was true for minimal product loss, favouring high crude DEHiBA to acetonitrile ratios, whilst water hindered product loss. As this optimisation explored the design space less than the nitric acid extractions, the data was modelled using a quadratic linear regression model (**Figure S36**) to better understand the interactions

between parameters and validate our understanding of this purification route. Overall, these models confirm the influence of water content on DEHiBA loss but no influence on the purity.

The purity and product loss trade-off data for this purification route is overlaid with the data from the 0.2 M nitric acid purifications for comparison **Figure 36**; Similar performance is achieved between 94-96% purity yielding similar product losses, however maximum purity is reduced when using water, struggling to exceed 97%. For optimal overall performance 94-95% purity minimizes product losses to ~3% after a single extraction stage. The optimum conditions are highlighted in **Figure S37** using the weighted objective function, seemingly requiring less MeCN compared to the nitric acid purifications.

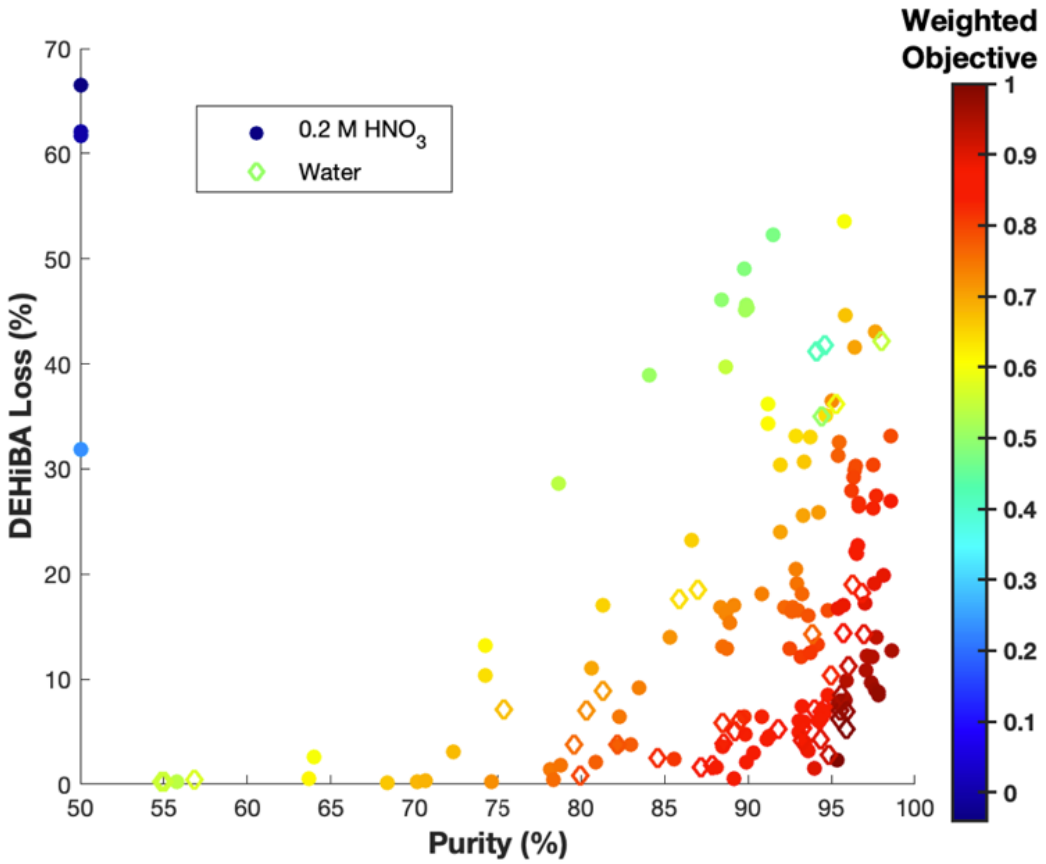

Figure 36: Comparing purity and product loss metrics for the purifications with water vs 0.2 M nitric acid using the weighted objective indicating the more optimal conditions.

Despite sustainability benefits of water over nitric acid these benefits are lessened by the greater volume of aqueous waste for the optimal conditions (**Table 11**) compared to the nitric acid purifications. For example, the optimum condition yields 94.9% product purity, losing ~3% DEHiBA but requiring three times the aqueous volume as the optimum nitric acid condition that produced 94% purity, losing ~1.5% DEHiBA. Again, the higher purity conditions here lose a greater percentage of DEHiBA, especially over 96% purity. Lower volumes of aqueous waste are possible but result in greater losses of DEHiBA so this must be assessed from a cost perspective.

Table 11: Performance metrics for the optimal conditions when using acetonitrile and water to purify crude DEHiBA.

Crude DEHiBA Flow Rate (mL min^{-1})	MeCN Flow Rate (mL min^{-1})	Water Flow Rate (mL min^{-1})	MeCN:Water Flow Ratio	Purity (%)	DEHiBA Loss (%)	Aqueous: Organic Ratio
0.500	4.251	4.997	0.85	94.9	2.8	18.5
0.500	5.088	4.810	1.06	95.4	6.2	19.8
0.500	4.603	4.002	1.15	95.5	7.7	17.2
0.500	4.944	4.639	1.07	95.5	7.0	19.2
0.769	6.071	4.272	1.42	95.6	8.5	13.4
0.500	5.147	4.454	1.16	95.9	6.9	19.2
0.500	5.289	5.000	1.06	95.9	5.3	20.6
0.750	6.869	4.696	1.46	96.0	11.2	15.4
0.500	6.057	4.296	1.41	96.9	14.3	20.7

Purities >99.9% are possible via both routes, though require multiple extraction stages to achieve this. Both routes performed best between 94-96% purity due to the trade-off with product loss causing product loss to increase significantly over 95-96% purity. As these conditions require the same number of extraction stages to achieve >99.9% purity, total product loss is important for identifying optimal conditions.

In summary, water offers similar optimal trade-off performance between purity and product loss to the nitric acid purifications. To its benefit water is a more favourable reagent than nitric acid in terms of sustainability and safety. Nitric acid benefits from less aqueous waste for similar

purity and product losses, this must be weighed up against the cost and risk of nitric acid storage and disposal. Finally, the aqueous waste stream from the water purifications makes recycle of this phase simpler and likely more cost effective than disposal of the nitric acid waste stream. Both routes have benefits, particularly water being more risk averse than nitric acid, however, a cradle to grave economic analysis is needed to identify the most optimum route.

3.4.3.3 Targeting iBA Removal: Sodium Bicarbonate and Acetonitrile Purifications

Isobutyric acid (iBA) is the major impurity in the crude DEHiBA used, even after purification via the other routes. Purifications with sodium bicarbonate proved successful in batch with complete removal of iBA, but no removal of DiEHA. The addition of acetonitrile therefore hoped to yield >99.9% purity removing both DiEHA and iBA in fewer stages with less aqueous waste. Preliminary work with saturated sodium bicarbonate and acetonitrile proved challenging due to precipitation and blockages when combined. The concentration of sodium bicarbonate was reduced to 0.4 M to facilitate the mixing of this phase with acetonitrile without precipitation, the result being solubility until a 1:3 ratio of sodium bicarbonate to acetonitrile which then prompted precipitation. This was coded into the MATLAB optimisation code to avoid exceeding this, preventing blockages. Sodium bicarbonate was chosen over bases like sodium hydroxide due to being less hazardous and corrosive, plus similar solubility challenges were also faced with sodium hydroxide.

As fewer experiments were conducted during this optimisation, due to limited crude material and a refined objective for the BOAEI algorithm, the purity data was modelled to verify the parameter interactions for this purification. Experimental work suggests (**Figure 37**, a) that sodium bicarbonate has a greater effect on product purity than water or nitric acid, promoting

aqueous solubility of iBA, with high product purities achievable even at low acetonitrile flow rates. The purity model, **Figure S40** confirms the benefit of increased sodium bicarbonate content for product purity. Additionally, product loss is again hindered when aqueous (base) content increases, therefore this route is capable of high purities at low acetonitrile flow rates, reducing the trade-off between purity and product loss.

This purification appears to better overcome the trade-off between purity and product loss (**Figure 37**, **a-b**), benefitting from the reduced acetonitrile content due to enhanced sustainability and lower cost even at high purity low product loss conditions. However, the reduction in acetonitrile content results in incomplete removal of DiEHA as illustrated in four dimensions alongside purity and product loss (**Figure 37**, **c-d**), an issue not encountered with the other purification routes. As a result, the observed optimal conditions do not completely extract DiEHA despite its low concentration. This is of great concern especially if the reaction yield falls during manufacture as this route may not be able to handle an increase in DiEHA resulting in an impure product even with multiple extraction stages.

It is possible to operate at less optimal conditions that ensure DiEHA removal, however despite purities up to 99%, 9-10% product loss results in this route being comparable to the higher purity nitric acid purifications (**Figure 37**, **e-f**). Additionally, this route did not grant any reduction in aqueous waste with 0.2 M nitric acid generating less waste, though the cost for disposal of nitric acid may outweigh this difference in volume. The most optimal condition for this purification yields 96.9% purity with 0.7% product loss and less aqueous waste compared to the other conditions, though DiEHA is not completely removed and may require numerous stages for removal. Alternatively, for complete DiEHA removal 99% purity is possible but at the cost of 10% product loss and higher volumes of aqueous waste (**Table 12**).

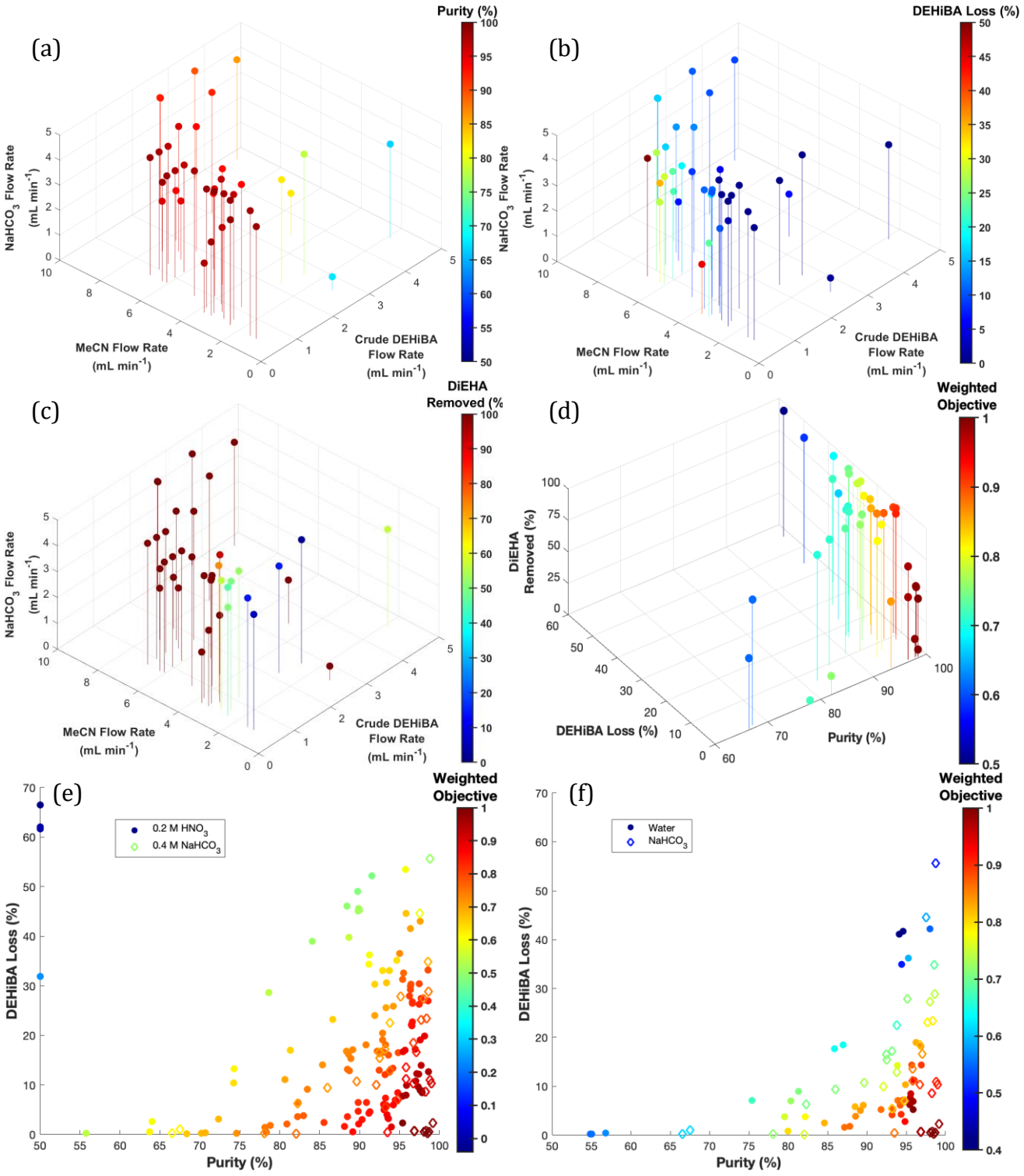

Figure 37: Purity, product loss and DiEHA removal performance across the parameter space for the optimisation with 0.4 M sodium bicarbonate and acetonitrile (a-c) respectively. Comparison of these performance metrics using the weighted objective to highlight that the optimum Purities and product losses lead to incomplete removal of DiEHA (d). The bottom plots (e-f) compare the purity and product loss performance of this route to the other routes.

Table 12: Performance metrics for the optimal conditions when using acetonitrile and 0.4 M sodium bicarbonate to purify crude DEHiBA.

Crude DEHiBA Flow Rate (mL min^{-1})	MeCN Flow Rate (mL min^{-1})	$NaHCO_3$ Flow Rate (mL min^{-1})	MeCN: $NaHCO_3$ Flow Ratio	Purity (%)	DEHiBA Loss (%)	DiEHA Removed (%)	Aqueous: Organic Ratio
0.692	2.608	5.000	0.52	96.8	0.7	49.8	11.0
0.914	3.624	5.000	0.72	96.9	0.7	74.0	9.4
0.500	1.441	5.000	0.29	98.1	0.5	14.8	12.9
0.591	2.911	5.000	0.58	98.3	0.8	55.8	13.4
0.502	1.141	4.484	0.25	98.5	0.3	6.0	11.2
0.512	2.453	4.994	0.49	98.7	0.5	45.8	14.6
0.612	3.437	4.852	0.71	99.0	10.3	100.0	13.5
0.556	2.526	4.147	0.61	99.2	2.3	50.8	12.0

Ultimately this route demonstrates promise for removing large quantities of iBA, but is let down by the lack of DiEHA removal, leading to the question as to whether acetonitrile is required for this step to achieve similar performance. Removal of acetonitrile from the purification would allow the removal of iBA as demonstrated in the batch purification work, preventing the extraction of DEHiBA, but not facilitating DiEHA removal, requiring an additional step before reaching the target purity.

3.4.4 An Optimum Purification Route

The optimisation of these purification routes has not identified a purification route capable of >99.9% purity in a single stage, yet all routes are capable of this target purity via multiple extraction stages. This has escalated the importance of minimizing product loss and aqueous waste to ensure optimal performance. By first using acetonitrile and water or 0.2 M nitric acid, the organic phase is then contacted with sodium bicarbonate to yield >99.9% product purity (**Figure S41**) avoiding a multi-stage purification that utilizes the same route and conditions. The second step of this route has not been optimized in this work but represents a successful proof of concept with no DEHiBA identified in the aqueous phase, limiting DEHiBA losses to 1-3% whilst achieving

>99.9% product purity. The purified products from the optimum purifications with water and 0.2 M nitric acid were used in batch to achieve the target purity using an equal volume of saturated sodium bicarbonate.

Alternatively, purifying with sodium bicarbonate first, followed by an acetonitrile and water or 0.2 M nitric acid extraction to remove residual DiEHA and iBA could reduce aqueous waste and further minimize product loss, however this would require further testing and optimisation. Whereas the first proposed route is more readily implemented.

3.5 Conclusion

In summary, the development of lab-scale purification equipment for continuous flow, in this case a coalescing filter, has facilitated the development of a self-optimizing continuous purification platform that utilizes machine-learning and automation to test, develop, and optimize purification routes prior to pilot plant. This minimizes material consumption during the development of a suitable and optimized purification route, reducing complexity and labour. The optimisation of purification conditions is no less important than synthetic optimisation, improving overall process sustainability, economics and ultimately the final product.

The crude DEHiBA used in this work is required to be at least 99.9% pure, requiring removal of iBA and DiEHA, also the degradation products of DEHiBA in nuclear reprocessing. Batch purifications found DiEHA troublesome to remove with a purely aqueous workup, which could cause problems for an industrial reprocessing flowsheet. This work compared three different purification routes in continuous flow, all employing acetonitrile and an aqueous phase (nitric acid, water, and sodium bicarbonate) to purify crude DEHiBA derived from optimum synthetic conditions identified in previously published work. The aqueous phases included two nitric acid

concentrations, water and 0.4 M sodium bicarbonate. All routes were capable of purities >95% up to 99%, however the minimization of product loss became an important objective with all routes capable of losing <3% but at the cost of purity. Sodium bicarbonate was most hindered resulting in poor DiEHA extraction or high product losses >9%. 0.2 M nitric acid marginally outperformed water for a single stage extraction losing less DEHiBA, 1.5% vs 3% and a third of the aqueous waste, at the minor cost of 1% purity. Unfortunately, nitric acid adds further complications and increases the cost of the aqueous waste compared to water adding complication to the decision.

A multi-step purification platform has been devised for the purification of crude DEHiBA that is capable of <3% product loss and 99.9% product purity. Pure DEHiBA can be manufactured on demand using this platform, improving accessibility to this specialized ligand for uranium extraction.

3.6 Future Work

Next, the optimisation of a multi-stage or multi-step purification would be interesting to further optimise the system and achieve desired purities more easily. This system was planned to be telescoped to the synthetic continuous flow platform for the constant manufacture of purified DEHiBA, however, time did not allow completion of this work. Additionally, other purification routes would be investigated potentially eliminating the need for acetonitrile. The following chapter (4) tests the performance of purified and crude DEHiBA for the extraction of uranium(VI) to ensure the suitability of the manufacture route. Although the pure DEHiBA was not obtained from this continuous purification platform, similar chemicals were used to purify DEHiBA, so that the suitability of DEHiBA produced via these routes can be confirmed. Further work could work on minimising the volume of the coalescing separator or CSTRs to reduce material consumption further during process optimisation.

3.7 References

1 R. A. Sheldon, Metrics of green chemistry and sustainability: past, present, and future, ACS Sustain Chem Eng, 2018, 6, 32–48.

2 P. M. Murray, F. Bellany, L. Benhamou, D.-K. Bučar, A. B. Tabor and T. D. Sheppard, The application of design of experiments (DoE) reaction optimisation and solvent selection in the development of new synthetic chemistry, Org Biomol Chem, 2016, 14, 2373–2384.

3 A. D. Clayton, J. A. Manson, C. J. Taylor, T. W. Chamberlain, B. A. Taylor, G. Clemens and R. A. Bourne, Algorithms for the self-optimisation of chemical reactions, React Chem Eng, 2019, 4, 1545–1554.

4 A. M. Schweidtmann, A. D. Clayton, N. Holmes, E. Bradford, R. A. Bourne and A. A. Lapkin, Machine learning meets continuous flow chemistry: Automated optimisation towards the Pareto front of multiple objectives, Chemical Engineering Journal, 2018, 352, 277–282.

5 M. Baumann, T. S. Moody, M. Smyth and S. Wharry, A perspective on continuous flow chemistry in the pharmaceutical industry, Org Process Res Dev, 2020, 24, 1802–1813.

6 M. Movsisyan, E. I. P. Delbeke, J. Berton, C. Battilocchio, S. V Ley and C. V Stevens, Taming hazardous chemistry by continuous flow technology, Chem Soc Rev, 2016, 45, 4892–4928.

7 J. Britton and C. L. Raston, Multi-step continuous-flow synthesis, Chem Soc Rev, 2017, 46, 1250–1271.

8 T. Ichitsuka, M. Sato, S. Miura, T. Makino and T. Ishizaka, Telescoped two-step continuous-flow synthesis of vanillin, ACS Sustain Chem Eng, 2023, 11, 16322–16329.

9 A. D. Clayton, Recent Developments in Reactor Automation for Multistep Chemical Synthesis, Chemistry-Methods, 2023, 3, e202300021.

10 A. D. Clayton, A. M. Schweidtmann, G. Clemens, J. A. Manson, C. J. Taylor, C. G. Niño, T. W. Chamberlain, N. Kapur, A. J. Blacker and A. A. Lapkin, Automated self-optimisation of multi-step reaction and separation processes using machine learning, Chemical Engineering Journal, 2020, 384, 123340.

11 F. F. Cantwell and M. Losier, in Comprehensive analytical chemistry, Elsevier, 2002, vol. 37, pp. 297–340.

12 P. Jorayev, D. Russo, J. D. Tibbetts, A. M. Schweidtmann, P. Deutsch, S. D. Bull and A. A. Lapkin, Multi-objective Bayesian optimisation of a two-step synthesis of p-cymene from crude sulphate turpentine, Chem Eng Sci, 2022, 247, 116938.

13 S. T. Knox, S. J. Parkinson, C. Y. P. Wilding, R. A. Bourne and N. J. Warren, Autonomous polymer synthesis delivered by multi-objective closed-loop optimisation, Polym Chem, 2022, 13, 1576–1585.

14 M. R. Chapman, M. H. T. Kwan, G. King, K. E. Jolley, M. Hussain, S. Hussain, I. E. Salama, C. González Niño, L. A. Thompson and M. E. Bayana, Simple and versatile laboratory scale CSTR for multiphasic continuous-flow chemistry and long residence times, Org Process Res Dev, 2017, 21, 1294–1301.

15 A. Adamo, P. L. Heider, N. Weeranoppanant and K. F. Jensen, Membrane-based, liquid–liquid separator with integrated pressure control, Ind Eng Chem Res, 2013, 52, 10802–10808.

16 J. Daglish, A. J. Blacker, G. de Boer, S. J. Russell, M. Tausif, D. R. J. Hose, A. R. Parsons, A. Crampton and N. Kapur, A Coalescing Filter for Liquid–Liquid Separation and Multistage Extraction in Continuous-Flow Chemistry, Org Process Res Dev, 2024, 28, 1979–1989.

17 A. D. Clayton, L. A. Power, W. R. Reynolds, C. Ainsworth, D. R. J. Hose, M. F. Jones, T. W. Chamberlain, A. J. Blacker and R. A. Bourne, Self-optimising reactive extractions: towards the efficient development of multi-step continuous flow processes, J Flow Chem, 2020, 10, 199–206.

18 A. D. Clayton, E. O. Pyzer-Knapp, M. Purdie, M. F. Jones, A. Barthelme, J. Pavey, N. Kapur, T. W. Chamberlain, A. J. Blacker and R. A. Bourne, Bayesian Self-Optimisation for Telescoped Continuous Flow Synthesis, Angewandte Chemie, 2023, 135, e202214511.

19 S. Bourg, A. Geist, J.-M. Adnet, C. Rhodes and B. C. Hanson, Partitioning and transmutation strategy R&D for nuclear spent fuel: the SACSESS and GENIORS projects, EPJ Nuclear Sciences & Technologies, 2020, 6, 35.

20 R. Malmbeck, D. Magnusson, S. Bourg, M. Carrott, A. Geist, X. Hérès, M. Miguirditchian, G. Modolo, U. Müllich and C. Sorel, Homogenous recycling of transuranium elements from irradiated

fast reactor fuel by the EURO-GANEX solvent extraction process, Radiochim Acta, 2019, 107, 917–929.

21 M. Miguirditchian, L. Chareyre, C. Sorel, I. Bisel, P. Baron and M. Masson, Development of the GANEX process for the reprocessing of Gen IV spent nuclear fuels.

22 T. Shaw, A. D. Clayton, R. Labes, T. M. Dixon, S. Boyall, O. J. Kershaw, R. A. Bourne and B. C. Hanson, A self-optimised approach to synthesising DEHiBA for advanced nuclear reprocessing, exploiting the power of machine-learning, React Chem Eng, 2024, 9, 426–438.

23 M. Carrott, K. Bell, J. Brown, A. Geist, C. Gregson, X. Hères, C. Maher, R. Malmbeck, C. Mason and G. Modolo, Development of a new flowsheet for co-separating the transuranic actinides: the "EURO-GANEX" process, Solvent Extraction and Ion Exchange, 2014, 32, 447–467.

24 S. Tachimori and Y. Morita, Ion exchange and solvent extraction, 2010, 19, 1–63.

25 A. Baker, A. Fells, M. J. Carrott, C. J. Maher and B. C. Hanson, Process intensification of element extraction using centrifugal contactors in the nuclear fuel cycle, Chem Soc Rev, 2022, 51, 3964–3999.

26 A. Geist, J.-M. Adnet, S. Bourg, C. Ekberg, H. Galán, P. Guilbaud, M. Miguirditchian, G. Modolo, C. Rhodes and R. Taylor, An overview of solvent extraction processes developed in Europe for advanced nuclear fuel recycling, part 1—Heterogeneous recycling, Sep Sci Technol, 2021, 56, 1866–1881.

27 D. Whittaker, A. Geist, G. Modolo, R. Taylor, M. Sarsfield and A. Wilden, Applications of diglycolamide based solvent extraction processes in spent nuclear fuel reprocessing, part 1: TODGA, Solvent Extraction and Ion Exchange, 2018, 36, 223–256.

28 A. Baker, A. Fells, T. Shaw, C. J. Maher and B. C. Hanson, Effect of scale-up on residence time and uranium extraction on annular centrifugal contactors (ACCs), Separations, 2023, 10, 331.

29 G. B. Hall, E. L. Campbell, N. P. Bessen, T. R. Graham, H. Cho, M. RisenHuber, F. D. Heller and G. J. Lumetta, Extraction of Nitric Acid and Uranium with DEHiBA under High Loading Conditions, Inorg Chem, 2023, 62, 6711–6721.

30 G. B. Hall, N. P. Bessen, P. R. Zalupski, E. L. Campbell, T. S. Grimes, D. R. Peterman and G. J. Lumetta, Extraction of Neptunium, Plutonium, Americium, Zirconium, and Technetium by Di-(2-

Ethylhexyl)-Iso-Butyramide (DEH i BA) at High Metal Loadings, Solvent Extraction and Ion Exchange, 2023, 41, 545–563.

31 D. Vopálka, K. Štamberg, A. Motl and B. Drtinová, The study of the speciation of uranyl–sulphate complexes by UV–Vis absorption spectra decomposition, J Radioanal Nucl Chem, 2010, 286, 681–686.

Chapter 4: Optimising Key Process Variables for the Extraction of Uranium with DEHiBA

Thomas Shaw, Alastair Baker, Richard A. Bourne, Bruce C. Hanson*

4.1 Abstract

Hydrometallurgical nuclear reprocessing involves the selective extraction of radionuclides from an extremely radioactive and oxidising environment. This selectivity is controlled predominantly by the type of ligand used, whilst the process can be further refined through variables such as ligand (DEHiBA), nitric acid, and metal (uranium) concentration, the ratio of organic to aqueous phase (SA ratio) and temperature. This work firstly verifies the performance of DEHiBA manufactured via two different routes, comparing purities and how this affects the forward extraction of 0.10 M uranyl nitrate against commercially sourced DEHiBA and literature data. DEHiBA concentrations of 1.00 M and 1.50 M were investigated and compared for their performance across a range of SA ratios and nitric acid concentrations with uranium extraction efficiencies up to 90% and 80% achievable when using 1.50 M and 1.00 M DEHiBA respectively. Process intensification by operating at a four-fold increase in throughput of uranium led to some loss in extraction efficiency, down to 85% and 72% respectively although not detrimental given the increased throughput. This work highlights the influence of temperature on this extraction and the need to assess this variable prior to pilot plant or hot tests.

4.2 Introduction

DEHiBA (*N,N*-di-(2-ethylhexyl)isobutyramide) is an organic ligand specifically designed for the selective extraction of uranium(VI) from irradiated nuclear fuel,[1-3] with uses in advanced nuclear reprocessing such as the GANEX (Grouped ActiNide EXtraction) 1st cycle process (**Figure 38**),[4] and more recently interest for HALEU (High Assay Low Enriched Uranium) production.[5-7] This completely incinerable, CHON based ligand offers a proliferation resistant alternative process to the likes of PUREX (Plutonium, Uranium, Reduction, Extraction) which has used tri-n-butyl phosphate (TBP)[8,9] for decades to recover uranium and plutonium.[10-17] The improved separation factor of DEHiBA facilitates the extraction of uranium devoid of plutonium, which can then be coextracted downstream with remaining actinides (minor actinides). These advantages paired with the supposedly less troublesome degradation products of DEHiBA lends this ligand to being of great interest to the nuclear industry.[18]

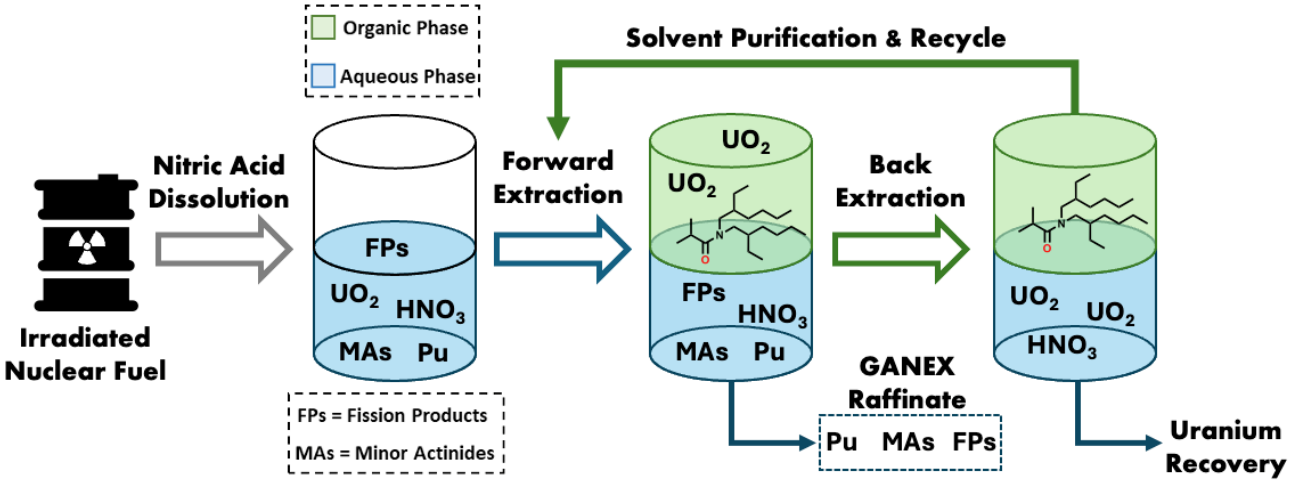

Figure 38: Simplified illustration of the GANEX 1st cycle process.

GANEX promises to revolutionise nuclear reprocessing by providing a more secure and sustainable management option for used nuclear fuel. The initial recovery of uranium, with options to recover the remaining valuable materials such as the actinides substantially reduces the long-term radiotoxicity and volume of nuclear waste for disposal.[19-21] Industrial

implementation of this technology requires concerted efforts from scientific and engineering research to regulatory and economic planning.[20,22-24]

Until recently, literature investigating the extraction of uranium with DEHiBA has focussed on using 1.00 M DEHiBA as per the GANEX 1st cycle process,[25-27] likely due to legacy concentrations for TBP, but also viscosity limitations when loaded with uranium. However, recent work from Pacific Northwest National Laboratory (PNNL), specifically G. B. Hall *et al.*[6] has investigated uranium(VI) extractions with 1.50 M DEHiBA to enhance uranium loading, improving process efficiency whilst maintaining minimal extraction of tri, tetra and pentavalent actinides, though issues with technetium extraction were faced.

Despite global interest in DEHiBA, the technology readiness level of processes that utilise DEHiBA are behind that of the PUREX process and must address performance and safety criteria for DEHiBA to be implemented for nuclear reprocessing on an industrial level.[28] This requires more published and/or in-house testing of DEHiBA with uranium and mock or irradiated nuclear fuel. To support this, the performance of DEHiBA across a range of conditions and equipment must be understood, however the cost of such tests is a limiting factor,[29] with access to ligands limited to those that can afford to purchase these high-cost research materials. Such costs negatively impact advanced nuclear reprocessing flowsheets as the economics are even less favourable than the PUREX process due to the specialised nature and novelty.[30] By achieving the necessary performance, safety and economic requirements, the nuclear industry can move towards a future where the efficient use and recovery of nuclear materials is balanced with the imperative of minimising environmental impact whilst enhancing global security.

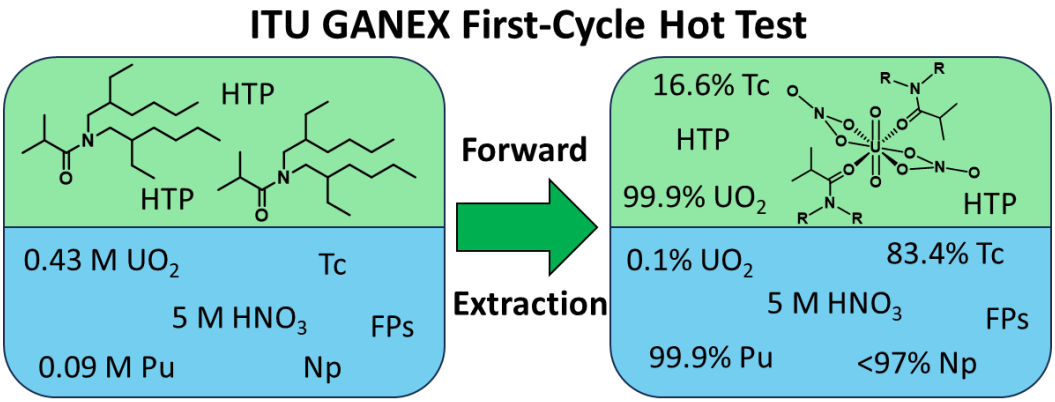

Figure 39: Extraction performance of 1.00 M DEHiBA in a GANEX first-cycle hot test as reported by G. Modolo, A. Geist and M. Miguirditchian.[25]

Further testing of DEHiBA is needed to better understand the compatibility and performance of this ligand, whereby an optimised flowsheet can be implemented for the recovery of uranium. Few pilot plant scale tests employing DEHiBA have been published,[31-33] of these, the irradiated tests show promise, yielding >99.9% uranium recovery and good separation factors when using 1.00 M DEHiBA (**Figure 39**). Though the literature is sparse on research covering performance optimisation of DEHiBA for the extraction of uranium, it is essential that the effect of parameters like DEHiBA, nitric acid, and uranium concentration, organic (often referred to as solvent in this discipline) : aqueous phase ratio (SA ratio), temperature and the impact of impurities is understood. This work provides greater understanding of extraction conditions, screening DEHiBA and nitric acid concentrations across a range of SA ratios for a simple uranium(VI) only system, aiding to underpin more complex extractions and hot tests so that optimal process conditions can be rigorously tested.

In these studies, we have used DEHiBA manufactured in-house via two routes from iBAnhydride (isobutyric anhydride) and the thermal amidation of iBA; (e) and (f) respectively, as described in previous work.[29] We also compare the performance to commercially sourced DEHiBA to understand how uranium(VI) extractions with DEHiBA are affected by impurities and starting materials (potential degradation products) to ensure performance prior to pilot

plant extraction testing. Recent literature from PNNL,[6] has also been used as a benchmark to verify the performance of our material to for the extraction of uranium(VI).

4.3 Experimental

4.3.1 Materials

Uranyl nitrate hexahydrate ($UO_2(NO_3)_2.6H_2O$, 98–102%) was procured by ABSCO Ltd., UK, from International Bio-Analytical Industries, Inc., Boca Raton, FL, USA. Nitric acid (>65%, Analytical Reagent, catalogue number 20429.320) were supplied by VWR International. *n*-dodecane and sodium hydroxide pellets were sourced from Sigma Aldrich. All commercially sourced materials were used without purification. DEHiBA from routes (e) and (f) were sourced from previous synthetic work.[29]

4.3.2 DEHiBA Materials & Purities

DEHiBA was manufactured for this work via two synthetic routes detailed by T. Shaw *et al.*[29] referred to as routes (e) and (f) illustrated by **Scheme S7**.

The two crude materials, denoted as e56 and f23 were collected from a range of experimental conditions explored over the optimisation of each route, thus contain biphenyl as the internal standard and an array of impurities. **Figures S42 & S43** detail the composition of each crude product, although the concentration of iBA and the degradation products from route (f) have not been determined. Purities were determined as weight percentages via gas chromatography-flame ionization detection (GC-FID) analysis to be 56-58% DEHiBA for crude e56 and 23-24% DEHiBA for crude f23, both containing biphenyl as the internal standard. The concentration of iBA was not

determined due to column contamination when calibrating with the GC-FID, resulting in non-linear calibration curves. The following purities have been determined by weight via GC-FID:

Table 13: Quantified composition of the five DEHiBA materials studied.

Material	Shorthand	DEHiBA (%)	iBA (%)	DiEHA (%)	iBAnhydride (%)
Crude (e) DEHiBA	e56	56-58	40-42	0	2
Purified (e) DEHiBA	e99	99	0	0	0
Crude (f) DEHiBA	f23	23-24	N/A	20	0
Purified (f) DEHiBA	f88	88-90	0	0	0
Commercial DEHiBA	CD	>99	0	0	0

These crude and purified DEHiBA materials were made to the desired concentration of DEHiBA by dilution in n-dodecane, using the quantified mass of DEHiBA present.

4.3.3 Batch Purification of Crude e56 to Yield e99 DEHiBA

The purity of the crude (e) material taken from a combination of >99 experiments of varying conditions when optimising route (e) was established to be 56-58% by weight and is henceforth referred to as e56. The crude e56 product was purified in batch via liquid-liquid extraction to yield pure DEHiBA for comparison when extracting uranium(VI).

The crude e56 (300 g) was diluted in hexane (300 mL), then saturated sodium bicarbonate (300 mL) was added leading to a cloudy emulsion (3rd phase) that did not clear. Acetonitrile (300 mL) was added with methylamine (10 mL) to clear the emulsion and to aid removal of iBAnhydride. A subsequent wash with 0.1 M NaOH (300 mL) and acetonitrile (300 mL) with

methylamine (10 mL), and then a 1:1 water : acetonitrile wash (300 mL) clarified the organic phase yielding 160 g of 99% pure DEHiBA (**Figure S44**) by mass (residual biphenyl), this purified material is referred to as e99.

The purified material (e99) was a colourless oil, with a density measured to be 0.85 g mL^{-1}. Mass spectroscopy of e99 confirmed a molecular weight of 311.77 g mol^{-1} (**Figure S22**). ^{1}H and ^{13}C NMR (**Figures S20 & S21**) confirmed the purity of e99 against commercially sourced DEHiBA.

4.3.4 Batch Purification of Crude f23 to Yield f88 DEHiBA

The purity of the crude (f) material taken from a combination of >80 experiments of varying conditions when optimising route (f) was established to be 23-24% DEHiBA by weight and is henceforth referred to as crude f23. Degradation products like 3-methylheptane and the secondary amide of DEHiBA (*N*-(2-ethylhexyl) isobutyramide) are observed at 6.4 and 7.4 minute retention times (**Figure S43**) respectively from the thermal degradation of DEHiBA.

The crude f23 (100 g) was diluted in hexane (100 mL), this was then washed with 0.1 M NaOH (2x 100 mL) with methylamine (2x 5 mL). The organic phase was then washed with acetonitrile (2x 50 mL), to yield an organic phase comprised largely of DEHiBA and DiEHA. To purify this material, 2.0 M nitric acid (4x 25 mL) and acetonitrile (4x 50 mL) washes led to a product purity of 87-90% by weight (**Figure S45**) and is referred to as f88.

4.3.5 Uranium(VI) Extractions, Analysis and Calibrations

Stock aqueous uranyl nitrate solutions were made to the desired concentration (typically 0.1 M) using uranyl nitrate hexahydrate, and the respective nitric acid stock solution (2.0-6.0 M) in a volumetric flask.

Extractions were performed by contacting the desired organic phase (crude or purified DEHiBA in *n*-dodecane) with an equal volume of desired nitric acid twice, over 3 hours at ambient conditions (15-22 °C), ensuring pre-acidification of the organic phase. The phases were then separated via centrifugation at 2500 rpm for 2 minutes and the organic phase was then contacted with the desired volume of uranyl nitrate solution, each extraction was mixed for an hour at a recorded room temperature before centrifugation. The separated phases were then analysed separately by UV-Vis spectroscopy.[3]

The spectrometer (FLAME-S-UV-VIS, 200–850 nm) with thermoregulator (USB-TC) was connected to a high-power MINI deuterium tungsten halogen source with shutter (200–850 nm) via a cuvette holder (1 cm pathlength) with solarization-resistant fibres (2 m, P400-2-SR). The system was equilibrated for 60 minutes, a reference sample, either nitric acid or *n*-dodecane was then used to collect the background for the aqueous and organic phases respectively, using an 'integration time' of 96 milliseconds, with 64 'scans to average' the final spectrum.

Uranyl nitrate has a distinct signal between 350-500 nm, typically a multiplet of nodes.[34] From this the maximum peak height or peak area can be used to quantify the amount of uranium(VI) present. However, the neighbouring nitric acid signal (330-400 nm) can overlap with the uranium(VI) signal, therefore, measurements were taken above 400 nm where possible.

To calibrate the aqueous phase a 0.10 M uranyl nitrate solution in 4.0 M nitric acid was composed, aliquots were taken and serially diluted with 4.0 M nitric acid to afford uranium(VI)

concentrations from 0.10 to 0.01 M. The aqueous uranium(VI) calibration spectra are shown in **Figure S46**, presenting three obvious peaks. Calibrations used the peak height and area as a means of comparison and validation. Two aqueous calibration curves were generated using the peak area between 400-440 nm, and maximum absorbance at 419 nm for **Figures S47 & S48** respectively. This was repeated for 2.0-6.0 M nitric acid concentrations.

Attempts to dissolve uranyl nitrate directly in 1.50 M DEHiBA led to three phases including incomplete dissolution (**Figure S49**), leading to inaccurate uranium(VI) concentrations. Instead, organic uranium(VI) calibrations loaded uranium(VI) into the organic phase via solvent extraction using pre-acidified 1.50 M e99 DEHiBA in *n*-dodecane through contact with an equal volume of 0.10 M uranyl nitrate in 4.0 M nitric acid. The resultant aqueous phase was analysed by UV-Vis and quantified to contain 0.011 M uranium(VI), therefore the organic phase contains 0.089 M uranium(VI). Subsequently the organic phase was diluted in series with the 1.50 M e99 DEHiBA solution yielding a range of uranium(VI) concentrations for the calibration (**Figures S50 & S51**). UV-Vis analysis of these organic solutions resulted in more peaks and a shift in wavelength compared to the aqueous calibration measurements (**Figure S52**), with the maximum absorbance at 430 nm.

4.3.6 Working with Open Sources of Ionising Radiation: Uranium

All work with radioactive substances at the University of Leeds is carried out under a strict management protocol to ensure compliance with health, safety, and environmental legislation. In the human body, this ionization can cause adverse health effects such as the induction of cancer. The risk of an adverse health effect is related to the level of exposure to radiation, and the risks are, therefore, controlled by limiting the exposure of workers to radiation. Radiation workers have

to complete radiation safety training, log risk assessments, order and confirm the receipt of sources, record the usage of sources, and log radioactive waste disposal.

Only individuals holding a valid University of Leeds Radiation Work Permit are permitted to handle unsealed radioactive substances. The University's permits for radiation work, issued under the Environmental Permitting Regulations 2010, specify that 'Best Available Techniques' must be used to minimize the radiological impact of discharges on people and the environment. Contamination control techniques are used to minimize the creation and spread of contamination, as follows:

- Careful dispensing and handling of materials to minimize the risk of contamination.
- Immediate disposal of contaminated material: tips, syringes, etc.
- Containment of any samples created in a secondary container.
- Storage or disposal of any stocks and samples not in use as soon as practicable.
- Radiation monitors are used to identify contaminated areas or equipment.

Equipment like pumps that comes in to contact with alpha emitting materials risks being contaminated and confined to the 'hot' lab if it cannot be decontaminated. For this reason HPLC pumps and other flow equipment used in the other chapters were not used for this work and the majority of the work was carried out using traditional batch chemistry and one variable at a time optimisation.

4.4 Results and Discussion

To understand and compare the performance of DEHiBA manufactured via routes (e) and (f), crude and purified DEHiBA materials (e56, e99, f23, and f88) were investigated to determine the effect of impurities on the extraction of uranium(VI). Commercially sourced DEHiBA was used as a benchmark material for comparison. The extraction of uranium(VI) can be tailored and optimised via a number of variables such as: type/structure of ligand, ligand concentration, metal (uranium) concentration, nitric acid concentration, phase or SA ratio, and temperature. This work employs 0.10 M uranyl nitrate as a model system where DEHiBA concentration, SA ratio and nitric acid concentration were screened to provide insight for the development of industrial processes. This work found temperature to be highly influential on the extraction as mentioned in the literature,[35] and aims to highlight the importance of this process metric that can be overlooked. Only the forward extraction has been studied in this work, though the impurities may influence the back extraction (stripping) or extraction of other nuclides which will need to be investigated in future work.

4.4.1 Performance Testing of Crude and Purified DEHiBA for the Forward Extraction of Uranium(VI)

In this work DEHiBA of various purities and compositions (**Table 13**) has been tested for the extraction of uranium(VI), with focus on varying the DEHiBA concentration to understand how impurities affect the forward extraction of uranium(VI) from 0.10 M uranyl nitrate in 4.0 M nitric acid using a 1:1 SA ratio. Initial screening compared 1.50 M DEHiBA solutions of e99, crude e56, f88, and commercial DEHiBA (CD) at 15 °C (**Table S21**), finding comparable distribution ratios (D_U) around 8 even for the crude material (**Figure 40**). Initial measurements however, found crude

e56 to extract more uranium(VI), with a 9.3 D_U (**Figure S53**), but was found to be due to interference from oxidised DiEHA absorbing between 410-430 nm due to its yellow appearance, increasing the organic absorbance (**Figure S54**). Similarity of the aqueous phase measurements (**Figure S55**) for the extractions with crude and purified DEHiBA gave confidence of similar performance with an expected D_U of ~8 for all. Therefore, the UV-Vis methodology was modified for the crude e56 organic measurements, where the background was taken using the crude material before contact with uranium. Additionally, extractions with 1.50 M crude e56 led to a 10% volume redistribution where the aqueous phase increased in volume, likely due to phase transfer of isobutyric acid. These findings highlight the added complexity when using crude DEHiBA due to the interference of impurities, whereby DiEHA interferes with UV-Vis analysis, and the solubility of isobutyric acid (and potentially other materials) in both phases not only changes the SA ratio, but also has the potential to chelate to uranium(VI) or other nuclides, which could unknowingly contaminate waste or product streams. As these impurities are potential degradation products of DEHiBA any impact that these could impose on the process must be understood.

Although the purified (e99 & f88) and crude (e56) DEHiBA materials demonstrated similar uranium(VI) extraction performance to one another (D_U ~8), this differed from the distribution ratio of 6.2 published by G.B. Hall *et al*.[6] when using the same concentration of uranium(VI) and nitric acid at the same SA ratio, notably the temperature of this extraction was not referenced but was later confirmed to be around 25 °C by the author. Comparable performance was achieved at 22 °C with 1.50 M e99, this time a D_U of 6.3 was measured. This exemplifies the exothermic nature of this extraction as described by P. Pathak *et al.*[35] emphasising the need to understand how these extractions perform across a range of temperatures.

The concentration effect of DEHiBA was investigated for crude (e56 and f23) and purified (e99 and f88) DEHiBA materials (**Figure 40**), typically ranging between 0.75 M up to 1.50 M, these were

contacted with an equal volume of 0.10 M uranyl nitrate solutions in 4.0 M nitric acid to understand how the concentration and purity of DEHiBA affects the extraction of uranium(VI) and whether any benefits from increasing the concentration of DEHiBA plateau. Crude f23 was only investigated at a concentration of 0.33 M due to its low purity (restricting access to high concentrations) and the formation of three liquid phases following contact with aqueous uranyl nitrate, the colouration of this material also increased the organic UV-Vis absorbance making extractions with this material highly unfavourable to work with so was not investigated further. Organic and aqueous UV-Vis measurements can be found in **Figures S54-S62.**

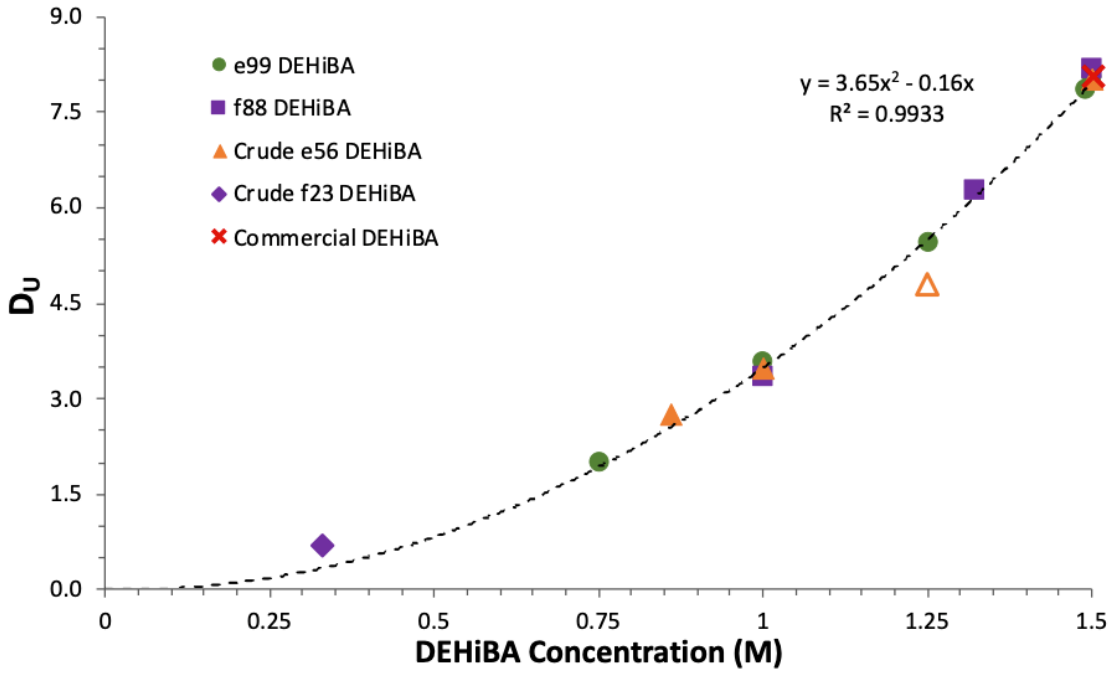

Figure 40: The effect of DEHiBA concentration on the distribution ratio of uranium(VI) comparing e99, crude e56, f88, and crude f24 solutions when using an equal volume of 0.1 M uranyl nitrate in 4.0 M nitric acid. The hollow triangle experiment at 1.25 M DEHiBA was conducted at 22 °C whilst all other experiments took place at 15 °C.

Overall, uranium(VI) extraction reduces as DEHiBA concentration reduces, in a non-linear fashion. Instead the majority of datapoints fit to a second order polynomial equation despite differences in purity, facilitating prediction of uranium(VI) extraction efficiency for varying

DEHiBA concentrations when using an equal volume of 0.10 M uranyl nitrate in 4.0 M nitric acid at 15 °C. This implies that impurities like isobutyric acid and di-(2-ethylhexyl)amine (DiEHA) have little if any effect on the forward extraction of uranium(VI) at these conditions. The majority of these experiments took place at 15 °C, however the extraction with 1.25 M crude e56 DEHiBA took place at 22 °C due to the difference in ambient temperature, as the other extractions with crude e56 demonstrate similar extraction performance for uranium(VI), it is most likely that this drop in performance is due to the increase in temperature hindering the exothermic extraction.[35] Over-quantification of uranium(VI) in the organic crude e56 phase was only observed when using 1.50 M DEHiBA as a greater concentration of DiEHA is present, therefore the accumulation of degradation products such as DiEHA without suitable purification could add complications with analysis, especially given the difficulty to remove fatty amines via liquid-liquid extraction.

The reduction in extraction performance at lower DEHiBA concentrations was expected due to lesser moles of available ligand for chelation. However, the non-linear relationship (**Figure 40**) means that the ratio of DEHiBA to uranium(VI) reduces from ~16:1 when using 1.50 M DEHiBA, down to 11:1 when using 0.75 M DEHiBA (**Table S21**). From this data alone it is unclear why the ratio of DEHiBA to uranium is not constant with varying DEHiBA concentrations. This could be influenced by the amount of free ligand from nitric acid adduct formation. However, it does mean that higher DEHiBA concentrations have more 'free' DEHiBA so can accommodate higher uranium loadings by increasing the SA ratio.

To expand the explored DEHiBA concentration range, 2.00 M and 2.73 M (neat DEHiBA) e99 DEHiBA solutions were contacted with an equal volume of 0.10 M uranyl nitrate in 4.0 M nitric acid, although these extractions were contacted at 22 °C not 15 °C again due to the difference in ambient temperature, making comparison difficult (**Table S21 and Figure S63**). The 2.00 M DEHiBA solution extracted a significantly greater amount of uranium(VI) than 1.50 M DEHiBA with

a D_U of 11.6 vs ~8. This did not follow the second order polynomial curve from **Figure 40**, most likely due to the increased temperature. Therefore, further work is required to repeat this extraction at 15 °C to ascertain whether the second order polynomial equation continues when using 2.00 M DEHiBA, as additional factors may restrict the extraction of uranium(VI) at higher DEHiBA concentrations. The extraction with neat DEHiBA resulted in reduced performance compared to the 2.00 M DEHiBA with a D_U of 9.8, potentially due to the absence of dodecane and the increased viscosity of the organic phase (as observed during manipulation), however inspection of the organic UV-Vis measurement suggests increased uranium(VI) extraction due to greater absorbance (**Figure S56**). The reduced D_U was deduced to be a result of the aqueous UV-Vis measurement (**Figure S57**), where an overall shift in wavelength is observed compared to the other extractions, leading to a poorer mass balance and over-quantification of the uranium(VI) concentration. It is unclear as to why the aqueous phase was affected, however the actual D_U is expected to be greater than the 2.00 M DEHiBA extraction based on the organic UV-Vis measurement (**Figure S56)**.

The ability to predict uranium(VI) extraction performance across a range of temperatures, SA ratios, nitric acid, DEHiBA and uranium concentrations supports the optimisation and operation of a next generation reprocessing facility. The understanding that typical degradation products do not hinder the forward extraction of uranium for the conditions tested in this work reinforces the robustness of these materials and extraction conditions. Further work is needed exploring a range of temperatures for these extractions to predict performance alongside measuring viscosity of the phases, prior to industrialisation due to the significant impact temperature has, as has been highlighted here.

4.4.2 The Impact of Nitric Acid Concentration on Uranium(VI) Extractions with 1.50 M and 1.00 M Purified DEHiBA

The influence of nitric acid concentration was next investigated for the forward extraction of uranium(VI) between 2.0-6.0 M nitric acid with 1.00 M and 1.50 M e99 DEHiBA due to the relevance of these concentrations in the literature.[6] The extraction performance of e99 DEHiBA was further verified against literature data published by G.B. Hall *et al*.[6] for the extraction of 0.10 M uranyl nitrate in 2.0-6.0 M (1.0 M increments) nitric acid using a 1:1 SA ratio at 22 °C. Although G.B. Hall *et al*.[6] focussed on using 1.50 M DEHiBA, our results with 1.00 M DEHiBA are directly compared using the same extraction conditions (**Figure 41**). Back extraction/stripping conditions at lower nitric acid concentrations (0.01 M to 1.00 M) were not explored.

Extractions with 1.50 M DEHiBA demonstrate comparable performance to the data published in the literature as illustrated in **Figure 41**, validating the suitability of the synthetic route (e) and purification methodology and reagents used. Comparably, 1.00 M DEHiBA is far less efficient at extracting uranium(VI), this is exacerbated at 5.0 M and 6.0 M nitric acid with >10% difference in extraction efficiency. Therefore, for the extraction of 0.10 M uranyl nitrate at 22 °C, 1.50 M DEHiBA provides better uranium(VI) loading and thus throughput, requiring fewer extraction stages to achieve 99.9% uranium removal compared to the GANEX 1st cycle process using 1.00 M DEHiBA. Of course, the feasibility of using 1.50 M (or other concentrations) DEHiBA relies on the suitability of phase densities, as if a phase is too dense/viscous compatibility issues with equipment like annular centrifugal contactors and pulsed columns will be met, as density is also dependent on the uranium loading extraction performance may need to be limited to not exceed viscosity limitations. Further investigation of phase densities for promising extraction conditions is needed prior to scale-up or pilot plant testing. The temperature of the aqueous feed in a hot test or reprocessing facility may be elevated aiding the handling of viscous phases, however this will

reduce the extraction efficiency of the system and must be understood and balanced. Additionally, 1.00 M DEHiBA may be favoured for the management and separation of a greater number of radionuclides, specifically technetium.[6] Overall, both 1.50 M and 1.00 M DEHiBA concentrations demonstrate increased uranium(VI) extraction as nitric acid concentration increases, both tailing off around 5.0 M nitric acid, but to a greater extent when using 1.00 M DEHiBA. Third order polynomial equations were fitted generating good fits as per the equation used to fit the PNNL data (**Figure S68**).[6]

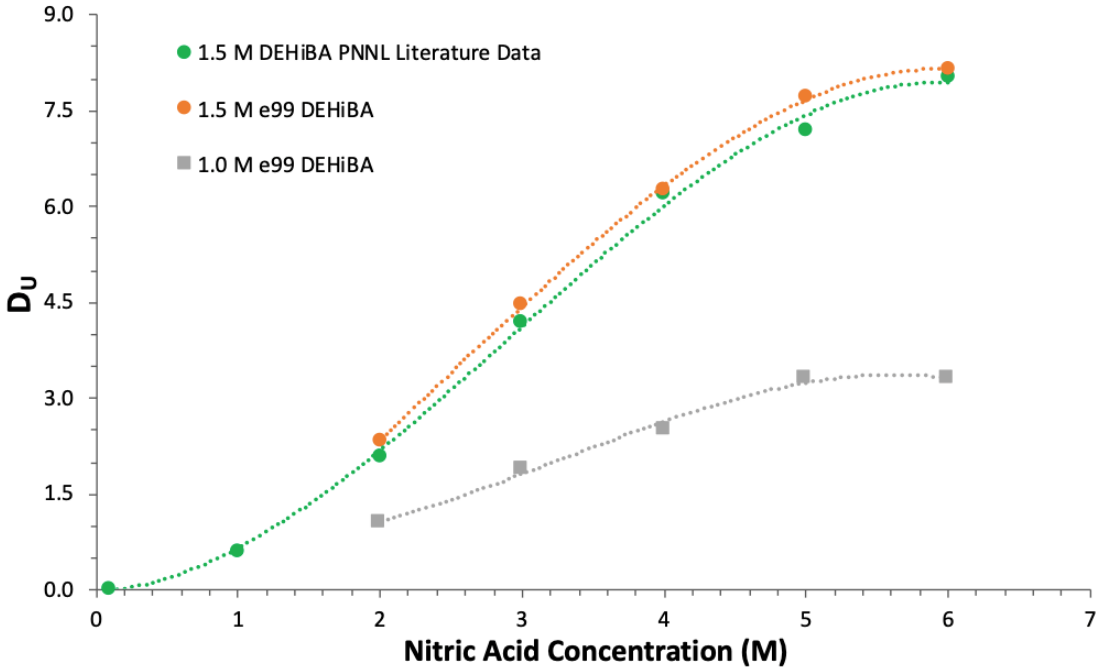

Figure 41: The effect of nitric acid concentration on the distribution ratio of uranium(VI) at 22 °C comparing 1.50 and 1.00 M e99 DEHiBA to 1.50 M DEHiBA literature data,6 using a 1:1 SA ratio for the extraction of 0.10 M uranium(VI).

All mass balances for these extractions were within ±10% of 100% (**Table S22**). Interestingly, the UV-Vis measurement of organic uranium(VI) when using >5.0 M nitric acid led to a shift in wavelength (**Figures S64 & S65**), likely due to a change in the electronics of the uranium complex. Little difference is observable for the aqueous uranium(VI) UV-Vis measurements besides intensity (**Figures S66 & S67**), although the low absorbance of uranium(VI) for the 5.0 M and 6.0 M nitric acid phases may subdue any noticeable differences.

Ultimately, 5.0 M and 6.0 M nitric acid promotes the best extraction efficiency of uranium(VI) for both DEHiBA concentrations when using a 1:1 SA ratio, the plateau of this metric illustrates little need to increase nitric acid concentration further. Instead, uranium loading and thus throughput can be further optimised by exploring differing SA ratios. Higher uranium loading can also be achieved through higher aqueous uranium concentrations, as investigated by G.B Hall *et al*.[6] However, in the work presented here on a uranyl nitrate concentration of 0.10 M is used, and the effect of SA ratio is investigated for improving uranium throughput.

4.4.3 Investigating Organic : Aqueous Phase Ratio to Optimise the Extraction of Uranium(VI) with 1.50 M and 1.00 M DEHiBA

This section of work aims to understand how the SA ratio impacts the extraction efficiency of uranium(VI) with 1.50 M and 1.00 M DEHiBA. This data can then be used to maximise extraction efficiency and throughput or identify trade-off conditions for these objectives, aiding to inform scale-up operations and improve process efficiency.

SA ratios from 2:1 down to 1:2 are reported in **Figure 42** using 1.00 M and 1.50 M DEHiBA, across 2.0-6.0 M nitric acid concentrations. The majority of extractions here were conducted at 22 °C, however four of the extractions with 1.50 M DEHiBA using 3.0 M and 5.0 M nitric acid were conducted at 15 °C, identifiable by the non-filled markers. This further highlights the influence of temperature on this extraction, whereby the extractions at 15 °C do not follow the trend of the 22 °C extractions, over-extracting uranium(VI). This emphasises the need to investigate these conditions across a range of temperatures. The polynomial equations for the trendlines are not displayed due to the difference in temperatures for some of the data, the trendlines should only be used as a visual guide.

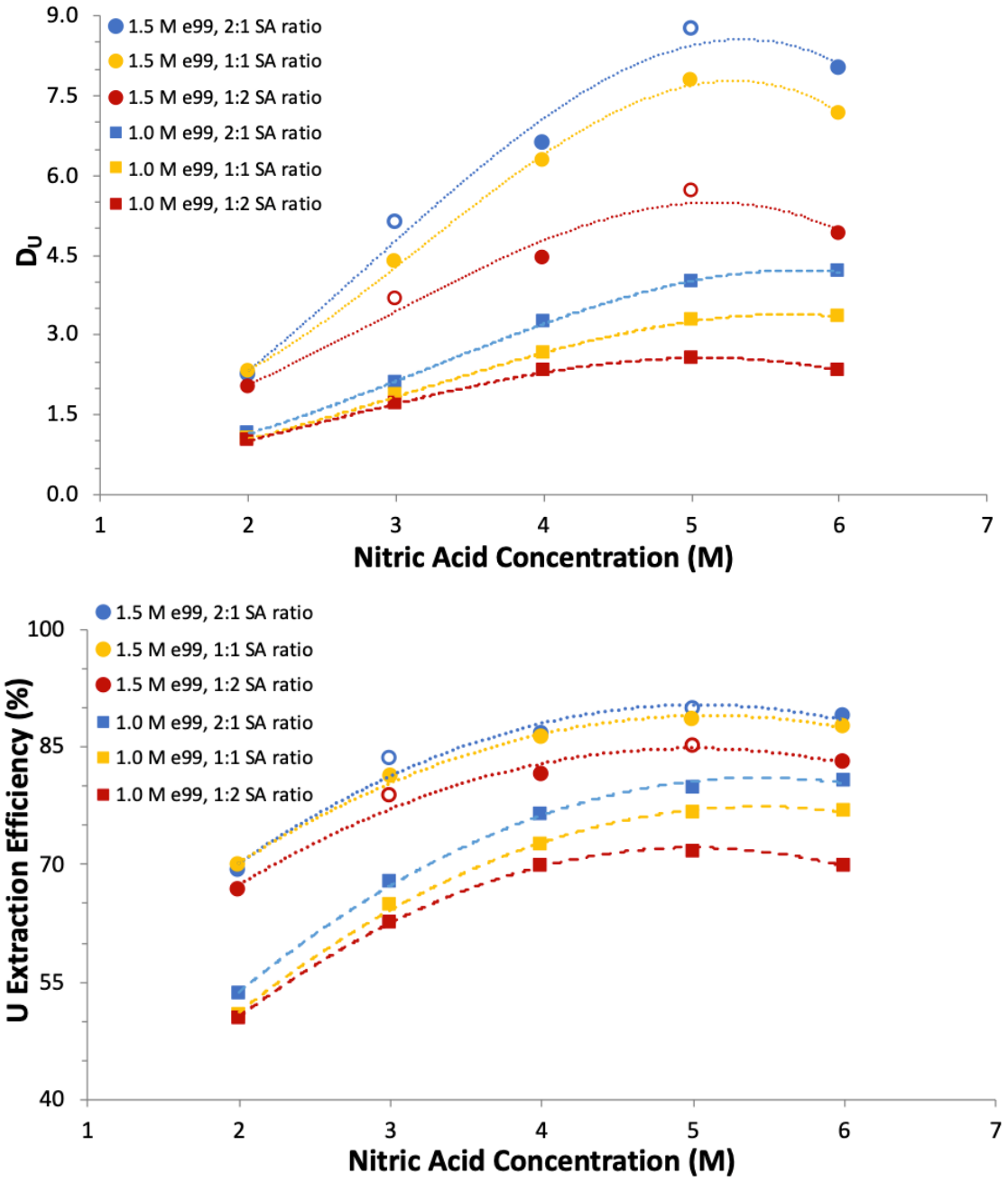

Figure 42: Comparing the uranium(VI) extraction performance of 1.50 M and 1.00 M e99 DEHiBA concentrations for the extraction of 0.10 M uranyl nitrate with varying nitric acid concentration and SA ratio at 22 °C (filled ● markers) and 15 °C (empty ○ markers).

Similar trends are observed for both the 1.00 M and 1.50 M DEHiBA extractions, where D_U increases steadily from 2.0 M to 4.0 M nitric acid, before this trend starts to plateau, although to different extents depending on the SA ratio used. For example, the 6.0 M nitric acid 1:2 SA ratio with 1.00 M DEHiBA shows reduced performance compared to the same extraction but in 5.0 M

nitric acid. This reduction in performance is less noticeable and harder to determine given the difference in temperature when using 1.50 M DEHiBA. The D_U is best at higher (2:1) SA ratios for both DEHiBA concentrations, therefore for maximum extraction efficiency, uranium throughput must be sacrificed and thus a trade-off between these metrics must be defined. This trade-off tends to increase with nitric acid concentration, being most notable with 6.0 M nitric acid as the difference between D_U is greatest between the 2:1 and 1:2 SA ratio. For example, when using 1.50 M DEHiBA the difference in extraction efficiency between a 2:1 and a 1:2 SA ratio is 2.5% with 2.0 M nitric acid, increasing to ~5% with 3.0-5.0 M nitric acid, and finally 6% with 6.0 M nitric acid. Comparatively, when using 1.00 M DEHiBA the difference in extraction efficiency increases from 3% to 6.5% to 10.7% when using 2.0 M, 4.0 M and 6.0 M nitric acid respectively. A maximum extraction efficiency of ~90% can be achieved when using 5.0 M and 6.0 M nitric acid at a 2:1 SA ratio with 1.50 M DEHiBA, only dropping to ~85% when using a 1:2 SA ratio, a ~5% loss in efficiency for a four-fold increase in uranium throughput. Whereas extraction efficiency drops from 80% down to ~70% for the same conditions when using 1.00 M DEHiBA, representing a 10% loss, double that observed with 1.50 M DEHiBA. Ultimately, these losses are not detrimental to performance given the increased uranium throughput, although a greater number of sequential extraction stages is needed to attain 99.9% extraction.[36]

Overall, 5.0 M nitric acid is seemingly optimal for both DEHiBA concentrations, affording a lesser reduction in extraction performance as the SA ratio reduces, facilitating better uranium throughput with minimal loss to extraction efficiency. Extractions with 1.50 M DEHiBA significantly improves extraction performance for all conditions compared to using 1.00 M DEHiBA, with up to a 13% difference when using 4.0-6.0 M nitric acid and up to 16% when using 2.0-3.0 M nitric acid. Further visual comparison of uranium(VI) extraction performance when using 1.50 M and 1.00 M DEHiBA is plotted in **Figure S69** allowing visual comparison across four-

dimensional space, illustrating the sheer difference in performance, yet similar trends between datasets. The mass balances for each of these extractions is listed in **Tables S23-S26**, where all extractions provided good confidence in the data, within 10% of a 100% mass balance.

From this data, the ratio of DEHiBA to uranium in each organic phase can be plotted to understand how effectively each condition utilises DEHiBA to partition uranium(VI). In general, higher nitric acid concentrations and lower SA ratios lead to a more effective utilisation of DEHiBA for the chelation of uranium(VI). However, the difference in temperature for the extractions with 1.50 M DEHiBA makes interpretation of this unclear (**Figure S74**), thus **Figure 43** only contains the data for 1.00 M DEHiBA. Linear relationships between SA ratio and the ratio of DEHiBA to uranium(VI) are observed for all nitric acid extractions within the SA ratios explored. Interestingly, 4.0 M and 5.0 M nitric acid conditions look to outperform extractions in 6.0 M nitric acid if lower SA ratios were explored, this supports the comparatively reduced performance at low SA ratios when using 6.0 M nitric acid vs 4.0 M and 5.0 M. Further investigation as to whether these linear relationships continue towards the y-axis would be interesting in future work.

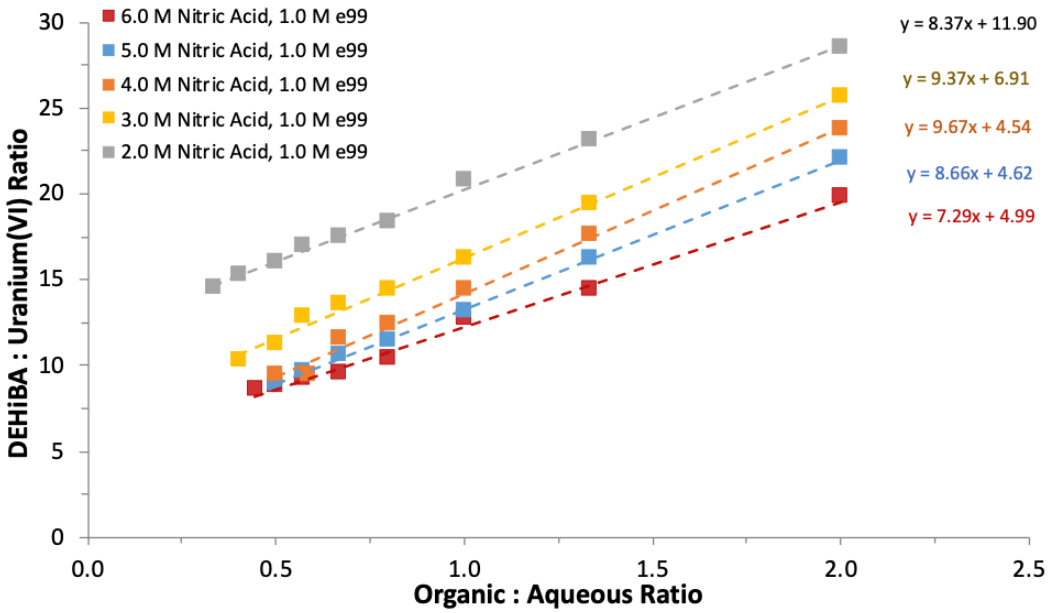

Figure 43: The effect of SA ratio and nitric acid concentration on the ratio of DEHiBA to uranium(VI) at 22 °C using 1.00 M e99 DEHiBA to extract 0.10 M uranyl nitrate.

4.5 Conclusions

This work verifies the performance of DEHiBA manufactured in-house via two synthetic and purification pathways,[29] comparing the performance to that of commercial DEHiBA and available data in the literature.[6] The purified DEHiBA from routes (e) and (f), e99 and f88 respectively possessed near identical performance to commercially sourced DEHiBA at 15 °C when using a 1.50 M DEHiBA concentration. Even crude DEHiBA from route (e) demonstrated comparable performance to purified DEHiBA for the forward extraction of DEHiBA despite the significant amounts of impurities like iBA. The performance of DEHiBA purified from route (e) was also found to be near identical to that published by G. B. Hall *et al.*[6] when extracting an equal volume of 0.10 M uranyl nitrate in 2.0-6.0 M nitric acid concentrations with 1.50 M DEHiBA. These investigations validate the scalable synthetic routes proposed in previous work and purification methods devised in this work as DEHiBA performs as expected even in the presence of impurities such as potential degradation products.

Three variables, ligand concentration, nitric acid concentration and SA ratio, were investigated throughout for the extraction of 0.10 M uranyl nitrate. Temperature effect was observed to be influential on the extraction but has not yet been investigated thoroughly. Purity was also investigated to some extent and found to have little influence if any on the forward extraction of uranium(VI).

The concentration of DEHiBA was assessed for the purpose of process intensification to facilitate increased uranium loading of the organic phase and understand when the benefits of increasing DEHiBA concentration are optimal. As the proposed GANEX 1st cycle forward extraction employs 1.00 M DEHiBA, this work investigated greater concentrations of DEHiBA (1.50 M, 2.00

M, and 2.73 M) which resulted in increased extraction efficiency for the conditions explored. Thus, theoretically fewer extraction stages are required for an industrial process, although the density of the organic phase must be monitored as higher DEHiBA concentrations can lead to complications when loaded with large amounts of uranium(VI).

The effect of SA ratio was assessed between 2:1 and 1:2, investigating the trade-off between extraction efficiency and uranium throughput. Lower SA ratios (1:2) only reduced extraction efficiency marginally in comparison to the four-fold improvement in uranium throughput, from ~90% extraction efficiency down to 85% at 5.0 M nitric acid with 1.50 M DEHiBA. This provides options for plant design where the number of extraction stages can be optimised with uranium throughput, providing insight prior to scale-up and pilot plant demonstrations in future work.

Overall, 1.50 M DEHiBA for the extraction of 0.10 M uranyl nitrate provides superior forward extraction performance over the suggested concentration of 1.00 M DEHiBA for the GANEX 1st cycle forward extraction, with at least a 10% extraction efficiency increase. It should, however, be noted that this system does not account for the added complexity of other species found in irradiated nuclear fuel, higher uranyl nitrate concentrations and temperatures, or organic phase density when loaded with uranium, which may better suit 1.00 M DEHiBA. However, at this stage, with the available data 1.50 M DEHiBA outperforms 1.00 M DEHiBA without issue.

4.6 Future Work

This work highlights the temperature dependence of such extractions and the need for studies that investigate this variable alongside the other variables mentioned and investigated here. Additionally further work with 2.00 M DEHiBA and potentially beyond across these variables would be of interest for process intensification as no observable issues were encountered for the limited extractions investigated for these DEHiBA concentrations. Additionally, the investigation

of lower SA ratios may yield valuable operating conditions, whilst density measurements for organic phases would provide valuable insight across a range of temperatures.

The investigation of these variables at higher uranium concentrations would improve industrial relevance and potentially uranium throughput, allowing comparison of process metrics and densities for compatibility with equipment like annular centrifugal contactors.[37]

Extraction studies with industrial process equipment is the next logical step to ensure compatibility with equipment and to compare the effect of equipment on the extraction efficiency relative to small scale laboratory methods and equipment. Additionally, increased complexity of the aqueous phase, simulating the composition of used nuclear fuel through the addition of nuclides like plutonium, will ensure DEHiBA behaves as reported and is suitable across a range of promising process conditions.

These extractions were conducted in batch using a one variable at a time optimisation approach, this deviates from the other work completed in this thesis due to equipment limitation in the alpha active laboratory at the University of Leeds. In the future design of experiments or machine-learning algorithms should be employed to optimise process conditions, aiding to explore and understand synergistic effects between the various process variables that influence these extractions. This work could be done in continuous flow using microfluidics and the separators used in Chapter 3 (or smaller versions) to automate these processes, minimising material consumption, allowing higher uranium concentrations to be investigated and improving repeatability, however this was not achievable in this work due to the cost and time restrictions but would be beneficial to research in this field and would aid to minimise operator dose. By conducting these tests in small-scale continuous flow, the outlet streams could be monitored by UV-Vis spectroscopy to further reduce analysis time and maximise the number of extraction

conditions that can be assessed in minimal time. These setups could be used to assess temperature dependence and any temperature increases caused by the extraction.

4.7 References

1 A. Tessier, P. G. C. Campbell and M. Bisson, Sequential extraction procedure for the speciation of particulate trace metals, Anal Chem, 1979, 51, 844–851.

2 N. Condamines and C. Musikas, THE EXTRACTION BY N, N-DIALKYLAMIDES. I. HNO3 AND OTHER INORGANIC ACIDS., Solvent extraction and ion exchange, 1988, 6, 1007–1034.

3 N. Condamines and C. Musikas, The extraction by NN-dialkylamides. II. Extraction of actinide cations, Solvent extraction and ion exchange, 1992, 10, 69–100.

4 M. Miguirditchian, L. Chareyre, C. Sorel, I. Bisel, P. Baron and M. Masson, Development of the GANEX process for the reprocessing of Gen IV spent nuclear fuels.

5 M. L. Hill, C. Pereira and A. G. Servis, Kinetics and Mechanism of Ce (IV) Phase Transfer by the Neutral Extractants Tributyl Phosphate and N, N-Di (2-ethylhexyl) isobutyramide, Ind Eng Chem Res.

6 G. B. Hall, E. L. Campbell, N. P. Bessen, T. R. Graham, H. Cho, M. RisenHuber, F. D. Heller and G. J. Lumetta, Extraction of Nitric Acid and Uranium with DEHiBA under High Loading Conditions, Inorg Chem, 2023, 62, 6711–6721.

7 G. B. Hall, N. P. Bessen, P. R. Zalupski, E. L. Campbell, T. S. Grimes, D. R. Peterman and G. J. Lumetta, Extraction of Neptunium, Plutonium, Americium, Zirconium, and Technetium by Di-(2-Ethylhexyl)-Iso-Butyramide (DEHiBA) at High Metal Loadings, Solvent Extraction and Ion Exchange, 2023, 41, 545–563.

8 J. Drader, G. Saint-Louis, J. M. Muller, M. C. Charbonnel, P. Guilbaud, L. Berthon, K. M. Roscioli-Johnson, C. A. Zarzana, C. Rae and G. S. Groenewold, Radiation chemistry of the branched-chain monoamide di-2-ethylhexyl-isobutyramide, Solvent Extraction and Ion Exchange, 2017, 35, 480–495.

9 G. M. Gasparini and G. Grossi, Review article long chain disubstituted aliphatic amides as extracting agents in industrial applications of solvent extraction, Solvent Extraction and Ion Exchange, 1986, 4, 1233–1271.

10 E. R. Bertelsen, M. R. Antonio, M. P. Jensen and J. C. Shafer, Electrochemistry of PUREX: R is for reduction and ion transfer, Solvent Extraction and Ion Exchange, 2022, 40, 64–85.

11 H. A. C. McKay, in Science and technology of tribuytl phosphate, 1990.

12 J. M. McKibben, Chemistty of the purex process, Radiochim Acta, 1984, 36, 3–16.

13 R. S. Herbst, P. Baron and M. Nilsson, in Advanced separation techniques for nuclear fuel reprocessing and radioactive waste treatment, Elsevier, 2011, pp. 141–175.

14 W. B. Lanham and T. C. Runion, PUREX process for plutonium and uranium recovery, Oak Ridge National Lab.(ORNL), Oak Ridge, TN (United States), 1949.

15 J. E. Birkett, M. J. Carrott, O. D. Fox, C. J. Jones, C. J. Maher, C. V Roube, R. J. Taylor and D. A. Woodhead, Recent developments in the Purex process for nuclear fuel reprocessing: Complexant based stripping for uranium/plutonium separation, Chimia (Aarau), 2005, 59, 898.

16 G. Modolo, A. Wilden, A. Geist, D. Magnusson and R. Malmbeck, A review of the demonstration of innovative solvent extraction processes for the recovery of trivalent minor actinides from PUREX raffinate, Radiochim Acta, 2012, 100, 715–725.

17 R. J. Taylor, C. R. Gregson, M. J. Carrott, C. Mason and M. J. Sarsfield, Progress towards the full recovery of neptunium in an advanced PUREX process, Solvent Extraction and Ion Exchange, 2013, 31, 442–462.

18 J. Drader, G. Saint-Louis, J. M. Muller, M. C. Charbonnel, P. Guilbaud, L. Berthon, K. M. Roscioli-Johnson, C. A. Zarzana, C. Rae and G. S. Groenewold, Radiation chemistry of the branched-chain monoamide di-2-ethylhexyl-isobutyramide, Solvent Extraction and Ion Exchange, 2017, 35, 480–495.

19 M. Salvatores and G. Palmiotti, Radioactive waste partitioning and transmutation within advanced fuel cycles: Achievements and challenges, Prog Part Nucl Phys, 2011, 66, 144–166.

20 J.-P. Glatz, P. Souček and R. Malmbeck, in Reprocessing and recycling of spent nuclear fuel, Elsevier, 2015, pp. 49–62.

21 T. A. Kurniawan, M. H. D. Othman, D. Singh, R. Avtar, G. H. Hwang, T. Setiadi and W. Lo, Technological solutions for long-term storage of partially used nuclear waste: A critical review, Ann Nucl Energy, 2022, 166, 108736.

22 K. L. Nash and G. J. Lumetta, Advanced separation techniques for nuclear fuel reprocessing and radioactive waste treatment, Elsevier, 2011.

23 R. S. Herbst, P. Baron and M. Nilsson, in Advanced separation techniques for nuclear fuel reprocessing and radioactive waste treatment, Elsevier, 2011, pp. 141–175.

24 S. Bourg, A. Geist and J. Narbutt, SACSESS–the EURATOM FP7 project on actinide separation from spent nuclear fuels, Nukleonika, 2015, 60, 809–814.

25 G. Modolo, A. Geist and M. Miguirditchian, Minor actinide separations in the reprocessing of spent nuclear fuels: recent advances in Europe, Reprocessing and recycling of spent nuclear fuel, 2015, 245–287.

26 C. Poinssot, C. Rostaing, P. Baron, D. Warin and B. Boullis, Main results of the French program on partitioning of minor actinides, a significant improvement towards nuclear waste reduction, Procedia Chem, 2012, 7, 358–366.

27 R. Malmbeck, D. Magnusson, S. Bourg, M. Carrott, A. Geist, X. Hérès, M. Miguirditchian, G. Modolo, U. Müllich and C. Sorel, Homogenous recycling of transuranium elements from irradiated fast reactor fuel by the EURO-GANEX solvent extraction process, Radiochim Acta, 2019, 107, 917–929.

28 P. Baron, S. M. Cornet, E. D. Collins, G. DeAngelis, G. Del Cul, Y. Fedorov, J. P. Glatz, V. Ignatiev, T. Inoue and A. Khaperskaya, A review of separation processes proposed for advanced fuel cycles based on technology readiness level assessments, Progress in Nuclear Energy, 2019, 117, 103091.

29 T. Shaw, A. D. Clayton, R. Labes, T. M. Dixon, S. Boyall, O. J. Kershaw, R. A. Bourne and B. C. Hanson, A self-optimised approach to synthesising DEHiBA for advanced nuclear reprocessing, exploiting the power of machine-learning, React Chem Eng, 2024, 9, 426–438.

30 M. Bunn, J. P. Holdren, S. Fetter and B. Van Der Zwaan, The economics of reprocessing versus direct disposal of spent nuclear fuel, Nucl Technol, 2005, 150, 209–230.

31 M. Miguirditchian, H. Roussel, L. Chareyre, P. Baron, D. Espinoux, J. N. Calor, C. Viallesoubranne, B. Lorrain and M. Masson, in Proceedings Global, 2009.

32 R. Malmbeck, M. Carrott, B. Christiansen, A. Geist, X. Hérès, D. Magnusson, G. Modolo, C. Sorel, R. Taylor and A. Wilden, in Proceedings of Sustainable Nuclear Energy Conference, 2014.

33 R. Malmbeck, D. Magnusson, S. Bourg, M. Carrott, A. Geist, X. Hérès, M. Miguirditchian, G. Modolo, U. Müllich and C. Sorel, Homogenous recycling of transuranium elements from irradiated fast reactor fuel by the EURO-GANEX solvent extraction process, Radiochim Acta, 2019, 107, 917–929.

34 F. Rodrigues, G. Ferru, L. Berthon, N. Boubals, P. Guilbaud, C. Sorel, O. Diat, P. Bauduin, J. P. Simonin and J.-P. Morel, New insights into the extraction of uranium (VI) by an N, N-dialkylamide, Mol Phys, 2014, 112, 1362–1374.

35 P. N. Pathak, L. B. Kumbhare and V. K. Manchanda, Effect of structure of N, N dialkyl amides on the extraction of U (VI) and Th (IV): a thermodynamic study, Radiochim Acta, 2001, 89, 447–452.

36 A. Tessier, P. G. C. Campbell and M. Bisson, Sequential extraction procedure for the speciation of particulate trace metals, Anal Chem, 1979, 51, 844–851.

37 A. Baker, A. Fells, T. Shaw, C. J. Maher and B. C. Hanson, Effect of scale-up on residence time and uranium extraction on annular centrifugal contactors (ACCs), Separations, 2023, 10, 331.

Chapter 5: Overall Conclusion

The work in this project has devised and employed methodologies to optimise the synthesis and purification of DEHiBA in continuous flow using Industry 4.0, exploiting automation and machine-learning algorithms to efficiently achieve desirable process metrics for the manufacture of DEHiBA. This work has utilised self-optimising flow platforms, using this technology for an industrially relevant application in the area of nuclear reprocessing. These methodologies are time and resource efficient, requiring minimal operator input, facilitating the efficient optimisation of key process metrics like cost, throughput, and purity. Bayesian machine learning algorithms were preferred for this work due to their ability to identify optima in minimal experimental iterations, minimising research and development timelines and material consumption. The use of a weighted objective for the purification optimisations with BOAEI was very effective and could have been useful in the synthetic optimisation work to more effectively identify optimal trade-off conditions.

Such methodologies and platforms outlined are applicable to many other industrially relevant chemicals including other ligands for nuclear reprocessing. Such applications are incredibly relevant due to limited accessibility to ligands like DEHiBA, especially on the large scale and the high-cost barrier associated with ligands in this area of research. However, further work is required for the optimisation of telescoped synthetic steps to make this methodology better suited to multi-step syntheses.

Further work in this thesis ensured that DEHiBA manufactured via these promising routes behaved as suggested in the literature, also comparing to industrially sourced DEHiBA. This work ensured that chosen starting materials and reagents were compatible with the end application of extracting uranium(IV). Additionally testing in the presence of potential degradation products allowed performance comparison to pure DEHiBA for the forward extraction of uranium(VI). Additionally other variables were explored to expand on relevant published studies with DEHiBA.

When designing chemical processes, the consideration of multiple performance metrics is crucial to success. Work in Chapters 2 and 3 optimises multiple objectives to achieve this and develop well rounded processes with a choice of operating conditions depending on performance criteria motives. TSEMO and BOAEI are used to do this, respectively, where TSEMO works well for the synthetic work identifying Pareto Fronts for a variety of objectives whereas the purification work in Chapter 3 was material intensive and focussed on achieving specific performance criteria of high purity (>95%) and low product loss. As the synthetic optimisations were less material intensive these optimisations used a greater number of experiments and were able to fully explore the Pareto Front, the purification work however was limited in terms of crude DEHiBA and thus a more targeted method was used in the form of BOAEI with a weighted objective. Both approaches used significant quantities of reagent, especially when performing continuous chemistry solvent-free, the optimisation of these reactions with slug-flow would have further minimised cost and

material waste however this approach would have been difficult to adopt for the purification work with the coalescing separator used. Both approaches optimised and compared multiple routes to identify an optimum on-demand continuous manufacture route to DEHiBA finding that crude DEHiBA could be synthesised for £23.60 mol^{-1} at 14.7 kg L^{-1} h^{-1} or £24.50 mol^{-1} at 75.8 kg L^{-1} h^{-1} using iBAnhydride and DiEHA. An alternative route was devised in the event that iBAnhydride became less or no longer viable, using iBA and DiEHA via a thermal amidation route for £27.20 mol^{-1} with a reduced throughput of 3.5 kg L^{-1} h^{-1}. Additionally, it would also be possible to manufacture iBAnhydride from iBA, although this was out of the scope of this project but could further reduce the cost of DEHiBA. Cost analysis of the purification routes and conditions were not included in this work due to uncertainty with disposal costs of the aqueous waste, however, assumptions can be made that nitric acid waste streams would be more costly and problematic than a water waste stream or even the bicarbonate waste stream. These optimisations aimed to reduce the volume of aqueous waste in order to minimise the cost of DEHiBA further, although the priority of this work was low product loss and high product purity.

Performance testing of DEHiBA identified promising conditions for the forward extraction of uranium investigating key process variables to understand how this affects the extraction efficiency of DEHiBA. SA ratio was used to vary the throughput of aqueous uranium and determine how extraction efficiency is affected by this variable, providing a range of process conditions that could be employed depending on process criteria and goals. The DEHiBA manufactured from routes (e) and (f) were found to be comparable to literature data and one another, justifying the use of either route to manufacture DEHiBA for uranium extraction in the future. Additionally crude DEHiBA did not negatively affect the forward extraction of uranium, however further work is needed on the back extraction (stripping) to ensure no issues are faced, furthermore more complex studies with a greater range of nuclides would be beneficial to ensure no extraction of unwanted

species. This work highlighted the importance of temperature control on the extraction of uranium, with future work needed to determine the extraction performance across a range of potential operating conditions.

Overall, this work has implemented and developed an efficient methodology to manufacture DEHiBA in continuous flow with limited human intervention required to optimise process conditions. Such an approach is applicable to other industrially relevant molecules like the diamides (TODGA) where there is a demand for further studies, including large-scale testing with these materials to improve the technology readiness of advanced reprocessing flowsheets. However, further work is needed to tackle more complex multi-step processes, in these cases slug or droplet flow is likely better suited but is more complex. The DEHiBA manufactured from the optimum routes in this work has proven to be successful for the extraction of uranium(VI) and provides comparable data to the literature and commercially sourced DEHiBA, justifying the effectiveness of these methodologies. The ability to have ligands like DEHiBA on demand aids to reduce barriers to research by increasing supply and reducing the cost of these specialised ligands. The current demand for DEHiBA and other ligands does not currently require continuous manufacture, however this work opens such a possibility and by publishing the findings of this research others in the field are able to manufacture their own DEHiBA using 'optimised' conditions if they choose to. Furthermore, the flow platform for DEHiBA can be reconfigured to manufacture other ligands like DEHBA or DHOA on demand.

It is likely that future advancements in self-optimising flow platforms will focus on improving the usability of slug flow for more complex multi-step synthetic optimisations. This will aid minimise material consumption and simplify the challenges faced when optimising telescoped reaction steps allowing more complex molecules like TODGA or active pharmaceutical ingredients to be optimised efficiently in continuous flow. Additionally, it is likely that research and

development in the nuclear industry will adopt digital chemistry techniques using industry 4.0 to reduce operator dose and minimise material consumption, moving away from one variable at a time optimisations and using DOEs or machine learning algorithms to optimise research challenges. The coalescing separator used in Chapter 3 also has the potential to revolutionise complex extraction processes where solids or hard to break emulsions are faced due to its potential for compatibility with solids, a trait that traditional solvent extraction equipment like pulsed columns and centrifugal contactors lack. This capability is of interest to electronic waste recycling however work is needed to modularise the separator and exchange the filter media when it blinds.

Chapter 6: Appendix

6.1 Chapter 2 Supporting Information

Self-Optimising Flow Reactor Platform Setup

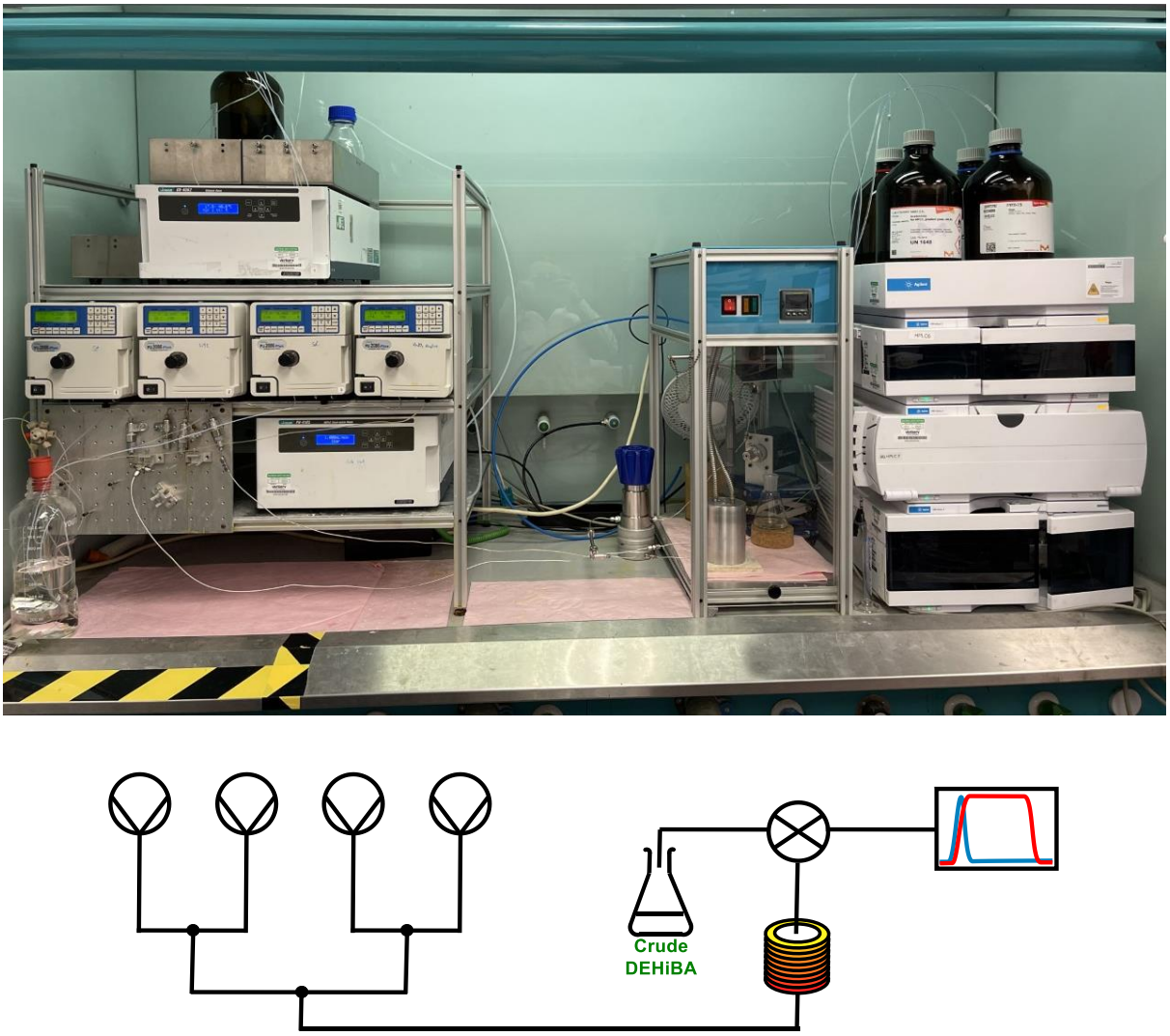

Figure S44: The self-optimising flow reactor platform and its visual schematic

Reagents were made up to their desired concentrations in the stock solutions, loaded into glass bottles and primed on the dual piston reciprocating JASCO PU-2800 HPLC pumps. These solutions were then pumped where streams would be mixed using Swagelok SS-100-3 tee-pieces according to **Figure 28**. Tubular reactors were made from PFA, PTFE and 316 stainless steel tubing

(1/16” OD), these were fitted to cylindrical aluminium blocks and heated via a Eurotherm 3200 temperature controller, this enabled the reaction mixtures to be heated rapidly. After the reactor, the tubing enabled rapid cooling back to roughly ambient temperature prior to an aliquot of the reaction solution being sampled using a VICI Valco EUDA-CI4W sample loop (4-port) with 0.5 and 0.06 μL injection volume. The sample was then fed directly into an Agilent 1260 Infinity II series HPLC instrument fitted with an Agilent Poroshell 120 EC-C18 reverse phase column (5 cm length, 4.6 mm ID and 2.7 μm particle size) for quantitative analysis. The flow system was maintained under a constant back pressure using an Upchurch Scientific back pressure regulator (100/250 psi) for all setups however route (e) also employed the Tescom™ 26-1762-22 control pressure regulator to achieve a pressure of 210 bar. The automated system was controlled using a custom written MATLAB program to enable real-time control and monitoring of all the optimisation variables. The machine-learning algorithms in MATLAB were initiated with Latin hypercube sampling where the number of experiments for this was $2n+1$, n being the number of variables. This formula guarantees that each dimension is divided into $n + 1$ subintervals, and that there will be one sample in each subinterval. This helps achieve a more even coverage of the parameter space, thus reducing the risk of missing important regions. The analytical data from this and following experiments enabled the generation of new conditions for the optimisation to proceed. To determine process metrics, biphenyl was included as an internal standard in reservoir 1 solutions, here the internal standard and compound signal areas allow for accurate calculations to be completed using calibration data previously obtained. During the process, Microsoft Teams screen sharing capability is also utilised to allow for the user to monitor the equipment remotely.

Reagent Costs

The lowest cost for each reagent was acquired as of March 2022 for the cost calculations used by this research.

Table S14: The reagent costs for the raw materials used in this research as of March 2022 using the largest quantity possible to determine this

Raw Material	Molecular weight (g mol^{-1})	Cost per mole (£ mol^{-1})
Di(2-ethylhexyl)amine (**DiEHA**)	241.46	18.18
Isobutyryl chloride (**iBCl**)	106.55	14.75
Isobutyric acid (**iBA**)	88.11	0.59
1-ethyl-3-(3-dimethylaminopropyl)carbodiimide hydrochloride (**EDC.HCl**)	191.77	23.96
4-dimethylaminopyridine (**DMAP**)	122.17	17.25
Isobutyric anhydride (**iBAnhydride**)	158.19	5.31
Triethylamine	101.19	1.68

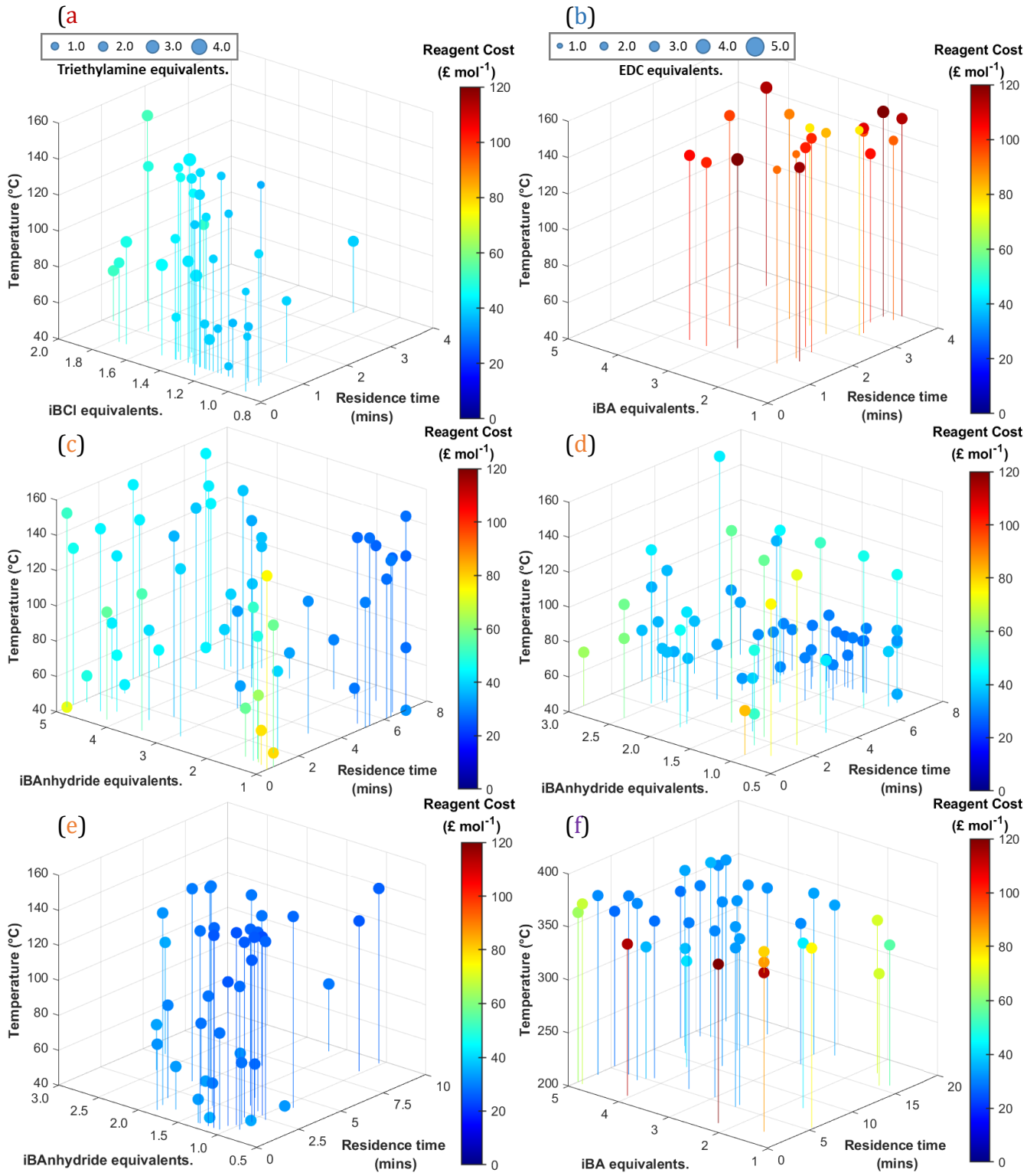

Figure S45: Six 4/5D plots demonstrating the reagent cost for routes (a-f), the synthetic route for each is defined above the plots for ease of comparison. A consistent colour bar is illustrated throughout, ranging between 0-80%, whilst the x, y, z and size ranges are subject to the parameter space for each optimisation, finally a reduced dataset has been presented for clarity.

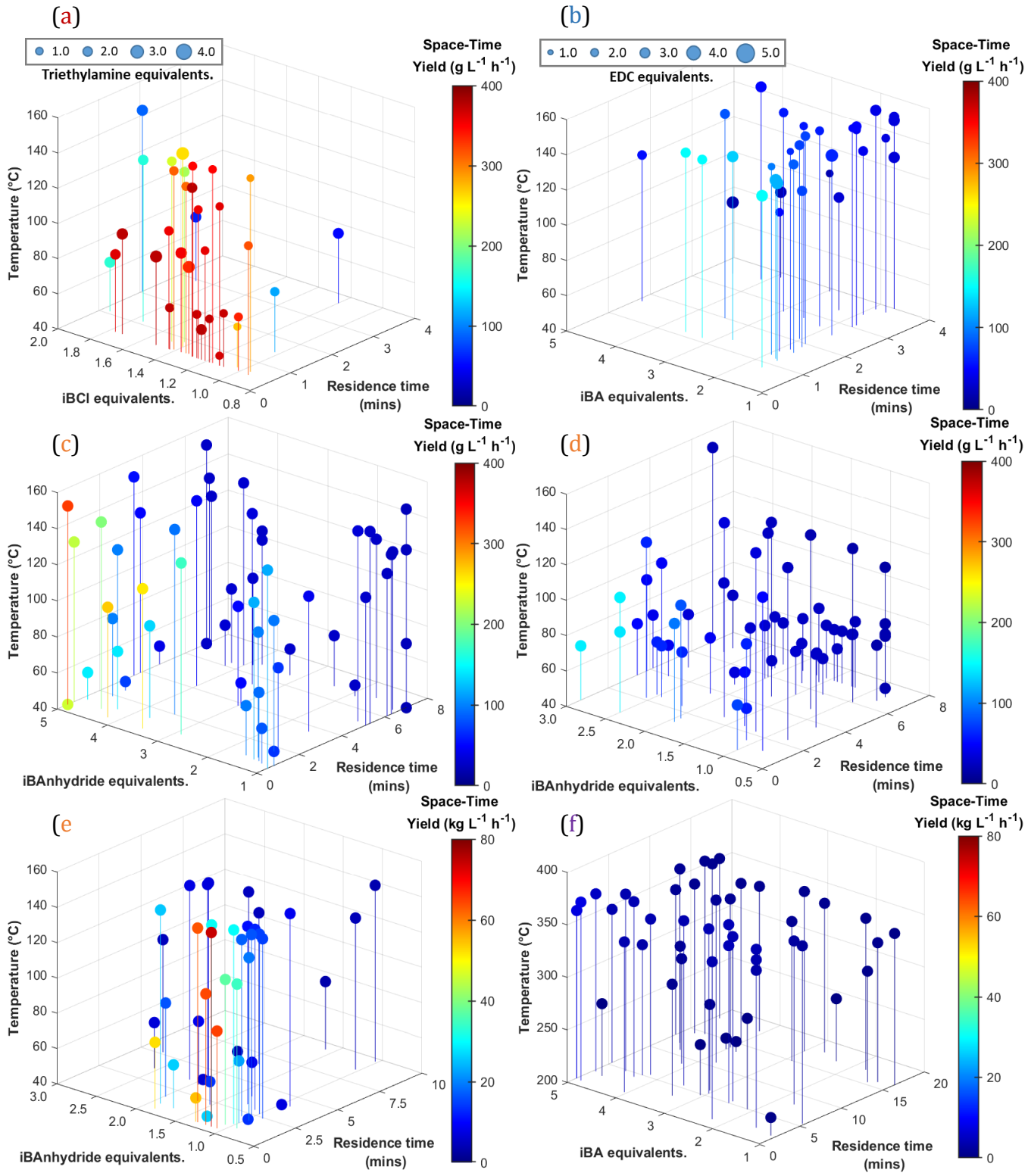

Figure S46: Six 4/5D plots demonstrating the space-time yield for routes (a-f), the synthetic route for each is defined above the plots for ease of comparison. A consistent colour bar is illustrated throughout, ranging between 0-80%, whilst the x, y, z and size ranges are subject to the parameter space for each optimisation, finally a reduced dataset has been presented for clarity.

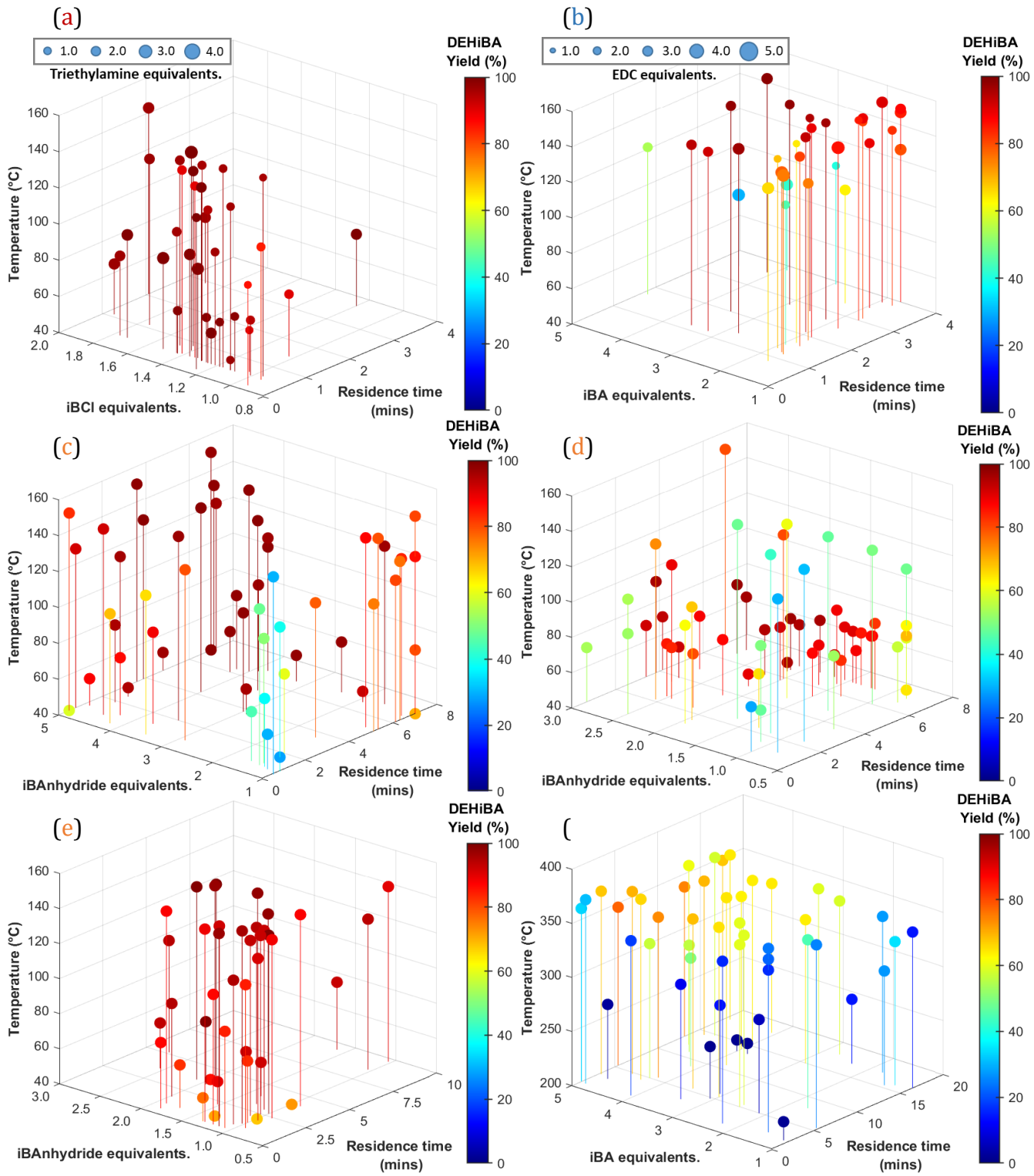

Figure S47: Six 4/5D plots demonstrating the product yield for routes (a-f), the synthetic route for each is defined above the plots for ease of comparison. A consistent colour bar is illustrated throughout, ranging between 0-80%, whilst the x, y, z and size ranges are subject to the parameter space for each optimisation, finally a reduced dataset has been presented for clarity.

The Optimum Conditions for Each Route

Table S15: The optimum conditions from routes (a-f) with a normalised colour scale across each route for ease of process metric comparison

Route	Residence Time (min)	Equivalents. of iBA Derivative	Equivalents. of Reagent	Temperature (°C)	Yield of DEHiBA (%)	Reaction Mass Efficiency (%)	Space-Time Yield (g L^{-1} h^{-1})	Cost of DEHiBA (£ mol^{-1})
(a)	0.6	0.95	0.95	150	99.9	68.6	285	35
	0.5	1.19	1.15	35	99.9	64.8	374	37.4
	0.5	1.09	1.44	35.5	99.2	61.4	374	36.9
	0.5	1.09	1.19	70.5	98.4	64.1	371	36.9
	0.2	1.12	1.08	71	98.8	65.6	933	36.9
	0.2	1.24	1.18	124	99.9	63.2	944	38.5
(b)	1.4	1.66	2.53	169	75.6	29.9	98.2	79.7
	3.3	1.90	1.7	153	84.8	34.7	47.6	77.3
	0.7	4.90	2.64	150	91.2	20	240	151
	1.0	3.08	3.16	144	93.8	26.2	168	101
	3.1	2.20	2.5	149	95	33.3	57.1	77.1
	3.0	2.50	2.1	151	96.2	32.9	60	83.3
(c)	0.5	5.00	-	150	83.2	26.3	326	51.2
	7.0	1.00	-	127.5	86.1	70.4	24.1	26
	0.8	2.00	-	128.5	91.4	28.9	224	46.6
	0.9	3.00	-	143.5	91.8	31.5	200	43.7
	7.0	4.00	-	127.5	96	65.5	26.9	25.9
	6.5	1.80	-	127	97.5	60.6	29.4	27.1
(d)	0.7	2.50	-	105	54.2	26.5	145	58
	2.4	1.35	-	70.5	64.9	44.4	51.6	39
	7.0	2.35	-	69.7	86.8	62.4	23.2	28.4
	3.7	3.35	-	71.5	86.8	46.5	43.8	34.1
	7.0	4.35	-	69	90.5	59.9	24.2	28.6
	3.9	3.00	-	91.5	95.8	41.7	46.5	35.6
(e)	0.5	1.07	-	149	95.5	72.6	74700	24.9
	0.5	1.15	-	150	97.2	71.9	74110	24.9
	2.7	2.15	-	141.9	99.3	77.5	14720	23.6
	0.7	3.15	-	147.9	92.1	71.9	51590	25.4
	1.3	1.02	-	150	96	74.3	30090	24.5
(f)	1.7	5.00	-	366	52.3	23.8	7320	40.5
	4.8	4.60	-	369	69.8	33.5	3731	30
	6.3	5.60	-	353	71	34.7	2921	29.4
	5.5	6.60	-	348	73.7	37.4	3619	28.1
	13.2	7.60	-	338	74.3	33.8	1378	28.5
	10.6	8.60	-	339	75.6	34.4	1734	28
	5.4	5.00	-	346	77.7	35.4	3495	27.2

Experimental

HPLC and GC-FID Methods

HPLC analysis was performed on an Agilent 1260 Infinity II series HPLC instrument fitted with an Agilent Poroshell 120 EC-C18 reverse phase column (5 cm length, 4.6 mm ID and 2.7 μm particle size) with a binary pump and a variable wavelength detector.

The same HPLC method was used for all routes and calibrations. Water (A, 18.2 MΩ) and acetonitrile (B) HPLC mobile phases were used, starting with a 50:50 method of A:B, the amount of A was reduced to 5% over 3 minutes and held here for a further 3 minutes before returning to 50:50 over 0.5 minutes at a flow rate of 1.50 mL min^{-1} and a column temperature of 30 °C. 210 nm was used to detect the product DEHiBA, whilst 254 nm was used to detect biphenyl.

GC analysis was carried out on an Agilent 7890B instrument fitted with an Agilent Technologies 7693 Autosampler and a HP-5 column (30 m x 0.32 mm, 0.25 μm film thickness), H_2 carrier gas, FID detector.

The same GC method was used throughout, starting at 40 °C and holding at this for 1 minute, then the temperature was ramped up to 55 °C over 1 minute and held here for a further 1 minute. The temperature was then gradually increased to 150 °C over 3.8 minutes. Finally the temperature was raised to 300 °C over 3 minutes before cooling to 40 °C.

Calibrations for Quantitative Analysis

All raw materials were purchased from suppliers and calibrated where possible via GC-FID and HPLC. N,N-di-(2-ethylhexyl)isobutyramide (DEHiBA) was synthesised as well as purchased from a commercial supplier (Technocomm) for analytical calibrations to enable the quantitative analysis of all reactions for calculating key process metrics. Two calibration curves are shown in Figure S5 for HPLC and GC-FID:

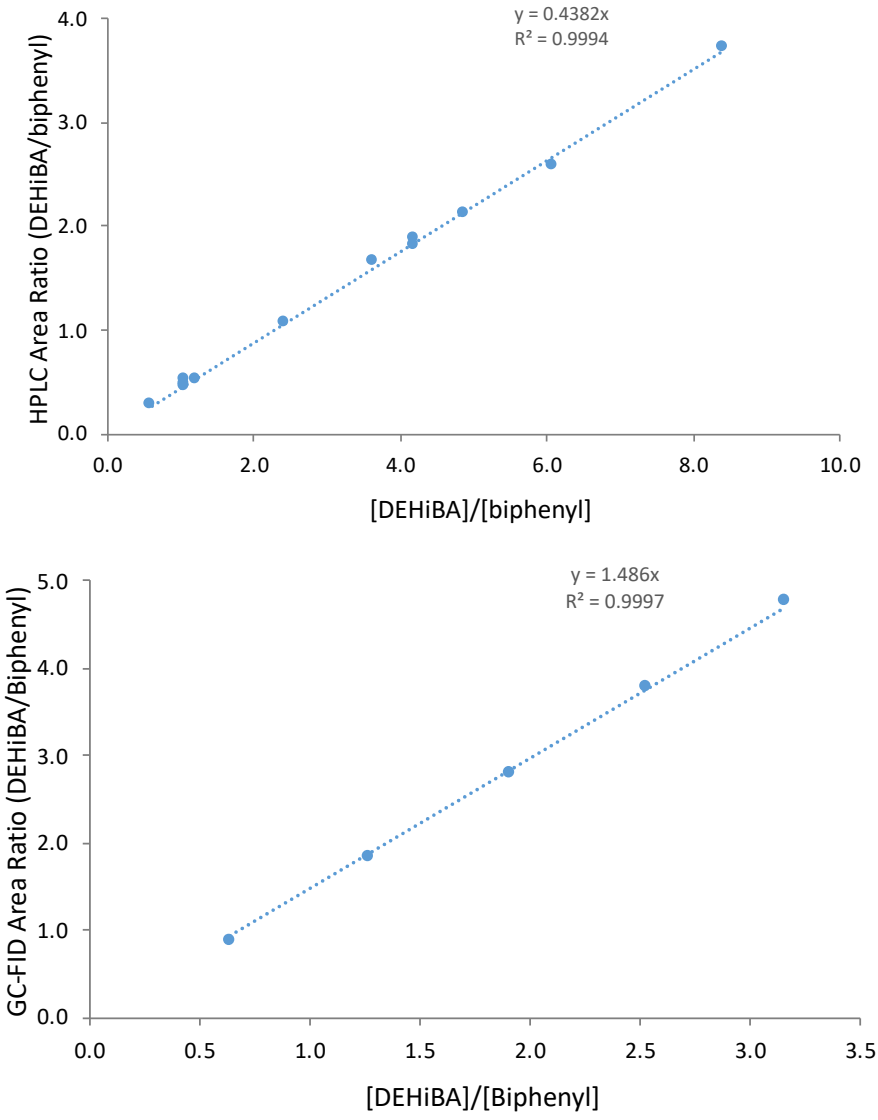

Figure S48: HPLC (top) and GC-FID (bottom) calibration curves for DEHiBA from the commercial supplier, our purified DEHiBA is also in agreement with these plots

Route (a) Acyl Chloride Route: Synthesis from Isobutyryl Chloride

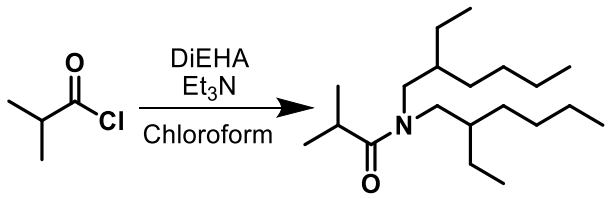

Scheme S8: Amide bond formation using isobutyryl chloride and di(2-ethylhexyl)amine (DiEHA) to yield N,N-di-(2-ethylhexyl)isobutyramide (DEHiBA)

Batch Chemistry:

Batch studies were conducted prior to any flow chemistry to ensure homogeneity and product formation. A range of common organic solvents were screened one of which being toluene, all reagents showed good solubility separately, however when combined in the reactor the solution instantly precipitated and stirring came to a halt at a concentration of 0.1 mol dm^{-3} due to the amount of precipitate. As solids are problematic in flow, chloroform was adopted as the reaction solvent to solubilise the $Et_3N.HCl$ precipitate.

Di-2-ethylhexylamine (0.28 g, 1.16 mmol) and triethylamine (0.1450 g, 1.43 mmol) were combined with chloroform in a 10 mL volumetric flask. Likewise, Isobutyryl chloride (0.1483 g, 1.39 mmol) was combined with chloroform in a 10 mL volumetric flask. The di-2-ethylhexylamine solution was charged to an ice bath cooled 50 mL round bottom flask with stirring, slow addition of iBCl over 2 minutes gave a slightly yellow, homogenous solution that was left to stir for 4 hours at room temperature before HPLC analysis confirmed a 98% yield.

Continuous Flow Chemistry:

Reservoir solutions were prepared to the desired concentrations by dissolving the reagents in solvent with stirring at ambient conditions.

Setup (i):

Reservoir 1: Di(2-ethylhexyl)amine (6.0401 g, 0.025 mol, 0.05 mol dm^{-3}), triethylamine (10.5 mL, 0.075 mol, 0.15 mol dm^{-3}) and biphenyl (5.4127 g, 0.035 mol, 0.07 mol dm^{-3}) in chloroform (500 mL).

Reservoir 2: Isobutyryl chloride (5.3205 g, 0.05 mol, 0.05 mol dm^{-3}) in chloroform (1000 mL).

Reservoir 3: Chloroform.

Setup (ii):

Reservoir 1: Di(2-ethylhexyl)amine (6.0365 g, 0.025 mol, 0.05 mol dm^{-3}), and biphenyl (5.3974 g, 0.035 mol, 0.07 mol dm^{-3}) in chloroform (500 mL).

Reservoir 2: Isobutyryl chloride (2.6638 g, 0.025 mol, 0.05 mol dm^{-3}) and triethylamine (4.2 mL, 0.03 mol, 0.06 mol dm^{-3}) in chloroform (500 mL).

Reservoir 3: Chloroform.

Setup (iii):

Reservoir 1: Di(2-ethylhexyl)amine (12.0730 g, 0.05 mol, 0.1 mol dm^{-3}), and biphenyl (5.3965 g, 0.035 mol, 0.07 mol dm^{-3}) in chloroform (500 mL).

Reservoir 2: Isobutyryl chloride (5.3275 g, 0.05 mol, 0.1 mol dm^{-3}) in chloroform (500 mL).

Reservoir 3: Triethylamine (7.0 mL, 0.05 mol, 0.1 mol dm^{-3}) in Chloroform (500 mL).

Reservoir 4: Chloroform.

An example chromatogram is shown in Figure S6.

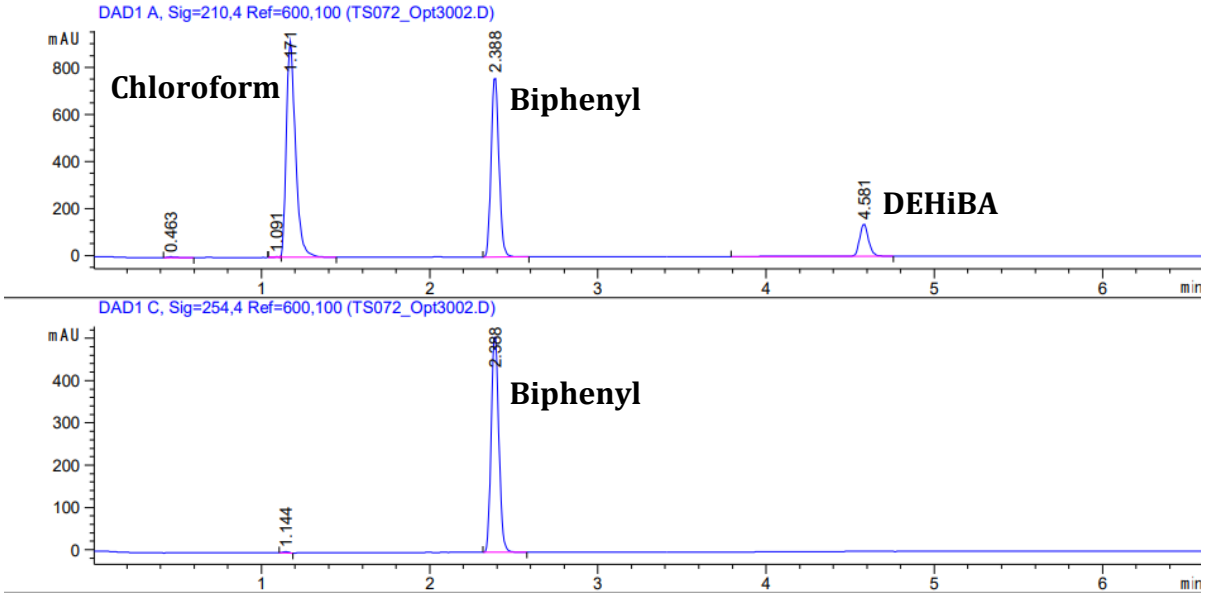

Figure S49: A typical HPLC chromatogram for route (a)

The flow platforms were set up according to **Figure 28** all using a reactor volume of 2.7 mL with PFA tubing and a back pressure of 100 psi. The self-optimisation was conducted with respect to three continuous parameters for setups (i) and (ii): residence time, iBCl equivalents, and temperature. Whilst setup (iii) optimised four continuous parameters: residence time, iBCl equivalents, triethylamine equivalents, and temperature. The upper and lower parameter bounds are described in Tables S3. The initial objective for each optimisation was to maximise yield, then simultaneously maximize reaction mass efficiency and space-time yield.

Tables S16: Upper and lower parameter bounds for setups (i), (ii), and (iii). Equivalents are determined with respect to DiEHA

Setup (i)	Residence time (mins)	iBCl equivalents.	Temperature (°C)	Triethylamine equivalents.	[DiEHA] in reactor (mol dm^{-3})
Lower bound	0.5	0.95	35	3	0.01
Upper bound	10	3	150	3	0.01

Setup (ii)	Residence time (mins)	iBCl equivalents.	Temperature (°C)	Triethylamine equivalents.	[DiEHA] in reactor (mol dm^{-3})
Lower bound	0.5	0.95	35	1.14	0.01
Upper bound	10	3	150	3.6	0.01

Setup (iii)	Residence time (mins)	iBCl equivalents.	Temperature (°C)	Triethylamine equivalents.	[DiEHA] in reactor (mol dm^{-3})
Lower bound	0.5	0.95	35	0.95	0.01
Upper bound	5	2	150	4	0.01

Route (a) Data and Further Analysis

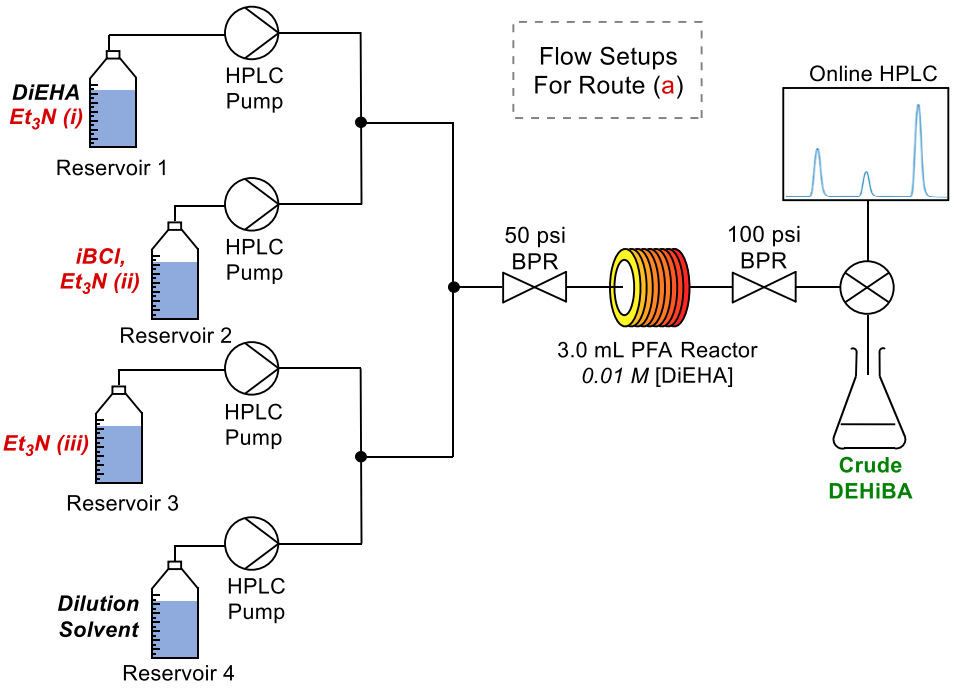

Figure S50: The various flow setups (i-iii) for route (a)

Three flow setups were investigated for route (a), each an attempt to improve on the last setup, with setup (iii) being discussed in the paper. The reservoir configuration and concentrations define the feasible parameter space for each self-optimisation, therefore this screening provides an insight into feasible reservoir configurations whilst allowing access to different parameter spaces to further the optimisation in the search for improved process metrics. The setups investigated here differed in the location and amount of triethylamine in the reservoirs:

- Setup (i) combined a large excess of triethylamine with DiEHA in reservoir 1, to match the maximum possible equivalents of iBCl (3 with respect to DiEHA).
- Setup (ii) combined equal amounts of triethylamine and iBCl into reservoir 2.
- Setup (iii) separated each reagent into individual reservoirs for the optimisation of both the equivalents of iBCl and triethylamine.

Figure S7 illustrates these setups as well as the setups for routes (b-f). Despite the convenience and simplicity offered by setup (i), the optimisation was limited by its inability to vary the equivalents of triethylamine, this large and constant excess of triethylamine limited the RME to a

theoretical maximum of 39.5%. Nevertheless setup (i) performed exceedingly well with minimal trade-off between the key process metrics. All the reactions conducted were high yielding at >90%, and an optimum RME of 38.8% was achieved at just 40 °C, with 0.95 equivalents of iBCl, the large excess of triethylamine, and a 10 minute residence time which substantially diminished the STY. Impressively, several conditions were close to this optimum RME, but to their advantage, far outperformed in terms of productivity with the optimum requiring only a 0.5 minute residence time at 150 °C, achieving an RME of 38.4% and an exceptional improvement in STY to 367 g L^{-1} h^{-1}. This condition provided little trade-off between key process metrics, proving itself as the overall optimum condition in this case.

A clear trend between temperature and residence time was observed, with higher temperatures favouring lower residence times for the best conversion due to thermal degradation of starting materials. Therefore, in addition to improving the STY, shorter residence times aided to improve the RME. Overall route (a), setup (i) showed great promise, with the maximum RME and STY just 0.7% and 6 g L^{-1} h^{-1} from their theoretical maximum, in addition to the insignificant trade-off as demonstrated by the insignificant Pareto front (**figure S8**).

However, in an attempt to improve on this, setup (ii) was designed so that only a slight excess of triethylamine was maintained with respect to iBCl. This was initially promising, however starting material degradation over a period of just 6 hours resulted in a loss of reproducibility, with large yield losses in some cases, verifying the impracticality of combining triethylamine and iBCl. This degradation is caused by ketene formation which is highly reactive and in this case has degraded somewhat in the reservoir.

A plot comparing the RME and STY metrics for setups (i) and (iii) was produced and can be found in **Figure S8**.

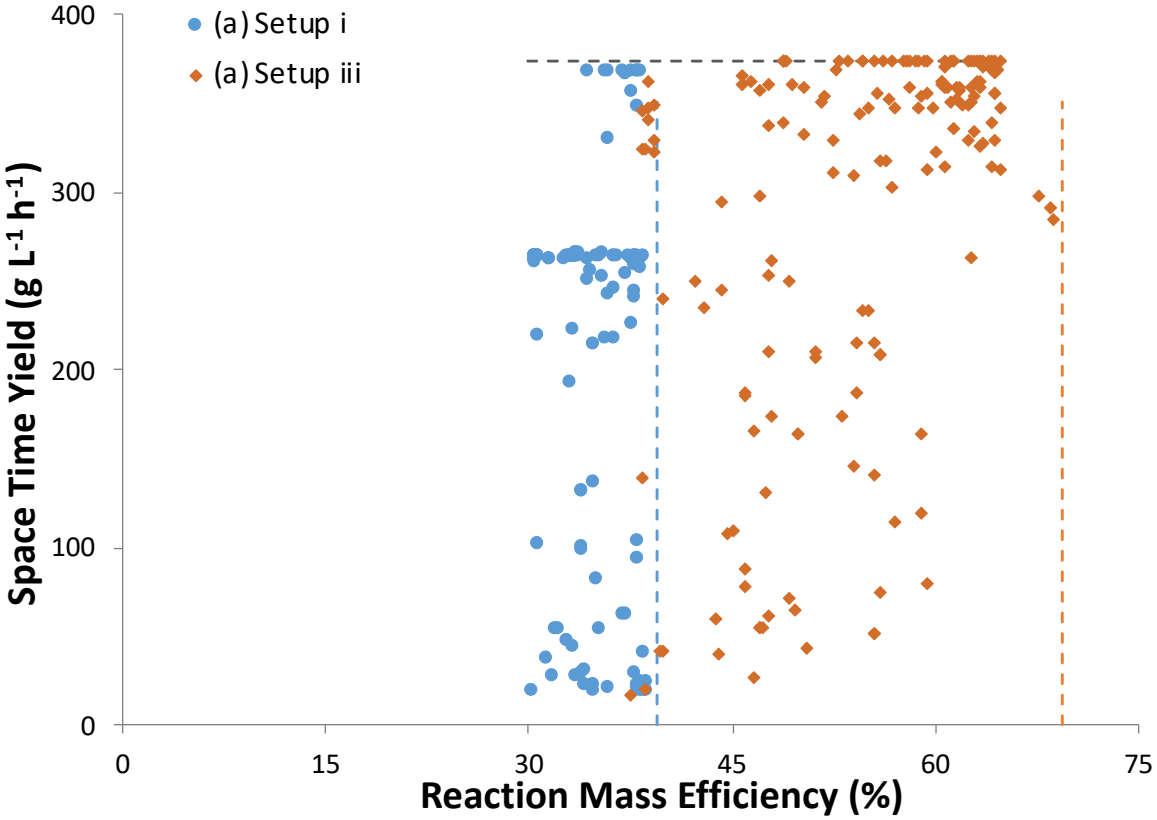

Figure S51: Reaction data for route a, setups (i) and (iii), where the dashed lines show the theoretical maxima for their accessible parameter space during each optimisation

A plot demonstrating the performance of route (a) even at 12 second residence times is shown in Figure S9 where little trade-off is observable even at these flow rates.

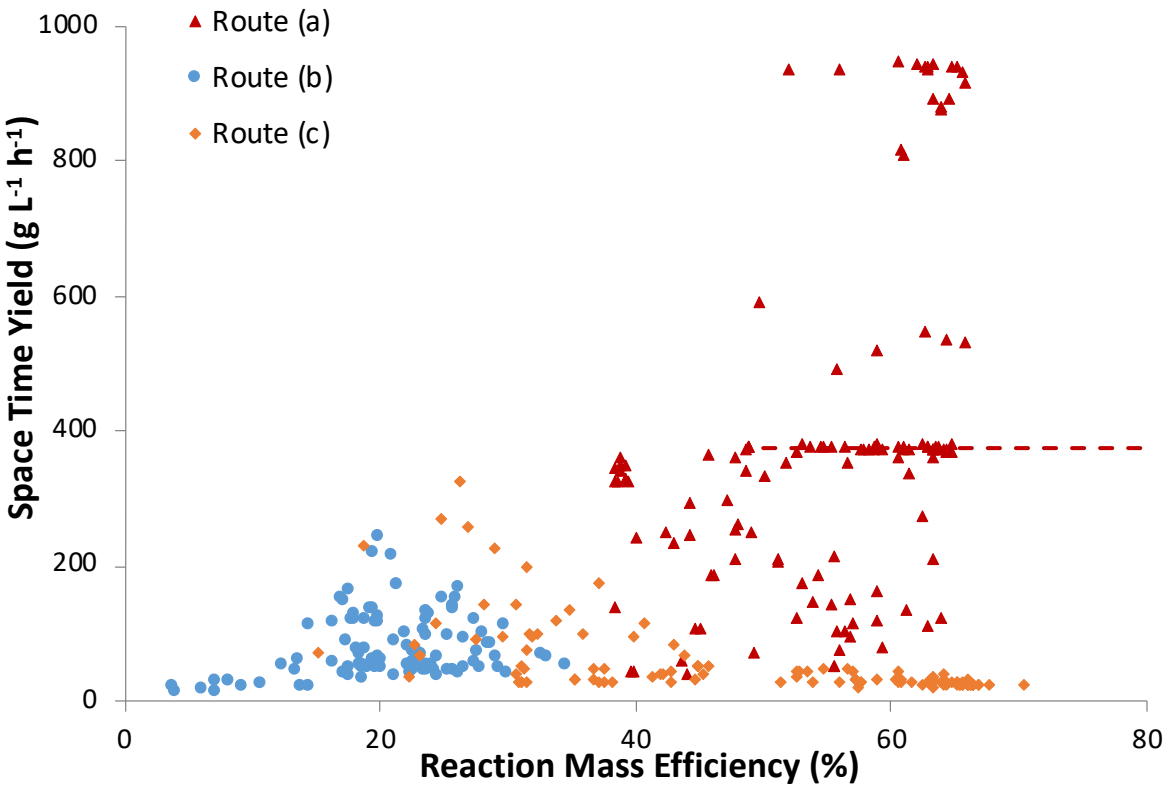

Figure S52: STY, RME Pareto fronts for routes (a-c) with the additional data from route (a) exploring residence times below 0.5 minutes the limit that was set and shown by the dashed line as the upper STY limit

To further add to the data provided in Chapter 2we have hereby included the entirety of the reaction conditions explored for route (a) and the outcome of each experiment.

Table S17: Reaction conditions and outcomes from the optimisation of setups (i) and (iii)

Setup	Residence time (min)	iBCl equivalents.	Et_3N equivalents.	Temp (°C)	DEHiBA Yield wrt DiEHA (%)	Reaction mass efficiency (%)	Space-Time Yield (g L^{-1} h^{-1})	Cost of DEHiBA (£ mol^{-1})
(i)	6.7	2.18	3	41.9	99.4	33.9	27.8	50.6
(i)	3.5	2.56	3	65.9	98.8	32.3	52.8	56.6
(i)	9.4	1.64	3	78.5	98.5	35.9	19.6	43
(i)	1.4	2.01	3	93.1	97.5	33.9	130.2	49
(i)	5	2.76	3	103.8	98.5	31.5	36.8	59.8
(i)	8.6	1.09	3	125.9	98.2	38.4	21.4	34.9
(i)	3	1.3	3	140.8	97.9	37.2	61.1	38.1
(i)	3.5	2.56	3	65.9	98.2	32.1	52.5	56.9

Setup	Residence time (min)	iBCl equivalents.	Et_3N equivalents.	Temp (°C)	DEHiBA Yield wrt DiEHA (%)	Reaction mass efficiency (%)	Space-Time Yield (g L^{-1} h^{-1})	Cost of DEHiBA (£ mol^{-1})
(i)	1.4	2.01	3	93.1	97.4	33.9	130.2	49.1
(i)	3	1.3	3	140.8	97.7	37.2	60.9	38.2
(i)	6.2	2.07	3	45	98.9	34.2	29.8	49.2
(i)	7	2.62	3	45	98.5	32	26.3	57.7
(i)	7	2.2	3	45	98.6	33.6	26.3	51.3
(i)	7.9	0.95	3	40	97.2	38.7	23	33.1
(i)	0.7	0.95	3	40.1	91.4	36.4	244.3	35.2
(i)	10	0.95	3	40.1	97.3	38.8	18.2	33.1
(i)	6.4	0.95	3	40	95.1	37.9	27.8	33.8
(i)	8.4	0.95	3	49.8	95.8	38.2	21.3	33.6
(i)	10	0.95	3	150	96.8	38.5	18.1	33.3
(i)	10	1.75	3	150	97.3	34.9	18.2	45.2
(i)	10	0.95	3	150	96.5	38.4	18	33.3
(i)	7.8	0.95	3	150	96.5	38.4	23.1	33.3
(i)	0.7	1.72	3	149.9	98.2	35.4	262.4	44.4
(i)	0.7	2.68	3	149.9	98	31.6	261.8	58.8
(i)	0.7	0.95	3	149.3	90.3	36	241.1	35.7
(i)	0.7	1.97	3	149.6	98.2	34.4	249.3	48
(i)	0.7	3	3	40	97.9	30.5	261.6	63.7
(i)	0.7	2.4	3	40	98.1	32.6	262.2	54.6
(i)	0.7	2.7	3	40	98	31.5	261.9	59.1
(i)	0.7	3	3	40	98.1	30.5	262	63.6
(i)	0.7	2.98	3	149.9	98	30.6	260.3	63.4
(i)	0.7	3	3	150	98.1	30.6	262.1	63.6
(i)	0.7	1.95	3	40.2	98	34.4	260.9	47.9
(i)	0.7	2.99	3	150	98	30.5	261.7	63.6
(i)	0.7	3	3	96.8	98.1	30.6	261.4	63.6
(i)	10	3	3	150	97.2	30.3	18.2	64.2
(i)	0.7	2.19	3	40.3	98.3	33.5	262.4	51.3
(i)	0.7	1.8	3	40	98.3	35.1	262.6	45.5
(i)	0.7	3	3	103.2	98.2	30.6	262.5	63.5
(i)	0.7	3	3	48.4	98.1	30.6	262.2	63.6
(i)	0.7	3	3	62.3	98.3	30.6	262.7	63.4
(i)	0.7	3	3	71.7	98.1	30.6	262.3	63.6
(i)	0.7	3	3	131.9	98.3	30.6	262.7	63.4
(i)	0.7	3	3	65.9	98.4	30.6	262.9	63.4
(i)	0.7	3	3	136.1	98.4	30.6	262.9	63.4
(i)	0.7	3	3	103.1	98.5	30.7	263.2	63.3
(i)	0.7	3	3	124	98.4	30.6	262.9	63.4
(i)	0.7	3	3	135.5	98.5	30.7	263.1	63.4
(i)	0.7	3	3	148.4	98.6	30.7	263.4	63.3
(i)	0.7	3	3	40.7	98.3	30.6	262.7	63.4
(i)	0.7	3	3	149.6	98.4	30.6	262.9	63.4
(i)	0.7	3	3	112.9	98.4	30.6	262.9	63.4

Setup	Residence time (min)	iBCl equivalents.	Et_3N equivalents.	Temp (°C)	DEHiBA Yield wrt DiEHA (%)	Reaction mass efficiency (%)	Space-Time Yield (g L^{-1} h^{-1})	Cost of DEHiBA (£ mol^{-1})
(i)	0.7	2.99	3	74.2	98.4	30.7	263	63.3
(i)	0.7	3	3	102.9	98.3	30.6	262.8	63.4
(i)	0.7	3	3	87.5	98.5	30.7	263.2	63.3
(i)	0.7	3	3	75.1	98.5	30.7	263.2	63.3
(i)	0.7	2.99	3	69.7	98.5	30.7	262.8	63.2
(i)	0.7	3	3	86.6	98.5	30.7	263.2	63.3
(i)	0.7	3	3	130.5	98.5	30.7	263.2	63.3
(i)	0.7	3	3	110.1	98.5	30.7	263.2	63.3
(i)	0.7	2.33	3	126.6	98.7	33.1	263.6	53.2
(i)	0.7	2.29	3	101.4	98.5	33.2	263.2	52.7
(i)	0.7	2.27	3	127.2	98.6	33.3	263.4	52.3
(i)	0.7	2.23	3	75.9	98.7	33.4	263.6	51.8
(i)	0.7	2.36	3	93.8	98.6	33	263.6	53.7
(i)	0.7	2.33	3	118	98.7	33.1	263.7	53.2
(i)	0.7	2.31	3	54.3	98.7	33.2	263.8	53
(i)	0.7	2.29	3	107	98.7	33.2	263.7	52.7
(i)	0.7	2.28	3	149.4	98.6	33.2	263.3	52.6
(i)	0.7	2.27	3	99.2	98.5	33.2	263.2	52.5
(i)	0.7	2.26	3	114	98.6	33.3	263.5	52.2
(i)	0.7	2.25	3	148.2	98.6	33.3	263.4	52.1
(i)	0.7	2.25	3	142.4	98.4	33.3	262.9	52.1
(i)	0.7	2.24	3	74	98.5	33.4	263.1	52
(i)	0.7	2.28	3	126.2	98.6	33.3	263.4	52.5
(i)	0.7	2.26	3	147.6	98.4	33.3	262.8	52.3
(i)	0.7	2.26	3	117.7	98.6	33.4	263.5	52.1
(i)	0.7	2.23	3	119.3	98.5	33.4	263.1	51.9
(i)	0.7	2.25	3	150	98.7	33.4	263.6	52
(i)	0.7	2.24	3	150	98.4	33.3	262.8	52
(i)	0.7	2.23	3	149.9	98.5	33.4	263.3	51.8
(i)	0.7	2.23	3	150	98.6	33.5	263.5	51.7
(i)	0.7	2.2	3	149.4	98.5	33.6	263.3	51.3
(i)	0.7	2.23	3	150	98.7	33.5	263.6	51.7
(i)	0.7	2.22	3	150	98.9	33.6	264.2	51.5
(i)	0.7	2.22	3	150	98.5	33.5	263.3	51.7
(i)	0.7	2.22	3	149.9	98.7	33.5	263.8	51.6
(i)	0.7	2.21	3	150	98.8	33.6	264	51.3
(i)	1.8	3	3	150	98.6	30.7	100.7	63.3
(i)	0.7	2.21	3	150	98.6	33.5	263.6	51.4
(i)	0.7	2.2	3	150	98.5	33.5	263.2	51.4
(i)	0.7	2.2	3	150	98.8	33.6	264	51.2
(i)	0.7	2.17	3	149.5	98.9	33.8	264.1	50.8
(i)	0.7	2.19	3	150	98.6	33.6	263.6	51.2
(i)	0.7	1.34	3	48.4	98.3	37.2	252.7	38.6
(i)	0.7	1.93	3	108.9	98.9	34.7	254	47.2

Setup	Residence time (min)	iBCl equivalents.	Et_3N equivalents.	Temp (°C)	DEHiBA Yield wrt DiEHA (%)	Reaction mass efficiency (%)	Space-Time Yield (g L^{-1} h^{-1})	Cost of DEHiBA (£ mol^{-1})
(i)	9	1.18	3	148.4	98.7	38.1	20.6	36
(i)	4.6	1.09	3	148.9	98.6	38.6	40.1	34.7
(i)	0.8	0.95	3	87.8	89.6	35.7	216.3	35.9
(i)	2	0.95	3	88.3	87.9	35	80.9	36.6
(i)	0.7	1.29	3	146.2	98.6	37.5	263.5	37.8
(i)	0.7	1.73	3	146.5	98.6	35.5	251.3	44.3
(i)	3.2	0.95	3	113.9	88.7	35.3	52.6	36.3
(i)	0.7	1.48	3	133.3	98.6	36.6	263.4	40.6
(i)	0.7	1.74	3	136.2	98.9	35.5	264.2	44.4
(i)	0.7	1.11	3	149.3	98.7	38.5	263.6	35
(i)	0.7	2.13	3	51.1	98.6	33.8	263.5	50.3
(i)	0.7	1.19	3	136.4	98.7	38	263.7	36.3
(i)	1.2	0.93	3	141.8	87.3	34.9	136.3	36.5
(i)	1.6	0.9	3	142.4	84.6	33.9	99.9	37.2
(i)	1.6	0.9	3	150	84.7	34	97.1	37.1
(i)	0.7	1.53	3	88.3	98.5	36.4	263.1	41.4
(i)	0.7	1.53	3	95.6	98.6	36.4	263.4	41.3
(i)	0.8	1.51	3	95.8	98.6	36.5	217.4	41.1
(i)	7.8	0.94	3	99.2	87.7	35	21.1	36.5
(i)	3.6	0.9	3	50.1	83.1	33.3	42.7	37.9
(i)	3.3	0.9	3	53.7	82.3	33	47	38.2
(i)	0.7	1.17	3	112.7	98.1	37.9	262.1	36.2
(i)	7.4	0.9	3	150	85.2	34.2	21.6	36.9
(i)	0.8	2.94	3	41.1	98.3	30.8	217.7	62.6
(i)	1	2.26	3	45.2	98.1	33.1	192.6	52.6
(i)	0.8	1.17	3	108.1	98.3	38	239.1	36
(i)	0.8	1.17	3	112.9	98	37.9	242.4	36.2
(i)	0.7	1.17	3	51.2	98.2	38	262.3	36.1
(i)	0.7	1.16	3	93.9	98.3	38	261.2	36
(i)	0.8	1.24	3	128.6	98.2	37.6	225.8	37.1
(i)	0.9	1.83	3	140.1	98.4	35	213.9	46
(i)	0.7	1.05	3	75.2	96.7	38	258.3	34.8
(i)	0.7	1.11	3	76.6	98.1	38.2	262.1	35.3
(i)	0.7	1.22	3	87.9	98.1	37.7	262.1	36.9
(i)	0.7	0.9	3	88.1	83.1	33.3	222.1	37.8
(i)	0.7	1.09	3	53.6	98	38.3	261.9	35
(i)	0.7	1.12	3	63.4	98	38.2	261.9	35.4
(i)	0.7	1.09	3	63.8	98	38.3	261.7	35
(i)	0.7	1.09	3	65.5	97.9	38.3	261.6	34.9
(i)	0.7	1.15	3	54.5	98.1	38	262.2	35.8
(i)	0.7	1.19	3	61.1	98.2	37.9	262.4	36.3
(i)	0.7	1.09	3	80.2	98	38.3	256.1	35
(i)	0.7	1.09	3	84.6	97.9	38.3	261.5	35
(i)	0.7	1.12	3	67.8	98	38.2	261.9	35.3

Setup	Residence time (min)	iBCl equivalents.	Et_3N equivalents.	Temp (°C)	DEHiBA Yield wrt DiEHA (%)	Reaction mass efficiency (%)	Space-Time Yield ($g\ L^{-1}\ h^{-1}$)	Cost of DEHiBA (£ mol^{-1})
(i)	0.7	1.18	3	77.4	98.1	37.9	262.1	36.3
(i)	0.7	1.18	3	89.2	98.3	38	262.5	36.2
(i)	0.7	1.13	3	109.9	98	38.1	261.8	35.6
(i)	0.5	1.23	3	65.6	98.3	37.7	367.9	37
(i)	0.5	1.14	3	67.9	98.3	38.2	367.9	35.5
(i)	1.8	1.15	3	92.4	98.2	38.1	101.9	35.8
(i)	2	1.16	3	93.2	98.2	38.1	92.2	35.9
(i)	0.5	1.95	3	32.5	98.3	34.5	367.8	47.7
(i)	0.5	1.21	3	47.5	98	37.7	356.1	36.7
(i)	0.5	1.13	3	57.4	98.1	38.1	348.2	35.5
(i)	0.6	1.55	3	62.2	98	36	329	42
(i)	0.5	1.62	3	44	98.1	35.8	367.1	42.9
(i)	0.5	1.59	3	44	98.2	36	367.2	42.4
(i)	0.5	1.14	3	101.9	98.1	38.1	367.2	35.6
(i)	0.5	1.1	3	104.2	98.4	38.4	368	34.9
(i)	0.5	1.36	3	119.1	98.2	37	367.5	39
(i)	0.5	1.27	3	127.6	97.8	37.3	366	37.8
(iii)	2.1	0.98	0.98	46.6	70.8	49.6	64	46.1
(iii)	6.4	1.49	1.49	67.6	68.2	38.5	19.9	58.9
(iii)	3.3	1.94	1.94	81.5	97.8	47.3	54.9	47.8
(iii)	6.7	1.24	1.24	93.6	60.2	37.6	16.9	60.6
(iii)	4	1.58	1.58	106.8	92	50.4	42.5	45
(iii)	1.1	1.75	1.75	131.8	96.9	49.9	163.4	45.4
(iii)	5.4	1.32	1.32	133.8	77	46.5	26.8	48.9
(iii)	1.1	1.75	1.75	131.8	96.8	49.8	163.1	45.5
(iii)	3.3	1.94	1.94	81.5	97.1	47	54.6	48.2
(iii)	3.3	1.94	1.94	81.5	97.2	47	54.6	48.1
(iii)	1	1.88	1.88	65.2	97.3	47.9	174.5	47.2
(iii)	1.1	1.95	1.95	67.9	97	46.7	166.1	48.5
(iii)	1.4	1.9	1.9	68.9	96.9	47.5	130.2	47.6
(iii)	2.9	1.89	1.89	76.3	96.9	47.6	61.7	47.6
(iii)	0.9	1.45	1.45	123.8	97.1	55.8	209.2	40.7
(iii)	0.9	1.43	1.43	124.9	96.7	56	208.2	40.6
(iii)	2.3	2	2	140	96.9	46	77.3	49.2
(iii)	2	2	2	143	96.7	45.9	88.2	49.3
(iii)	0.5	1.18	1.18	131.4	97.3	62.3	348.8	36.5
(iii)	0.8	1.49	1.49	142.4	96.5	54.7	234.1	41.5
(iii)	0.8	1.52	1.52	144.9	97	54.2	215.1	41.8
(iii)	0.8	1.47	1.47	150	96.8	55.1	233.6	41.2
(iii)	0.5	0.99	0.99	100.8	92.6	64.4	329.6	35.5
(iii)	0.5	0.96	0.96	133.2	90.7	64.3	339.2	35.6
(iii)	0.5	1.27	1.27	145.7	96.2	59.3	354.9	38.4
(iii)	0.5	1.29	1.29	148.1	95.9	58.6	347.2	38.8
(iii)	0.5	1.22	1.22	71.7	97	61.2	350.8	37.2

Setup	Residence time (min)	iBCl equivalents.	Et_3N equivalents.	Temp (°C)	DEHiBA Yield wrt DiEHA (%)	Reaction mass efficiency (%)	Space-Time Yield (g L^{-1} h^{-1})	Cost of DEHiBA (£ mol^{-1})
(iii)	0.5	1.26	1.26	83	96.7	59.9	348	38
(iii)	0.5	1.15	1.15	87.5	96.6	62.6	350.5	36.4
(iii)	0.5	1.44	1.44	107.1	96.4	55.6	355.5	40.8
(iii)	0.5	0.95	0.95	144.7	89.5	63.6	327	36
(iii)	0.5	0.95	0.95	150	89	63.2	325.6	36.2
(iii)	0.5	0.99	0.99	150	89.8	62.5	328.4	36.6
(iii)	0.5	1	1	150	90.9	62.9	333.7	36.3
(iii)	0.7	1.06	1.06	65.8	92.9	62.6	262.4	36.4
(iii)	0.5	1.17	1.17	150	96.1	61.9	349.6	36.8
(iii)	0.5	0.99	0.99	35	86.1	60.1	322.1	38
(iii)	0.5	2	2	62	96.5	45.8	360.6	49.4
(iii)	0.5	1.13	1.13	118	96.8	63.3	362	36
(iii)	0.5	1.98	1.98	135.1	97	46.3	362.6	48.8
(iii)	0.6	1.26	1.26	53.1	96.3	59.5	312.3	38.3
(iii)	0.6	1.23	1.23	55.4	96.7	60.7	313.9	37.5
(iii)	0.6	1.09	1.09	84.9	96.2	64.2	313.7	35.5
(iii)	0.5	1.05	1.05	87.8	95.1	64.4	355.5	35.4
(iii)	0.5	1.5	1.5	94.1	96.7	54.5	344.3	41.7
(iii)	0.5	1.64	1.64	98.5	96.4	51.7	351	43.9
(iii)	0.5	1.05	1.05	106.2	95.1	64.5	355.4	35.4
(iii)	0.5	1.25	1.25	124.7	94.9	58.9	354.8	38.6
(iii)	0.5	1.25	1.25	51.3	97	60.4	362.5	37.7
(iii)	0.5	1.2	1.2	59.3	96	60.8	358.8	37.5
(iii)	0.5	1.14	1.14	130.5	94.4	61.5	353	37.1
(iii)	0.5	1.12	1.12	130.5	96.2	63.2	359.5	36.1
(iii)	0.5	1.18	1.18	74.7	96.2	61.5	359.6	37.1
(iii)	0.5	1.77	1.77	84	96.6	49.5	361.3	45.8
(iii)	0.5	1.7	1.7	85	95.9	50.2	358.4	45.1
(iii)	0.5	1.89	1.89	99.5	95.6	47	357.5	48.1
(iii)	0.5	1.23	1.23	102.1	96.6	60.5	361	37.6
(iii)	0.5	1.21	1.21	102.7	96.1	60.8	359.3	37.5
(iii)	0.5	1.16	1.16	108	95.9	61.9	358.6	36.8
(iii)	0.5	1.14	1.14	108.2	95.9	62.6	358.4	36.4
(iii)	0.5	1.47	1.47	54.8	96.6	55	346.7	41.3
(iii)	0.5	1.37	1.37	62.5	96.3	57	346.8	39.9
(iii)	0.5	1.17	1.17	74.2	96	61.7	357.3	36.9
(iii)	0.5	1.32	1.32	120.7	96.2	58.1	359.5	39.2
(iii)	0.5	1.06	1.06	91.3	96.3	64.9	346.8	35.2
(iii)	0.6	0.97	0.97	150	96	67.6	298.5	33.8
(iii)	0.6	0.95	0.95	150	96.6	68.6	284.6	33.3
(iii)	0.6	0.96	0.96	150	96.9	68.5	290.4	33.4
(iii)	0.6	1.06	1.06	102.2	96.1	64.8	313.5	35.2
(iii)	0.5	1.34	1.34	134.9	90	53.9	308.8	42.2
(iii)	0.5	1.66	1.66	140.9	90.1	47.8	336.7	47.4

Setup	Residence time (min)	iBCl equivalents.	Et_3N equivalents.	Temp (°C)	DEHiBA Yield wrt DiEHA (%)	Reaction mass efficiency (%)	Space-Time Yield (g L^{-1} h^{-1})	Cost of DEHiBA (£ mol^{-1})
(iii)	0.5	1.41	1.41	141.5	90.1	52.4	311.3	43.4
(iii)	3.2	1.73	2.86	65	100	43.7	59.2	43.6
(iii)	0.5	1.01	1.28	70.6	94.4	61.4	336.3	35
(iii)	0.5	1.39	2.16	87.7	100	52.9	373.9	37.4
(iii)	1.3	1.23	2.01	109.1	99.7	53.9	145.9	36.4
(iii)	0.8	1.54	2.95	90.6	100	44.3	245.4	40.9
(iii)	0.6	1.9	3.55	115.3	99.6	38.6	324.1	46.4
(iii)	0.6	1.78	3.51	150	99.3	39.3	323.2	44.8
(iii)	0.6	1.92	3.59	150	99.5	38.3	324	46.7
(iii)	0.8	1.77	2.98	35.4	100	43	235.2	43.9
(iii)	0.8	1.92	3.23	48.3	99.1	40	240	46.9
(iii)	0.5	1.97	3.47	49	99	38.4	346.1	47.7
(iii)	0.5	1.94	3.49	66.1	99.7	38.8	362.1	46.9
(iii)	1.3	1.08	1.73	35	94.4	55.4	141.5	36.1
(iii)	0.8	1.34	2.42	36.9	99.1	49.1	249.4	38.2
(iii)	0.7	1.46	2.47	37.4	99.1	47.7	252.8	40
(iii)	0.8	1.75	2.98	40.8	99	42.3	249.3	44.5
(iii)	0.5	1.25	2.15	36.2	99.8	52.6	369.6	36.6
(iii)	0.6	1.33	2.28	89.3	98.9	50.2	333.3	38.2
(iii)	0.5	1.08	1.85	109.7	98.8	56.7	352	34.5
(iii)	1.1	1.27	2.09	116.8	100	53.1	173.6	36.8
(iii)	0.9	1.2	2.37	95.1	100	51.1	209.8	35.8
(iii)	1.3	1.94	3.53	113.6	99.1	38.3	139.7	47.2
(iii)	0.9	1.32	2.62	131.1	99.1	47.7	210.3	37.9
(iii)	0.7	1.41	2.54	149.8	99.8	47.9	261.8	39
(iii)	0.5	1.52	2.3	60.8	100	48.9	373.9	40.7
(iii)	0.5	1.51	2.29	62.1	99.1	48.7	373.9	40.9
(iii)	0.5	1.66	2.51	74.4	98.6	45.7	365.2	43.3
(iii)	0.5	1.51	2.29	90.3	99.4	48.8	373.9	40.8
(iii)	0.6	1.96	3.35	121.1	99.5	39.3	329.5	47.3
(iii)	0.5	1.97	3.39	149.2	99.8	39.1	349	47.3
(iii)	0.5	1.98	3.41	150	99.3	38.8	347.2	47.7
(iii)	0.6	1.98	3.43	150	99.3	38.7	340.8	47.7
(iii)	1	1.21	2.05	42	100	54.3	186.4	35.7
(iii)	0.5	1.54	2.39	56.7	99.3	47.7	360.5	41.2
(iii)	0.6	1.38	2.42	69.1	99	48.7	339.9	38.8
(iii)	0.5	1.37	2.08	96.4	99.2	51.7	353.2	38.7
(iii)	0.9	1.34	2.34	100.5	100	51.1	206.7	37.2
(iii)	0.6	1.77	2.25	128.1	99.5	47.1	298.3	44.5
(iii)	0.6	1.95	2.5	132.1	99.7	44.3	294.2	47.1
(iii)	1.7	1.88	2.48	37	100	45	108.7	45.8
(iii)	1.7	1.88	2.48	45.3	99.3	44.6	107.7	46.2
(iii)	4.8	1.61	2.89	49	99.5	43.9	39.2	42.2
(iii)	3.3	1.25	1.26	65.5	89.5	55.6	50.9	40.9

Setup	Residence time (min)	iBCl equivalents.	Et_3N equivalents.	Temp (°C)	DEHiBA Yield wrt DiEHA (%)	Reaction mass efficiency (%)	Space-Time Yield (g L^{-1} h^{-1})	Cost of DEHiBA (£ mol^{-1})
(iii)	3.7	1.2	1.89	79.7	100	55.6	51.2	35.9
(iii)	4.5	1.79	3.44	87.9	99.2	39.6	41.8	45
(iii)	2.7	1.41	2.39	105.5	100	49.3	71.1	38.9
(iii)	2.3	1.01	1.51	114.9	95.6	59.3	79.9	34.6
(iii)	0.9	1.44	1.65	136.8	100	55.6	214.9	39.3
(iii)	1	1.74	2.46	142.1	99.5	45.9	185.9	44.1
(iii)	1	1.74	2.46	142.1	99.8	46	186.6	44
(iii)	2.3	1.01	1.51	114.9	90.2	55.9	75.3	36.7
(iii)	4.5	1.79	3.44	87.9	99.6	39.8	42	44.8
(iii)	1.1	1.03	1.41	71.4	93.4	58.9	163.2	35.7
(iii)	1.5	1.03	1.41	74.4	90.5	57.1	114.6	36.9
(iii)	1.5	1.03	1.41	74.4	93.4	58.9	118.4	35.7
(iii)	0.5	0.94	1.75	49.8	93.3	52.5	329.5	36.6
(iii)	0.5	0.94	1.27	106.2	90.5	56.4	317.8	37.6
(iii)	0.5	0.94	1.27	113.5	89.8	55.9	318.3	38
(iii)	0.5	0.94	1.17	148.6	89.3	56.9	303	38.1
(iii)	0.5	1.19	1.25	103.6	99.7	62.8	373.9	35.8
(iii)	0.5	1.38	1.86	118.3	99.4	53.6	373.9	38.8
(iii)	0.5	1.29	1.72	136	99.8	56.2	373.9	37.3
(iii)	0.5	1.48	1.66	136.1	99.5	54.7	373.9	40.2
(iii)	0.5	1.19	1.37	56	99.9	61.4	373.9	35.8
(iii)	0.5	1.06	1.1	60.5	93.9	62.9	354.7	36
(iii)	0.5	1.09	1.19	70.4	98.4	64.1	371	34.9
(iii)	0.5	1.44	1.49	105.7	99.4	56.7	373.9	39.6
(iii)	0.5	1.19	1.15	35	100	64.8	373.9	35.5
(iii)	0.5	1.12	1.09	37.2	97.8	64.7	369.3	35.5
(iii)	0.5	1.12	1.08	45.6	97.1	64.3	366.7	35.7
(iii)	0.5	1.16	1.12	63.9	99.1	64.5	373.9	35.7
(iii)	0.5	1.13	1.17	43	99.1	64.2	373.9	35.2
(iii)	0.5	1.29	1.88	50.4	99.6	54.5	373.3	37.4
(iii)	0.5	1.26	1.31	64.9	99	60.7	370.6	37.1
(iii)	0.5	1.34	1.47	68.4	99.1	57.9	373.9	38.3
(iii)	0.5	1.15	1.09	69.9	97.7	64.2	369.1	36
(iii)	0.5	1.22	1.16	78.3	99.1	63.1	373.9	36.5
(iii)	0.5	1.73	2.07	96.9	99.3	48.8	373.9	43.9
(iii)	0.5	1.34	1.27	110.5	99.4	60.5	362.4	38.1
(iii)	0.5	1.29	1.33	48.5	100	60.6	373.9	37.3
(iii)	0.5	1.45	1.38	62.6	99	57.6	373.7	39.9
(iii)	0.5	1.43	1.36	63.7	99	58	373.8	39.7
(iii)	0.5	1.21	1.16	104.2	99.2	63.3	373.9	36.4
(iii)	0.5	1.21	1.29	35	100	62.3	373.9	35.9
(iii)	0.5	1.09	1.44	35.5	99.2	61.4	373.9	34.5
(iii)	0.5	1.18	1.18	64.7	99.2	63.5	373.9	35.9
(iii)	0.5	1.18	1.19	108.8	99.1	63.3	373.9	36

Setup	Residence time (min)	iBCl equivalents.	Et_3N equivalents.	Temp (°C)	DEHiBA Yield wrt DiEHA (%)	Reaction mass efficiency (%)	Space-Time Yield (g L^{-1} h^{-1})	Cost of DEHiBA (£ mol^{-1})
(iii)	0.5	1.2	1.14	35.8	99.5	63.8	373.9	36.1
(iii)	0.5	1.19	1.13	56.3	98.3	63.5	371.3	36.3
(iii)	0.5	1.23	1.86	57.2	99.8	55.5	373.9	36.4
(iii)	0.5	1.32	1.25	94.1	99.5	61	373.9	37.7
(iii)	0.5	1.43	1.37	35	100	59.1	373.9	38.9
(iii)	0.5	1.4	1.34	37	99.4	58.8	373.9	39.1
(iii)	0.5	1.4	1.35	37.1	99.1	58.6	373.9	39.1
(iii)	0.5	1.14	1.08	103	95.8	63.1	361.7	36.5
(iii)	0.5	1.28	1.4	53.1	99	59.3	373.7	37.5
(iii)	0.5	1.24	1.18	117.6	99.2	62.6	373.9	36.8
(iii)	0.3	0.95	1.82	38.4	88.5	49.6	589.5	38.3
(iii)	0.3	1.05	1.43	88.1	94.1	58.8	520.5	35.8
(iii)	0.3	0.94	1.42	88.8	92.4	55.8	491.9	36.9
(iii)	0.3	1.11	1.13	89.9	97.9	64.3	534.4	35.3
(iii)	0.2	1.21	1.21	101.8	99.3	62.8	937.8	36.2
(iii)	0.2	1.21	1.23	106.8	99.5	62.6	939.1	36.2
(iii)	0.3	1.21	1.22	110.5	99.4	62.7	548.3	36.2
(iii)	0.2	1.2	1.2	119.1	98.9	62.8	934	36.2
(iii)	0.2	1.35	1.29	125.6	100.2	60.5	945.8	38.1
(iii)	0.2	1.74	1.66	125.7	99.2	52	935	44.2
(iii)	0.2	1.53	1.47	127.1	99.2	55.9	936.8	41.1
(iii)	0.2	1.09	1.07	150	94.6	63.2	892.7	36.2
(iii)	0.2	1.12	1.08	70.9	98.8	65.6	933	35.1
(iii)	0.2	1.15	1.14	89.9	99.3	64.6	937.6	35.3
(iii)	0.2	1.24	1.18	123.9	100.1	63.2	944.9	36.5
(iii)	0.2	1.14	1.11	128.4	99.6	65.2	939.9	35.2
(iii)	0.2	1.04	1.03	49.6	94.3	64.4	889.9	35.5
(iii)	0.2	1.03	1	54.4	92.6	63.8	874.3	36.1
(iii)	0.2	0.94	0.96	95.6	91.2	61	809.9	37.4
(iii)	0.2	0.97	0.97	96.1	88.8	60.7	814.6	37.7
(iii)	0.3	1.02	0.97	38.5	94.7	65.7	532.4	35.1
(iii)	0.8	1.05	1	58.2	92.5	63.4	211.6	36.4
(iii)	0.6	1.04	0.99	63.1	90.7	62.5	272.1	37
(iii)	0.2	1.05	1.01	94.8	93.4	63.8	881.4	36.1
(iii)	0.2	1.13	1.07	35	99.1	65.7	915.4	35.1
(iii)	0.2	1.29	1.23	70.4	100	61.9	943.9	37.2

Route (b) Coupling Reagent Approach: EDC.HCl Mediated Synthesis

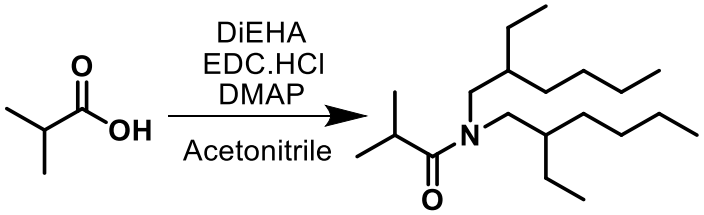

Scheme S9: Amide bond formation using 1-ethyl-3-(3-dimethylaminopropyl)carbodiimide hydrochloride (EDC.HCl) and catalytic amounts of 4-dimethylaminopyridine (DMAP) to couple isobutyric acid (iBA) and Di(2-ethylhexyl)amine (DiEHA), yielding *N,N*-di-(2-ethylhexyl)isobutyramide (DEHiBA)

Batch Chemistry:

Batch studies were initially conducted to ensure homogeneity and product formation via this route. Whilst later batch experiments were employed for kinetic understanding. Water and a range of common organic solvents including methanol, ethanol, tetrahydrofuran, *N,N*-dimethylformamide, dichloromethane, toluene, hexane, ethyl acetate, acetone, acetonitrile, and diethyl ether were screened to ensure the solubility of reagents. Acetonitrile, water, methanol, ethanol, *N,N*-dimethylformamide and chloroform were the only reagents to solubilise EDC.HCl, thus the only suitable solvents to transition this route into flow hence these were trialled in batch first.

Di-(2-ethylhexyl)amine (0.2976 g, 1.22 mmol) and isobutyric acid (0.1157 g, 1.30 mmol) were combined in a round bottom flask, note the exotherm of this combination. EDC.HCl (0.2769 g, 1.43 mmol) and DMAP (0.0079 g, 0.07 mmol) were then combined with solvent (see above) in a 10 mL volumetric flask. Once the di-2-ethylhexylamine and iBA solution had cooled to room temperature the EDC.HCl solution was charged, the reaction was stirred at 30 °C for repeatability over 24 hours to yield a colourless and homogenous solution. HPLC analysis confirmed yields of

96.3%, 99.9%, 55.5%, 9.0%, 2.1%, and 0% for acetonitrile, dichloromethane, *N,N*-dimethylformamide, ethanol, methanol and water respectively.

Although dichloromethane was best yielding the environmental impact of this solvent and the low boiling point causing cavitation in the HPLC pumps as well as a restrictive temperature range meant that acetonitrile was best suited for this reaction in flow.

Studies without DMAP saw a reduction in yield for reactions in acetonitrile to 45.8%. Replacement with DIPEA resulted in yields between 31.4-23.3% with varying equivalents from 0.5 to 1.5.

Kinetic studies were investigated using a recirculating batch reactor where the solution was pumped through a vici sample loop connected to a HPLC for online analysis. As described in section 2.4.3. A similar methodology was used to the one above however temperature was varied and concentration, but equivalents were maintained.

Continuous Flow Chemistry:

Reservoir solutions were prepared to the desired concentrations by dissolving the described reagents in solvent with stirring at ambient conditions, except for EDC.HCl, that was heated to 30 °C until dissolution and maintained at this temperature throughout the optimisation.

Reservoir 1: Di(2-ethylhexyl)amine (8.0554 g, 0.0334mol, 0.1334 mol dm^{-3}), isobutyric acid (2.0568 g, 0.0233 mol, 0.0934 mol dm^{-3}), 4-diaminopyridine (0.2049 g, 0.0017 mol, 0.0067 mol dm^{-3}), and biphenyl (0.7722 g, 0.0050 mol, 0.0200 mol dm^{-3}) in acetonitrile (250 mL).

Reservoir 2: 1-ethyl-3-(3-dimethylaminopropyl)carbodiimide hydrochloride (7.0320 g, 0.0367 mol, 0.1467 mol dm^{-3}) in acetonitrile (250 mL).

Reservoir 3: Isobutyric acid (2.8705 g, 0.0326 mol, 0.1303 mol dm^{-3}) in acetonitrile (250 mL).

Reservoir 4: Acetonitrile.

An example HPLC chromatogram is illustrated in Figure S6:

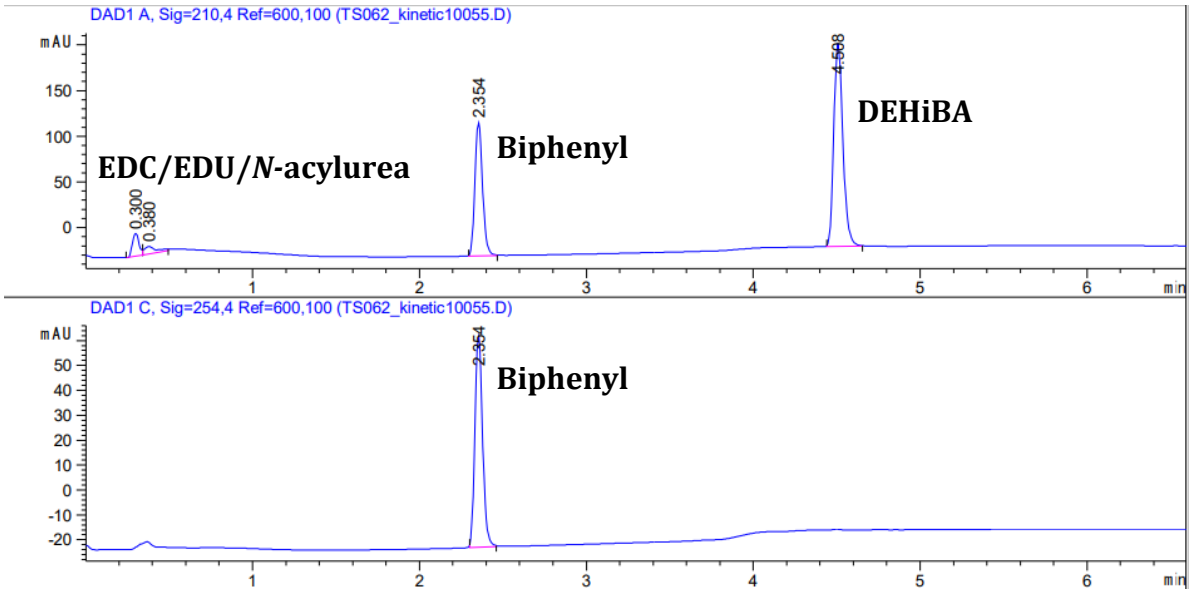

Figure S53: An example HPLC chromatogram from route (b)

The flow platform was set up according to **Figure 28** using a reactor volume of 2.7 mL with PFA tubing and a back pressure of 100 psi. The self-optimisation was conducted with respect to four continuous parameters: residence time, iBA equivalents, EDC.HCl equivalents and temperature. The upper and lower parameter bounds for each are described in Table S5. The initial objective for each optimisation was to maximise yield, then simultaneously maximize reaction mass efficiency and space-time yield.

Table S18: The upper and lower bounds for the variables optimised in route (b)

	Residence time (mins)	iBA equivalents.	EDC.HCl equivalents.	Temperature (°C)	[DiEHA] in reactor (mol dm^{-3})
Lower bound	0.5	1.7	1.5	40	0.01
Upper bound	4	5.2	5	170	0.01

Route (b) Data and Further Analysis

Kinetic studies were conducted in batch making use of online sampling for reaction monitoring. Clear concentration and temperature trends are identifiable in Figure S11, all studies were conducted at 30 °C with 1.15 equivalents of EDC and 1.1 equivalents of iBA respective to DiEHA.

The increase in by-product formation has not been directly quantified due to complications with the co-elution of N-acylurea with other signals in both HPLC and GC for a range of methods.

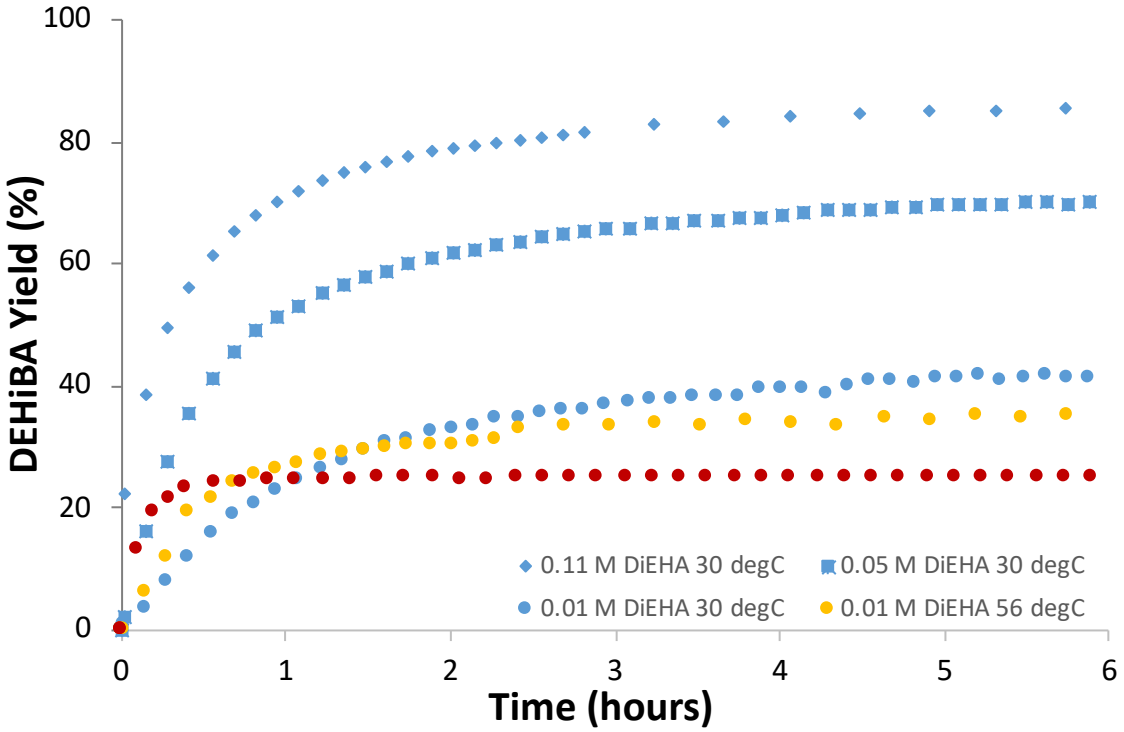

Figure S54: Kinetic studies for route (b) in batch at 30 °C with online sampling to a HPLC with 1.15 equivalents of EDC and 1.1 equivalents of iBA respective to DiEHA

The proposed reaction pathways that route (b) can take, discounting the inclusion of DMAP from the reaction can be found in Scheme S3.

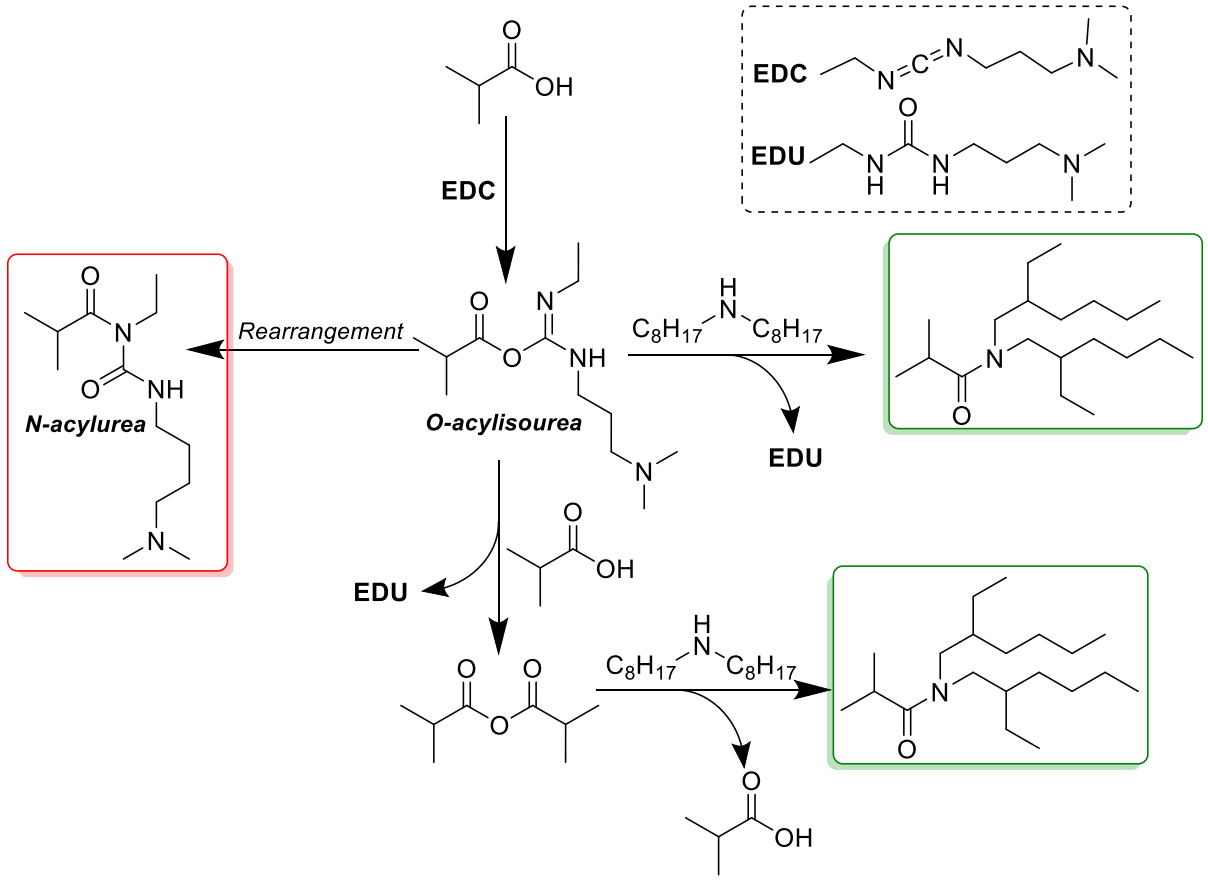

Scheme S10: The proposed reaction pathways feasible for route (b), discounting DMAP

GC-FID trace demonstrating the coelution of DiEHA and the *N*-acylurea by-product from 7.8-8 minute retention time, whilst DEHiBA and biphenyl are sharp signals.

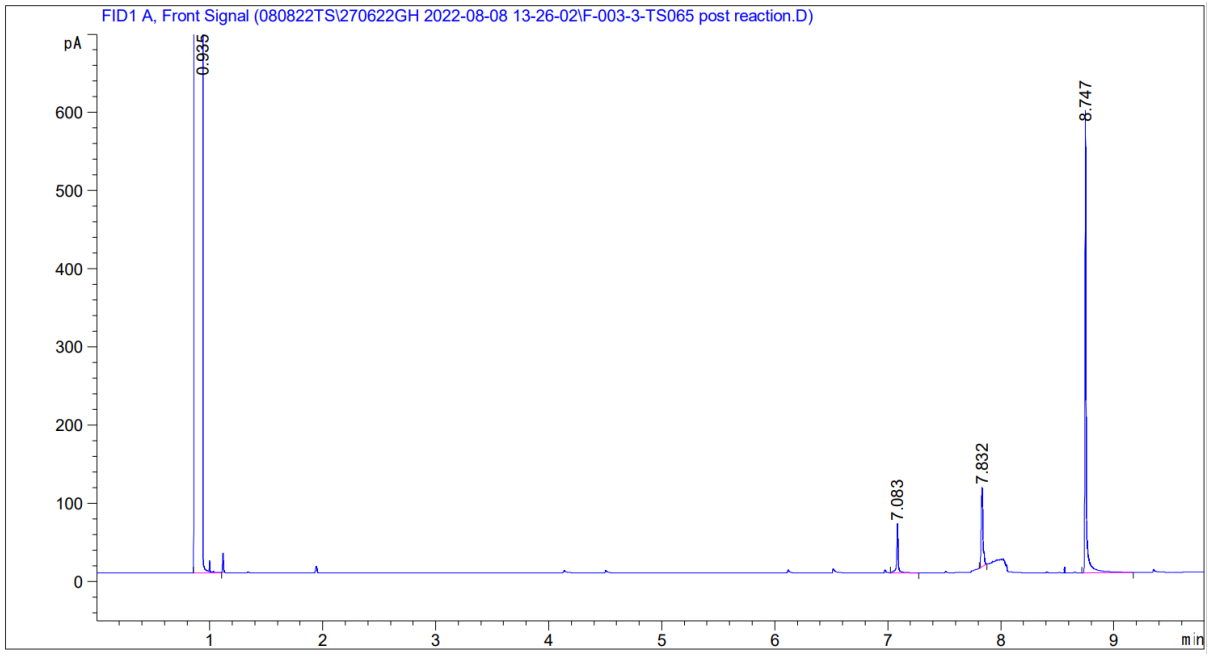

Figure S55: An example GC-FID trace of route (b) where biphenyl is observable at 7 minutes, DiEHA and N-acylurea coelute at 7.8-8 minutes and DEHiBA elutes at 8.7 minutes.

HPLC traces illustrating the overlap between EDC, EDU and the *N*-acylurea between 0.4 and 1.5 minutes. Biphenyl and DEHiBA are observable around 2.3 and 4.5-4.8 minutes respectively. Despite changes to the HPLC method these peaks were not resolved.

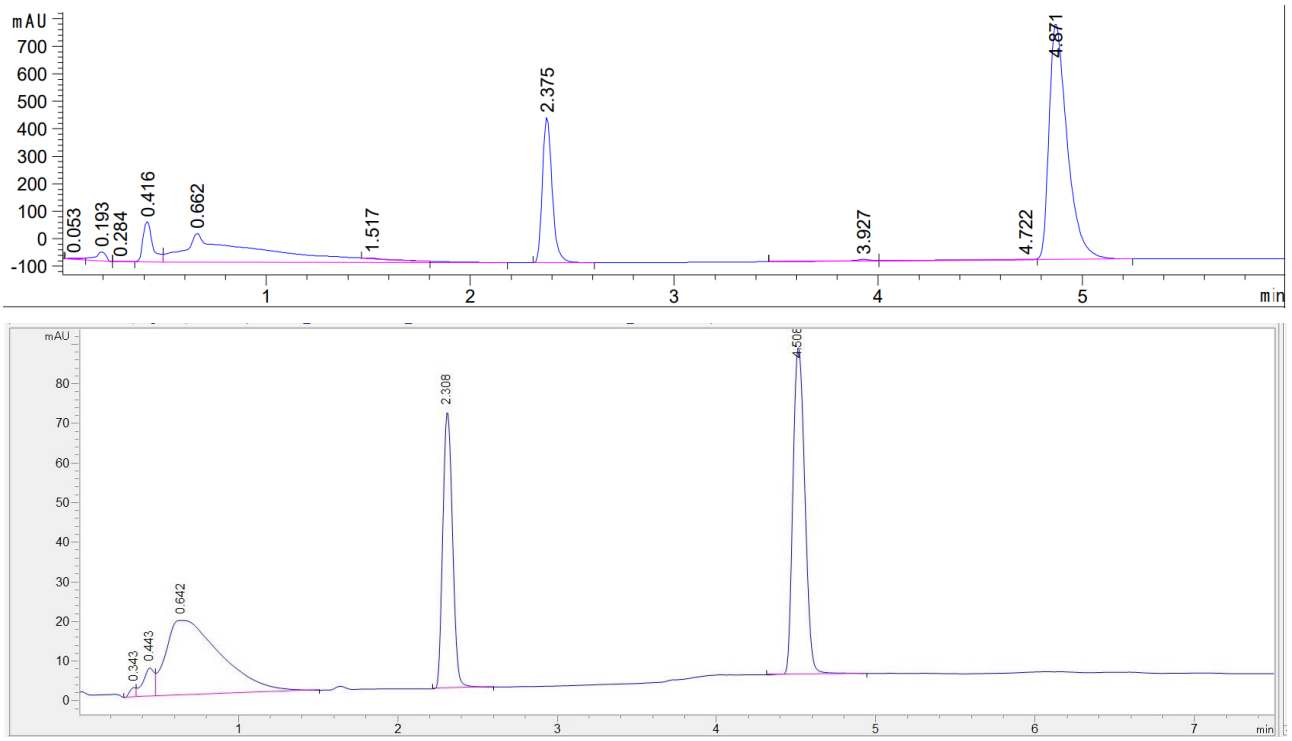

Figure S56: Typical HPLC traces for route (b) where EDC, EDU and the N-acylurea overlap between 0.4 and 1.5 minutes.

Table S6 provides the raw data for the experimental conditions exploited in the optimisation of route (b) and the performance metrics associated.

Table S19: complete dataset from the optimisation of route (b)

Residence time (min)	iBA equivalents.	EDC equivalents.	Temperature (°C)	DEHiBA Yield (%)	Reaction Mass Efficiency (%)	Space-Time Yield ($g\ L^{-1}\ h^{-1}$)	Cost of DEHiBA (£/mol)
1.9	3.72	2.31	100.1	13.4	4.1	12.1	568.9
3.4	3.24	3.89	135.3	97.4	23.8	47.6	117.2
1.7	1.85	1.63	152.4	64.1	27.7	64.6	92.3
2.6	3.57	4.13	169.8	98.7	22.8	62.9	121.7
1.8	1.74	2.83	100.3	24.8	8.2	23.5	355.1
3	2.96	1.66	126.4	49.6	18.8	27.8	122.2
1.7	5.02	2.99	152.1	95.7	23.7	92.2	97.9
1.3	2.58	1.66	170	75.6	29.9	98.2	79.7
3.5	5.11	5	113	98	18.5	47.1	144.7
1.5	1.93	2.3	119	45.1	16.4	50.6	166.9
2.1	4.5	4.1	139	97.1	21.3	77.9	123.4
4	5.21	4.5	161	99.2	19.8	41.8	130.7
3.9	2.96	1.9	107	40.4	14.5	17.4	164
3.5	1.93	3	133	89.2	28.1	42.9	103.2
3.3	2.65	1.5	146	60.4	24.6	30.8	93.5
2	1.83	2.9	158	89.2	28.9	75.1	100.4
2.3	4.29	3.3	107	54.2	13.5	39.7	185.4
4	5.32	1.5	136	44.7	14	18.8	130
4	4.91	5	136	98.7	18.9	41.5	143.6
4	1.73	4	147	84.4	22.6	35.5	137.2
3	1.73	4	158	85.3	22.8	47.9	135.8
3.8	1.73	2.4	139	82.8	30.1	36.7	93.6
1	1.73	4	147	72	19.3	121.2	160.9
2.1	1.73	5	147	82.7	19	66.3	169.2
1.6	4.91	4.6	155	98.6	19.8	103.8	133.9
4	1.73	4	126	79.6	21.3	33.5	145.6
2.4	4.5	2.2	133	60.2	17.7	42.2	123.5
3	5.32	4.5	139	98.6	19.6	55.3	131.8
2.7	5.32	5	148	99.5	18.6	62.1	142.6
3.2	4.8	2.4	104	39.2	10.9	20.6	202.2
2.8	1.73	4	140	84.7	22.7	50.9	136.8
3.1	5.32	4.3	147	99.8	20.3	54.2	125.4
3	1.73	1.9	153	84.8	34.7	47.6	77.3
1.6	4.91	4.6	126	99.8	20	105	132.4
4	5.32	2.9	151	96	23.7	40.4	95.4
3.6	5.32	3.3	152	98.2	22.9	45.9	103
2.8	4.6	3.5	155	99.3	23.5	59.7	106.3
2.5	5.32	5	143	98.8	18.5	66.5	143.7
4	5.32	2.9	144	92.7	22.9	39	98.8
3.6	5.32	3.3	146	96.1	22.4	44.9	105.3
1.6	1.73	3.1	147	81	25.5	85.2	116.4

Residence time (min)	iBA equivalents.	EDC equivalents.	Temperature (°C)	DEHiBA Yield (%)	Reaction Mass Efficiency (%)	Space-Time Yield (g L^{-1} h^{-1})	Cost of DEHiBA (£/mol)
1.4	4.5	2.2	161	75.1	22.1	90.3	99
4	5.32	4.7	149	99.1	19.2	41.7	135.9
4	5.32	4.3	151	99.9	20.3	42.1	125.2
4	5.32	3.4	154	99	22.7	41.7	104.6
1.5	2.96	4	164	96.9	23.8	108.7	120.3
3.5	5.32	4.9	146	99.7	18.9	48	139.9
3.7	1.73	3.4	148	85.4	25.4	38.8	118.9
2.8	2.55	2.2	149	95	33.3	57.1	77.1
2	3.47	3.1	156	97.9	26.7	82.4	97.3
1.7	4.91	2.9	123	54.1	13.7	53.6	168.9
4	3.67	3.8	145	98.1	23.6	41.3	114.3
4	1.73	3.3	149	87	26.3	36.6	113.9
3.7	1.73	3.3	151	85.6	25.9	38.9	115.8
1.7	4.8	2.4	104	26.3	7.3	26.1	301.2
3.1	1.73	2.4	151	81.1	29.5	44	95.6
2.7	2.14	2.5	151	96.2	32.9	60	83.3
3.1	1.73	3.2	153	89.4	27.6	48.5	108.2
3.4	2.34	3.5	104	63.4	17.6	31.4	164.5
2.1	2.03	3.1	150	93.1	28.5	74.7	101.4
3.8	1.93	3.9	153	90.9	24.3	40.2	125
2.8	2.96	2.8	153	98	29.4	58.9	89.6
1.4	5.01	1.5	154	38.7	12.5	46.5	149.5
3.5	4.58	4.57	80.4	29.9	6.1	16	439.5
1.5	4.86	2.62	86.2	14.4	3.8	18.4	587.8
3.8	3.91	4.26	88.5	41.8	9.3	20.3	295.1
2.7	2.61	1.54	98.6	18	7.3	12.5	319.8
3	2.44	3.53	107.2	62.8	17.2	39.4	167.3
3.6	4.54	4.73	112.2	96.5	19.3	50.2	139.9
2.2	3.16	3.94	122.9	91.8	22.3	78.8	125.7
1.9	1.78	3.25	128.7	75.3	22.8	75.5	130.1
0.8	3.29	2.02	142	48.9	16.4	114.4	142.2
0.9	4.38	2.92	145.2	81.8	21.3	171.2	112.1
1.3	1.93	1.79	146.9	68.5	28	97.6	92.1
0.6	1.98	1.63	149.3	46.3	19.6	135.6	128
0.5	1.85	1.52	149.4	38.8	17.3	145.3	145.4
0.7	2.49	1.59	150	44.9	18.1	126.2	130.5
1.1	2.63	2.4	131.5	52.7	17.5	85.9	148.2
1.2	3.21	3.01	141.2	92.2	25.9	149.7	100.9
1.2	3.56	3.21	141.8	94.1	24.9	150.4	104.1
1	3.16	3.08	143.7	93.8	26.2	167.8	100.8
0.8	1.84	4.22	137.3	69.1	17.6	161.3	175.7
0.8	1.7	4.21	137.5	65.8	17	150.6	183.9
3.6	4.4	3.27	149.2	97.9	24.2	50.7	102

Residence time (min)	iBA equivalents.	EDC equivalents.	Temperature (°C)	DEHiBA Yield (%)	Reaction Mass Efficiency (%)	Space-Time Yield (g L^{-1} h^{-1})	Cost of DEHiBA (£/mol)
3.6	4.09	3.8	149.4	98.6	23	51.4	114.1
1.5	4.67	4.6	143.5	98.6	19.9	124.3	133.9
1.4	2.82	4.03	144.1	97.2	23.8	127.9	120.8
1.4	2.79	4.03	144.1	96.7	23.8	129.9	121.3
1.1	5.21	3.43	147.4	63.9	14.6	112.2	163.5
3.3	2.16	3.07	124.4	87.5	26.6	49.6	107.2
1.2	1.7	4.71	140.7	74.6	17.9	118.5	178.2
1.2	1.7	4.69	141	75.2	18.1	119.1	176.2
1.2	1.78	4.63	141.4	78.2	18.9	118.9	167.6
3.6	3.77	2.56	136.7	81.4	23.7	42.7	101.6
0.6	2.2	3.78	142.6	73	19.5	219	152
0.7	1.84	2.74	146.1	67.5	22.5	175	127.3
0.7	2.64	4.9	150	91.2	20	240.1	151.4
1.4	2.51	2.99	141	92	27.5	120.6	100.4
0.7	2.27	3.56	144.2	76.5	21.1	215.8	138.4
1.2	2.25	3.37	145.6	90.5	25.8	138.3	111.9
1.5	3.61	2.43	146.6	78.6	23.7	96.3	101.1
2.5	1.75	4.88	142.1	85.6	19.9	63.1	160.2
1.2	2.25	2.95	142.2	84.2	25.9	135.4	108.2

Routes (c) and (d) Solvated Synthesis From iBAnhydride

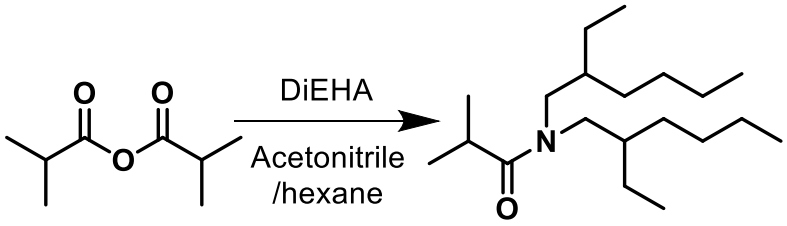

Scheme S11: Amide bond formations using isobutyric anhydride (iBAnhydride) and Di(2-ethylhexyl)amine (DiEHA) to yield N,N-di-(2-ethylhexyl)isobutyramide (DEHiBA) but with two different solvent systems, acetonitrile and hexane

Batch Chemistry:

No major solubility issues were encountered for iBAnhydride over a range of common organic solvents therefore batch reactions were trialled using tetrahydrofuran, toluene, hexane, ethyl acetate, acetone, acetonitrile, and diethyl ether via the following procedure:

DiEHA (0.0845 g, 0.35 mmol) was combined with solvent in a 5 mL volumetric flask, similarly iBAnhydride (0.0554 g, 0.35 mmol) was charged with the same solvent to a 5 mL volumetric flask. These solutions were combined in a 25 mL round bottom flask whereby a large temperature rise (not measured) saw most solutions reach boiling points and condensate formed on glassware. Yields were not recorded for these reactions and the chemistry was transitioned into continuous flow without further batch investigations.

Flow Chemistry

Reservoir solutions were prepared to the desired concentrations by dissolving the reagents in solvent with stirring at ambient conditions.

Route (c)

Reservoir 1: Di-(2-ethylhexyl)amine (4.2307 g, 0.0175 mol, 0.0701 mol dm^{-3}), and biphenyl (2.6969 g, 0.0175 mol, 0.0700 mol dm^{-3}) in acetonitrile (250 mL).

Reservoir 2: Isobutyric anhydride (2.7754 g, 0.0175 mol, 0.0702 mol dm^{-3}) in acetonitrile (250 mL).

Reservoir 3: Acetonitrile.

Route (d)

Reservoir 1: Di(2-ethylhexyl)amine (10.8706 g, 0.0450 mol, 0.0900 mol dm^{-3}), and biphenyl (5.4092 g, 0.0351 mol, 0.0702 mol dm^{-3}) in acetonitrile (500 mL).

Reservoir 2: Isobutyric anhydride (7.1190 g, 0.0450 mol, 0.0900 mol dm^{-3}) in acetonitrile (500 mL).

Reservoir 3: Acetonitrile.

An example HPLC chromatogram is illustrated in Figure S14:

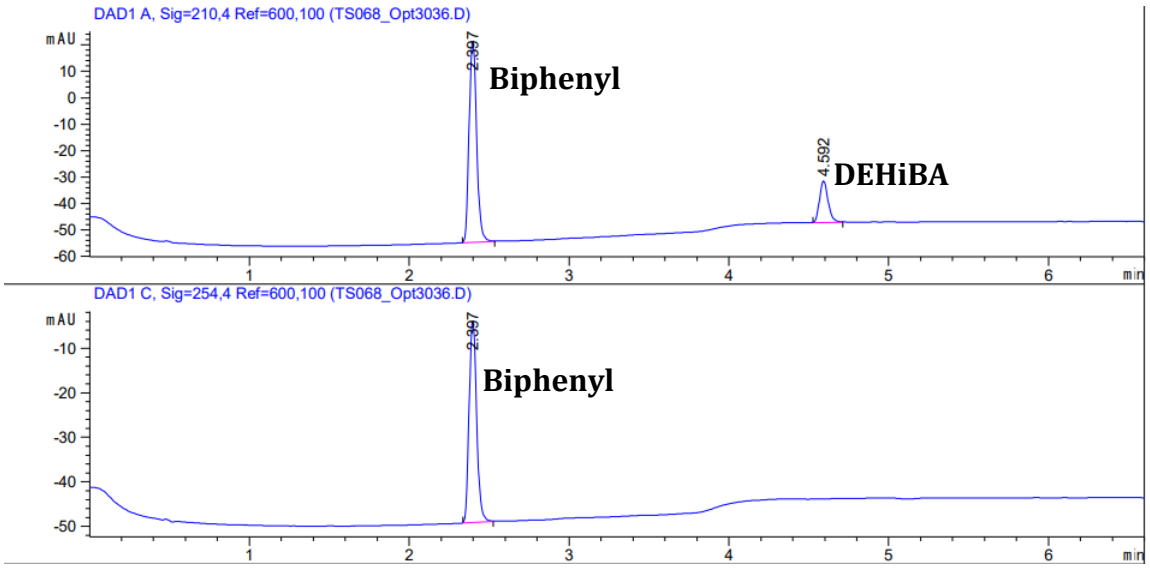

Figure S57: An example HPLC chromatogram from route (c/d)

The flow platform was set up according to **Figure 28** using a reactor volume of 2.7 mL with PFA tubing and a back pressure of 100 psi. The self-optimisation was conducted with respect to three continuous parameters: residence time, iBAnhydride equivalents, and temperature. The upper and lower parameter bounds for each are described in Table S7. The initial objective for each optimisation was to maximise yield, then simultaneously maximize reaction mass efficiency and space-time yield.

Table S20: The upper and lower bounds for the variables optimised in route (c) and (d), top and bottom table respectively

Route (c)	Residence time (mins)	iBAnhydride equivalents.	Temperature (°C)	[DiEHA] in reactor (mol dm^{-3})
Lower bound	0.5	1	40	0.01
Upper bound	7.5	5	150	0.01

Route (d)	Residence time (mins)	iBAnhydride equivalents.	Temperature (°C)	[DiEHA] in reactor (mol dm^{-3})
Lower bound	0.5	1	40	0.01
Upper bound	7.5	3	150	0.01

Routes (c-d) Data and Further Analysis

A comparison between the performance metrics, RME and STY demonstrates the improved performance of the reaction in acetonitrile over that of the reaction in hexane although similar trade-off curves are apparent.

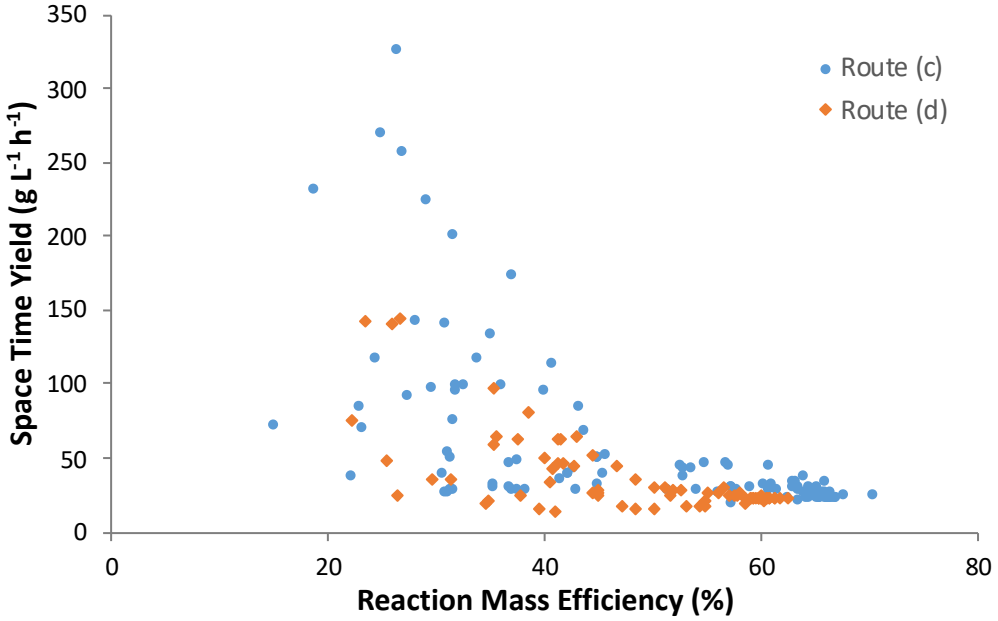

Figure S58: RME, STY comparison between routes (c) and (d)

Table S8 provides the raw data for the experimental conditions exploited in both optimisations and the performance metrics associated.

Table S21: complete dataset from the optimisation of routes (c) and (d)

Route	Residence time (min)	iBAnhydride equivalents.	Temperature (°C)	DEHiBA Yield (%)	Reaction Mass Efficiency (%)	Space-Time Yield (g L^{-1} h^{-1})	Cost of DEHiBA (£/mol)
(c)	0.5	1	40	18.5	15.1	72.4	121.3
(c)	0.5	5	40	58.8	18.6	230.7	72.5
(c)	7	1	40	70.1	57.3	19.6	31.9
(c)	7	5	40	98.4	31.2	27.6	43.3
(c)	3.8	3	95	98.3	44.9	50.7	33.1
(c)	3.8	3	95	100	45.6	51.6	32.5
(c)	3.8	3	95	98.2	44.8	50.7	33.1
(c)	0.5	1	150	29.8	24.4	116.9	75.1
(c)	0.5	5	150	83.2	26.3	326.2	51.2
(c)	7	1	150	80.6	65.9	22.6	27.8
(c)	7	5	150	97.5	30.9	27.3	43.7
(c)	6.7	3.2	54.5	98	42.8	28.7	34.2
(c)	0.9	1.6	67.5	44.6	29.5	97.2	57
(c)	1	1.4	109.5	50.9	35.9	99.8	48
(c)	7	4.9	122.5	96.3	31	27	43.7
(c)	6.3	4.2	81	97.8	35.3	30.4	39.4
(c)	6.9	2.2	103.5	97.3	54	27.7	29.2
(c)	0.9	2.9	135	79.4	37.1	173.1	40.3

Route	Residence time (min)	iBAnhydride equivalents.	Temperature (°C)	DEHiBA Yield (%)	Reaction Mass Efficiency (%)	Space-Time Yield (g L^{-1} h^{-1})	Cost of DEHiBA (£/mol)
(c)	6.4	4	141	98.2	36.7	30.1	38.2
(c)	0.8	1	48	28.3	23.1	69.3	79.2
(c)	6.2	1.9	73.5	94.7	57.1	30	28.4
(c)	1.7	1.3	87	59.8	43.7	69	40
(c)	0.8	1.4	127	47.8	33.8	117.3	51
(c)	6	4.2	62.5	97.7	35.3	31.9	39.5
(c)	0.8	1.3	78	37.5	27.4	92	63.7
(c)	0.5	3.5	117.5	65.4	26.9	256.7	53.5
(c)	6.9	4.9	133	98.1	31.5	27.9	43
(c)	6.7	1.9	46	92.7	55.9	27.1	29.1
(c)	0.7	1.2	59.5	30.1	22.8	84.2	77.8
(c)	6.8	3.8	114	96.7	37.5	27.9	37.8
(c)	0.9	4.5	143.5	91.8	31.5	200	43.7
(c)	1.2	4.9	55	87.7	28.2	143.3	48
(c)	1.2	4.3	72	86.5	30.7	141.3	45.2
(c)	6.6	3.9	88	97.3	37	28.9	38.1
(c)	0.5	4.2	101	68.7	24.8	269.5	56.1
(c)	2.5	4.7	45	95	31.5	74.5	43.2
(c)	6.8	3.8	109	98.3	38.1	28.3	37.2
(c)	6.4	2	128	97.8	57.3	30	28.1
(c)	5.2	1.2	145.5	87	66	32.8	26.9
(c)	6.9	2.4	68	97.5	51.3	27.7	30.2
(c)	1.9	4.7	83	95.4	31.7	98.5	43.1
(c)	1.3	3.7	91	88.3	34.9	133.2	40.8
(c)	1.9	4.6	122	96.1	32.4	99.2	42.2
(c)	4.8	5	50	96.6	30.6	39.5	44.1
(c)	3.9	5	128.5	98.7	31.3	49.6	43.2
(c)	5.4	3.4	134.5	98.5	41.3	35.8	35
(c)	3.6	5	150	98.4	31.1	53.6	43.3
(c)	7	1	80.5	79.8	65.3	22.4	28
(c)	7	1	123	79.6	65.1	22.3	28.1
(c)	4.1	2	130.5	96.7	56.6	46.2	28.4
(c)	5.9	1	134.5	79.1	64.7	26.3	28.3
(c)	4.4	2.2	67.5	95.3	52.8	42.5	29.9
(c)	7	1	75.5	79.9	65.4	22.4	28
(c)	6.1	1	119	80.6	65.9	25.9	27.8
(c)	7	1	127.5	86.1	70.4	24.1	26
(c)	3.7	2.9	54	95.9	44.8	50.8	33.4
(c)	0.8	1	120.5	38.9	31.8	95.3	57.6
(c)	3.6	1.5	115	78.3	53.4	42.6	31.8
(c)	6.3	1	128.5	76.2	62.3	23.7	29.4
(c)	7	1	131	77.5	63.4	21.7	28.9
(c)	5.1	1	111	75.2	61.5	28.9	29.8

Route	Residence time (min)	iBAnhydride equivalents.	Temperature (°C)	DEHiBA Yield (%)	Reaction Mass Efficiency (%)	Space-Time Yield (g L^{-1} h^{-1})	Cost of DEHiBA (£/mol)
(c)	7	1	126.5	80.8	66.1	22.6	27.7
(c)	4.2	4	142.5	98.4	36.8	46	38.2
(c)	5.3	1	146.5	79.7	65.2	29.5	28.1
(c)	0.8	5	128.5	91.4	28.9	224.1	46.6
(c)	7	1	130	81.8	66.9	22.9	27.4
(c)	2	3.5	142.5	97.2	39.9	95.3	36.1
(c)	7	1	144	81.7	66.8	22.9	27.4
(c)	2.2	3	100	94.2	43	84	34.5
(c)	7	1	128.5	80.1	65.5	22.4	28
(c)	3.1	1	128.5	69.6	56.9	44	32.2
(c)	5.2	1	143.5	78.7	64.3	29.7	28.5
(c)	4.1	2.1	107	96	54.7	45.9	29.1
(c)	3.6	1.3	126	82.9	60.6	45.1	28.8
(c)	5.1	1	129	76.9	62.9	29.6	29.1
(c)	5.2	2.3	146	97.6	52.7	36.8	29.7
(c)	3.7	1.8	54	84.7	52.6	44.9	31.2
(c)	5.3	1	124.5	77.5	63.4	28.7	28.9
(c)	6.1	1.8	128	97.1	60.3	31.2	27.2
(c)	6.8	1	129	80.7	66	23.3	27.7
(c)	4.7	1.4	146	90.7	64	37.8	26.9
(c)	4.5	3.2	67.5	97.8	42.8	42.6	34.3
(c)	6.5	1.8	127	97.5	60.6	29.4	27.1
(c)	6.9	1	127	78.4	64.1	22.3	28.5
(c)	5.5	1.6	145	95.7	63.2	34.1	26.6
(c)	1.4	2.6	89	81.3	40.7	113.9	37.5
(c)	4.5	1	118.5	74.4	60.8	32.4	30.1
(c)	7	2	126	98.3	57.6	27.5	27.9
(c)	7	1.2	127.5	89.3	67.6	25	26.2
(c)	6	3	77	98	44.7	32	33.2
(c)	7	2	126.5	98.3	57.6	27.5	27.9
(c)	7	1.5	127.5	96	65.5	26.9	25.9
(c)	7	1	128	81.3	66.5	22.8	27.5
(c)	4.9	2.9	54	97.1	45.3	38.8	33
(c)	7	1	121	81.1	66.3	22.7	27.6
(c)	6.9	1.4	127	93.8	66.2	26.7	26
(c)	5.8	1	145	79.7	65.1	26.9	28.1
(c)	7	1	145.5	80.7	66	22.6	27.7
(c)	6.5	1	116.5	78.7	64.3	23.7	28.5
(c)	7	1.8	126.5	97.8	60.7	27.4	27
(c)	2.5	2.9	134.5	47.7	22.3	37.4	67.1
(c)	4.9	3.3	104	98.2	42	39.3	34.7
(c)	6.5	1.1	127.5	83.5	65.7	25.2	27.4
(c)	6.2	1.6	128.5	95.9	63.4	30.3	26.5

Route	Residence time (min)	iBAnhydride equivalents.	Temperature (°C)	DEHiBA Yield (%)	Reaction Mass Efficiency (%)	Space-Time Yield (g L^{-1} h^{-1})	Cost of DEHiBA (£/mol)
(c)	7	1	143	81.2	66.4	22.8	27.6
(c)	4.6	1	146.5	77	63	32.8	29.1
(c)	4	3.9	108	98.6	37.5	48.3	37.6
(c)	7	1	124	80.9	66.1	22.7	27.7
(c)	6.3	1.9	128	97.6	58.9	30.4	27.6
(c)	7	1	144.5	80.9	66.2	22.7	27.7
(c)	4.9	3.3	119	98.6	42.2	39.4	34.5
(c)	6.6	1.1	127.5	84.3	66.3	25.1	27.1
(c)	7	1.6	128	96.8	64	27.1	26.3
(d)	4.8	2.12	46.9	89.6	48.4	35.2	32.8
(d)	2.6	2.53	69.7	84.9	41.3	61.9	37.2
(d)	6.6	1.54	81.7	88.6	56.9	25.1	29.7
(d)	1.2	1.94	95.7	62	35.2	96.8	45.9
(d)	3.6	2.74	105.9	89.2	41.1	46.3	36.7
(d)	6	0.95	127	49.5	39.3	15.4	46.9
(d)	2.2	1.17	141.2	42.7	31.2	35.9	57.1
(d)	7	2.74	70	96.2	44.4	25.7	34
(d)	7	1.41	58.6	87.9	58.9	23.5	29.2
(d)	7	1.67	52.5	93.2	57.3	24.9	29
(d)	7	0.8	45	64.6	54.7	17.2	34.7
(d)	5.9	1.3	60.4	83.1	57.9	26.3	30.2
(d)	7	1.23	69.5	86.2	61.7	23	28.6
(d)	7	0.8	75.7	69.1	58.5	18.4	32.5
(d)	7	1.21	69.7	86.8	62.4	23.2	28.4
(d)	7	3	150	79.9	34.8	21.3	42.7
(d)	7	1.18	77.3	82.4	59.9	22	29.7
(d)	7	1.22	68.2	85.3	61.2	22.8	28.9
(d)	7	1.23	68.5	85.6	61.2	22.9	28.9
(d)	7	1.23	68.6	82.9	59.2	22.1	29.8
(d)	7	1.23	68.5	83.5	59.8	22.3	29.6
(d)	7	1.23	68.7	83.9	59.9	22.4	29.5
(d)	7	1.23	68.7	83.7	59.9	22.3	29.5
(d)	7	1.23	68.8	83.5	59.7	22.3	29.6
(d)	7	1.23	68.8	82.5	59	22	29.9
(d)	7	1.23	68.9	83.7	59.8	22.3	29.5
(d)	7	1.24	68.8	85.2	60.8	22.8	29
(d)	7	1.23	68.9	83.6	59.8	22.3	29.5
(d)	7	1.23	69	84.4	60.3	22.5	29.3
(d)	7	1.23	69	83.9	60	22.4	29.4
(d)	7	1.23	69.1	83.2	59.5	22.2	29.7
(d)	7	1.23	69.1	84.8	60.6	22.6	29.1
(d)	7	1.23	69.1	84.3	60.3	22.5	29.3
(d)	7	1.23	69.2	82.7	59.2	22.1	29.8

Route	Residence time (min)	iBAnhydride equivalents.	Temperature (°C)	DEHiBA Yield (%)	Reaction Mass Efficiency (%)	Space-Time Yield (g L^{-1} h^{-1})	Cost of DEHiBA (£/mol)
(d)	7	1.23	69.1	65.7	47	17.6	37.6
(d)	0.7	1.01	65.3	28.6	22.2	75.2	82.3
(d)	5.4	1.5	64.5	86.9	56.6	30.4	30.1
(d)	6.6	2.1	69	96.6	52.5	27.4	30.3
(d)	7	1.85	69.5	95.8	55.9	25.6	29.2
(d)	7	1.55	70	90.1	57.7	24.1	29.3
(d)	4.8	1.65	138.5	60.8	37.7	23.9	44.3
(d)	6.2	1.65	62.5	88.8	55.1	26.8	30.3
(d)	7	1.45	69	90.5	59.9	24.2	28.6
(d)	2.4	1.35	70.5	64.9	44.4	51.6	39
(d)	6.6	2.75	79	97.5	44.9	27.6	33.6
(d)	6.5	2.1	45	95.4	51.8	27.7	30.7
(d)	7	1.35	69.5	85.3	58.4	22.8	29.7
(d)	6.6	0.8	71.5	57	48.2	16.1	39.4
(d)	2.2	2.55	128	73.6	35.6	64	43.1
(d)	4	2.75	57.5	92.4	42.6	43.8	35.4
(d)	3.4	3	69	91.8	39.9	50.5	37.1
(d)	7	1.15	73.5	81.9	60.3	21.9	29.6
(d)	7	0.8	113.5	48.3	40.9	12.9	46.4
(d)	1.1	0.8	127	29.9	25.3	48.6	75
(d)	7	2.1	63.5	95	51.6	25.4	30.9
(d)	4.2	3	70	93.4	40.6	42.1	36.5
(d)	3.7	2.15	71.5	86.8	46.5	43.8	34.1
(d)	7	0.8	81.5	62.6	53	16.7	35.8
(d)	1.5	1.1	94.5	49.9	37.4	62.2	48.1
(d)	1.5	1.1	58	46.9	35.2	58.5	51.2
(d)	7	0.8	69.5	64	54.2	17.1	35
(d)	0.7	3	70.5	53.6	23.3	143	63.7
(d)	0.7	2.5	85.5	52.6	25.7	140.5	59.7
(d)	3.7	0.8	81.5	52.9	44.8	26.7	42.4
(d)	3.9	3	91.5	95.8	41.7	46.5	35.6
(d)	1.5	1.95	104	67.7	38.3	81.6	42.1
(d)	0.7	2.5	105	54.2	26.5	144.8	58
(d)	5.9	2	121.5	80.4	44.9	25.5	35.8
(d)	5.8	2.2	65.5	94.7	50.1	30.5	31.5
(d)	7	0.8	74.5	59	50	15.8	38
(d)	4.8	1.15	138.5	47	34.6	18.5	51.6
(d)	2.5	1.65	150	47.8	29.7	35.8	56.3
(d)	4.9	2.75	70	88	40.5	33.6	37.3
(d)	2.3	2.15	70.5	80	42.9	63.6	37
(d)	6.6	1.05	77	71.6	54.7	20.3	33.2
(d)	2.4	0.8	137.5	31.2	26.4	24.8	71.9
(d)	2.5	2.45	69	83.7	41.4	62.6	37.3

(d)	5.7	2	70	91.5	51.1	29.7	31.5

Route (e) Solvent-free Direct Amidation with iBAnhydride

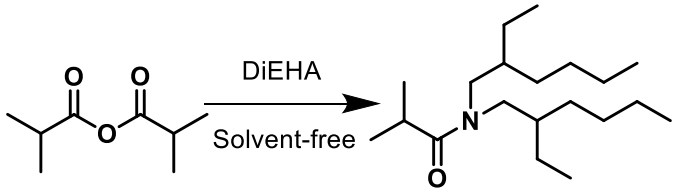

Scheme S12: Amide bond formation reaction using isobutyric anhydride (iBAnhydride) and Di(2-ethylhexyl)amine (DiEHA) to yield N,N-di-(2-ethylhexyl)isobutyramide (DEHiBA) in the absence of solvent

Reservoir one was prepared by dissolving the biphenyl in Di-(2-ethylhexyl)amine with stirring at ambient conditions.

Reservoir 1: Di-(2-ethylhexyl)amine (400 g, 1.66 mol), and biphenyl (8.7588 g, 0.0568 mol).

Reservoir 2: Isobutyric anhydride (477 g, 3.02 mol).

Reservoir 3: Acetonitrile.

An example HPLC chromatogram is illustrated in Figure S16.

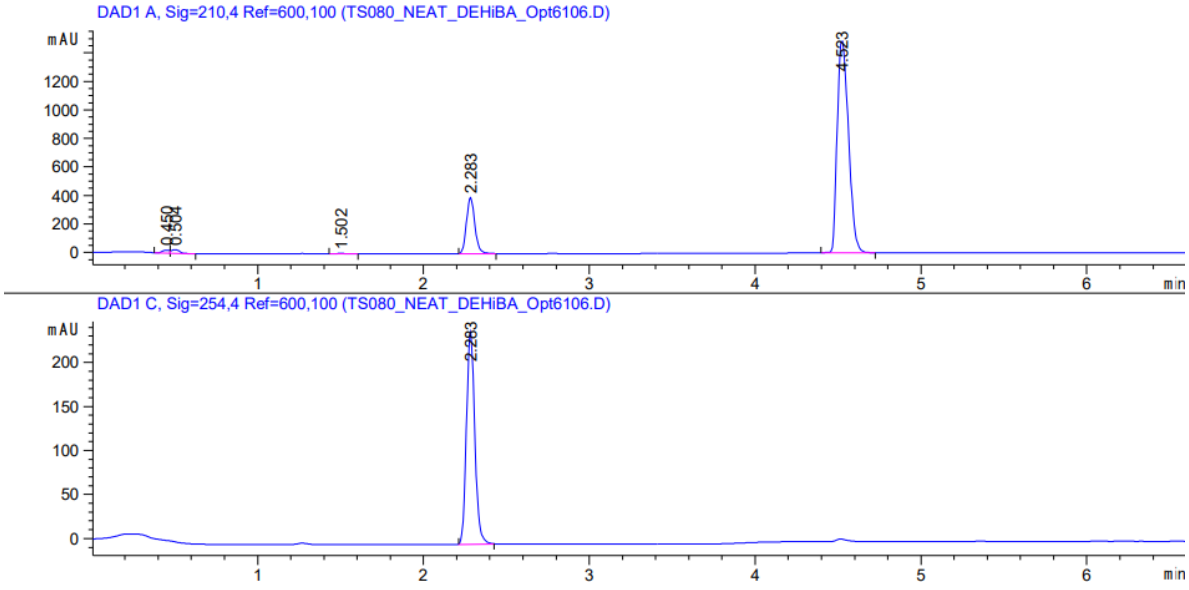

Figure S59: An example HPLC chromatogram from route (e)

The flow platform was set up according to **Figure 28** using a reactor volume of 4.0 mL with stainless steel tubing and a back pressure of 100 psi.

The self-optimisation was conducted with respect to three continuous parameters: residence time, iBAnhydride equivalents, and temperature. The upper and lower parameter bounds for each are described in Table S9. The initial objective for each optimisation was to maximise yield, then simultaneously maximize reaction mass efficiency and space-time yield.

Table S22: The upper and lower bounds for the variables optimised in route (e)

	Residence time (mins)	iBAnhydride equivalents.	Temperature (°C)	[DiEHA] after reactor (mol dm^{-3})
Lower bound	0.5	0.9	40	0.4
Upper bound	10	3	150	0.4

Route (e) Data and Further Analysis

A comparison between the trade-off between the solvated and solvent free synthesis of DEHiBA from iBAnhydride, whereby the trends are contrasting.

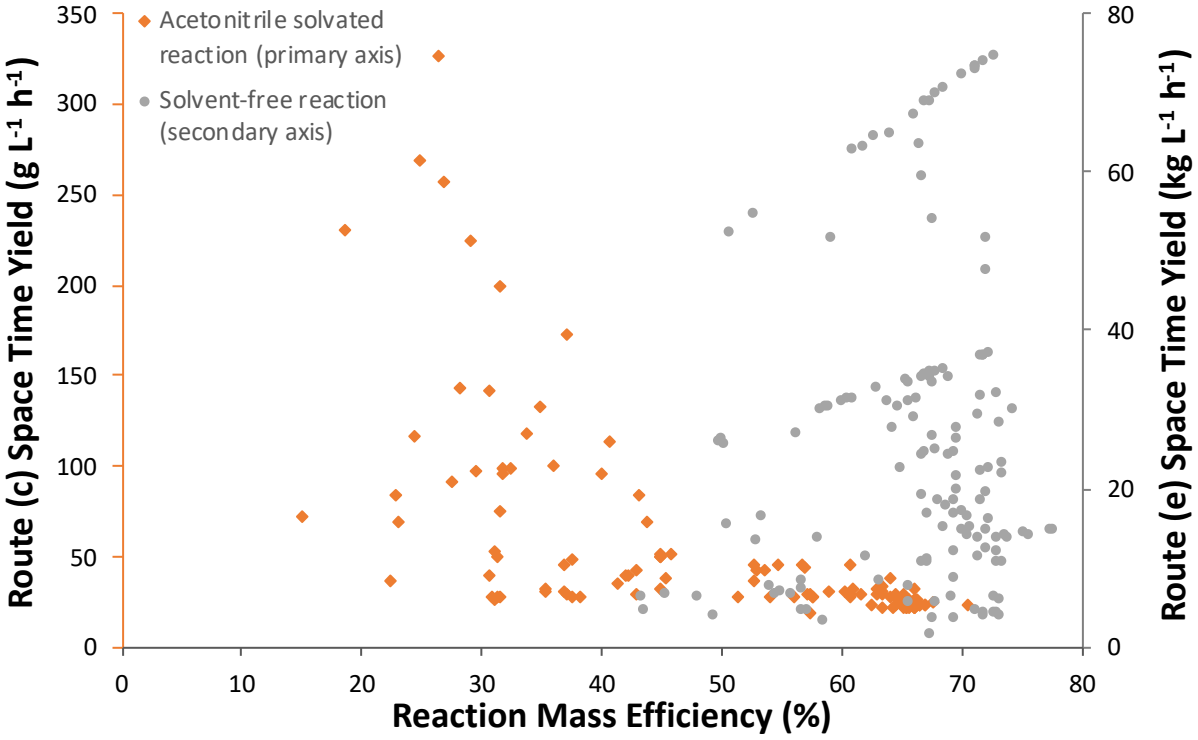

Figure S60: A comparison between the RME, STY trade-off curves for the solvated and solvent free reaction of iBAnhydride and DiEHA

Table S10 provides the raw data for the experimental conditions exploited in the optimisation of route (e) and the performance metrics associated.

Table S23: complete dataset from the optimisation of route (e)

Residence time (min)	iBAnhydride equivalents.	Temperature (°C)	[DiEHA] in reactor (M)	DEHiBA Yield (%)	Reaction Mass Efficiency (%)	Space-Time Yield (kg L^{-1} h^{-1})	Cost of DEHiBA (£/mol)
2.8	1	139	2.14	79.6	62	11.4	29.5
22.2	1	139	2.14	86.5	67.3	1.6	27.2
4	2	40	1.58	86	48.1	6.3	33.5
4	1	40	2.14	72.5	56.6	7.2	32.4
2	1	40	2.14	67.9	52.9	13.6	34.6
6.8	2.16	41.9	1.52	92.1	49.2	3.8	32.2
6	1	50	2.14	84.1	65.6	5.6	27.9
3.7	2.54	65.9	1.38	93.7	45.3	6.6	33.8
3.7	2.54	65.9	1.38	89.4	43.2	6.3	35.4
9.4	1.61	78.5	1.76	92.8	58.3	3.2	28.8
1.7	1.98	93.1	1.59	94.9	53.2	16.4	30.2
1.7	1.98	93.1	1.59	89.9	50.4	15.6	31.9
5.1	2.75	103.8	1.32	94.5	43.5	4.5	34.7
6	1	100	2.14	93.3	72.7	6.2	25.2

Residence time (min)	iBAnhydride equivalents.	Temperature (°C)	[DiEHA] in reactor (M)	DEHiBA Yield (%)	Reaction Mass Efficiency (%)	Space-Time Yield (kg L^{-1} h^{-1})	Cost of DEHiBA (£/mol)
8.6	1.05	125.9	2.10	93.9	71.9	4.3	25.3
3.2	1.26	140.8	1.96	94.3	66.8	10.9	26.3
8.6	1.05	125.9	2.10	95.2	72.9	4.4	24.9
3.2	1.26	140.8	1.96	94.8	67.1	10.9	26.2
3	1	150	2.14	92.3	72	12.3	25.4
1	1	150	2.14	85.8	66.9	34.3	27.4
8.8	0.9	149.7	2.22	92.1	72.6	4.2	25.6
9.4	0.9	128.8	2.22	92.9	73.2	4	25.5
8	0.9	138.2	2.22	90.3	71.2	4.5	26.2
6.2	1.88	139	1.63	97.9	56.6	4.8	28.8
6.6	1.85	125.7	1.64	98	57.2	4.5	28.6
3.7	2.1	150	1.54	99.3	54	7.8	29.5
4.3	2	150	1.58	100	55.8	6.8	28.8
4.2	1.98	150	1.59	96.8	54.3	6.8	29.6
4.2	1.98	150	1.59	97.6	54.8	6.9	29.4
1.1	1.27	150	1.95	91.9	64.7	30.3	27.1
3.2	1.17	150	2.02	91.8	67	10.8	26.6
1	1.47	150	1.83	88.3	58.1	30	29.4
2.7	1.13	150	2.05	98.3	73	13.9	24.6
2.5	0.9	128.9	2.21	89.2	70.5	14.2	26.4
3.2	0.94	135.5	2.19	89.2	71.4	11.3	25.9
1.1	1.02	150	2.12	85.6	66.2	31.3	27.6
1.2	1.05	150	2.10	86.4	65.9	29	27.5
8.9	0.98	108.2	2.15	91.3	71.7	4.1	25.6
2.1	1.1	140.1	2.07	93.2	69.9	17.3	25.8
1	0.99	148.3	2.15	86.3	67.7	33.5	27.1
1.4	0.99	148.3	2.15	85.5	67	24.7	27.4
4.1	0.91	149.4	2.21	87.6	69.3	8.7	26.8
1	1.91	149.7	1.62	87.5	50.2	25.5	32.3
1.6	0.9	150	2.21	90.4	71.5	22.2	26
1.1	0.92	150	2.20	81.7	65.4	31.1	28.4
1	1.35	140.6	1.90	91.7	62.8	32.6	27.6
2	1.16	140.8	2.02	91.5	67.1	16.9	26.6
2.9	1.11	142.3	2.06	92.6	69.3	12.2	26
1	0.98	148.2	2.16	83.2	65.5	33.6	28.1
1	1.07	122.3	2.09	88.8	67.4	34.7	26.8
1	1.08	140.5	2.08	86.2	65.3	33.6	27.7
1	1.29	145.9	1.94	87	60.8	31.5	28.8
2.7	1.01	150	2.13	94.8	73.5	14.1	24.8
1	1.07	122.3	2.09	94.4	71.7	36.9	25.2
1	1.08	140.5	2.08	90.5	68.5	35.2	26.4
1	1.29	145.9	1.94	83.9	58.6	30.4	29.8
2.7	1.01	150	2.13	92.1	71.4	13.7	25.6

Residence time (min)	iBAnhydride equivalents.	Temperature (°C)	[DiEHA] in reactor (M)	DEHiBA Yield (%)	Reaction Mass Efficiency (%)	Space-Time Yield (kg L^{-1} h^{-1})	Cost of DEHiBA (£/mol)
1	1.36	119.1	1.90	87.6	59.9	31.1	29
1	1.01	143.3	2.13	85.9	66.6	34.2	27.4
2	0.9	149.7	2.21	86.8	68.7	17.7	27.1
6.3	0.94	150	2.18	91.8	73.2	6	25.3
4.3	0.9	109.7	2.21	82.8	65.5	7.8	28.4
1	1.36	118.9	1.90	86.4	58.9	30.2	29.4
1	1.13	124.7	2.05	96.4	71.5	36.9	25.1
2.2	0.97	148.6	2.16	89.3	70.4	16.4	26.1
1.4	0.9	97.6	2.21	87.9	69.5	26.3	26.8
1	1.73	64.6	1.70	82.5	49.9	26.2	33.2
6.3	0.9	86.9	2.21	85.7	67.8	5.5	27.5
2.7	1	141.9	2.14	97	75.7	14.3	24.2
1.4	0.9	150	2.21	85.8	67.9	25	27.4
1	1.39	105.8	1.88	89.5	60.5	31.4	28.5
1.9	0.97	132.5	2.16	91.2	72.1	19.4	25.5
1.2	0.98	136.9	2.16	81.7	64.3	27.5	28.6
1.4	1	138.4	2.14	89	69.4	24.6	26.4
1	0.93	121.8	2.20	84.5	67.8	34.6	27.4
2	0.93	134.3	2.19	89.3	71.6	18.6	25.9
9.7	1.04	139.9	2.11	90.2	69.3	3.7	26.2
2.4	0.9	141.9	2.21	88.6	70.1	14.8	26.6
1	0.9	102.6	2.21	80.5	63.7	31	29.2
5.7	1.04	134.8	2.11	89.9	69.1	6.3	26.3
1.9	0.92	136.1	2.20	86.5	69.3	18.5	26.8
9.5	0.92	150	2.20	84.6	67.5	3.6	27.5
2.2	1.53	53	1.80	89.6	58	13.8	29.2
3.9	1.36	59.3	1.90	92	63.1	8.4	27.5
3.5	1.95	75.8	1.60	99.6	56.6	8.5	28.5
0.6	1.6	90.5	1.76	93.4	59.1	51.5	28.4
1.8	1.3	111.2	1.94	99.3	69.6	20	25.1
1	1.07	122.3	2.08	95.1	72.2	37.1	25
2.7	1.09	129.2	2.07	99.7	75.1	14.3	24
1	1.07	122.3	2.08	94.5	71.8	36.9	25.2
2.7	1	141.9	2.14	99.3	77.5	14.7	23.6
1.1	1.81	149.4	1.66	94.9	56.2	26.9	29.2
2.7	1	141.9	2.14	99.1	77.3	14.7	23.7
0.5	1.22	140	1.99	94.9	68.4	70.7	25.9
0.5	1	140	2.14	91	71.1	72.9	25.7
0.5	1.15	150	2.03	97.2	71.9	74.1	24.9
1.9	1.01	81.5	2.13	87.4	68	18.6	26.9
0.5	1.11	122.5	2.06	89.1	66.8	68.8	26.9
1.5	1	75.2	2.14	83.1	64.9	22.6	28.2
0.5	1.07	149	2.09	95.5	72.6	74.7	24.9

Residence time (min)	iBAnhydride equivalents.	Temperature (°C)	[DiEHA] in reactor (M)	DEHiBA Yield (%)	Reaction Mass Efficiency (%)	Space-Time Yield (kg L^{-1} h^{-1})	Cost of DEHiBA (£/mol)
1.2	1	120.2	2.14	91.6	71.5	31.8	25.6
1.3	1.02	150	2.12	96	74.3	30.1	24.5
1.7	1.05	136.7	2.10	95.6	73.4	22	24.8
1.6	1.06	146.1	2.09	96	73.4	23.1	24.7
0.5	1.12	149.2	2.05	90.8	67.8	69.9	26.5
3.5	1.04	133.3	2.11	95.3	73.3	10.7	24.8
1.3	1.04	139.3	2.11	92.9	71.4	29.2	25.4
0.8	1	142.4	2.14	92.3	72	47.7	25.4
1.7	1.16	150	2.02	94.6	69.6	21.4	25.6
0.5	1.32	150	1.92	88.9	61.7	63.1	28.2
2.8	1	150	2.14	94.5	73.7	13.7	24.8
0.7	1	147.9	2.14	92.1	71.9	51.6	25.4
0.5	1.05	134.9	2.10	86.8	66.5	63.4	27.3
2.3	1.02	143.3	2.13	92.8	72.2	16.3	25.3
2.1	1.02	143.2	2.13	89.1	69.3	16.9	26.4
0.5	1.11	84.6	2.06	81.4	60.9	62.8	29.5
1.8	1.12	125.4	2.05	89.3	66.7	19.1	26.9
3.5	1	146.8	2.14	93.3	72.8	10.7	25.1
0.5	1.07	95.1	2.08	84.1	63.9	64.8	28.3
0.5	1.05	149.9	2.10	92.7	71.2	73.2	25.5
1.6	1.02	143.3	2.12	93.1	72.3	22.5	25.2
0.5	1.16	150	2.02	89.7	66	67.1	27
2.4	1.06	149.5	2.09	92.6	70.7	15	25.6
0.5	1.03	149.9	2.12	92.2	71.2	73.1	25.6
1	1	144.9	2.14	88.2	68.8	34.2	26.6
3.1	1.02	128.3	2.13	93.8	72.9	12	25
0.5	1.22	114.2	1.99	86.9	62.6	64.4	28.3
1.2	1.01	150	2.13	93.7	73	32.2	25
0.5	1.34	53.5	1.91	76.6	52.7	54.8	32.9
1	1.3	41.5	1.93	71.1	49.7	26	35.2
1.3	1	149.1	2.14	93.6	73.1	28.2	25
1.3	1.08	117.4	2.08	91.6	69.5	27.5	26
1.4	1.08	119.2	2.08	87.7	66.6	24.2	27.1
0.5	1.01	135.5	2.13	86.3	67.3	69	27.2
1	1.08	110.9	2.08	88.9	67.4	33.9	26.8
2.5	1	114.7	2.14	92.1	71.9	14.8	25.4
0.6	1.07	150	2.09	88.8	67.7	54.1	26.8
1.3	1.03	149.1	2.12	87.2	67.4	26.7	27
0.6	1.06	150	2.10	87.1	66.6	59.4	27.2
2.3	1.28	142.6	1.95	97.2	68.5	15.2	25.6
0.5	1.86	77.5	1.64	87	50.7	52.4	32.1
0.5	1.15	142.7	2.03	94.8	70	72.2	25.5
1.5	1.05	136.1	2.10	89.9	69	24.2	26.3

Route (f) Direct Thermal Amidation From iBA

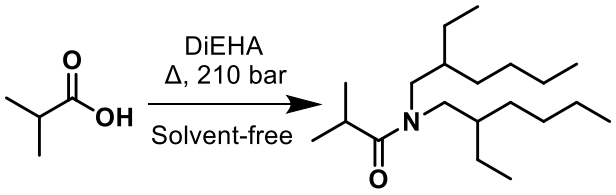

Scheme S13: A direct thermal amidation reaction to yield N,N-di-(2-ethylhexyl)isobutyramide (DEHiBA) by forcing isobutyric acid (iBA) and Di(2-ethylhexyl)amine (DiEHA) together via elevated temperatures and 210 bar of pressure

Reservoir one was prepared by dissolving biphenyl in Di(2-ethylhexyl)amine with stirring at ambient conditions.

Reservoir 1: Di-(2-ethylhexyl)amine (400 g, 1.66 mol), and biphenyl (8.7588 g, 0.0568 mol).

Reservoir 2: Isobutyric acid (475 g, 5.39 mol).

Reservoir 3: Acetonitrile.

An example HPLC chromatogram is illustrated in Figure S18 using the HPLC method previously described.

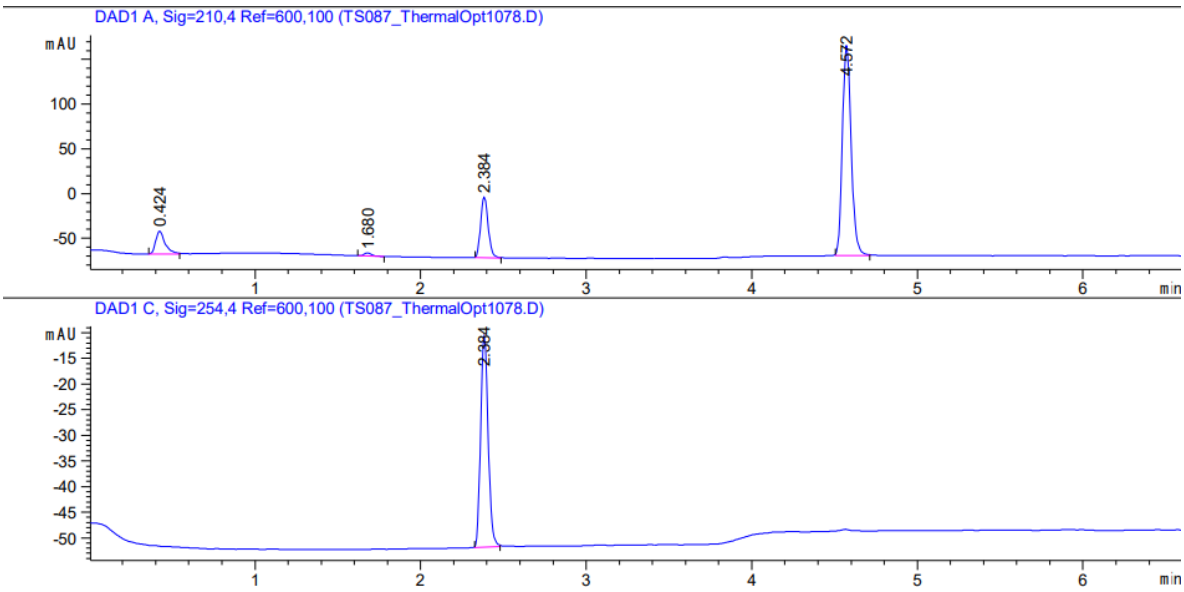

Figure S61: An example HPLC chromatogram from route (f)

The flow platform was set up according to Figure 2 using a reactor volume of 4.0 mL with stainless steel tubing a back pressure regulator set to 210 bar before the sample loop and a back pressure of 100 psi following the sample loop. The self-optimisation was conducted with respect to three continuous parameters: residence time, iBA equivalents, and temperature. The upper and lower parameter bounds for each are described in Table S9. The initial objective for each optimisation was to maximise yield and reaction mass efficiency, then simultaneously maximize reaction mass efficiency and space-time yield.

Table S24: The upper and lower bounds for the variables optimised in route (f)

	Residence time (mins)	iBA equivalents.	Temperature (°C)	[DiEHA] after reactor (mol dm^{-3})
Lower bound	1	0.9	200	0.4
Upper bound	18	5	370	0.4

Route (f) Data and Further Analysis

GC-MS used to identify the unknown signal that was in fact the thermal degradation product of DEHiBA:

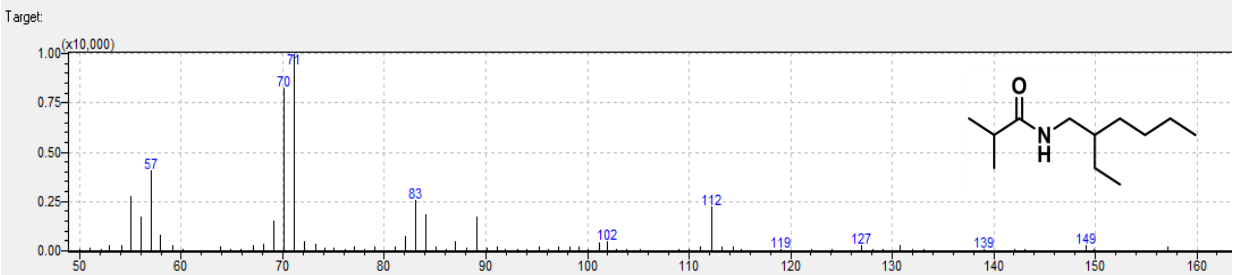

Figure S62: GC-MS chromatogram for the degradation product of DEHiBA

A concise dataset (Table S12) demonstrating the trend between conditions and the area ratio for the signals at 0.5 and 1.7 minutes. The signal at 0.5 minutes increases with increasing iBA equivalents predominantly whilst the signal at 1.7 minutes intensifies with both an increase in temperature and residence time.

Table S25: Area ratios for the signals at 0.5 and 1.7 minute retention times

0.5 min signal	1.7 min signal	Residence time (min)	iBA equivalents.	Temperature (°C)
0.57	0.08	5.00	2.50	330.0
0.45	0.15	5.00	2.50	350.0
0.43	0.23	5.00	2.50	370.0
1.03	0.16	5.92	5.00	344.9
0.98	0.14	5.04	5.00	345.5
1.00	0.15	5.43	5.00	346.1
0.80	0.16	5.50	4.21	348.3

0.65	0.19	5.50	3.52	356.9
0.53	0.18	5.50	3.00	356.9
0.41	0.18	5.50	2.50	356.9
0.85	0.07	8.85	4.14	300.0
0.49	0.03	17.19	2.35	259.5
0.61	0.03	6.03	3.07	282.0
0.82	0.11	10.99	4.53	298.6
0.14	0.25	15.99	1.28	332.8
0.22	0.28	8.15	1.68	355.7
0.54	0.37	18.00	4.08	338.0
0.64	0.29	13.98	4.00	341.1
0.80	0.59	14.75	4.66	364.7
0.80	0.53	12.09	4.73	365.6
0.41	0.34	18.00	2.73	341.9
0.07	0.28	17.34	1.76	344.3
0.03	0.21	16.40	1.00	344.4
0.38	0.38	18.00	2.78	345.4
0.82	0.31	14.35	4.81	342.2
0.95	0.42	17.62	5.00	347.1
0.89	0.48	17.64	4.98	352.0
0.90	0.49	18.00	4.91	352.2
0.76	0.01	13.54	3.81	209.7
0.80	0.01	13.47	4.00	210.3
0.68	0.32	15.34	4.01	351.1
0.72	0.18	6.34	4.48	352.7
0.47	0.36	17.12	3.00	352.3
0.48	0.35	16.41	3.06	352.3
0.42	0.36	17.30	3.05	352.6
0.58	0.29	10.78	3.75	354.9
0.86	0.22	13.17	5.00	338.0
0.87	0.18	10.65	5.00	338.7
0.94	0.19	5.43	2.91	359.1
0.40	0.16	5.13	2.87	359.5
0.20	0.07	15.47	1.40	305.6
0.77	0.07	5.00	4.30	324.3
0.82	0.14	9.42	5.00	324.3
0.46	0.23	14.96	2.89	332.8

Table S26: complete dataset for the optimisation of route (f)

Residence time (min)	iBA equivalents.	Temperature (°C)	[DiEHA] in reactor (M)	DEHiBA Yield (%)	Reaction mass efficiency (%)	Space-Time Yield (g L^{-1} h^{-1})	Cost of DEHiBA (£ mol^{-1})
5	2.5	330	1.874	44.6	30	3122	44.1
5	2.5	350	1.874	59.7	40.2	4181	33
5	2.5	370	1.874	59.5	40.1	4169	33.1
5.9	5	344.9	1.306	77.8	35.4	3210	27.2
5	5	345.5	1.306	77.3	35.2	3745	27.4
5.4	5	346.1	1.306	77.7	35.4	3495	27.2
5.5	4.2	348.3	1.444	73.7	37.4	3619	28.1
5.5	3.5	356.9	1.592	68.6	38.7	3713	29.6
5.5	3	356.9	1.724	65	39.9	3809	30.7
5.5	2.5	356.9	1.874	59.1	39.8	3765	33.3
8.8	4.1	300	1.459	50	25.6	1541	41.3
17.2	2.3	259.5	1.925	14.1	9.8	295	139.2
6	3.1	282	1.705	13.7	8.3	724	146.2
11	4.5	298.6	1.385	55.9	27.1	1317	37.4
16	1.3	332.8	2.377	34.4	30.2	956	55.1
8.1	1.7	355.7	2.186	44.7	35.7	2241	42.9
18	4.1	338	1.469	64.4	33.2	982	32.1
14	4	341.1	1.486	63.4	33.1	1260	32.5
14.8	4.7	364.7	1.362	57.9	27.6	999	36.2
12.1	4.7	365.6	1.351	60.8	28.7	1271	34.5
18	2.7	341.9	1.802	58.5	37.7	1094	33.9
17.3	1.8	344.3	2.151	27.4	21.5	635	70.3
16.4	1	344.4	2.534	14.2	13.4	409	132.6
18	2.8	345.4	1.786	55.7	35.5	1032	35.7
14.3	4.8	342.2	1.337	69.4	32.4	1210	30.3
17.6	5	347.1	1.306	68	30.9	942	31.2
17.6	5	352	1.309	64.4	29.4	894	32.9
18	4.9	352.2	1.32	64.3	29.6	882	32.8
13.5	3.8	209.7	1.527	1.3	0.7	27	1573.4
13.5	4	210.3	1.485	1.3	0.7	27	1593.3
15.3	4	351.1	1.484	63.9	33.3	1154	32.2
6.3	4.5	352.7	1.394	71	34.7	2921	29.4
17.1	3	352.3	1.724	59.1	36.3	1113	33.8
16.4	3.1	352.3	1.707	59.4	36.1	1156	33.7
17.3	3	352.6	1.71	56.2	34.2	1038	35.6
10.8	3.8	354.9	1.539	64.6	35.1	1726	31.6
13.2	5	338	1.306	74.3	33.8	1378	28.5
10.6	5	338.7	1.306	75.6	34.4	1734	28
5.4	2.9	359.1	1.749	60.9	38	3663	32.7
5.1	2.9	359.5	1.762	59	37.1	3782	33.7

15.5	1.4	305.6	2.315	27.3	23.3	764	69.6
Residence time (min)	**iBA equivalents.**	**Temperature (°C)**	**[DiEHA] in reactor (M)**	**DEHiBA Yield (%)**	**Reaction mass efficiency (%)**	**Space-Time Yield (g L^{-1} h^{-1})**	**Cost of DEHiBA (£ mol^{-1})**
5	4.3	324.3	1.428	56.8	28.4	3031	36.6
9.4	5	324.3	1.306	75.2	34.3	1950	28.2
15	2.9	332.8	1.755	64	40.1	1403	31.1
2.5	1.5	350	2.268	16.7	13.9	2826	114.5
1.6	2.3	350	1.955	16.9	11.9	3879	115.5
2.3	3.5	360	1.587	46.9	26.3	6182	43.3
2.5	1.5	360	2.268	21.4	17.8	3626	89.2
2.5	1.5	370	2.268	23.9	19.9	4048	79.9
2.5	1.5	350	2.268	16.7	13.9	2829	114.4
1.6	2.3	350	1.955	16.3	11.5	3733	120
2.3	3.5	360	1.587	46.4	26	6113	43.8
2.5	1.5	360	2.268	22	18.3	3731	86.7
2.5	1.5	370	2.268	25.8	21.4	4367	74.1
1.1	5	359.8	1.306	33.2	15.1	7224	63.7
1.1	5	359.9	1.306	32.6	14.8	7257	65
1.1	5	360	1.308	32.6	14.9	7282	64.9
1.1	5	360	1.307	33.3	15.2	7194	63.6
4.2	3.4	359.9	1.62	61.1	35.1	4409	33.1
4.7	3.9	360	1.516	64.7	34.6	3938	31.7
3.1	3.4	360	1.626	56.1	32.4	5488	36
2	1.1	217.2	2.469	1.9	1.8	446	970.4
4.8	3.1	248.2	1.708	1.4	0.8	92	1453.5
2.8	4.8	268.8	1.345	2.7	1.3	239	784.2
5	2.1	286.7	2.011	5.6	4.1	422	348.3
3.3	3.4	306.2	1.625	10.6	6.1	978	191.2
1.4	4.1	343.1	1.475	18.1	9.4	3584	114
4.1	2.4	346.1	1.902	35.3	24.1	3037	55.7
5.5	3.1	363.2	1.703	53.1	32.2	3072	37.7
5.5	3.1	363.2	1.705	57.2	34.7	3326	35
5.5	3	368.5	1.711	58.9	35.9	3423	34
4.5	3.8	361.4	1.525	61.7	33.2	3951	33.2
4.5	4	361.5	1.496	64.2	33.8	4006	32
4.6	3.9	362	1.514	64.5	34.4	3960	31.8
4.7	3.9	362.3	1.501	65.9	34.8	3908	31.2
5.2	2.7	368.5	1.812	56.6	36.7	3717	35
5.1	5	369.9	1.312	65.7	30	3176	32.2
5.1	5	370	1.306	68.4	31.1	3292	31
4.1	4.4	356.8	1.407	45.4	22.4	2907	45.9
4.1	4.3	357	1.419	59.7	29.7	3873	34.8
4	4.1	359.1	1.471	60.4	31.2	4185	34.1
3.9	4.9	364.5	1.316	68.3	31.3	4283	31
3.8	3.8	361.9	1.518	59.8	32	4495	34.3

4.3	4.4	366.8	1.417	66.4	33	4059	31.3
Residence time (min)	**iBA equivalents.**	**Temperature (°C)**	**[DiEHA] in reactor (M)**	**DEHiBA Yield (%)**	**Reaction mass efficiency (%)**	**Space-Time Yield (g L^{-1} h^{-1})**	**Cost of DEHiBA (£ mol^{-1})**
4.8	4.6	368.6	1.368	68.5	32.8	3641	30.6
4.8	4.6	368.6	1.371	69.8	33.5	3731	30
4.9	2.7	356.2	1.802	51.4	33.1	3531	38.6
4.8	2.7	356.4	1.804	49.9	32.2	3483	39.7
4.9	2.9	362.6	1.741	54.5	33.9	3646	36.6
4.8	2.9	363.2	1.757	54.9	34.4	3736	36.3
5.5	2.4	360	1.914	49.4	34.1	3216	39.6
5.5	2.3	360.3	1.926	48	33.3	3141	40.8
5.5	2.4	362.7	1.922	49.2	34	3211	39.8
5.5	2.5	367.9	1.874	52.3	35.2	3330	37.6
5.5	3.1	347.1	1.699	50.8	30.7	2935	39.4
5.4	3.2	354.5	1.675	56	33.3	3236	35.9
2.4	4.9	363.6	1.321	58.3	26.9	6116	36.2
3.2	5	369.1	1.312	67.9	31.1	5153	31.1
3.3	5	369.2	1.312	69.9	32	5184	30.3
5.5	1.1	369.5	2.502	25	23.3	2128	75.2
4.1	3.5	354	1.601	46	26.1	3387	44.1
3.7	3.7	354.4	1.561	52.4	28.9	4095	38.9
4.2	3.3	357.4	1.647	54.4	31.8	4020	37
5.2	2.9	370	1.757	57.5	36	3644	34.6
2.9	4.3	361.2	1.432	58.3	29.3	5326	35.6
3.1	3.7	364.4	1.543	58	31.6	5324	35.2
4.7	3.6	370	1.567	63.8	35.4	4020	31.9
4.5	3.6	370	1.582	63.8	35.7	4241	31.8
4.3	2.7	363.2	1.822	52	33.9	4152	38.1
1.9	4.3	366.5	1.434	48.6	24.4	6917	42.7
1.6	4.1	369.7	1.47	45.5	23.5	7619	45.3
1	4.9	370	1.324	31.1	14.3	7684	68
3.4	2.6	367.2	1.833	46.5	30.5	4715	42.5
2.7	3.2	370	1.659	49.6	29.2	5773	40.6
3.4	2.5	370	1.882	45.2	30.6	4656	43.5
3.6	2.4	370	1.894	45.2	30.8	4434	43.5
2.2	3.9	358.9	1.498	43.1	22.7	5480	47.7
4	4.1	367.4	1.462	64.7	33.2	4411	31.9
4	4	369	1.486	64.6	33.8	4538	31.9
1.9	3.9	370	1.51	49.5	26.3	7396	41.4
2.5	3.7	366.4	1.559	51.9	28.6	6105	39.3
3.4	4.6	368.4	1.377	66.2	31.9	5067	31.6
1.5	3.8	370	1.524	39.4	21.1	7610	52
3.5	4.6	370	1.365	65.6	31.3	4764	32
1.7	5	366.2	1.306	52.3	23.8	7320	40.5

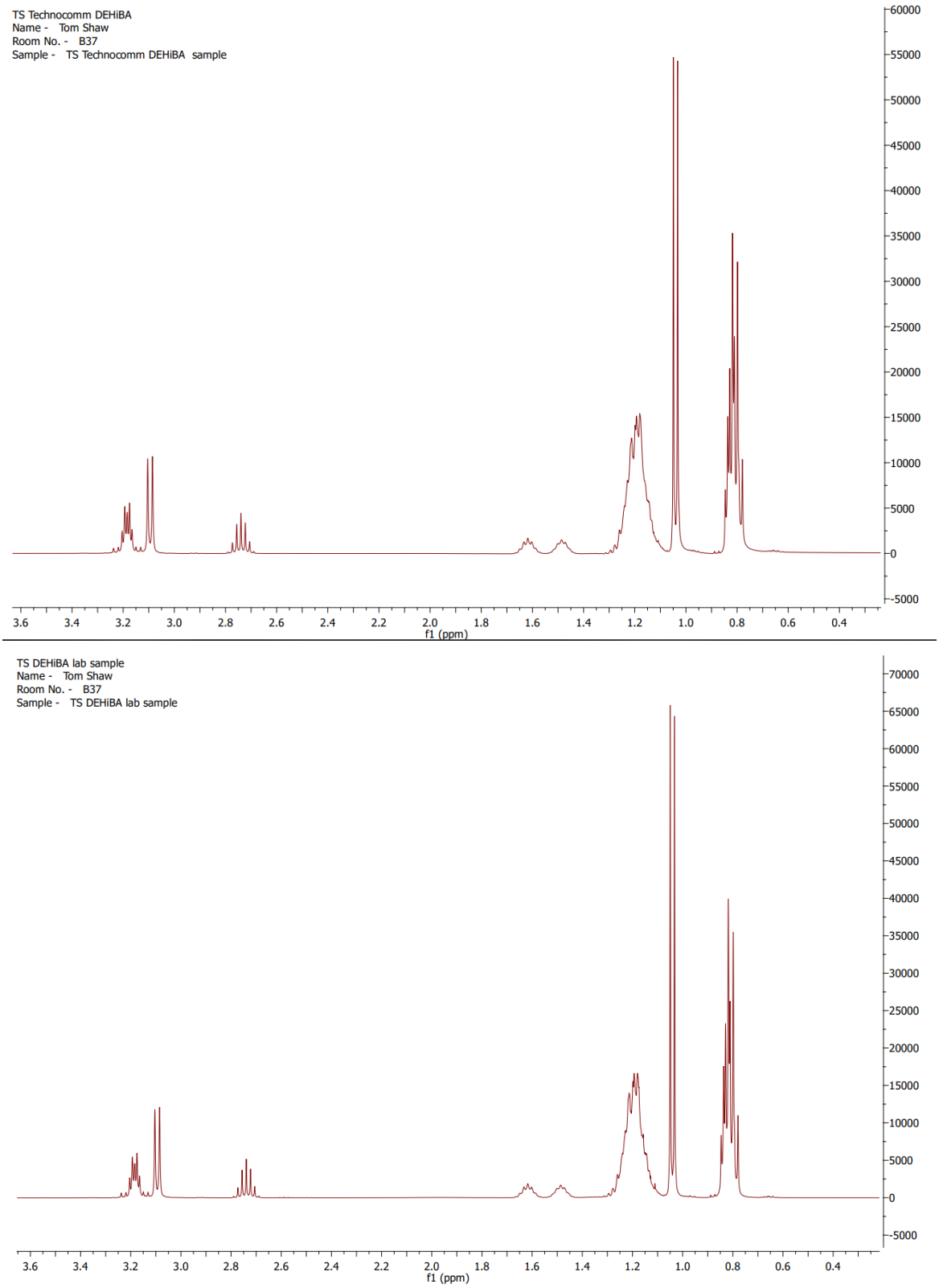

Figure S20: ^{1}H NMR spectra of DEHiBA from the commercial supplier (top) compared with DEHiBA manufactured and purified in this work

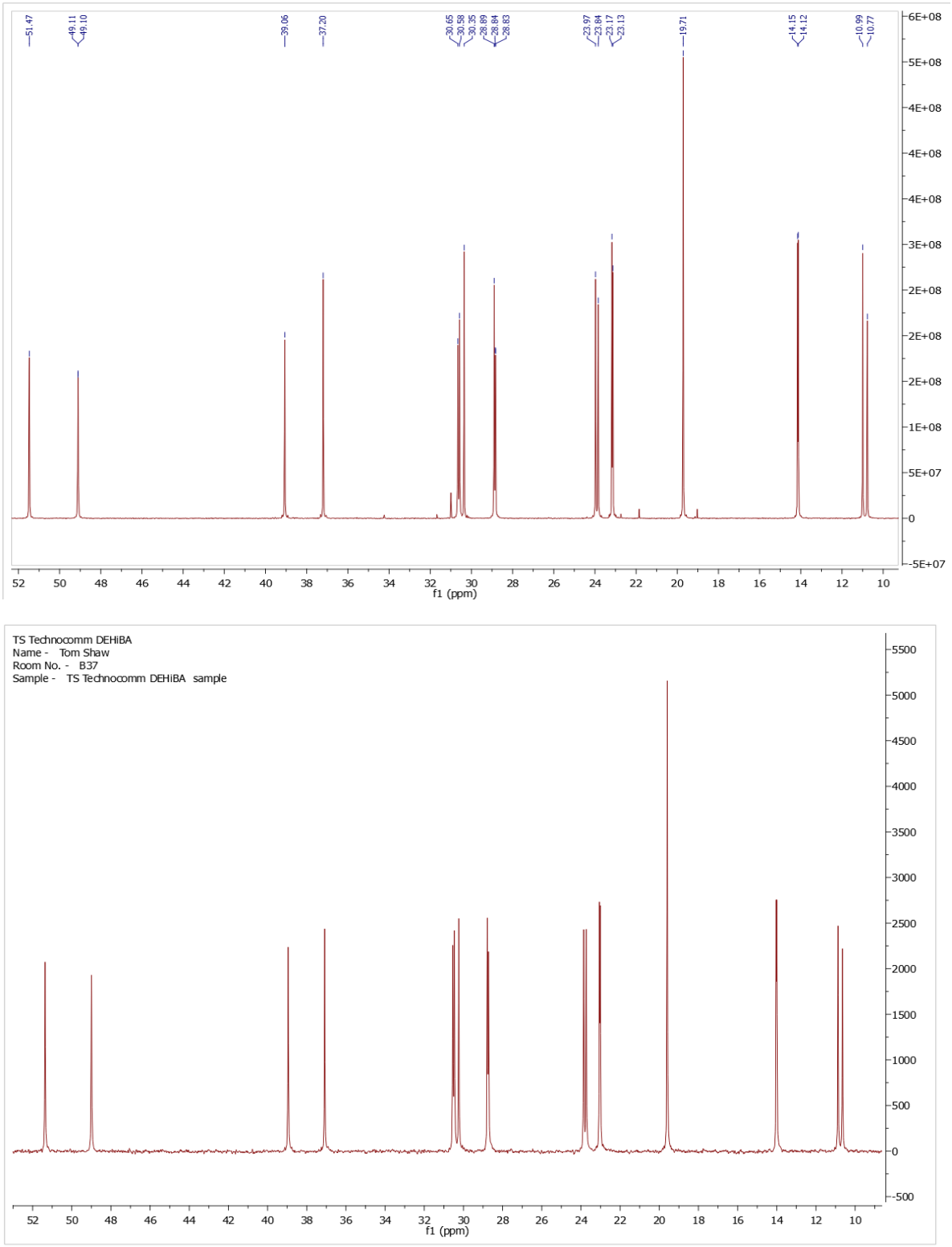

Figure S21: Comparison of DEHiBA purity by ^{13}C NMR. Top = purified e99 DEHiBA (biphenyl containing) from route (e). Bottom = DEHiBA from a commercial supplier

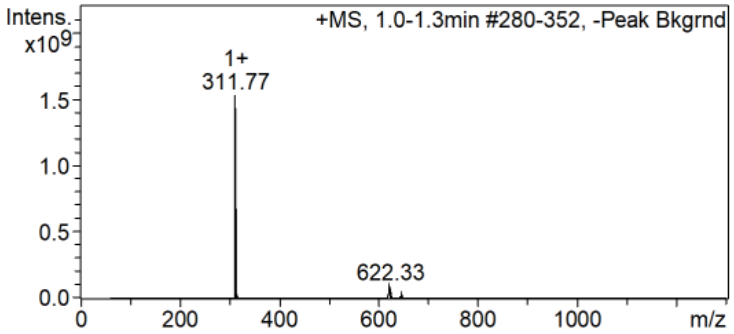

Figure S22: Mass spectroscopy of e99 confirming the molecular weight of DEHiBA.

6.2 Chapter 3 Supporting Information

Self-Optimizing Flow Purification Platform Setup

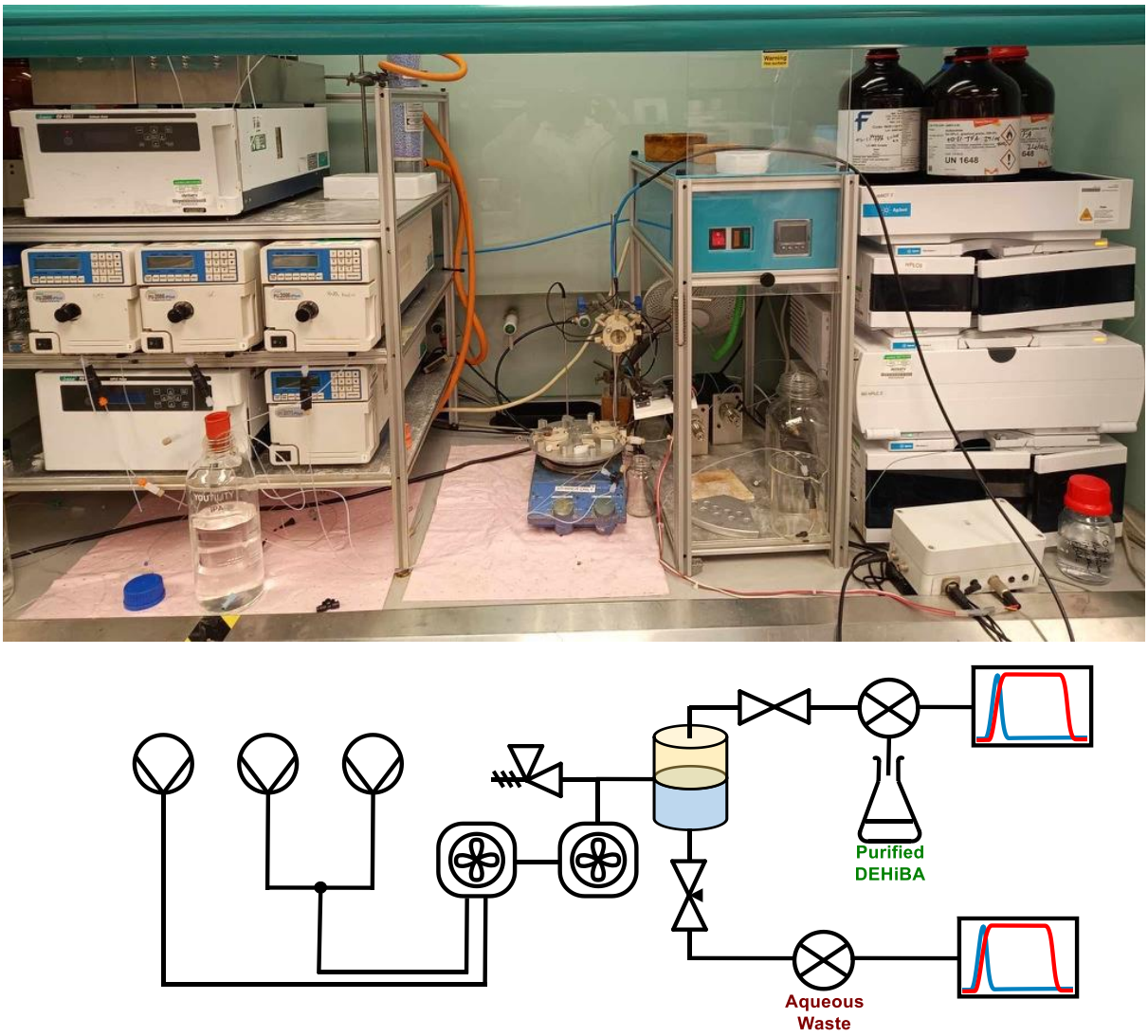

Figure S23: The self-optimizing flow purification platform and its visual schematic

Solutions and internal standards were made up to their desired concentrations, loaded into glass reservoirs and primed with the dual piston reciprocating JASCO PU-2800 HPLC pumps. These solutions were then pumped where streams would be mixed using Swagelok SS-100-3 or polymer tee-pieces according to Figure S23. Tubing was PFA (1/16" OD), from the pumps to two continuous-stirred tank reactors (CSTRs, specifically fReactors), the tubing then fed the mixture to

the coalescing filter to separate the phases,[298] a pressure relief valve was fitted before the separator to avoid overpressure. After the separator, the organic (top) feed led to a VICI Valco EUDA-CI4W sample loop (4-port) with 0.06 µL injection volume followed by an Upchurch Scientific back pressure regulator (40 psi) to maintain constant back pressure on this feed. The aqueous (bottom) feed led to a idex P-445 Micro-Metering Valve with ¼-28 UNF fittings that was automated via a Turnigy TGY-6114MD servo motor. The automation of this needle valve uses conductivity measurements via electrodes in the separator and is described by J. Daglish *et al.*[298] The aqueous phase also leads to a VICI Valco EUDA-CI4W sample loop (4-port) but with a 0.2 µL injection volume using multi-point sampling to analyse both phases.[228] These samples staggered and fed directly into an Agilent 1260 Infinity II series HPLC instrument fitted with an Agilent Poroshell 120 EC-C18 reverse phase column (5 cm length, 4.6 mm ID and 2.7 µm particle size) for quantitative analysis.

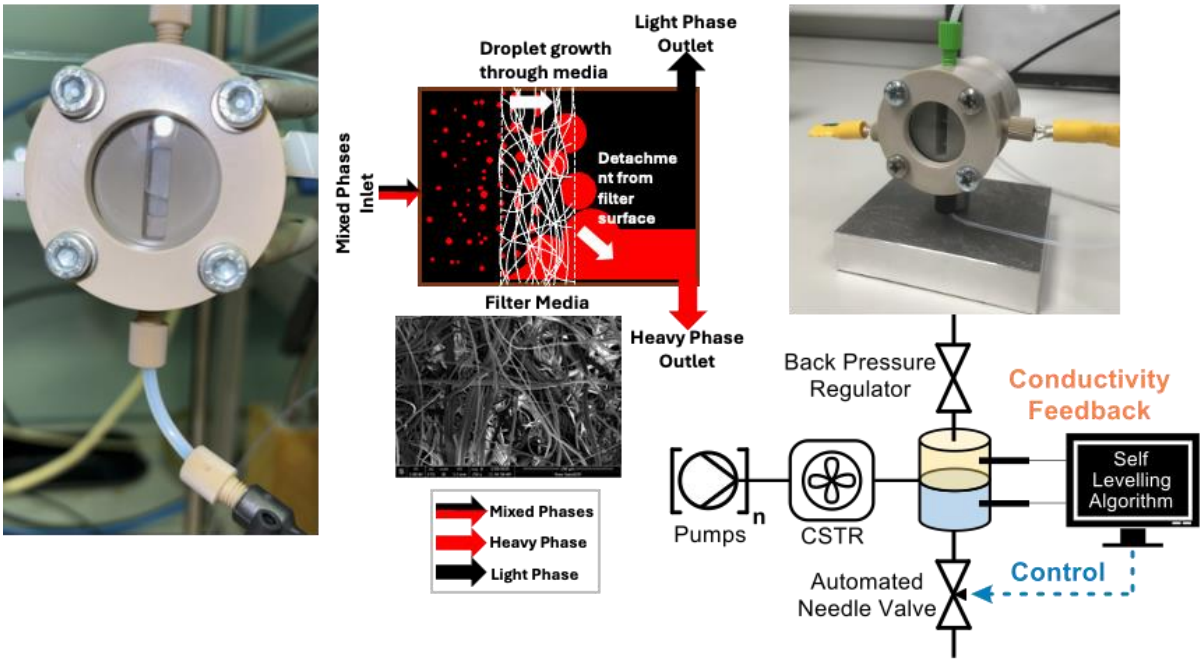

Figure S634: The coalescing separator used to separate the phases

The automated system was controlled using a custom written MATLAB program to enable real-time control and monitoring of all optimisation variables. The machine-learning algorithms in

MATLAB were initiated with Latin hypercube sampling where the number of experiments for this was $2n+1$, n being the number of variables. This formula guarantees that each dimension is divided into $n + 1$ subintervals, and that there will be one sample in each subinterval. This helps achieve a more even coverage of the parameter space, thus reducing the risk of missing regions of interest. The analytical data from this and following experiments enabled the generation of new conditions for the optimisation to proceed. To determine process metrics, internal standards were included in the aqueous and organic phase, allowing accurate calculations to be completed using calibration data.

The Weighted Objective Function

This objective was calculated automatically multiplying purities >95% by 1.1 to favour high purity performance. The newly weighted purities were then normalised between 0 and 1. Next, the product loss was normalised between 0 and 1 and before combining these objectives the normalised purity was multiplied by 2 before combined added to the normalised product loss data and again normalised between 0 and 1 to give the weighted response. The algorithm then took the log of each weighted response and optimised for this

Steady State Comparison

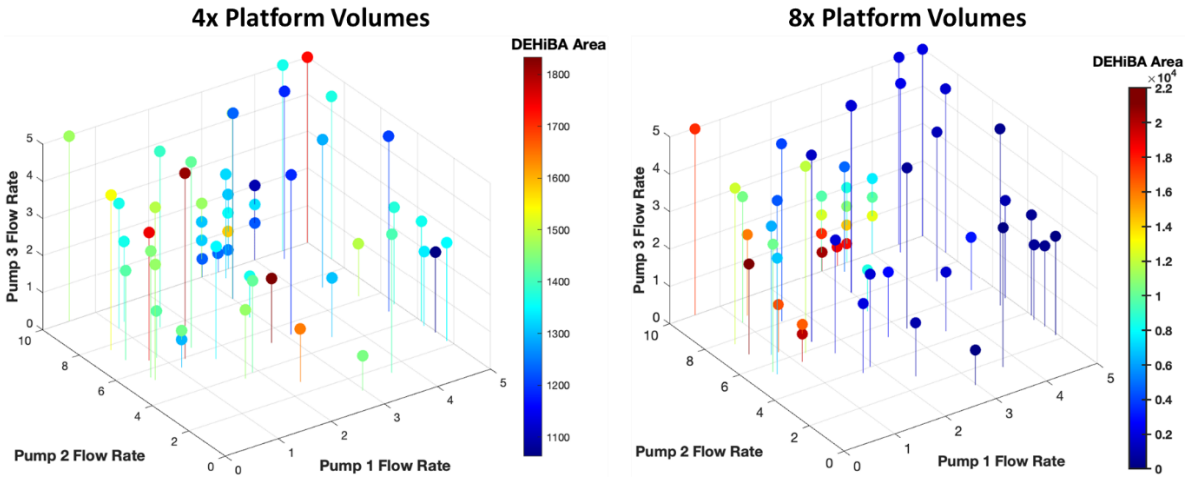

Figure S25: Platform volumes required to reach steady state.

HPLC and GC-FID Methods

HPLC analysis was performed on an Agilent 1260 Infinity II series HPLC instrument fitted with an Agilent Poroshell 120 EC-C18 reverse phase column (5 cm length, 4.6 mm ID and 2.7 µm particle size) with a binary pump and a variable wavelength detector.

The same HPLC method was used for all routes and calibrations. Water (A, 18.2 MΩ) and acetonitrile (B) HPLC mobile phases were used, starting with a 80:20 method of A:B, this ratio was maintained for 0.25 minutes followed by a reduction in the amount of A to 5% over 2 minutes, this was held for 3 minutes before returning to the starting ratio at a flow rate of 1.50 mL min^{-1} and a column temperature of 30 °C. 217 nm was used to detect the product DEHiBA and internal standards.

GC analysis was carried out on an Agilent 7890B instrument fitted with an Agilent Technologies 7693 Autosampler and a HP-5 column (30 m x 0.32 mm, 0.25 µm film thickness), H_2 carrier gas, FID detector.

The GC method started at 40 °C and was held here for 1 minute, then the temperature was ramped up to 55 °C over 1 minute, held for a further 1 minute, then the temperature was then increased to 150 °C over 3.8 minutes before increasing to 300 °C over 3 minutes. Finally, the oven cooled to 40 °C over 5/6 minutes.

Calibrations for Quantitative Analysis

All raw materials were purchased from suppliers and calibrated where possible via GC-FID and HPLC. *N,N*-di-(2-ethylhexyl)isobutyramide (DEHiBA) was synthesised as well as purchased from a commercial supplier (Technocomm) for analytical calibrations to enable the quantitative analysis of all reactions for calculating key process metrics.

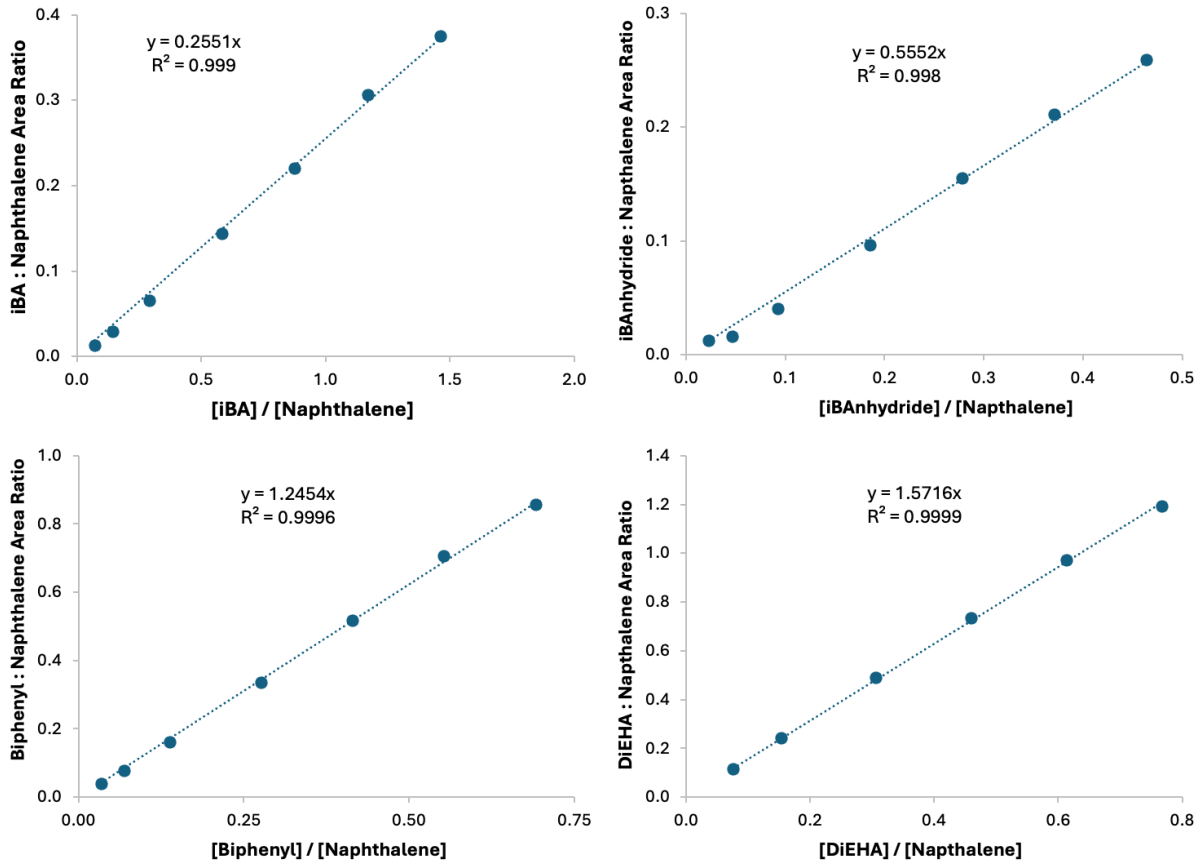

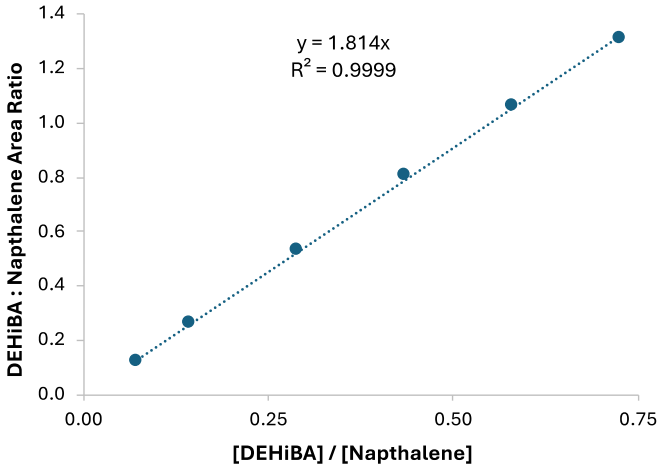

Figure S26: GC-FID calibration curves for isobutyric acid (iBA), isobutyric anhydride (iBAnhydride), biphenyl, *N,N*-di-2-ethylhexylamine (DiEHA), and N,*N*-di-2-ethylhexylisobutyramide (DEHiBA), all against naphthalene.

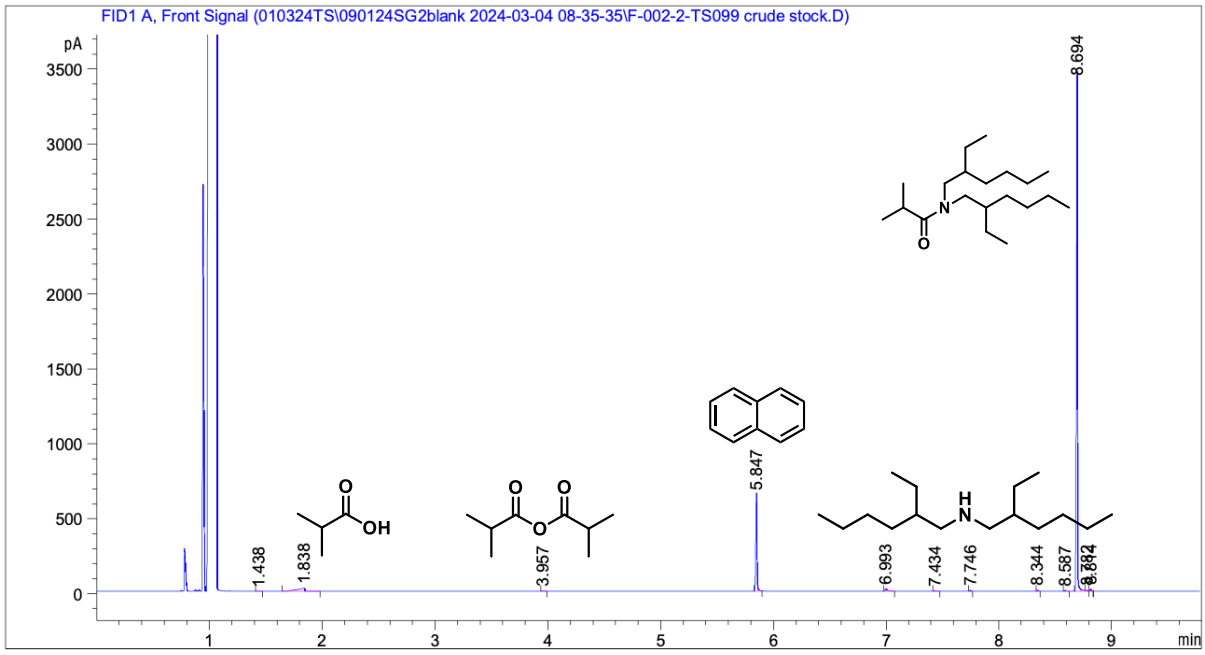

Figure S27: Example GC-FID chromatogram for the purifications.

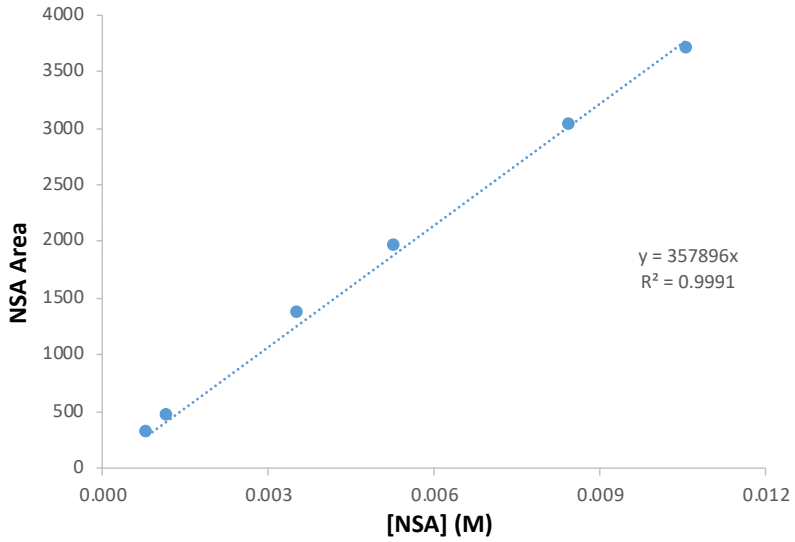

Figure S28: Calibration of sodium naphthalenesulfonate (NSA), the aqueous internal standard via HPLC analysis.

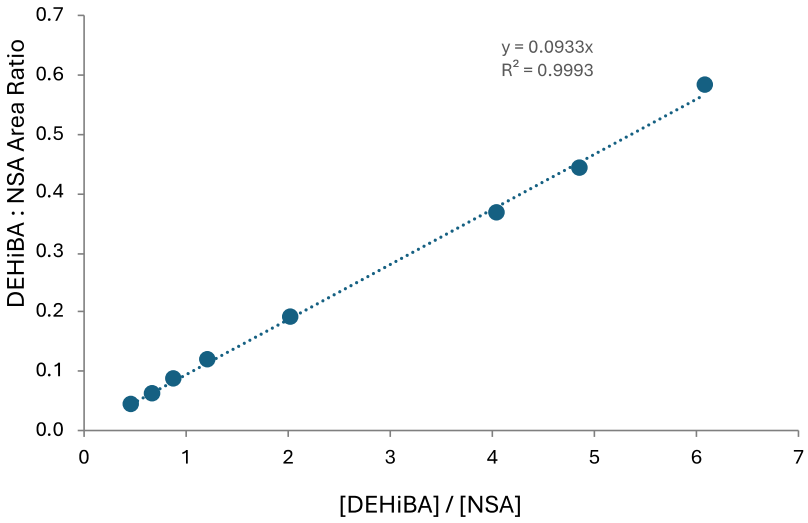

Figure S29: Calibration of DEHiBA with and without sodium naphthalenesulfonate (NSA), via HPLC analysis.

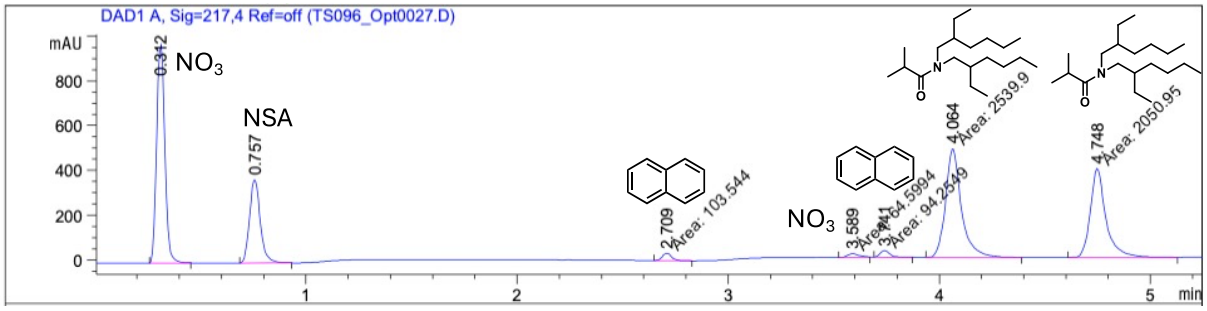

Figure S30: Example HPLC chromatogram for the purifications.

DEHiBA loss was determined by first calculating the volume change for each purification. NSA was used to do this by normalising the peak area using the aqueous flow rate, the difference in peak area and thus concentration allowed quantification of volume change, this was validated via Figure S28. The concentration of DEHiBA in the aqueous phase could then be quantified and verified via calibrations in Figure S29.

The percentage loss of DEHiBA from the organic phase can then be determined by converting the starting concentration of DEHiBA from moles per litre to grams per minute the same can be done for the aqueous concentration of DEHiBA, the percentage loss can then be calculated accounting for the difference in volume of the two phases.

Purity was quantified by diluting samples with external standard prior to GC-FID analysis. Calibration curves of all components (Figure S26) enabled quantification of concentrations for each component and from this the product purity.

Crude DEHiBA

Previous synthetic optimisation of DEHiBA identified an optimum route and two optimum conditions which underwent further testing in the form of continuous manufacture to generate crude DEHiBA for this work (Figure S31).

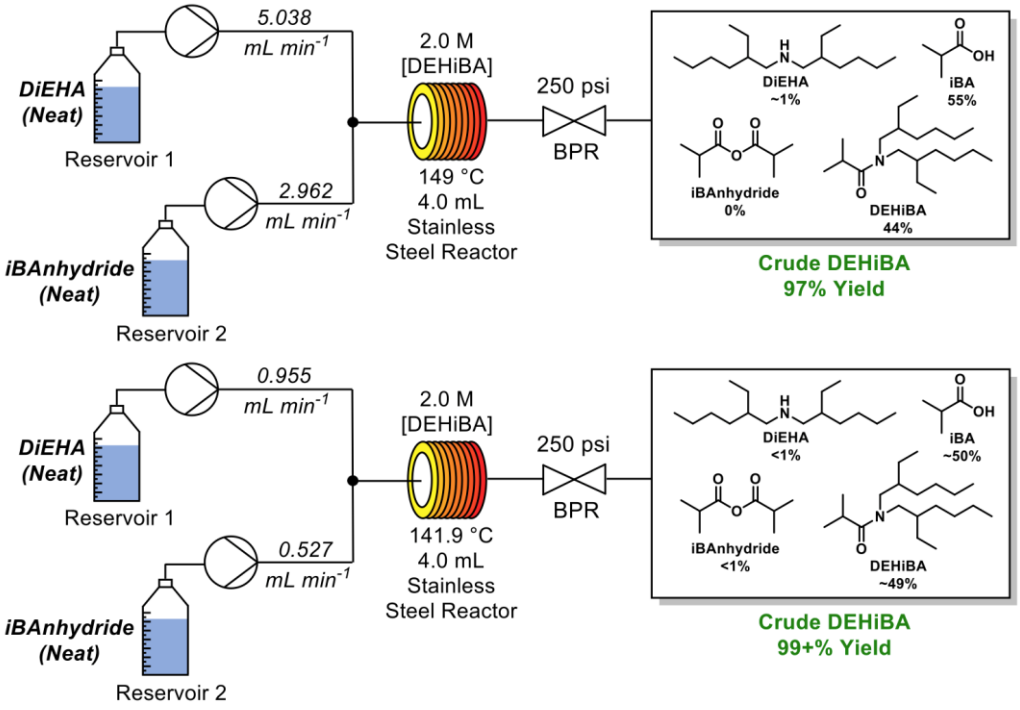

Figure S31: Two routes to crude DEHiBA of differing composition for purification optimisation. The first was used in the batch purification screening whilst the second was used in the continuous flow purification optimisations.

Batch studies were conducted prior to any flow chemistry to ensure homogeneity and identify a suitable route to optimise in continuous flow. A range of common bases and acids were screened for the purification of the lower yield crude product from Figure S31 (Top). Complete data from these acid and base screens can be found below:

Batch Purification Data

Table S14: Purity and composition data for the organic DEHiBA phase before and after contact with saturated sodium bicarbonate and 1 M sodium hydroxide solutions, the ratio of organic to base is varied throughout alongside the inclusion of hexane.

Sample	Volume Ratio and Composition	Purity (%)	mol% DiEHA wrt DEHiBA	mol% iBA wrt DEHiBA
Stock	Crude DEHiBA	44.6	3.0	121.1
Stock	Crude DEHiBA	44.0	2.9	125.4
Stock	Crude DEHiBA	43.0	2.8	129.9
P1	2:1 DEHiBA : sat. $NaHCO_3$	54.8	2.6	79.8
P1.1	1:1 DEHiBA : sat. NaHCO3	85.4	3.3	13.7
P3	1:1 DEHiBA : sat. $NaHCO_3$	83.6	2.5	17.2
P3.1	1:2 DEHiBA : sat. $NaHCO_3$	97.6	2.4	0.0
P6	1:2 DEHiBA : sat. $NaHCO_3$	95.5	2.6	2.2
P6.1	1:3 DEHiBA : sat. $NaHCO_3$	97.6	2.4	0.0
P4	1:1:1 DEHiBA : hexane : sat. $NaHCO_3$	84.1	2.3	16.6
P4.1	1:1:2 DEHiBA : hexane : sat. $NaHCO_3$	97.8	2.2	0.0
P7	1:1:2 DEHiBA : hexane : sat. $NaHCO_3$	95.9	2.5	1.8
P7.1	1:1:3 DEHiBA : hexane : sat. $NaHCO_3$	97.8	2.2	0.0
P2	2:1:1 DEHiBA : hexane : NaOH	83.0	2.6	17.9
P2.1	2:1:2 DEHiBA : hexane : NaOH	85.8	2.2	14.4
P5	1:1 DEHiBA : NaOH	97.5	2.6	0.0
P5.1	1:2 DEHiBA : NaOH	97.7	2.4	0.0
P8	1:2 DEHiBA : NaOH	97.6	2.5	0.0
P8.1	1:3 DEHiBA : NaOH	97.7	2.4	0.0
P9	1:1:1:1 DEHiBA : hexane : NaOH : $NaHCO_3$	97.7	2.3	0.0
P10	1:1:2:2 DEHiBA : hexane : NaOH : $NaHCO_3$	97.8	2.2	0.0

Table S15: Batch purifications with alternative bases.

	Composition	Purity (%)	mol% DiEHA wrt DEHiBA	mol% iBA wrt DEHiBA
P9	1:1:1:1 DEHiBA:hexane: NaOH: NaHCO3	97.7	2.3	0.0
P10	1:1:2:2 DEHiBA:hexane: NaOH: NaHCO3	97.8	2.2	0.0
P11	1:1:0.5:1 DEHiBA:hexane: methylamine 2M (THF): water	91.1	2.2	7.6
P12	1:1:1:1 DEHiBA:hexane: methylamine 2M (THF): water	98.0	2.1	0.0
P13	1:1:1 DEHiBA:hexane: ammonium hydroxide	97.9	2.2	0.0
P14	1:1:1:2 DEHiBA:hexane: pyridine (org): water	81.6	2.0	20.6

Table S16: Purity and composition data for the organic DEHiBA phase before and after contact with the various acids with and without hexane and acetonitrile, varying the volume ratio of these reagents as detailed.

Sample	Volume Ratio and Composition	Purity (%)	mol% DiEHA wrt DEHiBA	mol% iBA wrt DEHiBA
Stock	Crude DEHiBA	44.6	3.0	121.1
Stock	Crude DEHiBA	44.0	2.9	125.4
Stock	Crude DEHiBA	43.0	2.8	129.9
PH1	1:1 DEHiBA : 2M HNO_3	73.1	2.4	34.3
PH1.1	1:2	70.2	2.4	39.8
PH1.2	1:3	76.6	2.4	28.2
PH2	1:1:1 DEHiBA : hexane : 2M HNO_3	75.9	2.2	29.6
PH2.1	1:1:2	74.0	2.2	32.9
PH2.2	1:1:3	73.7	2.2	33.5
Ph7	1:1:1 DEHiBA : MeCN : 2M HNO_3	83.5	2.0	17.7
PH7.1	1:1:2	75.7	2.2	29.9
PH7.2	1:1:3	76.2	2.3	28.9
PH8	1:1:1:1 DEHiBA : hexane : MeCN : 2M HNO_3	87.9	1.3	12.5
PH8.1	1:1:1:2	78.9	1.9	24.9
PH8.2	1:1:1:3	77.8	2.1	26.5
PH3	1:1 DEHiBA : 10% H_2SO_4	67.8	2.2	45.2
PH3.1	1:2	66.1	2.2	49.2
PH3.2	1:3	67.5	2.2	45.9
PH4	1:1:1 DEHiBA : hexane : 10% H_2SO_4	70.7	2.0	39.4
PH4.1	1:1:2	68.9	1.9	43.1
PH4.2	1:1:3	71.5	1.9	38.0
PH9	1:1:1 DEHiBA : MeCN : 10% H_2SO_4	76.1	1.6	29.8
PH9.1	1:1:2	72.2	1.6	36.9
PH9.2	1:1:3	71.5	1.8	38.0
PH10	1:1:1:1 DEHiBA : hexane : MeCN : 10% H_2SO_4	80.3	1.1	23.5
PH10.1	1:1:1:2	75.7	1.4	30.7
PH10.2	1:1:1:3	74.9	1.9	31.7
PH5	1:1 DEHiBA : Sat. NH_4Cl	65.8	2.4	49.7
PH5.1	1:2	64.3	2.4	53.1
PH5.2	1:3	66.5	2.1	48.3
PH6	1:1:1 DEHiBA : hexane : Sat. NH_4Cl	68.8	2.3	43.0
PH6.1	1:1:2	66.8	2.2	47.6
PH6.2	1:1:3	65.2	2.3	51.1
PH11	1:1:1 DEHiBA : MeCN : Sat. NH_4Cl	68.6	2.2	43.6
PH11.1	1:1:2	67.2	2.2	46.7
PH11.2	1:1:3	68.0	2.3	47.2
PH12	1:1:1:1 DEHiBA : hexane : MeCN : Sat. NH_4Cl	69.5	2.2	41.6
PH12.1	1:1:1:2	73.3	1.7	34.7
PH12.2	1:1:1:3	70.5	2.1	39.8

Table S17: Purity and composition data for the organic DEHiBA phase after contact with nitric acid, hexane, and acetonitrile, varying the volume ratio of these reagents.

Sample	Volume Ratio and Composition	Purity (%)	mol% DiEHA wrt DEHiBA	mol% iBA wrt DEHiBA
PH13	2:1:1:1 DEHiBA : hexane : MeCN : HNO_3	67.4	2.1	46.4
PH13.1	2:1:1:2	69.5	2.2	41.7
PH13.2	2:1:1:3	72.0	2.2	36.7
PH14	1:1:2:1 DEHiBA : hexane : MeCN : HNO_3	89.1	0.0	12.3
PH14.1	1:1:2:2	87.6	1.2	12.9
PH14.2	1:1:2:3	85.2	1.9	15.5
PH18	1:2:1 DEHiBA : MeCN : HNO_3	80.4	1.1	23.2
PH18.1	1:2:2	80.1	1.6	23.3
PH18.2	1:2:3	80.0	1.9	23.1
PH17	1:1:1 DEHiBA : MeCN : HNO_3	73.3	2.0	34.4
PH17.1	1:2:1	81.0	1.0	22.5
PH17.2	1:3:1	86.1	0.6	15.6
PH16	1:1:1:0.5 DEHiBA : hexane : MeCN : HNO_3	63.0	2.2	56.6
PH16.1	1:1:2:0.5	79.7	0.7	24.7
PH16.2	1:1:3:0.5	90.1	0.0	10.9
PH15	1:1:3:1 DEHiBA : hexane : MeCN : HNO_3	95.2	0.0	5.1
PH15.1	1:1:4:1	100.0	0.0	0.0
PH15.2	1:1:5:1	100.0	0.0	0.0

Purifications in Continuous Flow

Tables S18: Upper and lower parameter bounds for all self-optimisations.

	Crude DEHiBA Flow Rate (mL min^{-1})	MeCN Flow Rate (mL min^{-1})	Water Flow Rate (mL min^{-1})
Lower bound	0.5	0.5	0.5
Upper bound	5	10	5

Nitric Acid, Acetonitrile Purifications

This purification used the flow setup illustrated in Figure S32 to initially optimise purity with the BOAEI algorithm, then purity and product loss with the TSEMO algorithm and finally purity and product loss using a weighted objective with the BOAEI algorithm.

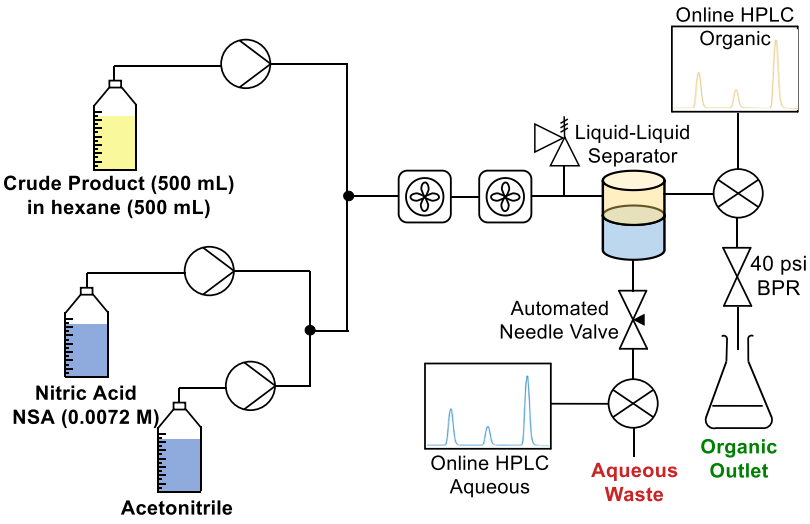

Figure S32: Continuous purification system for optimising the purification of DEHiBA with nitric acid and acetonitrile.

Reservoir solutions were prepared to the desired concentrations by dissolution in the desired medium with stirring at ambient conditions.

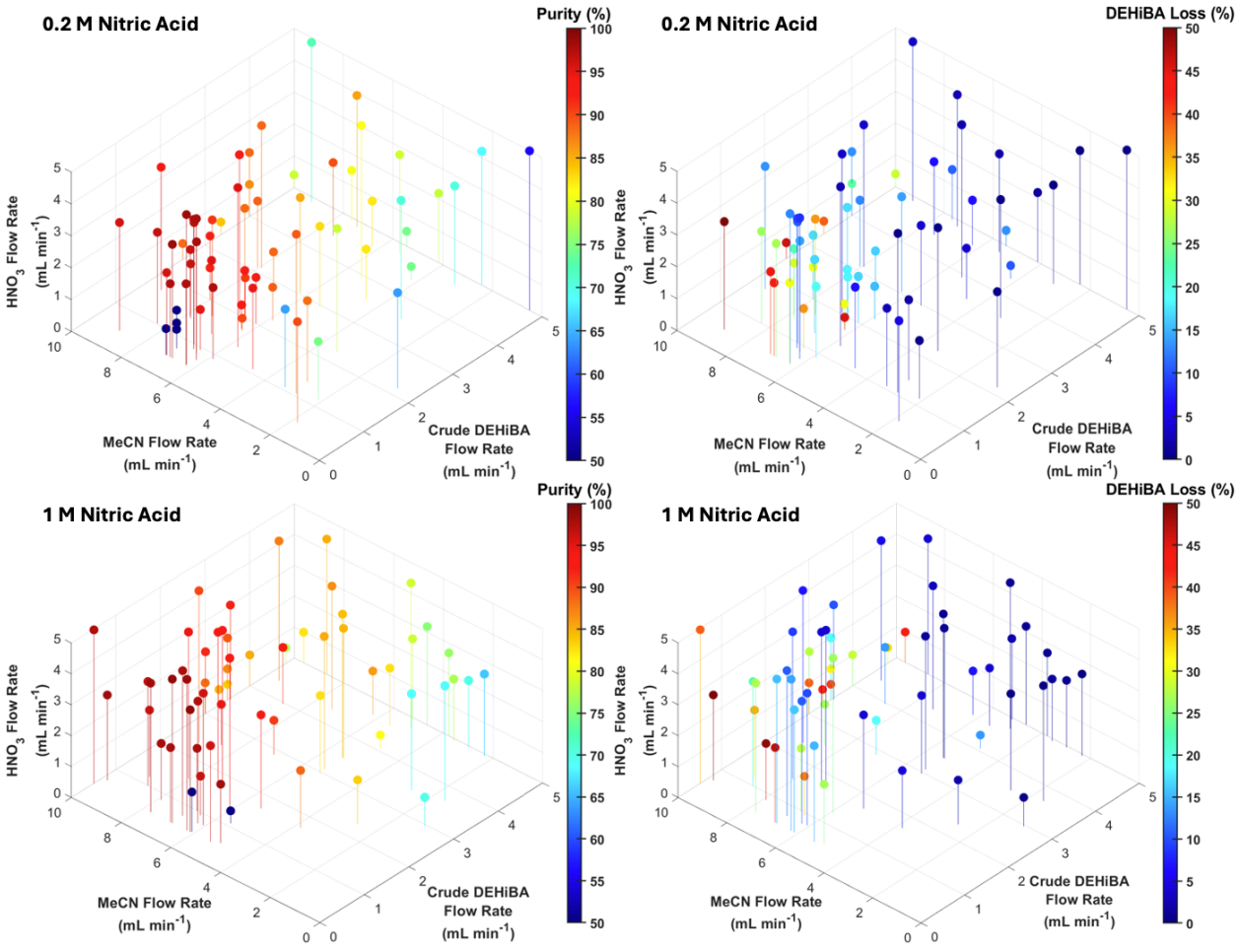

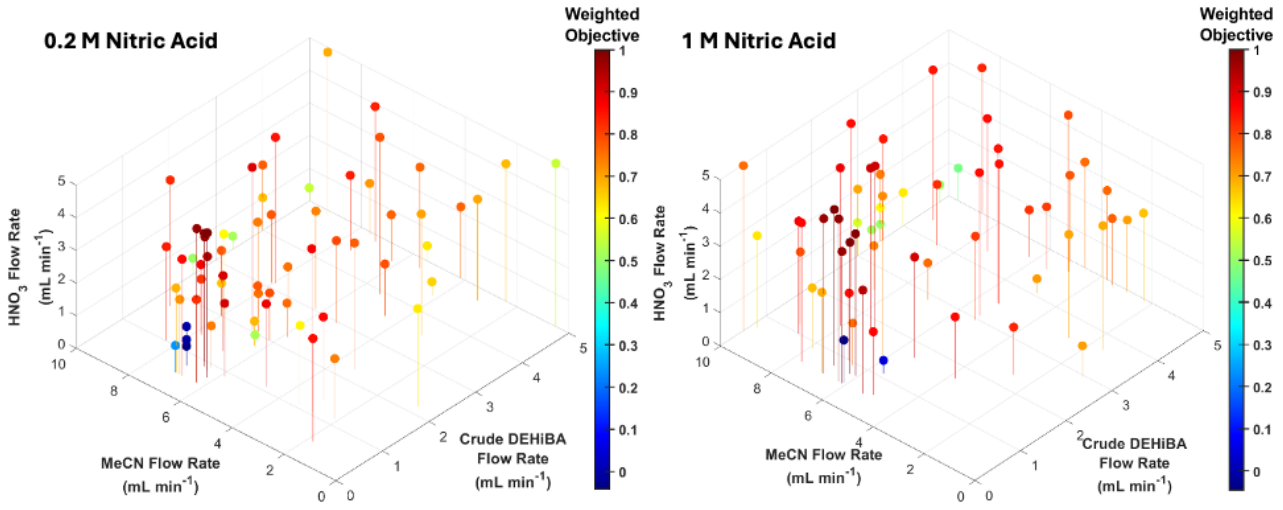

Figure S33: Purity and product loss comparisons between optimisations with 0.2 M and 1 M nitric acid, with weighted objective plots highlighting the optimum conditions for each optimisation. The number of datapoints has been reduced for ease of visualisation.

Table S19: Performance comparison of the optimal Pareto conditions for the purification with acetonitrile and 0.2 M nitric acid.

Crude DEHiBA Flow Rate (mL min^{-1})	MeCN Flow Rate (mL min^{-1})	0.2 M HNO_3 Flow Rate (mL min^{-1})	MeCN:HNO_3 Flow Ratio	Purity (%)	DEHiBA Loss (%)	Aqueous: Organic Ratio
1.575	5.387	5.000	1.08	94.0	1.5	6.6
1.370	5.746	5.000	1.15	95.4	2.3	7.8
1.481	5.803	2.569	2.26	95.9	9.9	5.7
0.888	6.659	4.071	1.64	97.4	9.6	12.1
0.727	6.239	4.270	1.46	97.8	8.8	14.5
0.705	6.226	4.431	1.41	97.8	8.5	15.1
0.518	6.291	4.703	1.34	98.6	12.7	21.2

Table S20: Performance comparison of the optimal Pareto conditions for the purification with acetonitrile and 1 M nitric acid.

Crude DEHiBA Flow Rate (mL min^{-1})	MeCN Flow Rate (mL min^{-1})	1 M HNO_3 Flow Rate (mL min^{-1})	MeCN:HNO_3 Flow Ratio	Purity (%)	DEHiBA Loss (%)	Aqueous: Organic Ratio
1.570	6.421	5.000	1.28	93.3	3.3	7.3
1.774	7.104	4.983	1.43	93.7	3.8	6.8
1.681	7.118	5.000	1.42	94.1	4.0	7.2
0.769	6.071	4.272	1.42	96.3	9.9	13.4
0.750	6.256	3.958	1.58	97.4	10.6	13.6
0.750	6.869	4.696	1.46	97.8	10.7	15.4

Water, Acetonitrile Purification Optimisations

This purification used the flow setup illustrated in Figure S34 to optimise purity and product loss using a weighted objective with the BOAEI algorithm.

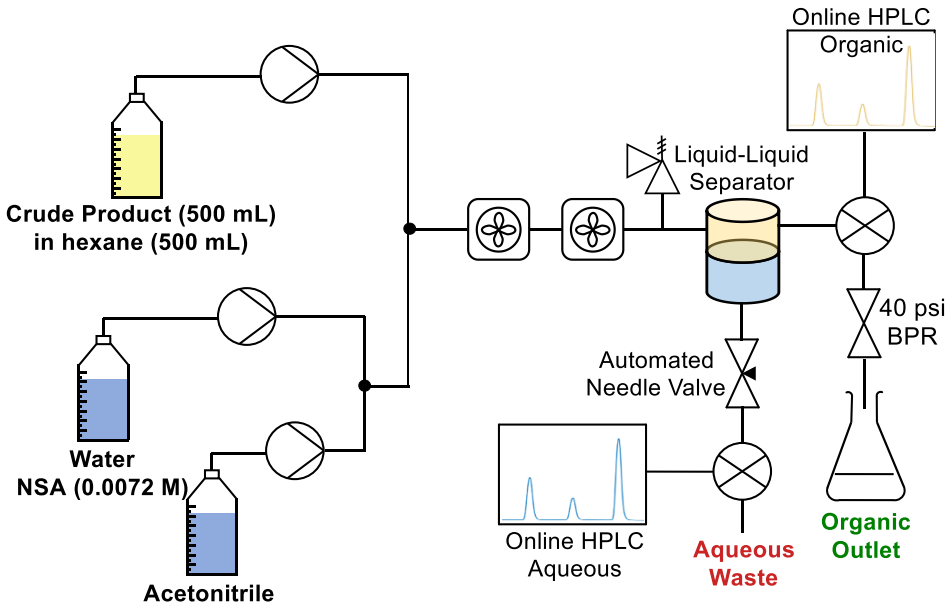

Figure S34: Continuous purification system for optimising the purification of DEHiBA with water and acetonitrile.

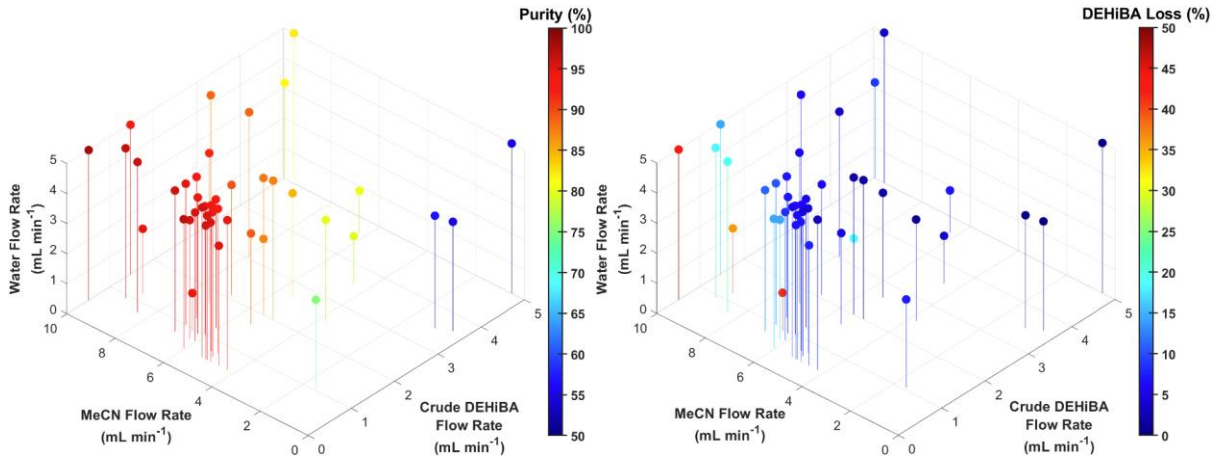

Figure S35: Purity and product loss 4D data plots for purification optimisations with water and acetonitrile.

As this optimisation explored the design space less than the nitric acid extractions, the data was modelled to better understand the interactions between parameters and validate our

understanding of this purification route. A quadratic linear regression model was used, the data was first logged then 90% of the data was used to train the model and 10% to validate with good prediction. This provided a 0.99 R-squared value and a 1.05 root mean squared error for the purity data, the product loss data was poorer, providing a 0.94 R-squared and a 3.15 root mean squared error. The poorer fit of the product loss model is likely due to the reduced spread of data, with most between 0-20% DEHiBA loss, whereas the purity data albeit skewed to high purity has a greater spread of purities across the design space. These models allow better understanding of the design space so that parameter interactions can be identified or verified. These models (Figure S36) confirm the influence of water on the loss of DEHiBA but no influence on the overall purity.

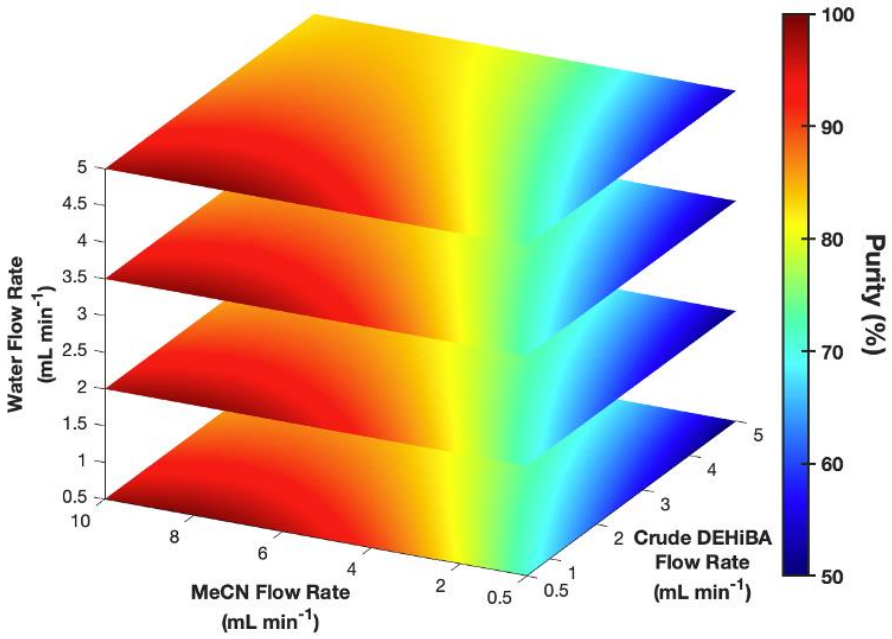

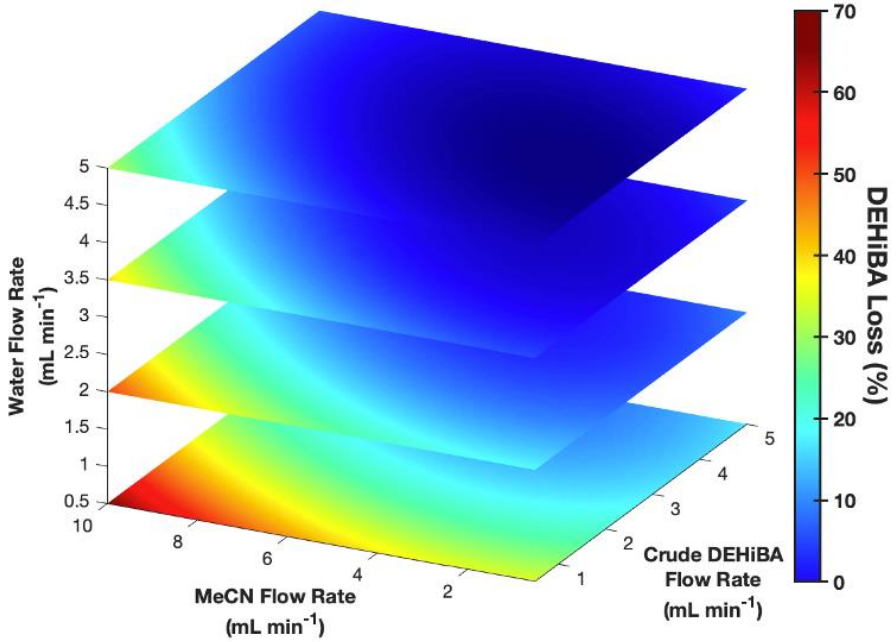

Figure S36: Quadratic linear regression models for purity and DEHiBA loss using the data from the purifications with water and acetonitrile.

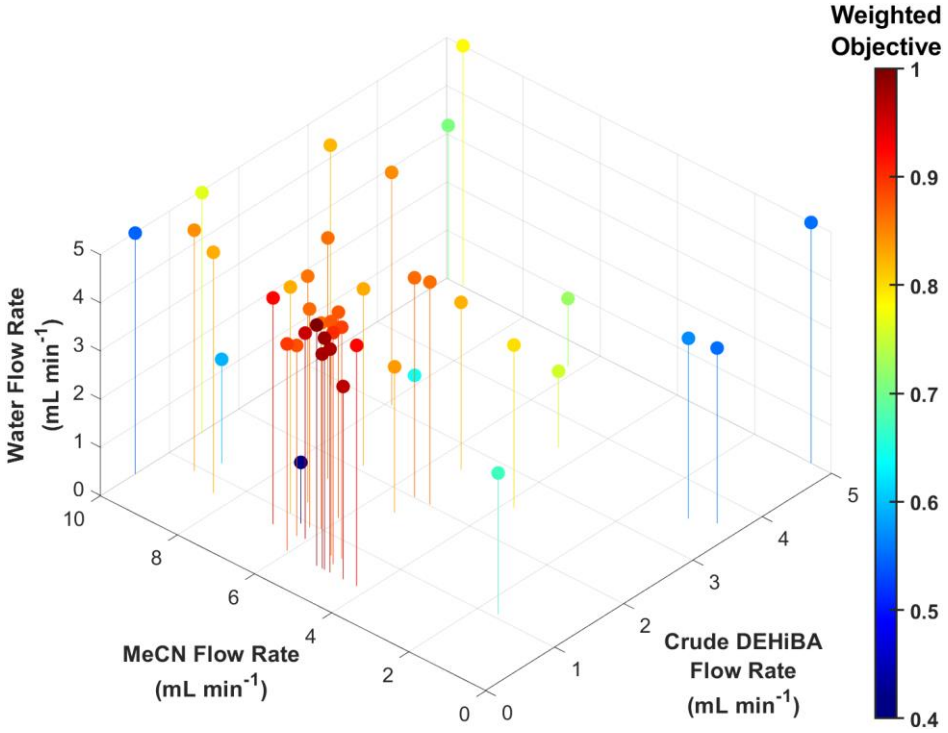

Figure S37: The optimum conditions for the purifications with water and acetonitrile, using the weighted objective as a visual aid.

0.4 M sodium bicarbonate, Acetonitrile Purifications

This purification used the flow setup illustrated in Figure S38 to optimise purity and product loss using a weighted objective with the BOAEI algorithm.

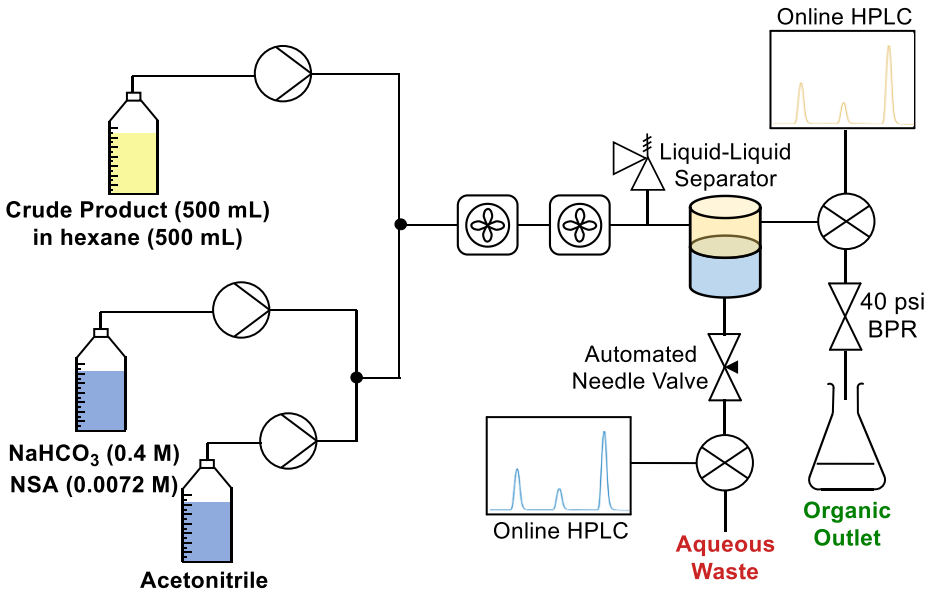

Figure S38: Continuous purification system for optimising the purification of DEHiBA with 0.4 M sodium bicarbonate and acetonitrile.

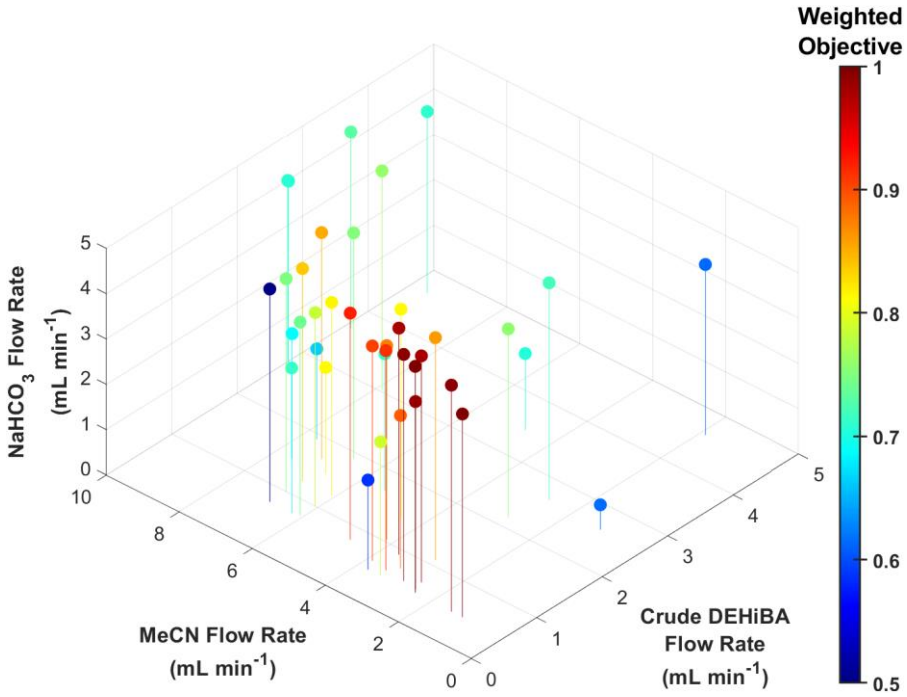

Figure S39: Purity and product loss 4D data plots along with weighted objective data for purifications with 0.4 M sodium bicarbonate and acetonitrile.

The purity data has again been modelled to visualise and better understand the parameter interactions for this parameter space. Figure S40 illustrates the benefit of increasing the amount of sodium bicarbonate for product purity. This was not the case for purifications with water or nitric acid. The R-squared for this model was 0.97 and the root mean square was 1.46 providing confidence in the model. The model for DEHiBA loss gave poor confidence with an R-squared of 0.77 so this was not used. It should be noted that R-squared should not be taken as a reliable indicator of goodness of fit on its own, instead it may reflect contributions from scatter in the data as well as quality of the fit. However, given the models produced the author believes the models describe the design space well as observable trends are identifiable.

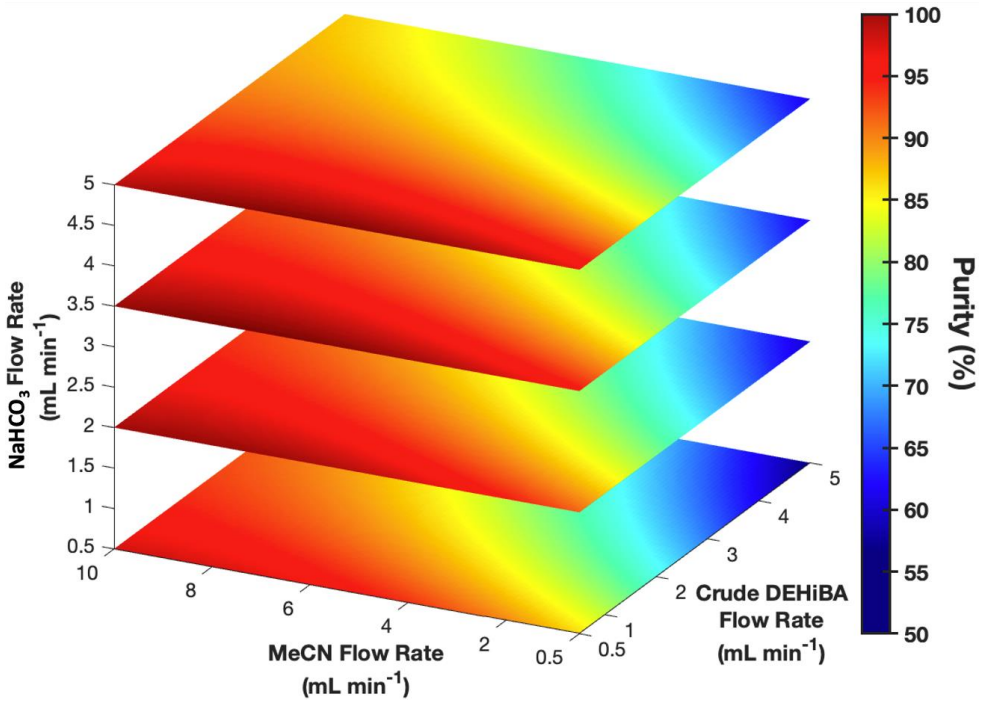

Figure S40: Quadratic linear regression model for product purity using the data from the purifications with sodium bicarbonate and acetonitrile.

An Optimised Manufacture Platform

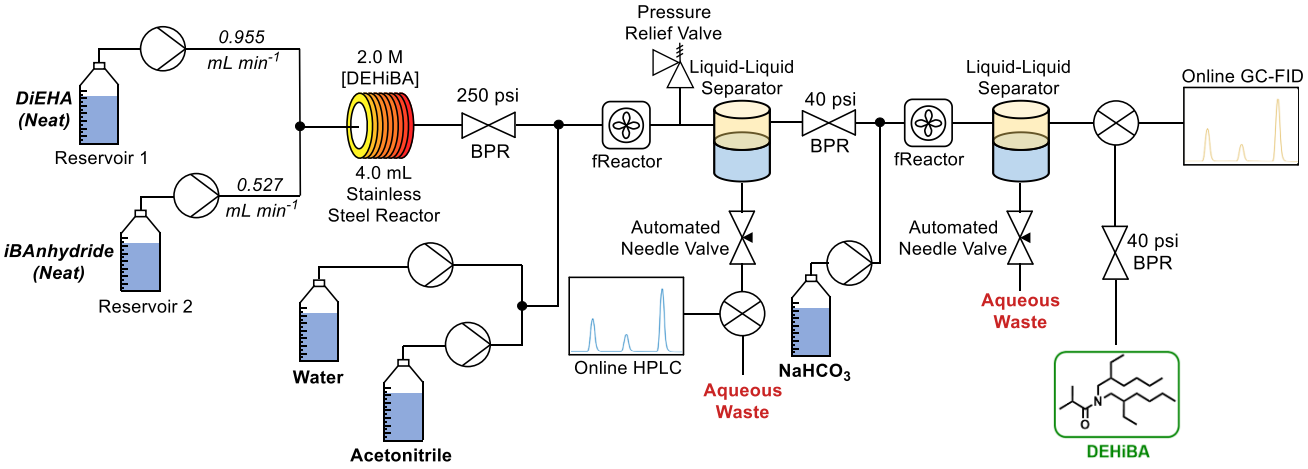

Figure S41: An optimised manufacture platform to generate pure DEHiBA on demand

6.3 Chapter 4 Supporting Information

DEHiBA Materials

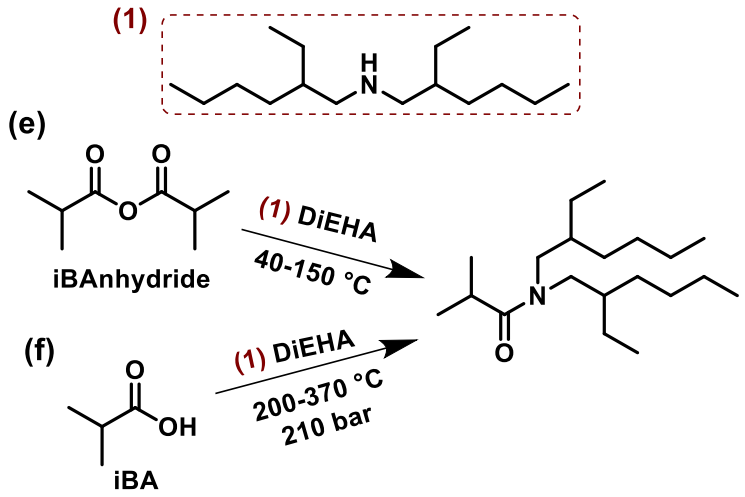

Scheme S7: Solvent-free synthetic pathways to DEHiBA referred to as routes (e) and (f) as described by T.Shaw *et al.*[156]

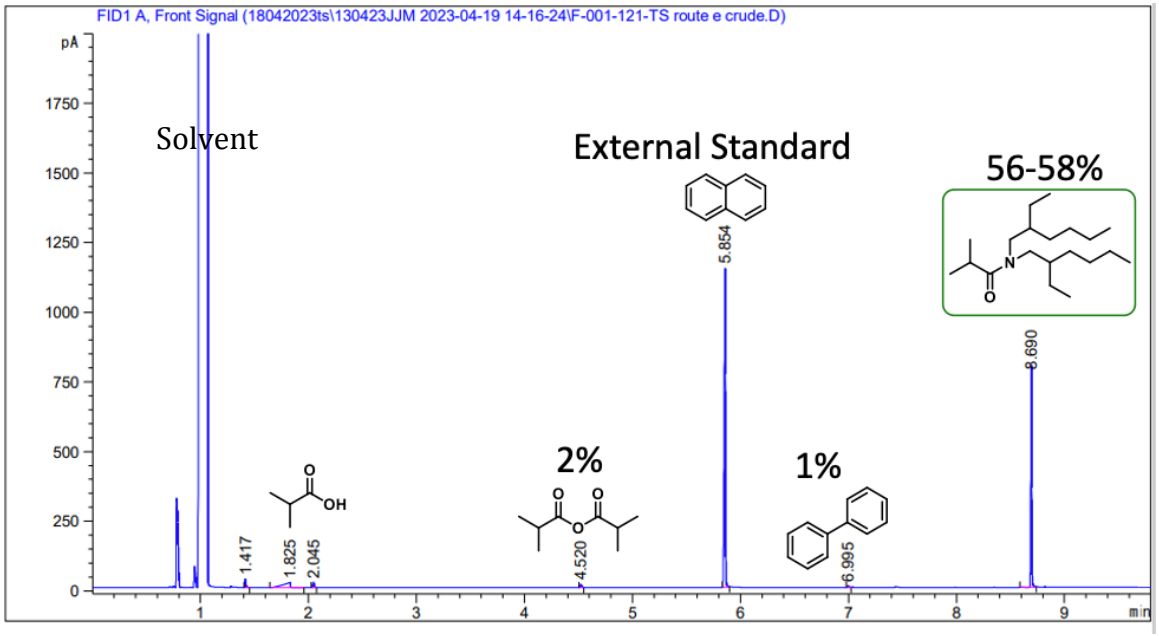

Figure S42: GC-FID trace for the crude e56 DEHiBA, a stock solution collected from the synthetic optimisation experiments for route (e). Percentages are determined by mass here, using naphthalene as the external standard.

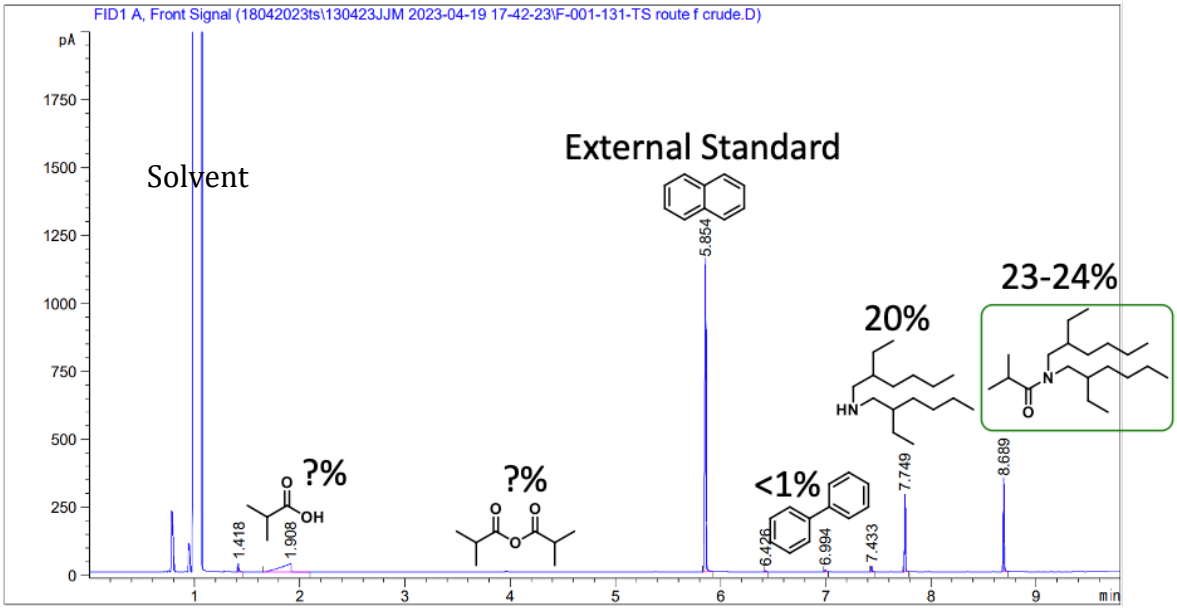

Figure S43: GC-FID trace for the crude f23 DEHiBA, a stock solution collected from the synthetic optimisation experiments for route (f). Percentages are determined by mass, using naphthalene as the external standard.

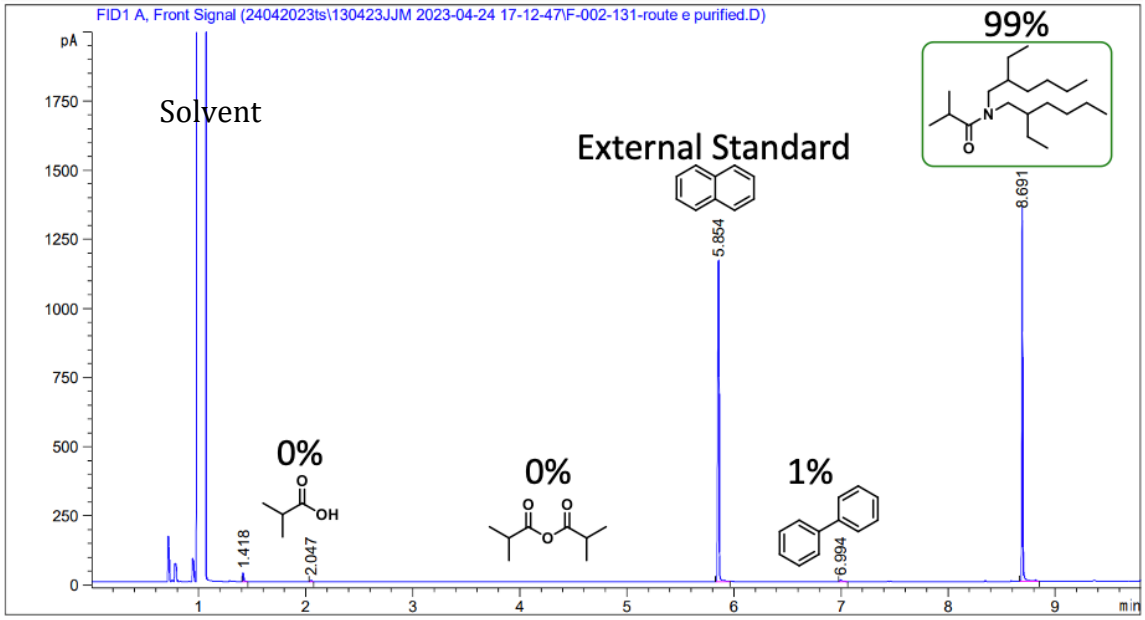

Figure S44: Quantitative GC-FID analysis of the purified DEHiBA (e99) from route (e), the only impurity being biphenyl, other signals being external standard and solvent. Purity is given as a weight percentage.

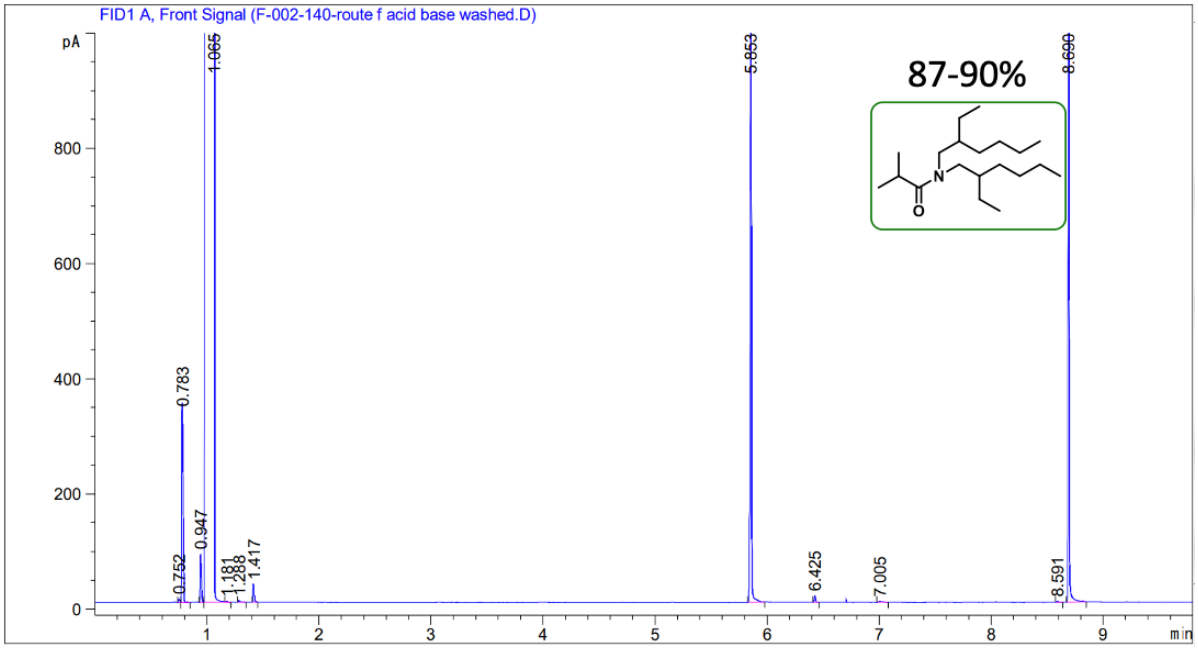

Figure S45: GC-FID of the final 'purified' DEHiBA (f88) following base and acid washes, purity is given as a weight percentage.

The degradation products were not isolated, synthesised or purchased for calibrations, it is unlikely 3-methylheptane and biphenyl account for 10% of the purity by weight. Instead, it is more likely that the remainder of the weight is entrained material such as nitric acid, or less likely could be methylamine.

Aqueous and Organic Uranium(VI) Calibrations

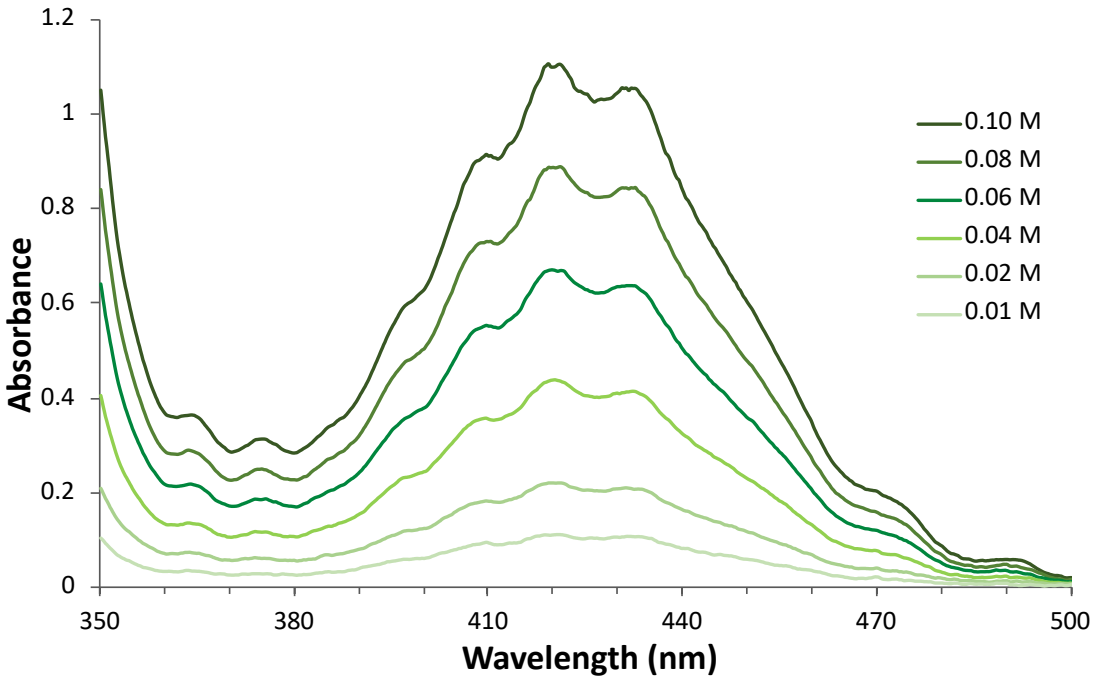

Figure S46: UV-Vis traces for a 350-500 nm wavelength range relevant to uranium(VI) illustrating the various uranium(VI) concentrations of aqueous uranyl nitrate in 4.0 M nitric acid for calibration.

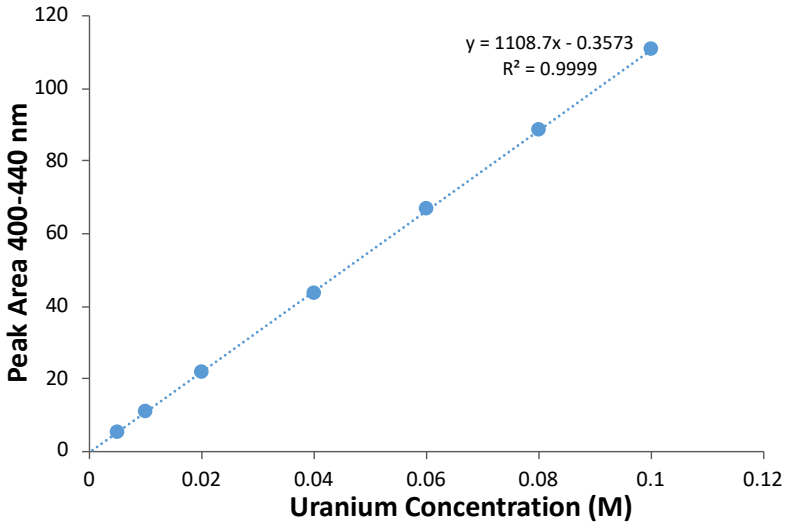

Figure S47: Calibration curve for the aqueous uranyl nitrate in 4.0 M nitric acid using the peak area between 400-440 nm.

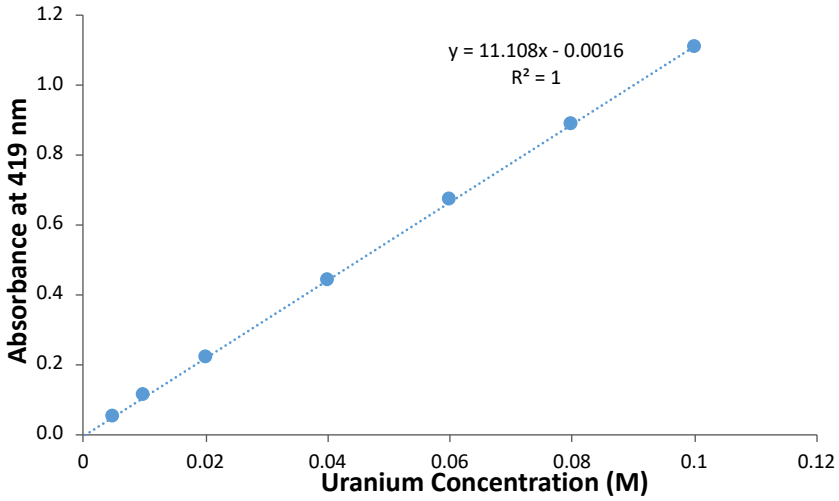

Figure S48: Calibration curve for the aqueous uranyl nitrate in 4.0 M nitric acid using the peak height at 419 nm.

OrgCal1 was calculated to contain 0.12 M of uranium(VI) (**Figure S**), however three phases were observed, a major organic phase, a small aqueous phase (likely from the hydrate), and finally a black/grey solid not observed in nitric acid dissolution.

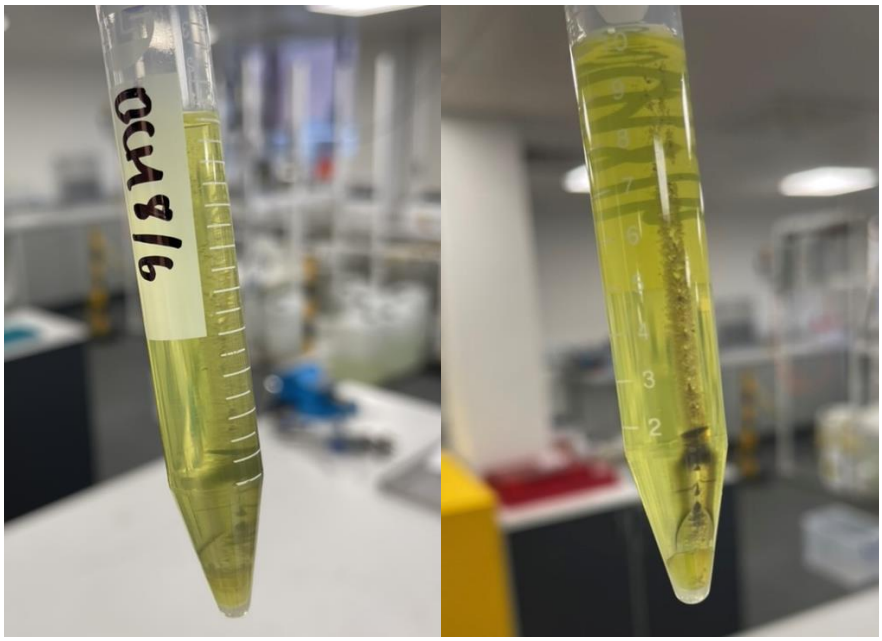

Figure S49: Three observed phases following direct dissolution of $UO_2(NO_3)_2.(H_2O)_6$ in 1.5 M e99 DEHiBA.

This lack of homogeneity adds complexity to this method and is likely to result in concentration inaccuracy, as it cannot be certain that all the uranium(VI) is in the organic phase.

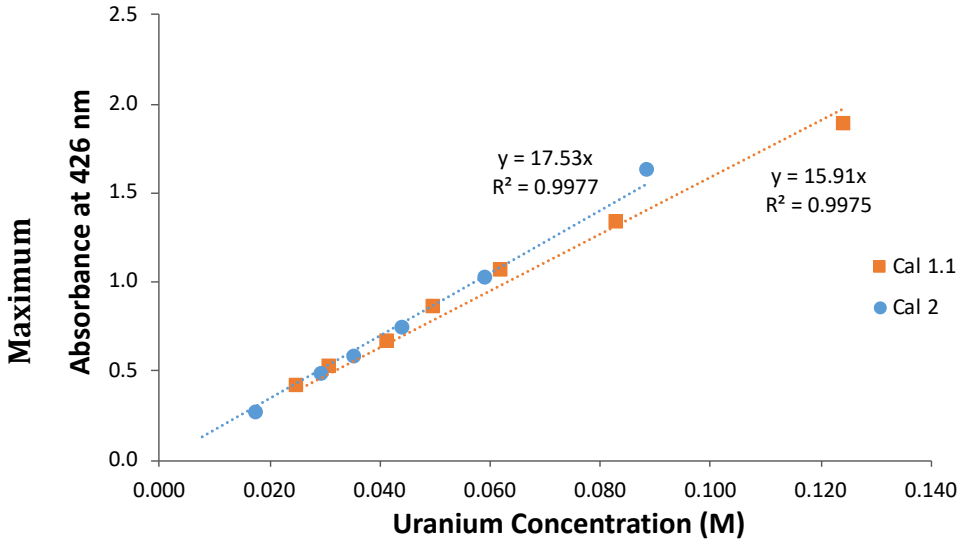

Figure S50: Comparison of organic calibration curves using max peak height from OrgCal1 and OrgCal2, direct dissolution and extraction methodologies respectively, with both using serial dilution.

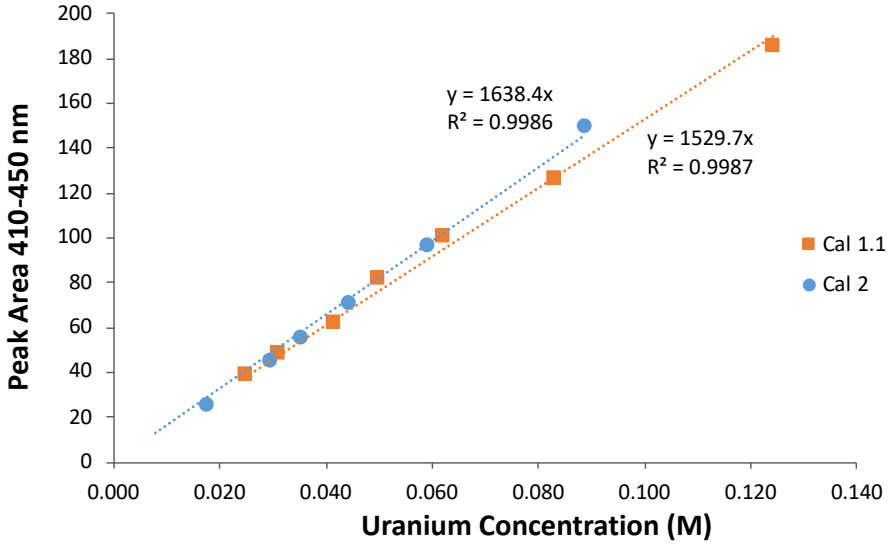

Figure S51: Comparison of organic calibration curves using peak area from OrgCal1 and OrgCal2, direct dissolution and extraction methodologies respectively, with both using serial dilution.

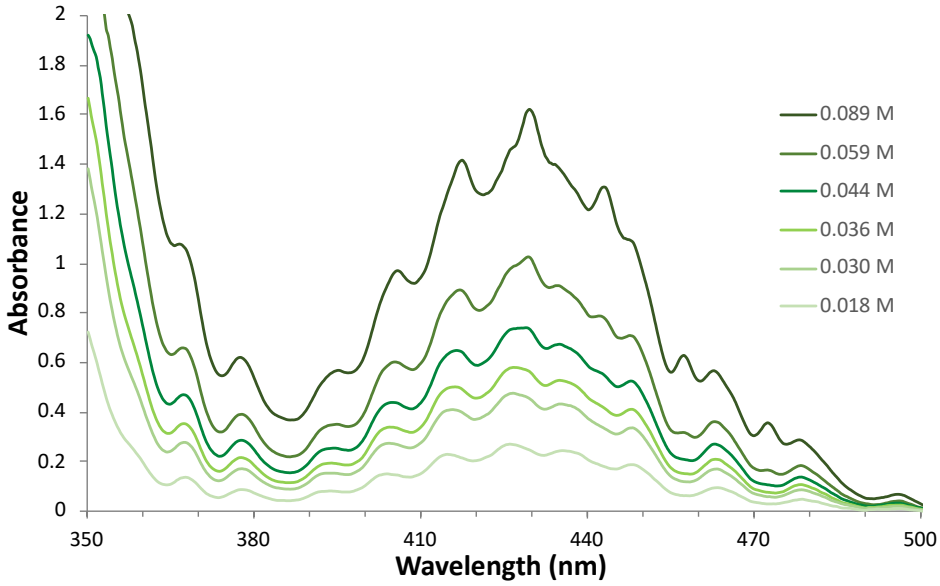

Figure S52: UV-Vis traces for varying organic uranium(VI) concentrations using the OrgCal2 method via uranium(VI) extraction from the aqueous phase using 1.5 M e99 DEHiBA in *n*-dodecane.

Testing the Performance of Different DEHiBA Compositions

Table S21: Uranium(VI) distribution ratios when extracting with high DEHiBA concentrations up to 2.73 M from 0.75 M at 15 and *22 °C, percentage mass balances are ± from 100%.

DEHiBA Sample	D_U From Max Abs	Molar Ratio of DEHiBA to U(VI)	Mass Balance (%)	D_U From Peak Area	Molar Ratio of DEHiBA to U(VI)	Mass Balance (%)
2.73 M e99 (neat)*	9.77	27.0	11.5	9.86	26.9	11.9
2.00 M e99*	11.62	20.2	7.4	11.34	20.5	6.3
1.50 M TC DEHiBA	8.04	16.7	0.9	7.97	16.8	0.4
1.50 M e99 (55% v/v)	8.03	16.0	5.5	8.07	15.9	6.2
1.49 M e99	7.85	16.5	2.1	7.80	16.5	2.1
1.25 M e99	5.45	14.7	0.8	5.58	14.5	1.8
1.00 M e99	3.56	12.8	0.0	3.66	12.5	2.1
0.75 M e99	2.00	11.4	-1.5	2.07	11.0	0.8
1.50 M Crude e56	8.02	16.9	5.0	7.86	16.9	4.4
1.25 M Crude e56*	4.78	13.2	2.4	4.85	13	1.3
1.00 M Crude e56	3.45	12.3	1.1	3.29	12.1	-1.7
0.86 M Crude e56	2.73	10.9	-1.7	2.61	10.6	-5.8
1.50 M f88	8.19	16.7	1.1	8.12	16.8	0.3
1.32 M f88	6.28	15.2	0.4	6.26	15.3	0.4
1.00 M f88	3.34	12.8	1.2	3.39	12.7	1.7
0.33 M Crude f23	0.68	8.2	-0.3	0.69	8.1	-0.4

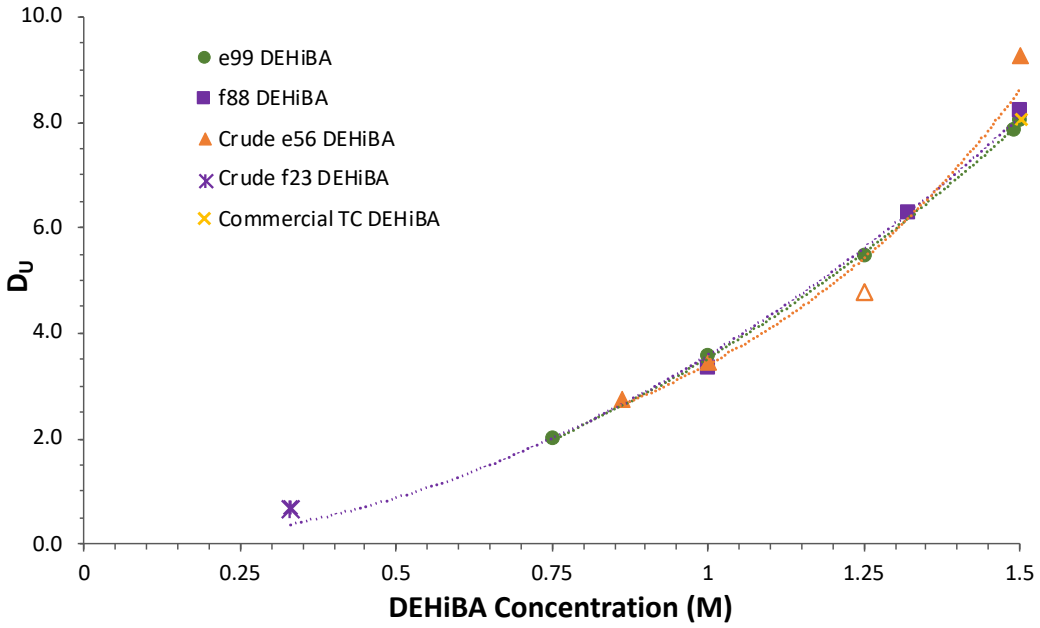

Figure S53: The effect of DEHiBA concentration on the distribution ratio of uranium(VI) comparing e99, crude e56, f88, and crude f24 solutions when using an equal volume of 0.1 M uranyl nitrate in 4.0 M nitric acid. The hollow triangle experiment at 1.25 M DEHiBA was conducted at 22 °C whilst all other experiments took place at 15 °C. The 1.50 M crude e56 measurement here illustrates the raw data without accounting for DiEHA absorbance.

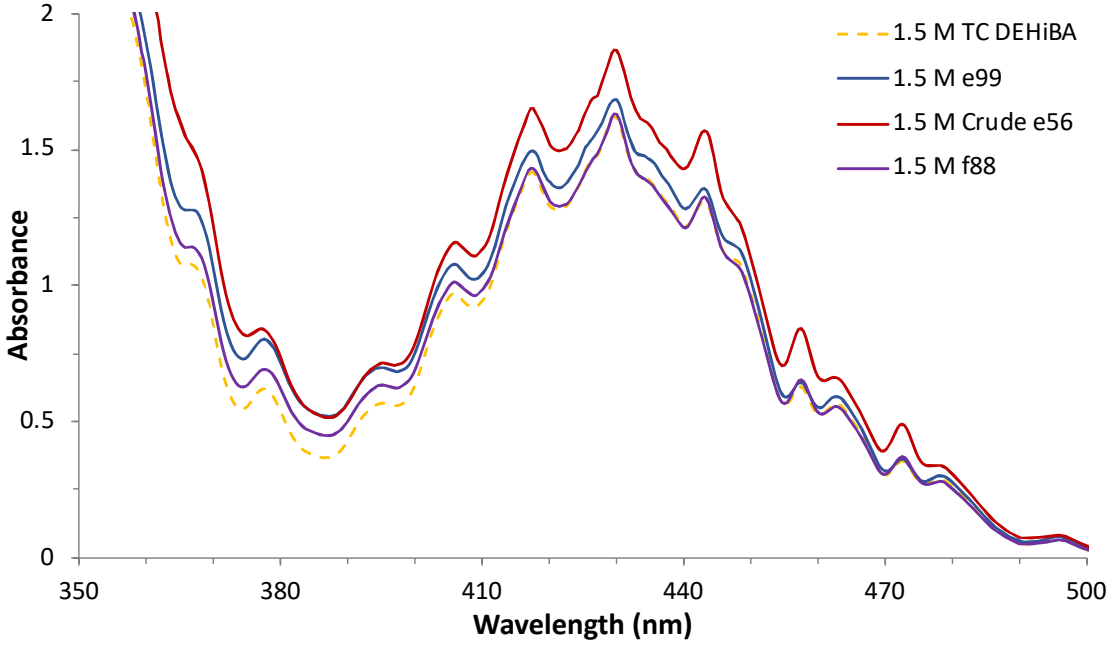

Figure S54: Organic UV-Vis traces following contact between 1.5 M DEHiBA solutions and 0.1 M uranyl nitrate in 4.0 M nitric acid at 15 °C using a 1:1 SA ratio.

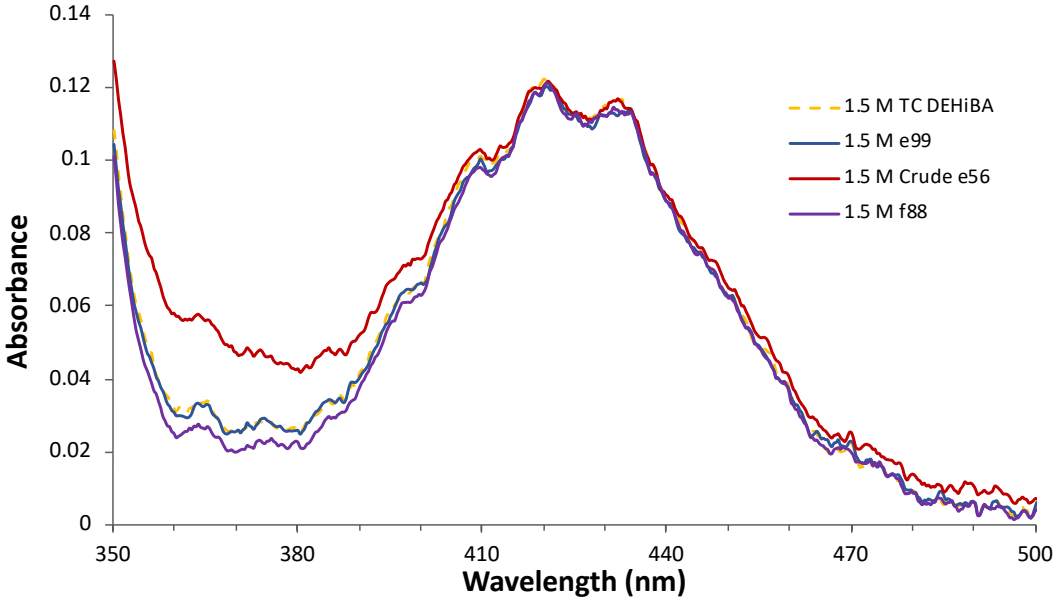

Figure S55: Aqueous UV-Vis analysis following contact between 1.5 M DEHiBA solutions and 0.1 M uranyl nitrate in 4.0 M nitric acid at 15 °C using a 1:1 SA ratio.

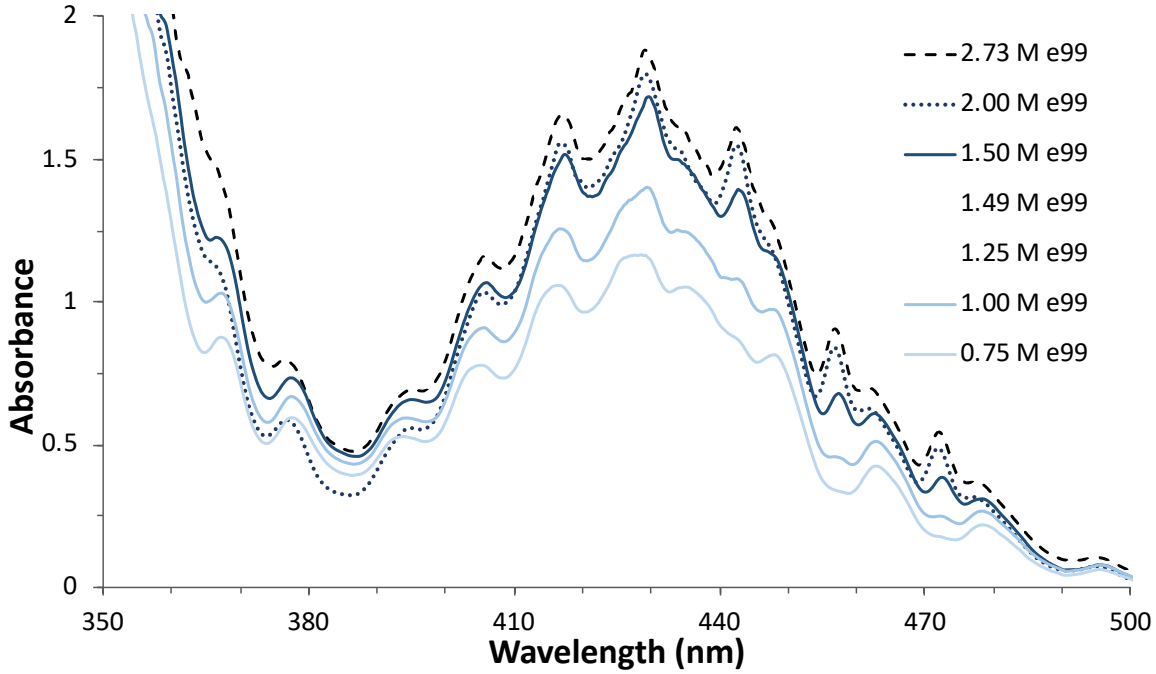

Figure S56: Organic UV-Vis spectra for the quantification of extracted uranium(VI) concentration in varying e99 DEHiBA concentrations. Illustrating increased uranium(VI) concentration with DEHiBA concentration.

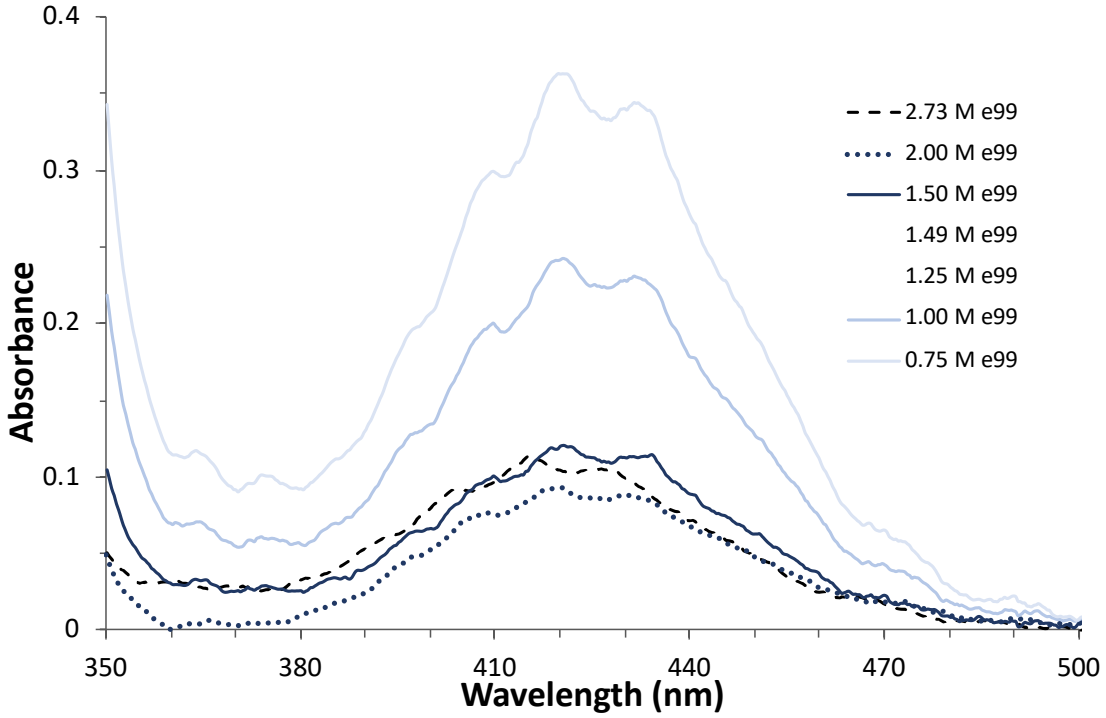

Figure S57: Aqueous UV-Vis spectra for the quantification of residual uranium(VI) concentration following contact with varying e99 DEHiBA concentrations. Illustrating the shift in wavelength for the neat DEHiBA extraction aqueous phase.

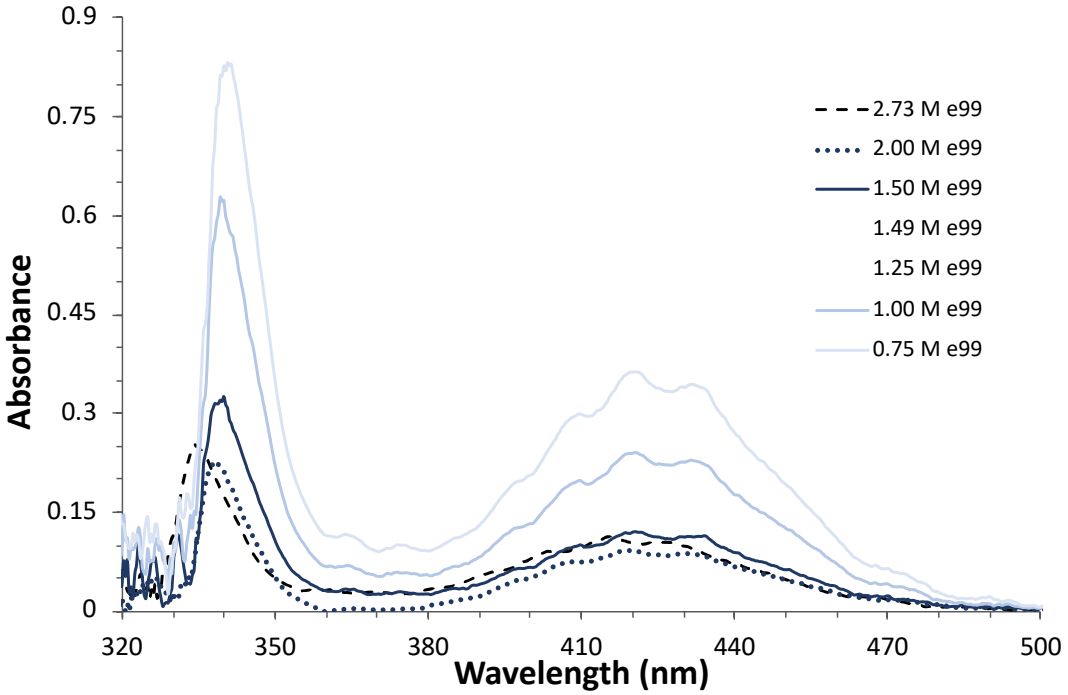

Figure S58: Aqueous UV-Vis spectra for the residual uranium(VI) and nitric acid following contact with varying e99 DEHiBA concentrations across a broader wavelength range.

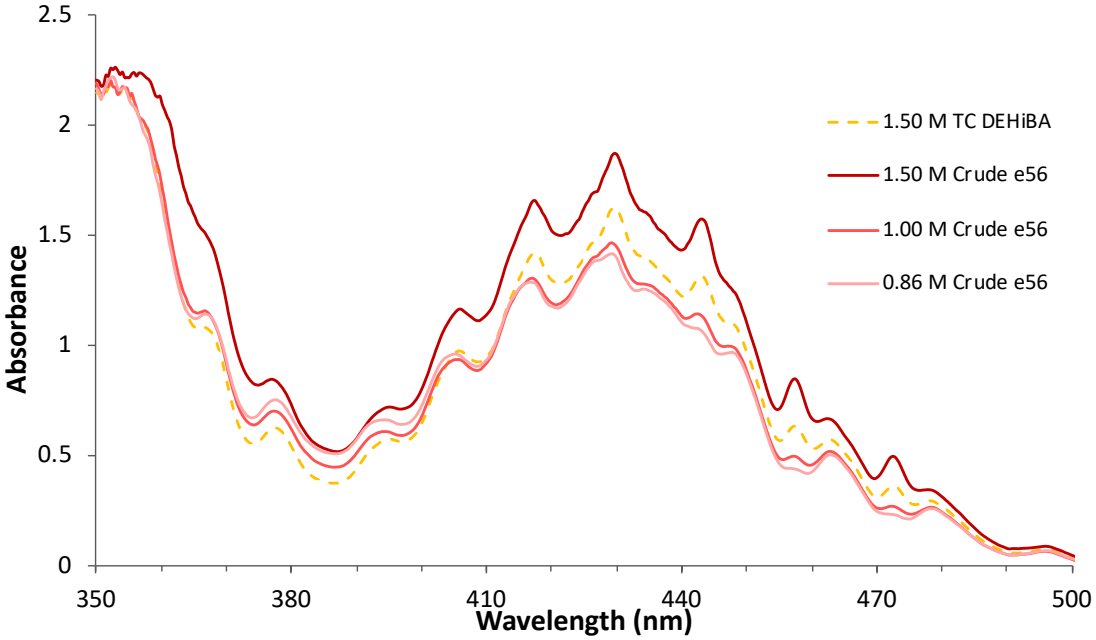

Figure S59: Organic UV-Vis spectra for the extraction of uranium(VI) with varying crude e56 DEHiBA concentrations. A 1:1 Sa ratio of 0.1 M uranyl nitrate solution in 4.0 M nitric acid was used for this extraction at 15 °C.

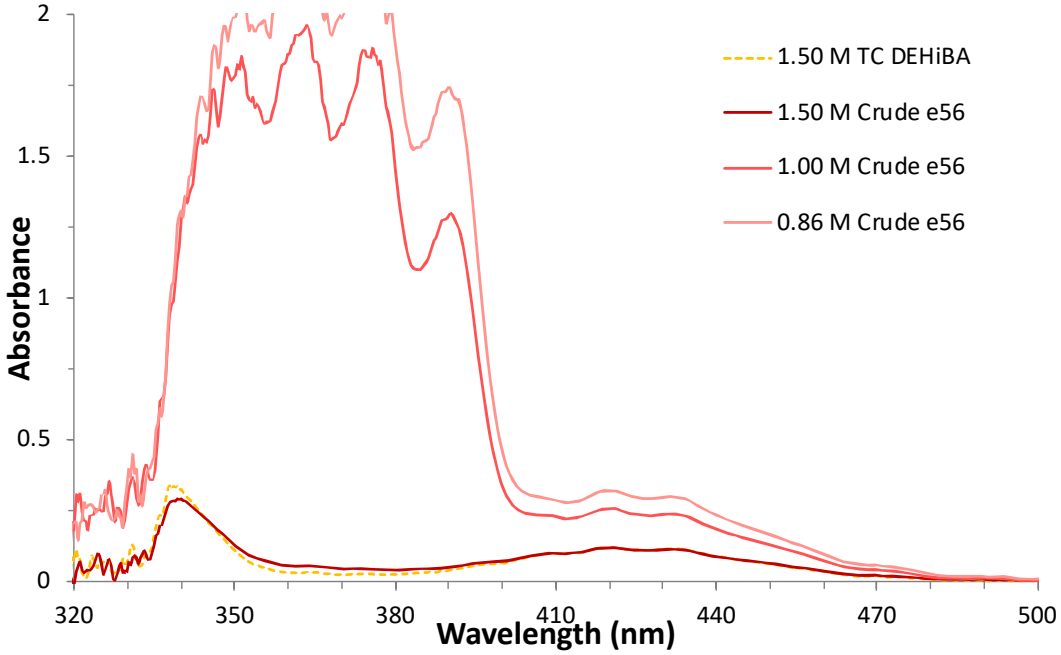

Figure S60: Aqueous UV-Vis spectra for the residual uranium(VI) following contact with varying crude (e) DEHiBA concentrations. A 1:1 Sa ratio of 0.1 M uranyl nitrate solution in 4.0 M nitric acid was used for this extraction at 15 °C.

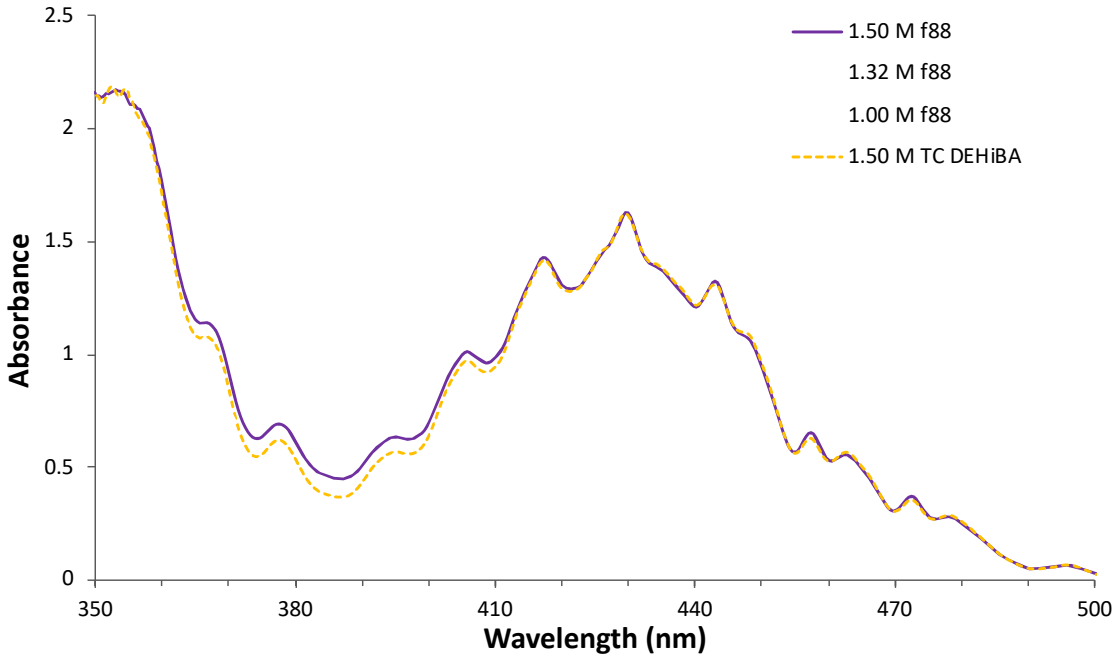

Figure S61: Organic UV-Vis spectra for the extraction of uranium(VI) with varying f88 DEHiBA concentrations when using 0.1 M uranyl nitrate in 4.0 M nitric acid with a 1:1 SA ratio at 15 °C.

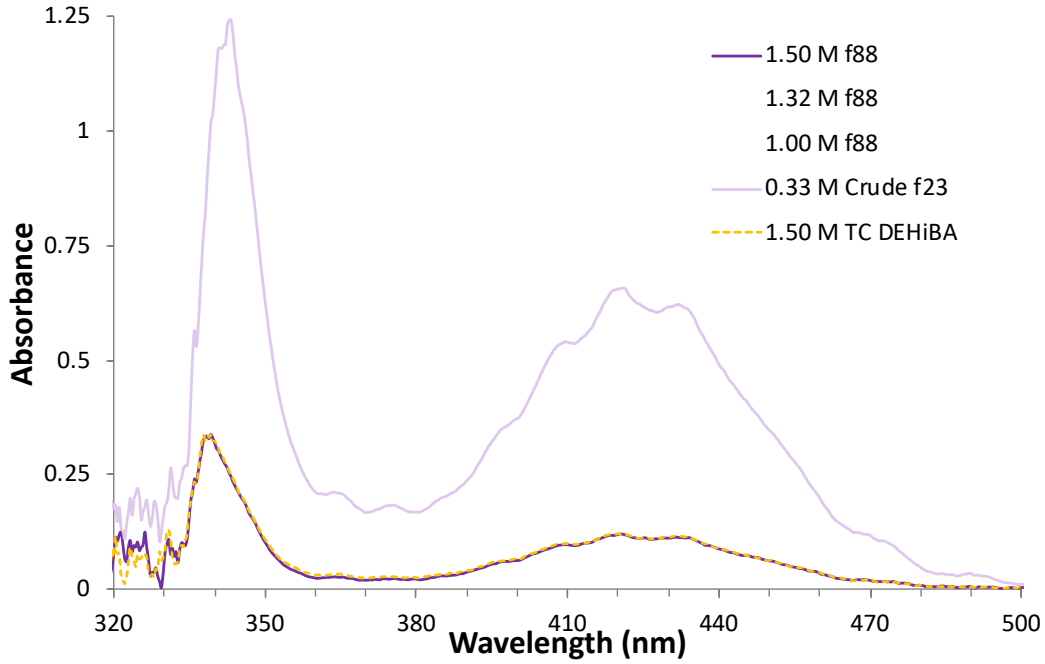

Figure S62: Aqueous UV-Vis spectra for the residual uranium(VI) following contact with varying f88 and crude f23 DEHiBA concentrations when using 0.1 M uranyl nitrate in 4.0 M nitric acid with a 1:1 SA ratio at 15 °C. Overlaid with the aqueous 1.50 M TC DEHiBA measurement.

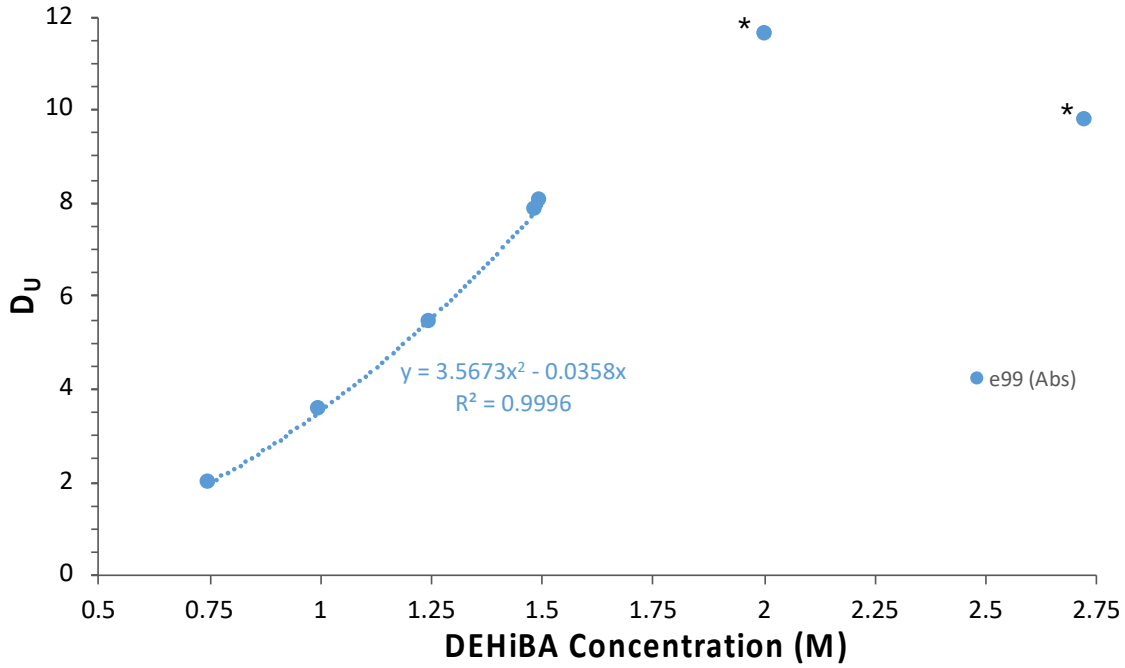

Figure S63: The effect of e99 DEHiBA concentration on the distribution ratio of uranium(VI) at 15 and *22 °C for the extraction of 0.1 M uranyl nitrate in 4.0 M nitric acid using a 1:1 SA ratio.

The Impact of Nitric Acid Concentration (2-6 M) for Uranium(VI) Extractions with 1.5 M and 1.0 M Purified DEHiBA (e99)

Table S22: Mass balance data for the extraction of 0.10 M uranyl nitrate with 1.50 and 1.00 M e99 across 2.0-6.0 M nitric acid concentrations at a 1:1 SA ratio at 22 °C.

DEHiBA Sample		Du from Max Abs	Mass Balance (%)	Du from Peak Area	Mass Balance (%)
6 M HNO_3		8.15	7.4	7.31	0.9
5 M HNO_3		7.71	5.5	7.13	-0.1
4 M HNO_3	**e99 1.5 M**	6.27	1.5	6.22	1.1
3 M HNO_3		4.48	-1.9	4.48	-3.6
2 M HNO_3		2.36	-2.5	2.40	-4.6
6 M HNO_3		3.30	2.3	3.06	-0.2
5 M HNO_3		3.32	1.7	3.15	-1.0
4 M HNO_3	**e99 1.0 M**	2.53	0.3	2.58	1.3
3 M HNO_3		1.90	-3.1	1.90	-4.9
2 M HNO_3		1.05	-7.2	1.08	-10.0

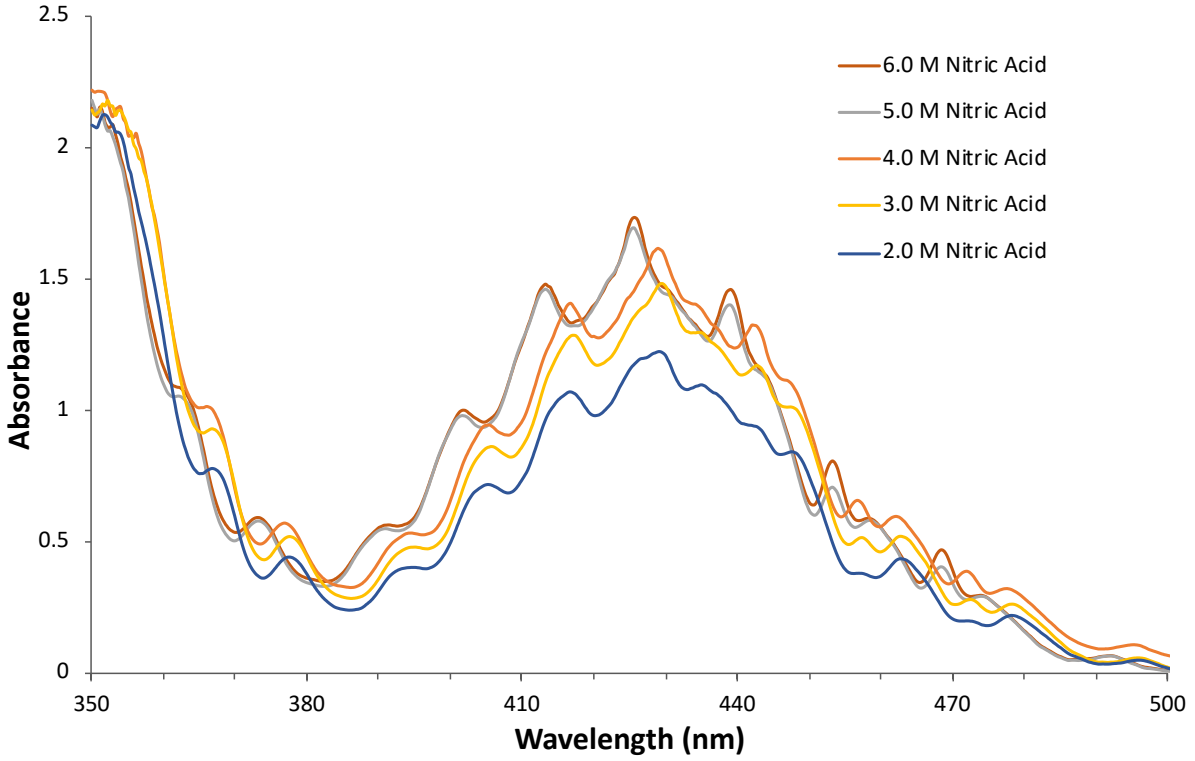

Figure S64: The effect of nitric acid concentration on the organic uranium(VI) UV-Vis spectra for the extraction of 0.1 M uranyl nitrate with 1.5 M e99 DEHiBA at 22 °C using a 1:1 SA ratio.

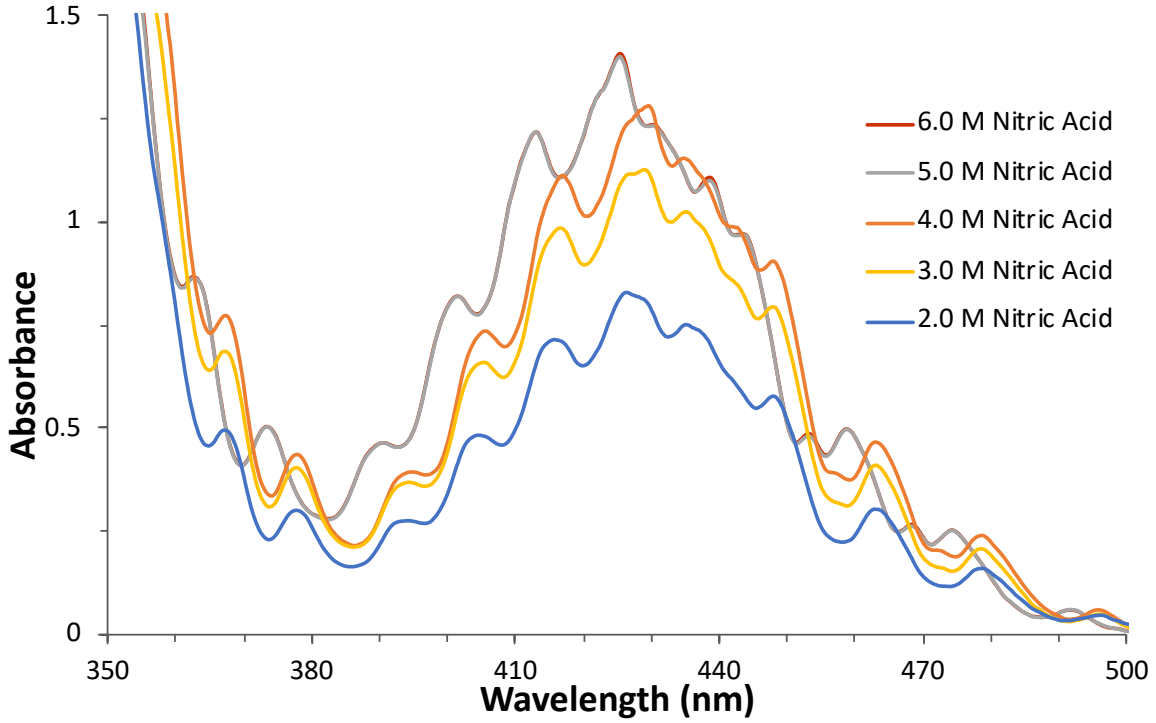

Figure S65: Nitric acid concentration effect on the organic uranium(VI) UV-Vis spectra for the extraction of 0.1 M uranyl nitrate with 1.0 M e99 DEHiBA at 22 °C using a 1:1 SA ratio.

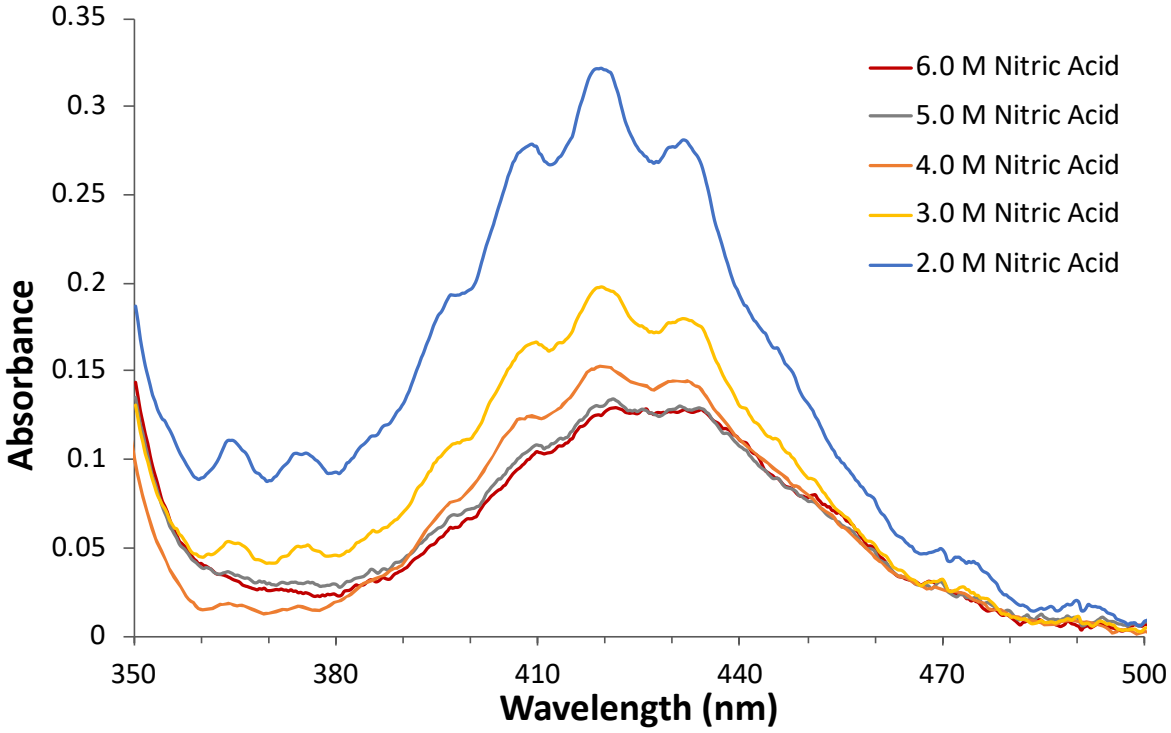

Figure S66: Nitric acid concentration effect on the residual aqueous uranium(VI) UV-Vis spectra from the extraction of 0.1 M uranyl nitrate with 1.5 M e99 DEHiBA at 22 °C using a 1:1 SA ratio.

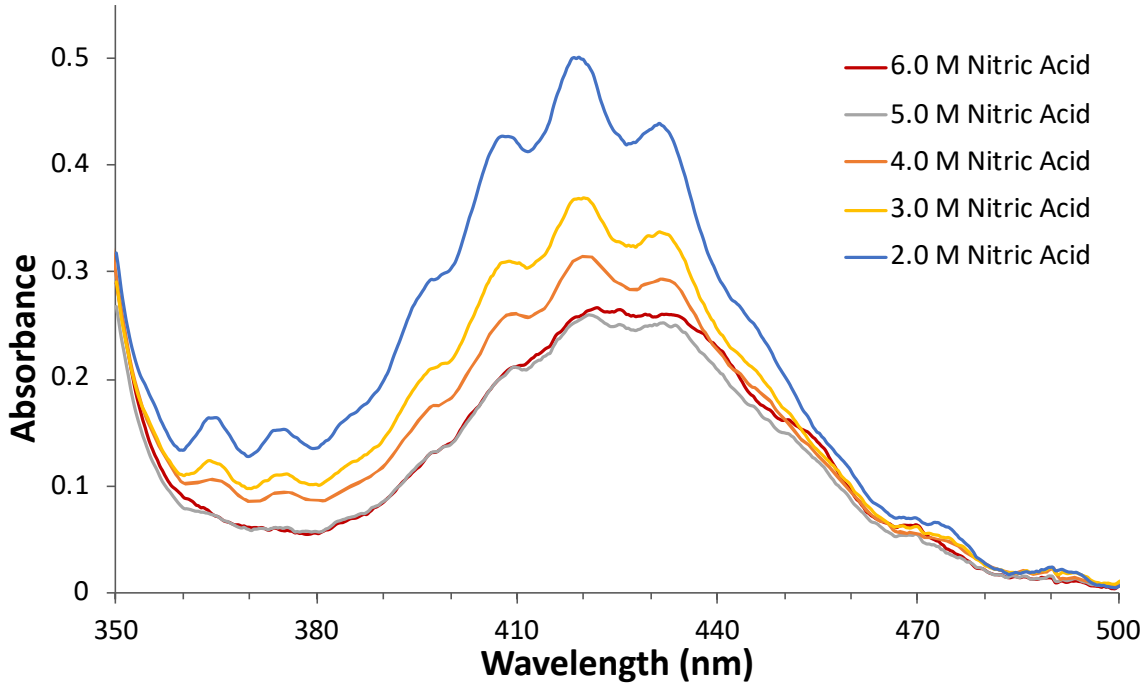

Figure S67: Nitric acid concentration effect on the residual aqueous uranium(VI) UV-Vis spectra from the extraction of 0.1 M uranyl nitrate with 1.0 M e99 DEHiBA at 22 °C using a 1:1 SA ratio.

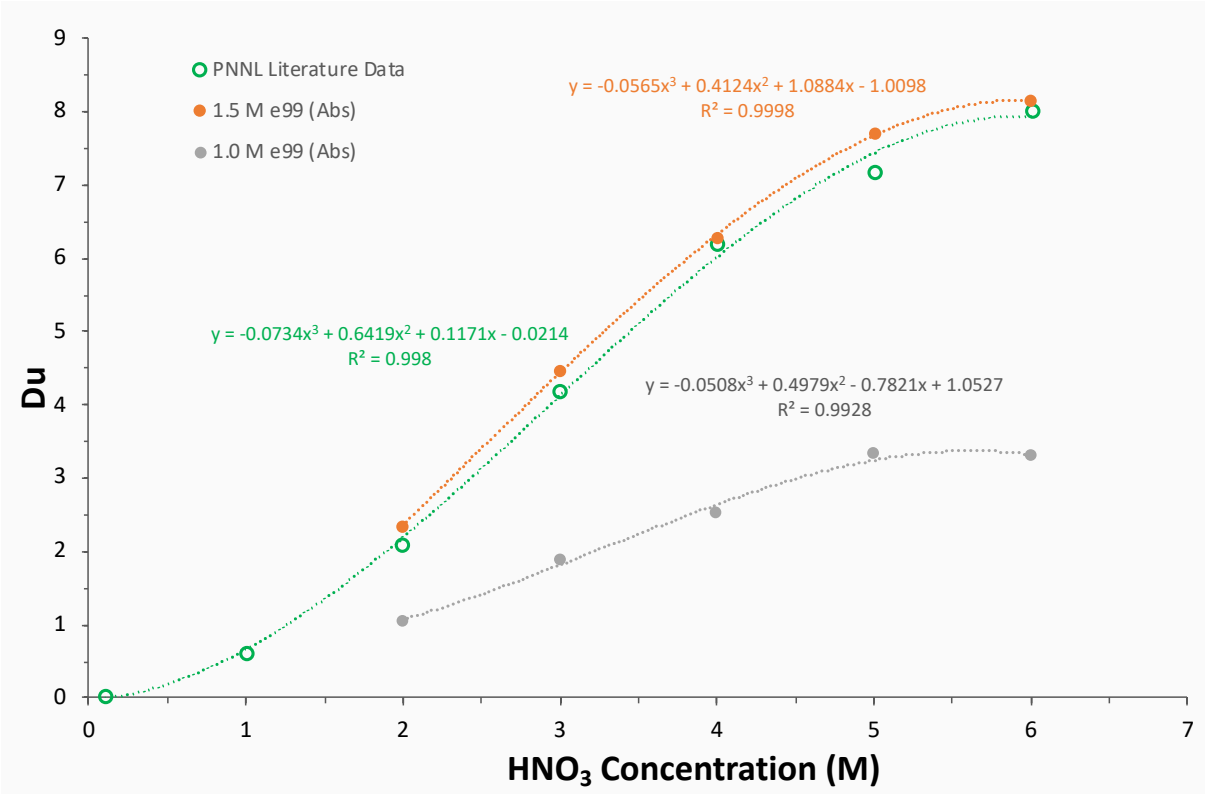

Figure S68: The effect of nitric acid concentration on the distribution ratio of uranium(VI) at 22 °C comparing 1.5 and 1.0 M e99 DEHiBA to 1.5 M DEHiBA literature data using a 1:1 SA ratio for the extraction of 0.1 M uranium(VI). With third order polynomial equations.

Investigating Organic : Aqueous Phase Ratio to Optimise the Extraction of Uranium(VI) with 1.50 M and 1.00 M DEHiBA

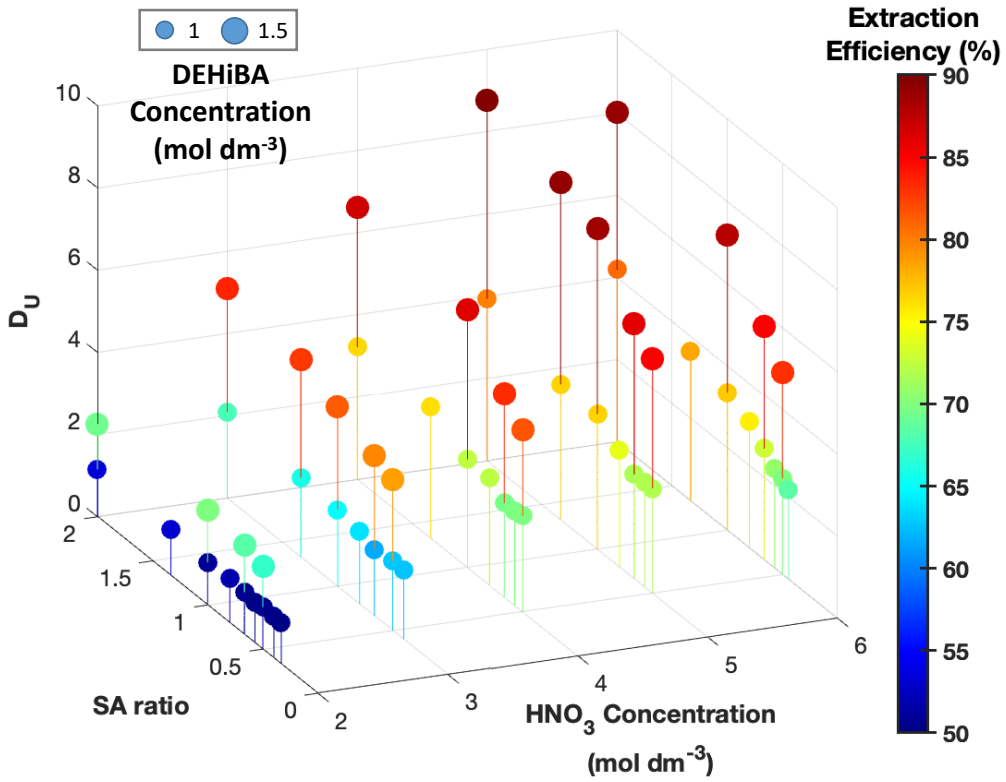

Figure S69: 4D plot comparing the uranium(VI) extraction performance of 1.0 M and 1.5 M e99 DEHiBA across a range of SA ratios and nitric acid concentrations when using 0.1 M uranyl nitrate.

Table S23: Mass balance data for the extraction of 0.1 M uranyl nitrate with 1.5 M e99 DEHiBA across 2.0-6.0 M nitric acid and varying SA ratios.

DEHiBA Sample		Temperature °C	SA ratio	Organic Uranium Concentration (M)	D_U	Aqueous Uranium Concentration (M)	Mass Balance (%)
5 M HNO_3	1.5 M e99	15	4	0.0283	**9.79**	0.0029	**16.1**
3 M HNO_3		15	4	0.0277	**5.39**	0.0051	**16.1**
6 M HNO_3		22	2	0.0490	**7.59**	0.0065	**4.5**
5 M HNO_3		15	2	0.0522	**8.76**	0.0060	**10.4**
4 M HNO_3	1.5 M e99	22	2	0.0491	**6.38**	0.0077	**5.8**
3 M HNO_3		15	2	0.0497	**5.08**	0.0098	**9.2**
2 M HNO_3		22	2	0.0420	**2.35**	0.0179	**1.9**
5 M HNO_3	1.5 M e99	15	1.5	0.0744	**7.75**	0.0096	**8.9**
3 M HNO_3		15	1.5	0.0699	**4.90**	0.0143	**7.5**
6 M HNO_3		22	1	0.0911	**6.85**	0.0133	**4.4**
5 M HNO_3		22	1	0.0950	**7.46**	0.0127	**7.8**
4 M HNO_3	1.5 M e99	22	1	0.0869	**6.24**	0.0139	**0.9**
3 M HNO_3		22	1	0.0865	**4.52**	0.0191	**5.6**
2 M HNO_3		22	1	0.0677	**2.46**	0.0275	**-4.8**
6 M HNO_3		22	0.67	0.1200	**5.60**	0.0214	**1.2**
5 M HNO_3		15	0.67	0.1247	**6.54**	0.0191	**2.2**
4 M HNO_3	1.5 M e99	22	0.67	0.1140	**5.03**	0.0227	**-1.5**
3 M HNO_3		15	0.67	0.1125	**4.12**	0.0273	**2.3**
2 M HNO_3		22	0.67	0.0851	**2.31**	0.0368	**-6.4**
6 M HNO_3		22	0.5	0.1453	**4.86**	0.0299	**-7.4**
5 M HNO_3		15	0.5	0.1542	**5.74**	0.0269	**4.0**
4 M HNO_3	1.5 M e99	22	0.5	0.1383	**4.55**	0.0304	**-9.4**
3 M HNO_3		15	0.5	0.1542	**4.42**	0.0349	**1.9**
2 M HNO_3		22	0.5	0.0948	**2.16**	0.0439	**-8.7**

Table S24: The extraction efficiency and DEHiBA to uranium(VI) ratio data for the extraction of 0.1 M uranyl nitrate with 1.5 M e99 DEHiBA across 2.0-6.0 M nitric acid and varying SA ratios.

DEHiBA Sample		Temperature °C	SA ratio	D_U	Extraction Efficiency (%)	Ratio of DEHiBA : Uranyl Nitrate
6 M HNO_3	1.5 M e99	22	2	7.59	88.9	29.7
6 M HNO_3			1	6.85	87.8	16.1
6 M HNO_3			0.67	5.60	85.0	12.6
6 M HNO_3			0.5	4.86	83.0	10.5
5 M HNO_3	1.5 M e99	15	4	9.79	91.5	49.6
5 M HNO_3		15	2	8.76	89.8	28.7
5 M HNO_3		15	1.5	7.75	89.1	19.4
5 M HNO_3		22	1	7.46	88.6	15.5
5 M HNO_3		15	0.67	6.54	86.1	12.9
5 M HNO_3		15	0.5	5.74	85.1	9.9
4 M HNO_3	1.5 M e99	22	2	6.38	86.9	29.5
4 M HNO_3			1	6.24	86.2	17.1
4 M HNO_3			0.67	5.03	83.2	13.3
4 M HNO_3			0.5	4.55	81.6	11.1
3 M HNO_3	1.5 M e99	15	4	5.39	84.4	52.2
3 M HNO_3		15	2	5.08	83.5	30.2
3 M HNO_3		15	1.5	4.90	82.7	21.3
3 M HNO_3		22	1	4.52	81.4	17.4
3 M HNO_3		15	0.67	4.12	79.5	13.8
3 M HNO_3		15	0.5	4.42	78.6	11.4
2 M HNO_3	1.5 M e99	22	2	2.35	69.3	35.8
2 M HNO_3			1	2.46	69.9	22.5
2 M HNO_3			0.67	2.31	68.4	18.1
2 M HNO_3			0.5	2.16	66.9	16.3

Table S25: Mass balance data for the extraction of 0.1 M uranyl nitrate with 1.0 M e99 DEHiBA across varying nitric acid concentrations and SA ratios.

Extraction Conditions		SA ratio	Organic Uranium Concentration (M)	D_U	Aqueous Uranium Concentration (M)	Mass Balance (%)
6.0 M HNO_3		2	0.0506	**4.19**	0.0121	**0.2**
5.0 M HNO_3		2	0.0450	**3.94**	0.0114	**1.4**
4.0 M HNO_3	**1.0 M e99**	2	0.0416	**3.21**	0.0130	**-3.8**
3.0 M HNO_3		2	0.0388	**2.09**	0.0186	**-3.8**
2.0 M HNO_3		2	0.0351	**1.15**	0.0305	**0.6**
6.0 M HNO_3		1.33	0.0695	**3.62**	0.0192	**3.4**
5.0 M HNO_3		1.33	0.0617	**3.29**	0.0188	**1.0**
4.0 M HNO_3	**1.0 M e99**	1.33	0.0568	**3.19**	0.0178	**-7.2**
3.0 M HNO_3		1.33	0.0515	**1.93**	0.0267	**-4.5**
2.0 M HNO_3		1.33	0.0434	**1.13**	0.0385	**-3.7**
6.0 M HNO_3		1	0.0785	**3.34**	0.0235	**2.3**
5.0 M HNO_3		1	0.0765	**3.28**	0.0234	**-0.2**
4.0 M HNO_3	**1.0 M e99**	1	0.0696	**2.63**	0.0264	**-4.0**
3.0 M HNO_3		1	0.0617	**1.86**	0.0333	**-5.0**
2.0 M HNO_3		1	0.0481	**1.03**	0.0465	**-5.3**
6.0 M HNO_3		0.8	0.0968	**3.08**	0.0315	**4.5**
5.0 M HNO_3		0.8	0.0875	**2.84**	0.0308	**0.8**
4.0 M HNO_3	**1.0 M e99**	0.8	0.0811	**2.61**	0.0311	**-4.0**
3.0 M HNO_3		0.8	0.0695	**1.77**	0.0394	**-5.0**
2.0 M HNO_3		0.8	0.0546	**1.07**	0.0509	**-5.4**
6.0 M HNO_3		0.67	0.1049	**2.70**	0.0389	**5.5**
5.0 M HNO_3		0.67	0.0942	**2.53**	0.0372	**0.0**
4.0 M HNO_3	**1.0 M e99**	0.67	0.0871	**2.28**	0.0382	**-3.8**
3.0 M HNO_3		0.67	0.0739	**1.61**	0.0460	**-4.8**
2.0 M HNO_3		0.67	0.0572	**1.02**	0.0561	**-5.8**
6.0 M HNO_3		0.57	0.1090	**2.41**	0.0452	**5.0**
5.0 M HNO_3		0.57	0.1038	**2.55**	0.0408	**0.1**
4.0 M HNO_3	**1.0 M e99**	0.57	0.0958	**2.30**	0.0416	**-3.6**
3.0 M HNO_3		0.57	0.0783	**1.52**	0.0517	**-3.6**
2.0 M HNO_3		0.57	0.0590	**0.99**	0.0597	**-6.6**
6.0 M HNO_3		0.5	0.1137	**2.33**	0.0488	**3.6**
5.0 M HNO_3		0.5	0.1125	**2.54**	0.0442	**0.5**
4.0 M HNO_3	**1.0 M e99**	0.5	0.1060	**2.33**	0.0456	**-1.4**
3.0 M HNO_3		0.5	0.0891	**1.68**	0.0529	**-2.5**
2.0 M HNO_3		0.5	0.0626	**1.02**	0.0614	**-7.3**

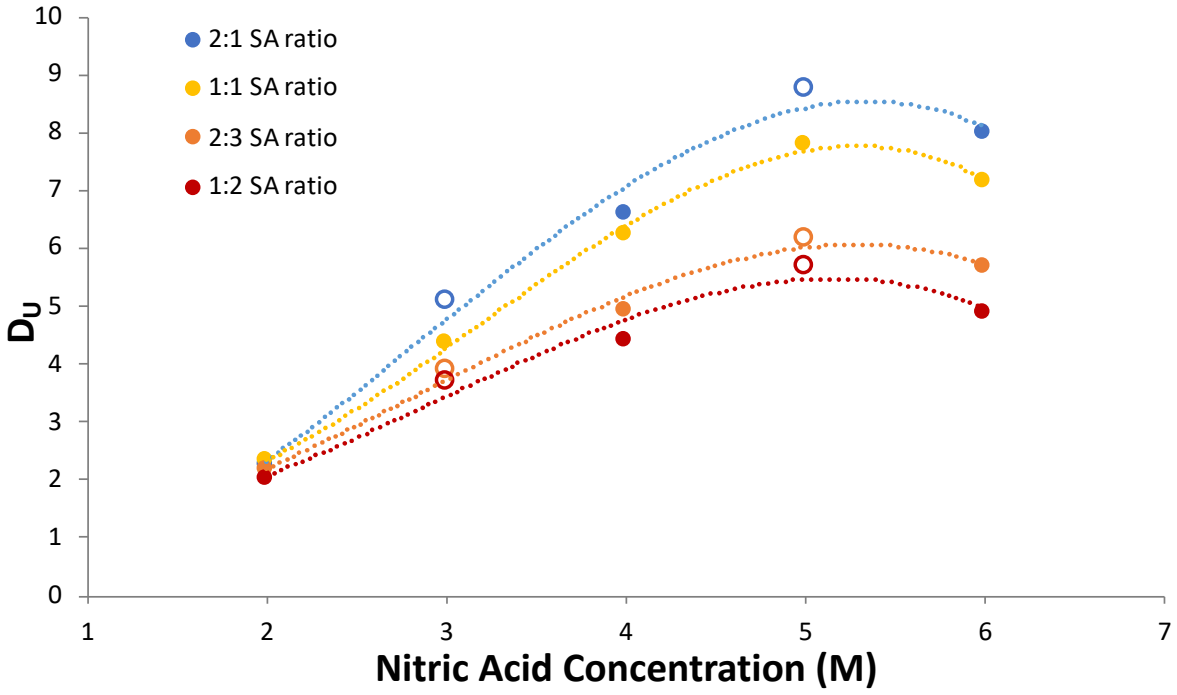

Figure S70: The effect of nitric acid concentration and SA ratio on the distribution ratio of uranium(VI) for the extraction of 0.1 M uranyl nitrate with 1.5 M e99 at 22 °C (filled ● markers) and 15 °C (empty ○ markers).

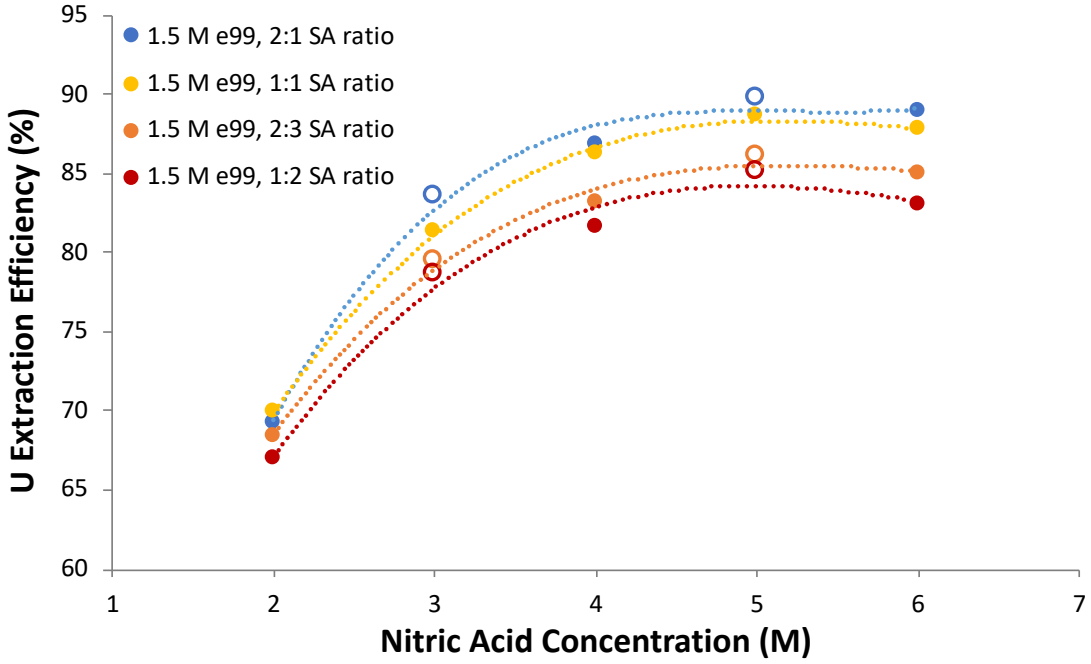

Figure S71: The effect of nitric acid concentration and SA ratio on the extraction efficiency of uranium(VI) using 0.1 M uranyl nitrate with 1.5 M e99 DEHiBA at 22 °C (filled ● markers) and 15 °C (empty ○ markers).

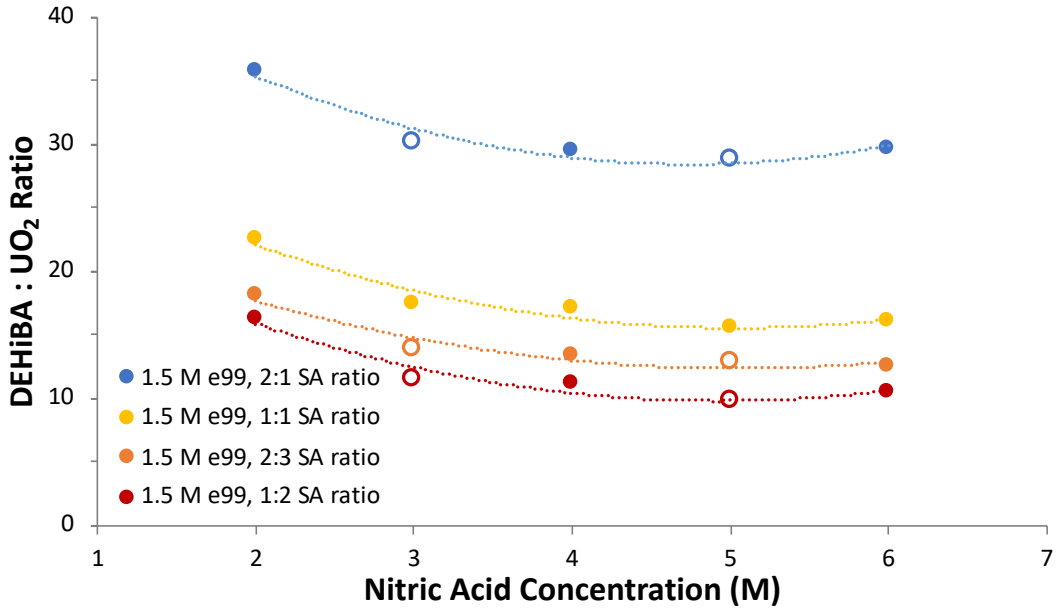

Figure S72: The effect of nitric acid concentration and SA ratio on the ratio of DEHiBA to uranium(VI) when using 0.1 M uranyl nitrate with 1.5 M e99 at 22 °C (filled ● markers) and 15 °C (empty ○ markers).

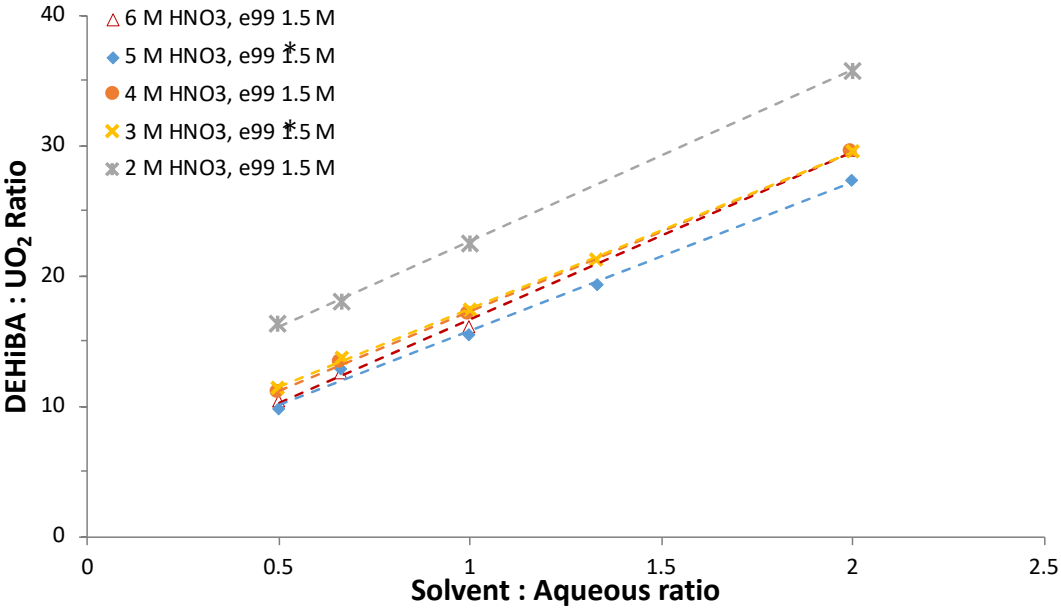

Figure S73: The effect of SA ratio and nitric acid concentration on the ratio of DEHiBA to uranium(VI) at 15* and 22 °C using 0.1 M uranium(VI) with 1.5 M e99.

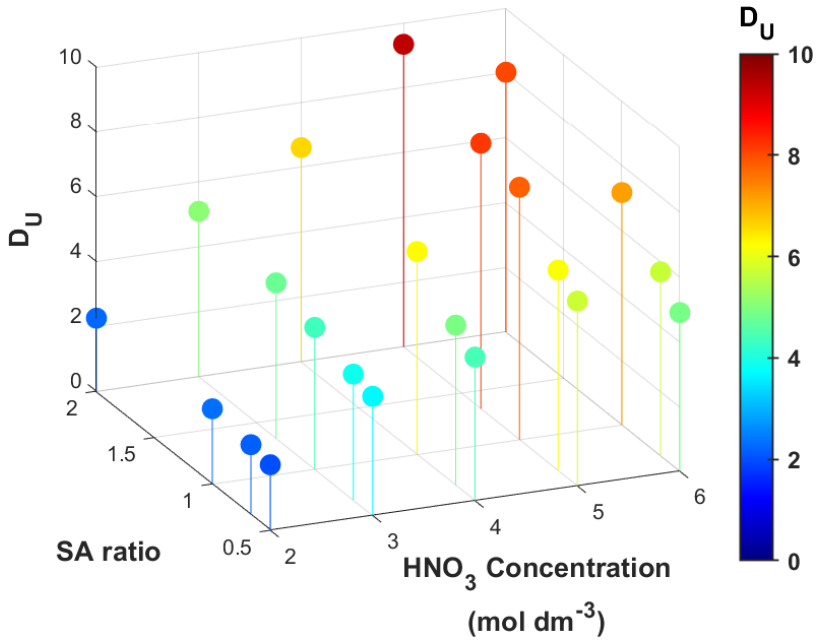

Figure S74: 4D plot illustrating the uranium(VI) extraction performance of 1.5 M e99 DEHiBA across 2.0-6.0 M nitric acid and a range of SA ratios.

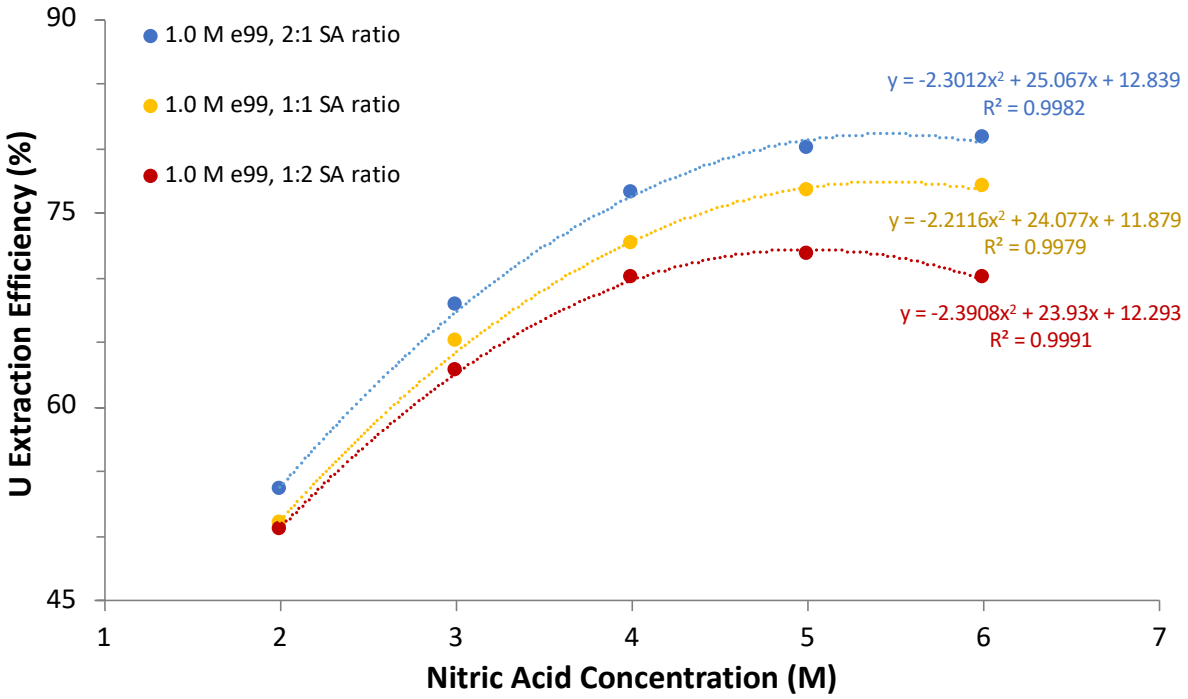

Figure S75: The effect of nitric acid concentration and SA ratio on the extraction efficiency of uranium(VI) at 22 °C using 0.1 M uranium(VI) with 1.0 M e99.

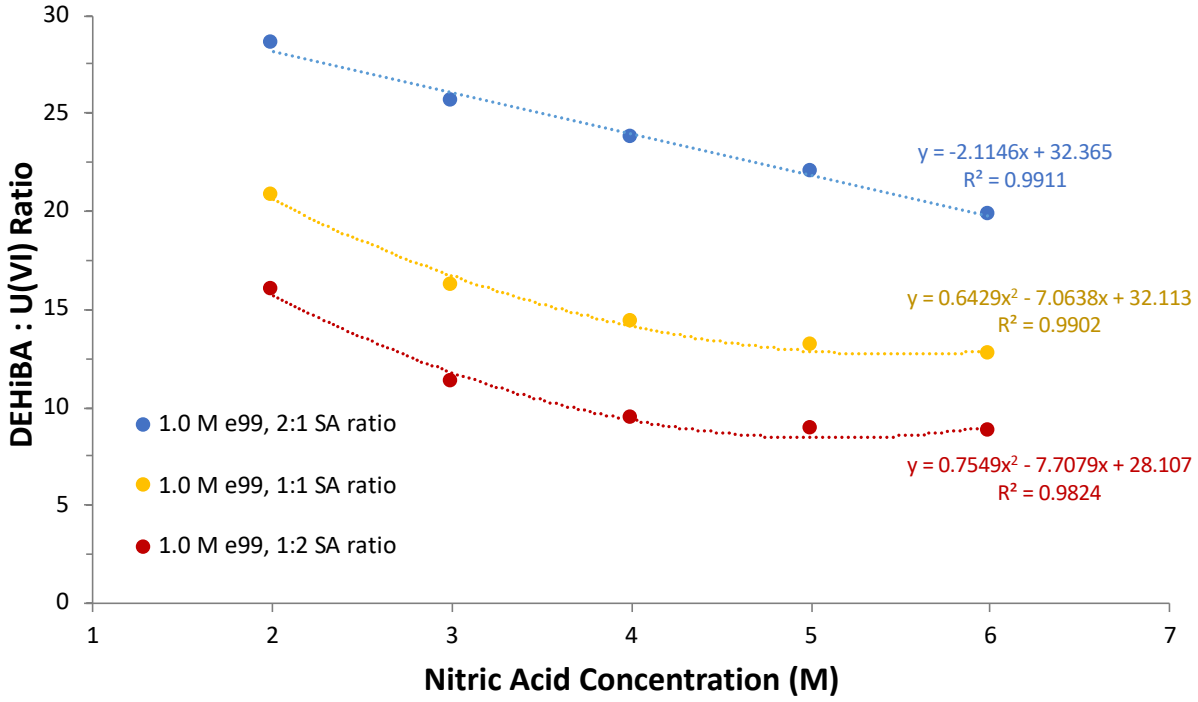

Figure S76: The effect of nitric acid concentration and SA ratio on the ratio of DEHiBA to organic uranium(VI) at 22 °C using 0.1 M uranyl nitrate with 1.0 M e99 DEHiBA.

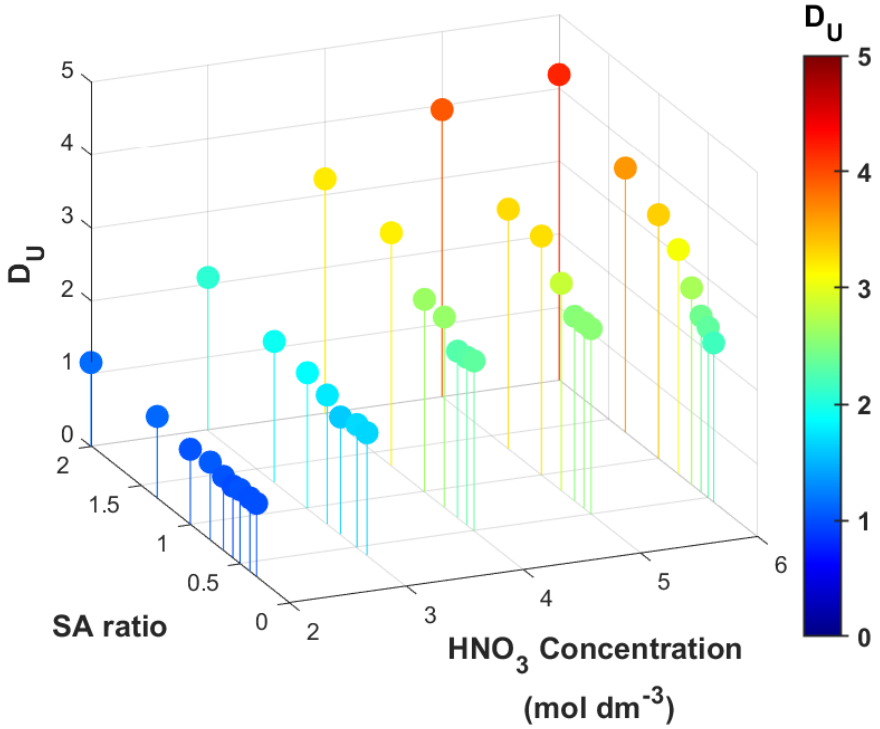

Figure S77: 4D plot illustrating the uranium(VI) extraction performance of 1.0 M e99 DEHiBA across a range of SA ratios and nitric acid concentrations when using 0.1 M uranyl nitrate at 22 °C.